DEVELOPMENT OF A PALEO FORAGE FISH INDEX AND COMPARISON OF MULTIPLE CORES FROM THE SANTA BARBARA BASIN

Alexander Dominic Filardo

A Thesis submitted in partial satisfaction of the requirements
for the degree Master of Science

in

Marine Science

College of Natural and Computational Sciences

Hawai‘i Pacific University

2019

Honolulu, Hawaii

Advisory Committee:

David B. Field, Chair
Keith E. Korsmeyer
Renato Salvatteci
John C. Field

ABSTRACT

Evidence from both fossil fish scale records and surveys of fish abundance suggest that small pelagic forage fish abundances in the California Current Ecosystem (CCE) have been declining since the late 20th century, however, the low values in the 1900s have never been put into the context of long-term records. This study compiled scale fluxes from sardine, anchovy, hake, and myctophid as well as a novel record of skeletal debris from three kasten sediment cores as well as numerous box core records from the Santa Barbara Basin (SBB) to develop a Paleo Forage Fish Index. The Paleo Forage Fish Index, which is a normalized compilation of the five time series, revealed periods of extended negative anomalies beginning around the 1930s and from the 1960s to the end of the record following a shift in plankton assemblages toward subtropical taxa, which suggests that the 20th century warming trend influences the abundance, distribution, and/or species assemblage of small pelagic forage fish in the CCE. In addition, this study developed a rigorous outlier detection procedure and determined that up to 30% of the sampling intervals contain identified outliers, although the presence of outliers do not have a major effect on the overall nature of the records. Comparison between cores shows significant differences between kasten cores and between composite core records, which emphasizes the need for a multi-core, composite record to average out decadal to interdecadal scale differences between cores. Furthermore, the skeletal debris record was determined to be a compilation of multiple species with vertebrae primarily coming from fish between two and eight centimeters in length.

HAWAI'I PACIFIC UNIVERSITY

Development of a Paleo Forage Fish Index and Comparison of Multiple Cores from the Santa Barbara Basin

by

Alexander Dominic Filardo

November 20, 2019

This thesis is submitted in partial fulfillment of the requirements for the degree of Master of Science in Marine Science at Hawai'i Pacific University. We the undersigned have examined this document and have found that it is complete and satisfactory in all respects, and all revisions required by the final examining committee have been made.

Author _____

Alexander D. Filardo

Committee Chair _____

David B. Field

Committee Member _____

Keith E. Korsmeyer

Committee Member _____

Renato Salvatteci

Committee Member _____

John C. Field

Dean _____

Brenda Jensen, PhD, Dean, College of Natural and Computational Sciences

Acknowledgements

I would like to thank a number people who have supported and mentored me throughout this journey that some call a Master's Thesis.

First of all, I would like to thank my thesis advisor Dr. David B. Field for the countless hours spent working with me and discussing fish scales, outliers and long-term variability in small pelagics. I thank you for your mentorship, patience, and immense scientific knowledge that guided me throughout my education. Most importantly I would like to thank Dr. Field for advising me to get out and go surfing after long hours of staring at the computer since it really does aid in mental health. I would also like to thank my thesis committee, Dr. John Field, Dr. Renato Salvatteci, and Dr. Keith Korsmeyer for their help in adding to the development of my thesis.

I would like to thank the professors and staff at Hawai'i Pacific University who taught me so much and made going to class enjoyable. I would also like to thank Melissa Bacallao for helping me process vertebrae samples and Poseidon Fisheries Research for allowing me to use their lab space and taking me to the fish markets.

I would like to thank my family for always supporting me, especially my parents who would brag to their friends about me regardless if they knew what I was studying or not. Mom and dad, I thank you for writing down my thesis topic on a notecard so you can read it off when people ask what I study. I would like to thank grampy (Marlin Lile) who took me on my first salmon fishing trip and originally sparked my interest in fisheries science.

I would like to thank my friends, both from Hawaii and California. I would like to thank my coworkers at the Western Pacific Regional Fisheries Management Council for giving me the

opportunity to work in fisheries management and my coworkers at Kamanu Composite for supporting me and covering all my shifts when I needed to stay home and work on my thesis.

And finally, I would like to thank my partner, Carissa Cabrera, for the endless encouragement and support. You are always there for me, whether its proofreading my paper, lifting my spirits during stressful times, getting me out of the house and off the computer, or challenging me to do better in all that I do.

I thank you all.

Table of Contents

Table of Figures

Table of Tables

CHAPTER 1: A Review of Using Fish Debris within Marine Sediment Cores as an Indicator of Small Pelagic Forage Fish Abundances

Scientific Background/Literature Review

Introduction

Evidence from both fish abundance surveys and fossil fish debris records suggest that small pelagic forage fish abundances have been declining since at least the late 20th century in the southern region of the California Current Ecosystem (CCE), and further evidence suggests that it may be related to the long-term warming trend (Rose, 2013; Koslow and Davison, 2016). Recent ichthyoplankton trawl survey data from the CCE indicates a decline in larval fish abundance by approximately 70% since the 1960s due to a decline in species with cool-water affinities (Koslow and Davison, 2016). Figure 1.1 shows the overall abundance of fish larvae where there is an apparent decline starting in the 1960s into the 21st century. In addition, fossil fish debris data show sardine (*Sardinops sagax)*, anchovy (*Engraulis mordax*), and hake (*Merluccius productus*) scale flux begin to decline in the mid-1930s and show additional decline after the mid-1970s (Rose, 2013; Field et al., in progress). However, it is unclear if this decline is a long-term decline in fish abundances or if this period of low fish abundance is common throughout the last few thousand years and is attributed to natural variability. The decline in forage fish abundance has large effects on the ecosystem, which has been seen in the unusual increase in juvenile California sea lion strandings around their breeding grounds off Santa Barbara, California from 2013-2016 (McClatchie et al., 2016). This decline in juvenile sea lion

health is likely due to the nursing female's inability to find quality food, such as sardine and anchovy, that is high in fat and oil content (McClatchie et al., 2016).

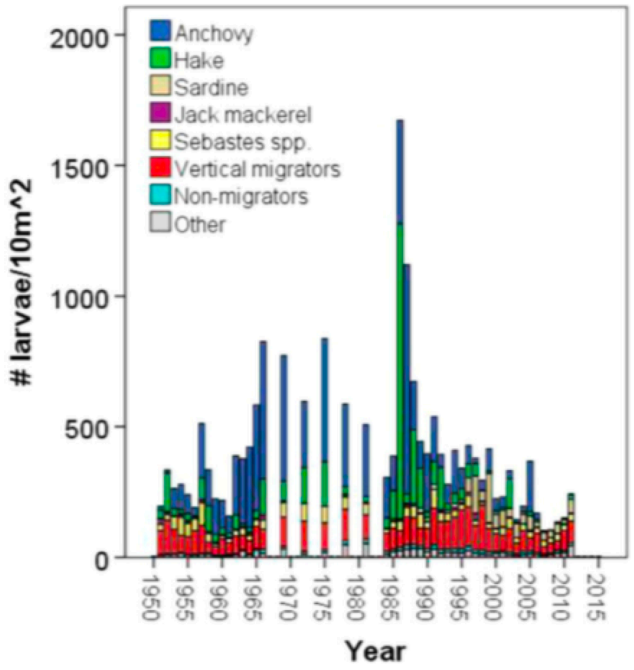

Figure 1.1: The overall mean annual abundance of fish larvae from California Cooperative Oceanic Fisheries Investigations (CalCOFI) ichthyoplankton trawl surveys from 1951 – 2011 (Koslow and Davison, 2016).

The cause of the decline in abundance of pelagic forage fish is currently unclear. On the one hand, these populations undergo large natural variations, fluctuating through periods of high and low abundance (Soutar and Isaacs, 1974). On the other hand, changes in environmental conditions such as an ocean warming trend and changes in subsurface oxygen levels can result in a shift in the food web structure, and other anthropogenic influences, such as commercial fishing and indirect effects through trophic cascades, may also affect forage fish populations (Field et al., in progress; Bertrand et al., 2011; Pikitch et al., 2012). With so many potential causes of variation, it is important to determine which have the greatest impacts on pelagic forage fish populations to better understand this decline in the face of a changing climate.

Quantifying fish debris within marine sediment cores allows us to infer past variability of fish population abundances prior to industrial fish catch records, stock assessments, and fishery-independent surveys. Soutar (1967) and Soutar and Isaacs (1969, 1974) pioneered the work reconstructing pelagic fish populations based on sediment cores from the Santa Barbara Basin (SBB) and first suggested that the collapse of the California sardine in the 1940s may be due to natural variability rather than overfishing. Since then, there have been numerous studies using organic debris within marine sediments to quantify plankton (e.g. Field et al., 2006), productivity (Field et al., in progress), and other sources of fish debris such as bones, vertebrae, and otoliths (Rose 2013; Jones 2016).

The primary objective of this paper is to review the paleoecological approach in understanding the dynamics of long-term variability in small pelagic forage fish in the CCE. I begin by discussing the background of the CCE, the primary small pelagic forage fish that inhabit it and leave debris in the marine sediments, and the factors that may affect these forage fish abundances. Next, I will discuss how fish debris is deposited to the sea floor followed by the sedimentary conditions required to preserve the sediment records. I conclude by synthesizing and analyzing recent fish debris studies.

Background of Key Small Pelagic Fishes in the California Current:

Small pelagic forage fish, found throughout the world's oceans, sustain higher trophic levels and industrial fisheries. Some of the major forage found in the central and southern CCE around the SBB include sardine, anchovy, juvenile hake, myctophids, small squid, rockfish, saury, and mackerel (Koehn et al., 2016; Szoboszlai et al., 2015). This review primarily focuses on

sardine, anchovy, juvenile hake, and myctophids because these species contribute to fish debris commonly found in SBB sediments (Soutar and Isaacs, 1969). Pacific saury (Cololabis saira), Pacific jack mackerel (Trachurus symmetricus), and Pacific mackerel (Scomber japonicus) are also found within SBB sediment cores, however in much lower abundances than the four major forage fish studied here.

There has been much debate as to how much fishing pressure should be put on small pelagic forage fish. Removing small forage fish from the ecosystem reduces the availability of prey for more valued commercially targeted species such as tuna, cod, and striped bass as well as piscivorous seabirds and marine mammals (Pikitch et al., 2012). Smith et al. (2011) found that fishing low trophic level species at the conventional maximum sustainable yield often results in reduced prey availability for higher trophic levels and halving exploitation rates from MSY levels would result in much lower impacts for the upper trophic levels, which in turn protect and maintain diversity.

Sardine:

Pacific sardine are found in regions throughout the coastal Pacific including the CCE (Emmett et al., 2005). Pacific sardine inhabit waters off central and southern California during the spring and migrate northwards along the coast toward northern California, Oregon, and Washington in the summer (Demer, 2012). Demer (2012) interprets that this movement between north and south habitats results from seasonal oceanographic changes, however, their distribution may also be largely dependent on stock size and migratory behavior (Field et al., 2009; Schwartzlose et al., 1999). For example, it is known that sardine migrate further north

when the population expands. Likewise, during El Niño years and periods of warm ocean regime, Pacific sardine are typically found closer to shore in warmer, more productive waters (Field et al., 2009; Emmett et al., 2005; Demer, 2012). However, in general, Pacific sardine are found further offshore in warmer, less productive waters compared to anchovy (Checkley et al., 2009). Sardine typically filter feed on both phytoplankton and small zooplankton, which are nourished by nutrient-rich waters due to upwelling or deep mixing (Checkley et al., 2017; Emmett et al., 2005). Sardine have a small mouth-gape and fine gill rakers designed to retain prey as small as 10 µm in size (Rykaczewski and Checkley, 2008), allowing them to take advantage of coastal waters that are dominated by small sized plankton.

The California sardine fishery began in the late 19th century and peaked around 1936 harvesting over 700,000 tons (Figure 1.2) (MacCall, 1979). After 1945, there was a dramatic decline in landings reaching a low of around 4,000 tons in the mid 1950s (MacCall, 1979), a reduction of greater than two orders of magnitude, and did not show signs of recovery until the early 1980s (Schwartzlose et al., 1999). As illustrated in Figure 1.2, landings of sardine started to recover after 1995. From 2001–13, commercial landings of sardine averaged over 42,000 tons over the thirteen-year period, which is still less than one order of magnitude of the height of the fishery (California Department of Fish and Wildlife, 2014). Nonetheless, in 2013, sardine was the fourth largest California fishery in terms of volume, generating an ex-vessel revenue of $1.6 million (California Department of Fish and Wildlife, 2014).

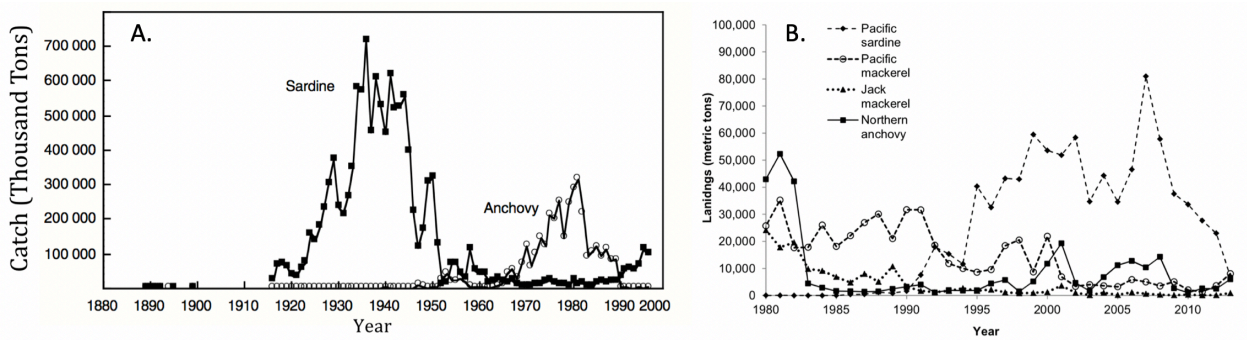

Figure 1.2: Time series of (A) catches of Pacific sardine and northern anchovy in the California Current from 1889 – 1997 and (B) landings of Pacific sardine, Pacific mackerel, jack mackerel, and northern anchovy from 1980 – 2013. (Modified from Schwartzlose et al., 1999 and California Department of Fish and Wildlife, 2014).

Anchovy:

Northern anchovy are typically found in productive, eastern boundary currents such as off central and southern California where there is an abundance of large planktonic prey due to strong coastal upwelling (Chavez et al., 2003; Rykaczewski and Checkley 2008). Anchovy have coarse gill rakers to feed on a variety of large phytoplankton using filter feeding techniques, however, anchovy primarily use a bite and pick feeding technique which allows them to feed on larger zooplankton providing them with most of their caloric energy (Hunter, 1981; Rykaczewski and Checkley, 2008; Espinoza, 2008; Espinoza et al., 2009). Based on the egg distribution collected from CUFES (Continuous, Underway Fish Egg Sampler), Checkley et al. (2000) found that northern anchovy in the CCE are more commonly found inshore of sardine eggs in regions of greater upwelling. Although anchovy are generally less migratory than sardine, the population expands and contracts in response to suitability of habitat, with less optimal habitats occupied largely during periods of high abundance (MacCall, 1990).

Industrial fishing for northern anchovy in the CCE began in the early 1950s, however, because the California anchovy fishery wasn't fully developed until later and catch records indicate that there was relatively low fish catch during this time, it is difficult to determine if the low catch was due to low fish abundance or minimal fishing effort (Figure 1.2; Schwartzlose et al., 1999). Figure 1.2 shows that fish catch peaked in the mid-1970s but had a sharp decline in 1983 and again in 1990 (Schwartzlose et al., 1999; California Department of Fish and Wildlife, 2014). The catch records showed a high abundance of anchovy in the 1970s reaching a maximum catch of 310,211 tons in 1981 (Figure 1.2) and lower catch through the 1990s averaging less than 100,000 tons per year (Lo and Methot, 1989; Schwartzlose et al., 1999). Since the early 1980s, anchovy landings off of California have been less than 25,000 tons due to both management measures (catch capped at 25,000 tons when biomass was below a threshold level) and poor market constraints (California Department of Fish and Wildlife, 2014). In 2013 the northern anchovy fishery off California earned ex-vessel revenue greater than $1.0 million with an export value of over $500 thousand (California Department of Fish and Wildlife, 2014).

Hake:

Pacific hake are found in patchy distributions throughout the northeastern Pacific from Queen Charlotte Sound, British Columbia to Southern California, United States (Methot and Dorn, 1995). Adult coastal Pacific hake feed in the northern region of their range (northern California to British Columbia) during the spring, summer, and fall and travel to the southern limits of their range (southern and Baja California) to spawn during the winter (Dorn 1995; Phillips et al., 2007), whereas juvenile hake are primarily found close to the coast of central and southern California

(Dorn, 1995). During spawning season, mature hake may be found several hundred kilometers off the coast (Dorn, 1995). Because adult coastal hake feed on a variety of small forage fish species, the hake's spawning migration may reduce potential cannibalism of their young (Phillips et al., 2007).

While adult hake are large, piscivorous fish, juveniles are found in large numbers in the water column and can be considered small pelagic forage fish (Brodeur et al., 2014). In addition, juvenile hake scales and skeletal debris are often found in the SBB sediment cores (Rose, 2013). This review refers to hake as forage fish, even though they become an important predator of small forage fish, including sardine, anchovy, and juvenile hake, as they grow in size (Livingston and Bailey, 1985; Brodeur et al., 2014; Buckley and Livingston, 1997). During the spring, summer, and fall months, adult hake undergo diel vertical migration and rise in the water column at night to feed on small fishes and invertebrates such as squid (Alverson and Larkins, 1969; Shaw et al., 1990), however, a diet analyses of 27 mature hake stomachs from the northern California Current contained approximately 80% of juvenile hake by weight of contribution (Figure 1.3; Brodeur et al., 2014). Figure 1.3 shows the ontogenetic shift from a predominantly plankton-based diet by fish smaller than 45 cm to a more piscivorous diet once the hake grow larger than 45 cm.

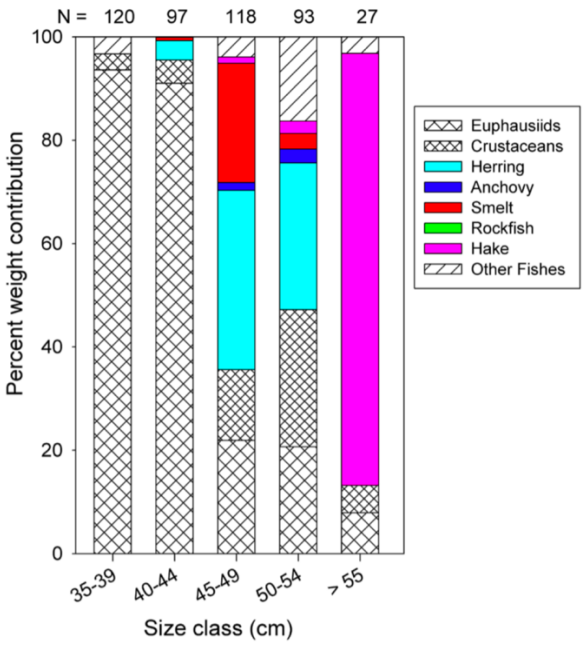

Figure 1.3: Diet composition of Pacific hake collected from the 1983 West Coast Trawl Survey conducted by the Alaska Fisheries Science Center off Oregon and Washington for five size classes (in cm) from Rextad and Pikitch, 1986. The number of stomachs analyzed is indicated at the top of each bar (Brodeur et al., 2014).

Since the mid 1990s, total landings between US and Canada averaged close to 300,000 tons per year making the hake fishery the largest fishery by volume on the US West Coast (Berger et al., 2019). Hake have supported a fishery averaging 170,000 tons from the mid 1960s to the mid 1990s, although most of the fishing occurs off Oregon, Washington, and British Columbia (Berger et al., 2019; Alverson and Larkins, 1969; Methot and Dorn, 1995; Phillips et al., 2007).

Myctophids:

Myctophids (Myctophidae) are a diverse family, consisting of many different species that inhabit epipelagic and mesopelagic ecosystems within the California Current (Wantabe et al., 1999). Many species are known for their diel vertical migration, feeding near the surface at night (Wantabe et al., 1999, Davison et al., 2015). Myctophids play a vital role in the ecosystem as prey

to higher trophic level predators as well as a link between surface production and the deep sea (Davison et al., 2015; Koslow et al., 2010). Most myctophid species consume zooplankton near the surface of the ocean under the cover of darkness and migrate to the depths during the day, thus these species become a potential transporter of organic matter from the surface to the deep ocean (Davison et al., 2015). Although these are ecologically important fish, particularly as forage to higher trophic levels, myctophids are not yet a commercially fished taxon. In 2016, the Pacific Fishery Management Council implemented a precautionary ban on the development of new fisheries on forage fish including myctophids and highly abundant, small fish (81 FR 19054).

Variability of Small Pelagic Forage Fish:

One of the problems with determining effects of global change on fisheries is the boom-and-bust nature of small pelagic forage fish, which can be attributed to a variety of different factors operating on different time scales including species interaction such as competition and predation (Koslow et al., 2010, 2014) and juvenile recruitment (Nishimoto and Washburn, 2002). Time series of catch records indicate that decadal to multi-decadal time scales contain a large amount of variability, which will be a primary focus of this review. Furthermore, factors acting on these short-term time scales can manifest on centennial to multi-centennial time scales where large scale climate change may also play a noteworthy role.

One potential cause of population variability seen in small pelagic fish is interspecific competition (Koslow et al., 2014). Simple trophic cascade models show that competitors, in a steady state, should be negatively correlated with each other. In this case, vertical migrating myctophids would compete with epipelagic planktivores such as sardine, anchovy, and juvenile

hake, potentially leading to an abundance of one species and near absence of others (Koslow et al., 2014). However, based on the CalCOFI ichthyoplankton time series, Koslow et al. (2014) found that mesopelagic myctophids are positively correlated with epipelagic planktivores such as anchovy and hake but not sardine. They also found positive correlations between epipelagic fishes (anchovy, hake, and mackerel) and environmental conditions that are indicative of low primary production, suggesting that the CCE is a dynamic region that is not in steady state and may be driven by bottom-up variations in productivity or other physical forcings.

Modern catch records of sardine and anchovy have led to a hypothesis indicating that the two species are out of phase with each other (Takasuka et al., 2008; Lluch-Belda et al., 1989). This hypothesis states sardine have more reproductive success during the warm regime and anchovy are more successful in recruitment during the cooler regime due to thermal preferences (Chavez et al., 2003; Lluch-Belda et al., 1989). However, because this hypothesis is based on catch records, the ratio of sardine to anchovy that were caught could be related to fishing pressure and market demand at any particular time. This hypothesis also does not take migration patterns into account. If the forage fish migrate to a region outside of the fishing grounds then the fish will not appear in the catch record and seem to be absent even though the population migrated to a different area and became unavailable to the fishing fleet (Lluch-Belda et al., 1989).

Juvenile fish recruitment may be sensitive to mesoscale processes such as local upwelling and eddies (Nishimoto and Washburn, 2002). For example, Nishimoto and Washburn (2002) conducted midwater trawl surveys and found a group of larval fishes to be in phase with some mesoscale phenomena. This relationship implies that forage fish recruitment may be subjected to mesoscale processes, which can then affect population abundances. However, recruits

disperse along a large spatial scale causing them to be affected by regional scale processes such as sea level anomalies and differences in water mass properties (Ralston et al., 2013; Schroeder et al., 2019). For example, rockfish recruitment in the CCE is greater equatorward geostrophic flow (e.g., lower relative sea level) seen throughout the California Current (Ralston et al., 2013). More recent work indicates that the mechanism for this relationship results in greater juvenile rockfish recruitment during years with more subarctic water mass conditions in the CCE, which correspond to cooler, fresher waters with higher dissolved oxygen (Schroeder et al., 2019).

While mesoscale processes may play a role in contributing to variability in recruitment, large-scale climatic processes are believed to affect variability, which may result in biological regime shifts related to changes in factors such as atmospheric and oceanic circulation, ocean temperature, and consequential changes in productivity and food availability (Chavez et al., 2003). These climate regime shifts may be due to a number of different influences including fluctuations in the Pacific Decadal Oscillation (PDO) and the 20th Century warming trend (Chavez et al., 2003; Field et al., in progress; Mantua et al., 1997). The PDO fluctuates between two phases, a positive phase and a negative phase (Mantua et al., 2002). During the positive phase the Aleutian Low-Pressure System intensifies, resulting in warmer than average sea surface temperature (SST) along the west coast of North America (and colder than average SST in the northeastern Pacific) and a decrease in coastal upwelling (Mantua et al., 2002). In contrast, the negative phase of PDO is due to a contraction of the Aleutian Low-Pressure System, which results in greater upwelling and cooler SST off the west coast of North America (and warmer than average SST in the 9northeastern Pacific; Mantua et al., 2002). The change in SST in the California Current associated with the fluctuations of the PDO may be related to changes in population

abundances, as well as the species assemblages of small pelagic forage fish. For example, Chavez et al. (2003) suggest that sardine prefer warmer SST and primarily dominate during the positive phase of the PDO, while anchovy are more abundant during the negative phase of the PDO when the northeast Pacific SST is cooler.

Sources of Fish Debris:

Many fish such as sardine, anchovy, hake, and most species of myctophid are caducous indicating that they naturally shed their scales (Field et al., 2009). It is likely that schooling forage fish populations contribute a rain of scales to the seafloor throughout their lifetimes. Additionally, it is hypothesized that fish also lose a large amount of scales from a predator strike, while also possibly serving as a predator defense tactic producing a flurry of scales which may induce visual confusion for the predator (O'Connell and Tunnicliffe, 2001). O'Connell and Tunnicliffe (2001) conducted an experiment quantifying the amount and type of Pacific herring scales shed to the floor of an aquarium. They added predators to the aquarium and found that herring lose approximately 100 times the scales in a predation avoidance event than natural shedding when schooling undisturbed. When consumed by a predator, herring scales were poorly preserved indicating an extensive breakdown in the gut, although the extent of breakdown is variable between types of scale and predator species (O'Connell and Tunnicliffe, 2001). O'Connell and Tunnicliffe (2001) concluded that natural shedding is the primary source of scales to the underlying sediments.

In contrast to scales, other fish debris such as bones, vertebrae, otoliths, and spines, are only deposited to the seafloor following predation and mortality events (O'Connell and

Tunnicliffe, 2001). When a fish is consumed, its skeletal debris may pass through the gut of the predator and then be deposited to the seafloor through fecal waste (O'Connell and Tunnicliffe, 2001). Studies found that bones could pass through the guts of some predators (i.e. black rockfish, hake, etc.) with varying degrees of degradation but not others (i.e. lingcod; O'Connell and Tunnicliffe, 2001; DeVries and Pearcy, 1982).

In some cases, the flux of fish debris will not accurately reflect fish abundances in the overlying water column due to outliers. On occasion, a predatory event may result in unconsumed pieces of a fish, causing a deposition of fish to the seafloor in a small region of the sediment. These pieces can range anywhere from a small piece to nearly an entire fish, with both scales and skeletal debris included in the chunk of fish (Field et al., 2009). Another potential source of outliers might come from small micro-accumulation zones where scales can accumulate by falling into small pits in the seafloor (Field, D.B., personal communication). Such outliers can be observed in sediment cores from the SBB where scales or bones show a high fish debris count in one sample surrounded by low fish debris counts within the same core (Field, D.B., personal communication). Additionally, O'Connell and Tunnicliffe (2001) observed an anomalously high peak in herring scales, that was an order of magnitude larger, in one sample that was not observed in their other four box cores. This high scale count denotes a clear outlier since the scale count is expected to be relatively consistent between cores at any particular time when the cores are taken from within close proximity to each other. If there are outliers present within the deposition rate time series, there is a false indication of sustaining larger fish populations in a given time period.

Industrial fisheries may also have an effect on the flux of fish scales and other skeletal debris such as bones, vertebrae, otoliths, and spines. It is possible that fishing operations would lead to an increased rate of scale shedding due to disturbances to the fish while being caught in large nets (Salvatteci et al., 2012). However, evidence based on the ratio of scales to skeletal debris from the cores off Peru does not explicitly support this trend. In addition, the fishery removes fish from the system, which eliminates the opportunity for forage fish to be eaten by predators so the skeletal debris will no longer pass through the guts of the predators or sink as a chunk of fish and be deposited into the sediments (Salvatteci et al., 2012).

Conditions Required to Preserve Fish Debris and Sediment Structure:

The SBB is composed of unique annually layered (varved) sediments due to low oxygen conditions and high sedimentation rates that result in a natural, high-resolution paleo record of pelagic fish populations (Soutar and Isaacs 1969; Baumgartner et al., 1992; Field et al., 2009). These varves facilitate the development of an accurate chronology that is needed to reconstruct a time series from the fish debris within the sediment record (Baumgartner et al., 1992). According to Field et al. (2009), three principal processes contribute to anoxia in the SBB, which has a maximum depth of approximately 630 m. First, the SBB has relatively less deep-water circulation due to a shallow sill found 475 m deep, which prevents the distribution of new, oxygen rich waters to the benthic environment. Second, the water that does enter the basin is old, intermediate water from the Pacific that is already depleted of oxygen due to biological respiration associated with deep-water circulation. Lastly, the SBB is located in an area of active upwelling, which leads to high primary productivity resulting in increased organic matter falling

to the seafloor. The relatively high export production allows bacteria to use the available oxygen to decompose organic matter, further reducing deep-water oxygen levels (Soutar 1967). Anoxic conditions reduce the presence of burrowing, benthic fauna that would otherwise bioturbate the lithologic layers (Soutar and Isaacs, 1974).

Soutar and Isaacs (1974) described the formation of the varves as a result of sediment deposition with different densities. Each year, a light and dark lamina pair form creating one annual varve. The dark layers have a higher density and contain more terrigenous debris that primarily represents detritus brought in from winter rains. The lighter, less dense varve layer contains more biological debris, such as diatoms, that accumulate from spring blooms (Soutar and Isaacs, 1974; Soutar and Crill, 1977). Most of the varve preservation from the last 2000 years is well preserved, however, there are still episodes of bioturbation and slumps that can cause homogenous layers and affect chronological development (Soutar and Isaacs, 1974; Baumgartner et al., 1992).

Coastal regions with all of these requirements are extremely rare, although some locations still have decent preservation of sediment structure and fish debris. For example, Effingham Inlet and Saanich Inlet have shallow sills which results in long residence time for the water and dysoxic conditions. However, the water entering the basin is not old and depleted of oxygen (Field et al., 2009; Tunnicliffe et al., 2001). Some regions off Peru are in active upwelling areas and have anoxic conditions due to the strong oxygen minimum zone, however the sedimentation rates vary regionally and the sediment layers are not necessarily annual (Field et al., 2009; Salvatteci et al., 2014). Thus, the SBB offers unique conditions that allows the preservation of varve patterns and provides the ability to construct a well-developed chronology.

Degradation and Preservation of Fish Debris:

Anoxic conditions not only preserve sediment varves, but also help minimize the degradation of fish debris (Salvatteci et al., 2012; Field et al., 2009). Fish scales are composed of 60-70% hydroxyapatite ($Ca_{10}(PO_4)_6(OH)_2$) crystals embedded in an organic matrix made of fibrous protein collagen (Field et al., 2009; Hutchinson and Trueman, 2006; Posner et al., 1984). The ocean is undersaturated in biogenous apatite, which may consequently result in dissolution of apatite in scales and bones in the water column and the top layer of the sediment (Atlas and Pytkowicz, 1977). In addition to the loss of apatite, bacterial degradation may also lead to a loss of organic matter in the fish scales (Field et al., 2009), which has been seen in a study where scanning electron microscope analysis showed that there were few holes in the external layers of scales while the internal collagen layers were full of channels and galleries due to bio-erosion by fungi, cyanobacteria, chlorophytes, and other micro-chemotrophs (Salvatteci et al., 2019; Wisshak et al., 2011). Some scales that have been bacterially degraded have fissures, vary in color, and/or become brittle and break when handled (Field et al., 2009).

Fish bones are rich in minerals such as calcium and phosphorous and are also composed of apatite (Hamada and Mikuni, 1990), therefore the skeletal debris is less subject to bacterial degradation. In addition, bones and vertebrae have a lower surface area to volume ratio suggesting that they have slower rates of dissolution (Salvatteci et al., 2012). Because skeletal debris undergoes less degradation than fish scales, Salvatteci et al. (2019) suggest that fish bones could be used as indicators of changes in fish abundance for longer sedimentation records containing glacial-interglacial periods that are associated with large changes in the oxygen

minimum zone. However, there are many other factors that must be taken into consideration when using skeletal debris as indicators of change in abundance, such as the different modes of loss and transport of fish debris to the seafloor, the predator type, predator abundance during a given period of time, and the difference in the relative number of scales to skeletal debris that is found in the sediment (Salvatteci et al., 2019).

In order to determine the relative role of degradation, Salvatteci et al. (2012) analyzed two box cores off the coast of Peru, at two different depths (201 m and 301 m), and documented signs of degradation based on fish scale integrity, which has not been observed in studies from the SBB. They found that the shallower core was exposed to more oxygenation events, which consequently led to greater degradation than in the deeper core. Salvatteci et al. (2012) also found differences in scale preservation between different temporal periods corresponding with a climatic shift (Gutiérrez et al., 2009). Gutiérrez et al. (2009) defined the shift as having higher productivity and lower water column oxygenation before the mid 19th century and lower productivity and higher water oxygenation after the sedimentary shift. Once again, Salvatteci et al. (2012) found that the period of high oxygenation and low productivity was associated with greater degradation of fish scales from within the cores. Salvatteci et al. (2012) found that the ratio of scales to bones and vertebrae could be a good indicator of degradation based on the theory that scales degrade faster than bones and vertebrae.

Fish debris may also go through a degradation process after the core has been taken (O'Connell and Tunnicliffe, 2001). O'Connell and Tunnicliffe (2001) took sediment core samples from the Ocean Drilling Program from Saanich Inlet, British Columbia and processed all of the samples within the 75 m core over the course of nineteen months. They found that the samples

that were processed later showed more scale degradation because the samples were stored in refrigerators where there was a potential for oxidation and bacterial growth. They also found a low ratio of scales to vertebrae downcore in the lower region of the core, which may suggest degradation of scales prior to coring, similar to the results found in Peru. However, Tunnicliffe et al. (2001) did note that bone dissolution was negligible. Another possible explanation of the low ratio of scales to vertebrae is a change in species assemblages. Different taxa lose scales at different rates and some predators may be more or less likely to digest skeletal debris so the assemblage of fish in the overlying water column may also play an important role in the ratio of scales to vertebrae and skeletal debris (O'Connell and Tunnicliffe, 2001).

The SBB shows little evidence of degradation of scales from the cores collected (Baumgartner et al., 1992; Field et al., 2009). Based on Baumgartner et al. (1992) analysis of sediment cores, the stratigraphic distribution of scales and clear tendencies toward increased scales downcore for both sardine and anchovy further indicates that degradation is most likely negligible. In addition, the anoxic sediment conditions found in the basin appear to have a relatively high pH (~8.0) resulting in the preservation of inorganic carbonates and apatites as well as minimizing the presence of aerobic bacteria (Soutar, 1967).

Using Fish Debris as Indicators of Changes in Fish Abundance:

One of the largest concerns with using fish debris flux from a sediment core to estimate population abundances is the uncertainty about how well a single core represents the variability in scale flux over an entire basin. To address this issue, Baumgartner et al. (1992) compared two time-series from sardine and anchovy scale deposition data from two piston cores (core 214 and

core 224) from the SBB. By comparing the two time-series, Baumgartner et al. (1992) were able to determine how well the scale deposition rates (SDR) characterized a "true" downcore signal that represented the abundance of fish in the overlying water column at any particular point in time. Baumgartner et al. (1992) first compared the linear correlations of sardine and anchovy between the two cores and found that correlations between cores 214 and 224 for sardine (R = 0.53) were similar to the between-core correlations of anchovy (R = 0.54), which indicates that the shared variability between cores for each species (R^2) is about 30%. This lack of between-core correlation for the two species may be largely due to the presence of outliers.

In order to further determine if there was a meaningful downcore signal that could be distinguished from the noise, or any signal that did not represent the abundance of fish in the overlying water column such as from an outlier, Baumgartner et al. (1992) performed a two-way analysis of variance (ANOVA) statistical analysis. They used an ANOVA to compare the ratio of downcore signal to the noise and the ratio of the between core effect to the noise for both the sardine and anchovy SDR time series for cores 214 and 224. For both sardine and anchovy SDR time series, the ANOVA clearly distinguished a meaningful difference between the downcore signal and the noise, showing that the downcore signal was three times greater than the noise for each species. Therefore, the downcore patterns can be reproduced in cores from different locations within the SBB. Similarly, the ANOVA was able to distinguish the between-core effect from the noise for the anchovy SDR, however, the sardine SDR time series did not show a significant difference between the intra core effect and the noise (Baumgartner et al., 1992). It is possible that the two cores contain a substantial amount of sardine outliers which could explain the difference between cores.

To determine the strength of the SDR signal as a proxy for estimating basin-wide fish abundances, O'Connell and Tunnicliffe (2001) compared multiple cores from the mid-inlet and near the basin's sill for herring and hake. The SDR time series shows a positive relationship in the downcore variations between most cores suggesting that large changes in SDR are replicated across the Saanich Inlet Basin. In addition, herring biomass estimates from 1939 to 1994 showed similar trends to the herring scale records (O'Connell and Tunnicliffe, 2001). These patterns indicate that the scale record is a reasonable proxy for changes in abundance in the recent record. Furthermore, Rose (2013) quantified fish scale and skeletal debris within six box cores from the SBB and found that high fish debris counts in one core was typically reflected in all of the other cores suggesting that the concentrations of fish debris are replicated across the SBB and are thus not highly affected by outliers. These three studies, however, did not perform a rigorous outlier analysis so it is likely that any between core comparisons that did not indicate a positive relationship is due to the presence of outliers. In the Humboldt current system, high resolution sediment core records from multiple locations reiterate the belief that the scale records taken form a single location reflect the primary downcore changes observed at multiple sites, however, the regional differences due to shifts in distribution and population dynamics are expected based on modern observations (Field et al., 2009; Salvatteci et al., 2018).

On rare occasions, the number of scales or skeletal debris may be abnormally high resulting in an outlier or noise, which may bias the data towards a high abundance of fish debris and not represent the fish density in the overlying water column for a given period of time. Many studies consider an interval an outlier when the scale or skeletal debris count is greater than two or three standard deviations from the mean (Rose, 2013; O'Connell and Tunnicliffe, 2001;

Salvatteci et al., 2012; Salvatteci et al., 2019). However, Kuwae et al. (2017) classified an abnormally high value as an outlier and removed it from the dataset but did not specify the criteria that defined an outlier. One study reported that less than one percent of all of the samples in their box core records were classified and treated as outliers (O'Connell and Tunnicliffe, 2001). When an outlier is corrected or removed from a fish debris flux time series, the data should show an improved downcore signal representing the fish abundance in the overlying water column.

Scales within Sediment Cores:

Time Scales of Variability:

Time series of SDR can be used to characterize populations of small pelagic forage fish prior to anthropogenic effects such as industrial fishing, however, different sampling techniques may alter the relative time series of variability. Baumgartner et al. (1992) created SDR time series of sardine and anchovy from 270 – 1970 AD using 10-year sampling intervals, however, they sampled at continuous one-centimeter intervals, which ranged from 4 – 20 years and they claim that sampling at a continuous interval only resulted in a slight loss of accuracy. In another study, McClatchie et al. (2017) continuously sampled at 0.5 cm intervals down the core, which should correspond to 2 – 4 years per sample assuming a sedimentation rate averaging 1.5 – 2 mm per year (Soutar and Crill, 1977; Biondi et al. 1977) and they claim to have an extremely high-resolution time series. However, studies such as those conducted by Rose (2013) and O'Connell and Tunnicliffe (2001) sampled at two-year varve intervals based on the varve structure and X-radiographs of the core to provide the finest chronological resolution. Because Baumgartner et

al. (1992) and McClatchie et al. (2017) did not follow the varve structure and X-radiograph template, the varves may not have the same uniform thickness or may not be perpendicular to the sampling procedure. So, sampling at one centimeter and 0.5 centimeter intervals, respectively, may result in sampling across varves, which would result in a coarser, less accurate resolution.

Baumgartner et al.'s (1992) time series are valuable for analyzing the variability throughout the last 1700 years, despite sampling at continuous intervals instead of following the varve structure. Since the 10-year resolution would not resolve the high frequency variability very efficiently, Baumgartner et al. (1992) only focused on multi-decadal scale variability of periods greater than 50 years. After the removal of centennial scale variability, Baumgartner et al. (1992) suggest there are high frequency peaks in sardine and anchovy SDR around 60 years, however, others argue that these multi-decadal scale peaks are a result from the oceanic integration of atmospheric white noise (Pierce, 2001) because periods of persistence occurred at longer and shorter timescales.

By using a calibration of fish scales to biomass to analyze periods of multi-decadal to centennial scale variability in sardine abundance based on SDR time series, Baumgartner et al. (1992) were able to create a record quantifying the major collapses and recoveries of the SBB sardine population. They defined a recovery as a population expansion from approximately one million metric tons or less increasing to four million metric tons or more, and vice versa for a collapse. Four million metric tons or greater was chosen as a threshold for recovery because that is the total biomass thought to be present in the mid-1930s during the peak of the California sardine fishery, however, Rose (2013) found that when looking at two-year sampling intervals,

sardine SDR is significantly lower after the 1930s than in the previous 200 years. In addition, McClatchie et al. (2017) used fish debris records to determine the collapse and recovery of sardine, anchovy, and hake populations, however, they did not account for potential outliers which may have affected their interpretations.

Sardine and anchovy fossilized fish scales are present in the Humboldt Current Ecosystem, off Peru, exhibiting non-alternating fluctuations (i.e. not out-of-phase) at centennial time scales (Gutierrez et al., 2009). In addition, the abundance of sardine, anchovy, hake, myctophids, and other epipelagic fishes exhibited large changes on multi-decadal to centennial timescales over the last 25 thousand years following shifts in the OMZ and productivity (Salvatteci et al., 2019). Records from the Humboldt Current Ecosystem over a 150-year period showed there were periods of high abundance for both sardine and anchovy as well as low abundance of both species, indicating that there are multiple time scales of variability and these two species do not show alternations in abundance (Salvatteci et al., 2018). In addition, these records consisted of an anchovy regime that lasted approximately 65 years and a sardine regime of approximately 20 years suggesting that sardine and anchovy persist over a wide range of timescales (Salvatteci et al., 2018).

Relationship with Climate and Industrial Fishing:

Based on catch records, it has been proposed that sardine dominate during a warm ocean regime associated with the positive phase of the PDO while anchovy are more abundant during the negative phase of the PDO which is associated with cooler SST in the CCE (Chavez et al., 2003). However, fossil fish records from the SBB suggest that there is no evidence of a correlation

between sardine and anchovy populations and the PDO throughout 20th century (Rose, 2013; McClatchie et al., 2010). Fossil fish scale evidence shows that sardine SDR decreases from around 1925 – 1945 even though this period is characterized by warmer SST during the positive phase of the PDO (Rose, 2013). Furthermore, McClatchie (2012) reconstructed a 370-year PDO record from six tree ring chronologies of mountain hemlock and compared it to a paleo sardine proxy to find that the abundance of sardine off California was not related to the PDO over long timescales, even though there was an apparent correlation over a 90-year record. SDR records from the Humboldt Current Ecosystem provide further evidence indicating that there is a weak relationship between anchovy and the PDO at multi-decadal timescales but not at a decadal scale suggesting that there is a nonlinear relationship (Salvatteci et al., 2018). However, Lindegren et al. (2013) developed a stock-recruitment model for sardine and anchovy in the California Current indicating that large scale climate forcing has the potential to generate long term variability, whereas density dependent processes may induce short term fluctuations in population abundance due to differences in life history traits between the two species.

The 20th century contains a warming trend superimposed on decadal scale variations. SST warming appears to have begun around the early 1930s based on a change in plankton assemblages, shifting towards more subtropical/warmer species and again in the 1970s (Field et al., in progress; Field et al., 2006). Based on fossil fish scale records, sardine, anchovy, and hake show a significant difference in the period before and after the 1930s-warming shift for mean SDR, while there was not a large difference in myctophid mean SDR (Figure 1.4; Rose, 2013). The change in mean SDR before and after the early 1930s suggests that sardine, anchovy, and hake populations all started to decline after this warming trend.

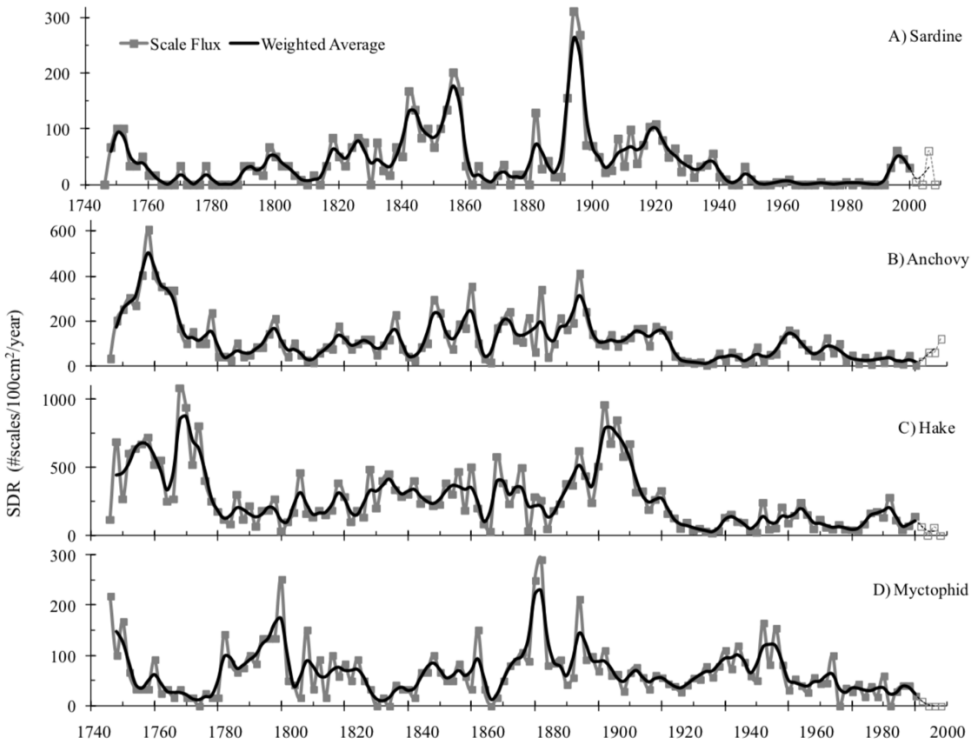

Figure 1.4. Time series of scale deposition rate and three-term weighted average for A) sardine, B) anchovy, C) hake, and D) myctophids. The fluxes are based on two-year sampling intervals from a composite of multiple cores. The flux at the end of the record, in the 21st century, was generated from one core and is indicated using a dashed line and open symbols (Rose, 2013).

The second period of the 20th century warming trend occurred around the mid-1970s and there were significant differences in mean SDR pre and post 1976 for all four of the major SBB forage fish *(sardine, anchovy, hake, and myctophids/mesopelagics)* (Rose, 2013). Myctophid mean SDR showed a greater difference in the 1970s warming shift than the 1930s shift, while sardine, anchovy, and hake mean SDR did not show a drastic decline after 1976 since these populations were already low. Sardine SDR was nearly absent for the majority of the second half of the 20th century, however, the decline persisted after the 1970s warming shift until about 1992 (Figure 1.4; Rose, 2013). Myctophid SDR begins a substantial decline around the early 1970s and continues to decline into the early 21st century (Figure 1.4; Rose, 2013). Since the main forage

fish were affected differently by the two major warming trends of the 20th century, it may suggest that climatic influences have different impacts on different species. Another issue is the lack of a long temporal record. This study was conducted based on ~250-year box core records which may not have the longevity to account for changes in abundance due to centennial scale natural variability.

Alternatively, the reduction in scale flux during the 20th century warming trend may be due to species shifting their distribution north out of the SBB, which has been observed during warmer years, although this could be more likely for the migratory sardine and hake than for anchovy (Field et al., in progress). In addition, scale flux may not be linearly related to adult biomass due to different life history stages between juveniles and adults of different species (Lasker and MacCall, 1982). For example, the SBB is near the center of preferred adult anchovy habitat so the variability of anchovy SDR is expected to be reduced compared to the more migratory sardine and hake, which encompass a greater distribution (Lasker and MacCall, 1982). Additionally, myctophids are restricted to a limited geographic range and do not horizontally migrate so myctophid SDR is also expected to have low variability compared to the more migratory species.

Another potential cause of variability in SBB forage fish abundance is the onset of commercial fisheries. Soutar and Isaacs (1974) were the first to propose that the collapse of the 1940s California sardine fishery was due to natural variability and not overfishing. Furthermore, Baumgartner et al. (1992) found that the recovery from the 1940s sardine crash was not unlike those of the past, although the record did not span to the end of the 20th century. Rose (2013) followed up on this issue by looking at mean SDR before and after the industrial fishery was

considered fully developed (1934 for sardine, 1967 for anchovy, and 1984 for hake). Each of the taxa showed a significant difference in mean SDR before and after the fishery was developed, however the ratio of scales to skeletal debris did not indicate that the decline corresponded to the onset of industrial fishing (Rose, 2013).

Skeletal Debris within Sediment Cores:

The use of fossilized fish skeletal debris, a fairly new concept in the SBB, is used to understand changes in fish populations response to natural and anthropogenic variability. The fossil fish debris record from the SBB consists of otoliths, vertebrae, jaw bones, spines, and other unidentified bones which are assumed to primarily come from sardine, anchovy, hake, and myctophids (Rose, 2013), however, species identification based on known morphological traits is not yet possible. Skeletal debris must pass through the guts of a predator before it can be deposited to the seafloor, therefore, the skeletal debris record is a function of availability to predators, reflecting prey consumption (Rose, 2013; Salvatteci et al., 2012).

There is the potential for different types of skeletal debris to be deposited to the seafloor in various different ways by many different taxa of forage fish. There was typically low shared downcore variability between most types of the skeletal debris and the scales deposited to the sediments for sardine, anchovy, and hake (Rose, 2013) suggesting that high/low abundances of one of these species does not directly result in a high/low amount of skeletal debris. However, myctophids shared the highest downcore variability between scale flux and skeletal debris (R^2 = 0.24) suggesting that myctophids are the primary contributors of skeletal debris to the seafloor (Rose, 2013; Field et al., in progress). Anchovy SDR shared only 5% of the downcore variability

with total skeletal flux, however, anchovy SDR shared nearly half of the downcore variability with the flux of spines suggesting that anchovy may be the primary source of spines to the skeletal debris record. Another study from the Humboldt Current Ecosystem found similar results indicating that spines were the most common bone debris found within the record consisting of over 13% of the total skeletal debris (Salvatteci et al., 2019). Since the Humboldt Current Ecosystem is dominated primarily by anchovy, it makes sense that spines were found disproportionately more than other types of skeletal debris.

There were times in the last ~250 years when myctophid scale flux was low but total skeletal debris flux was still high, suggesting that there are times when the skeletal debris may be primarily coming from species other than myctophids (cc. Figure 1.5 with Figure 1.4D; Rose, 2013). Jones (2013) found that many other species such as rockfish, mackerel, and saury also contribute to the sagittal otolith deposition from the SBB. In addition, some species such as skate, dogfish, and sharks are not represented in the fossils fish debris record because their dermal scutes and cartilaginous bones do not preserve over time (O'Connell and Tunnicliffe, 2001).

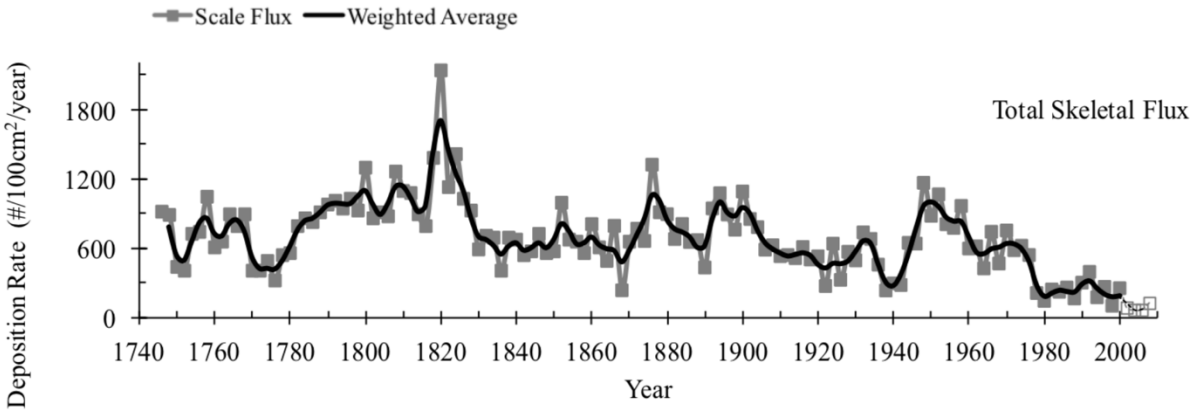

Figure 1.5. Time series of total skeletal debris flux and the three-term weighted average. The fluxes are based on two-year sampling intervals from a composite of multiple cores. The flux at the end of the record, in the 21st century, was generated from a single core and is indicated using a dashed line and open symbols (Rose, 2013).

Many factors may also play into the deposition of skeletal debris to the seafloor. Since skeletal debris often passes through the gut of a predator in order to be deposited to the sediment, the type of predator and digestion rate may play an important role in the composition of fish debris found within the sediments. Predators such as lingcod may be able to digest bones and vertebrae (O'Connell and Tunnicliffe, 2001), which would decrease the skeletal debris within the sediments even though the consumption rate and availability of prey to upper trophic level predators does not change. Furthermore, some predators, such as marine birds and large mysticetes, may consume forage fish as prey and then deposit the remains elsewhere. Because myctophids generally live in the mesopelagic, their predators may be different than those of sardine and anchovy, and may be less likely to digest skeletal debris resulting in greater quantities of skeletal debris being deposited to the seafloor.

Scales and skeletal debris arrive to the seafloor in different fashions, therefore, the ratio of scale to skeletal debris flux can be used to illustrate changes in consumption by upper trophic level predators due to fishing activities (Salvatteci et al., 2012). Salvatteci et al. (2012) used fish debris records from the Humboldt Current Ecosystem to detect an effect of the fishery on fish scales and skeletal debris deposition. They found that the flux of skeletal debris declined due to direct removal, thus increasing the ratio of scales to skeletal debris, during the periods of industrial fishing. Because fishing directly removes small forage fish from the ecosystem, it consequently reduces the availability of prey to upper trophic level predators.

Rose (2013) conducted a similar study from sediments from the SBB and determined that there are several reasons why the primary cause of the decline in small pelagic forage fish is not

industrial fishing. The ratios of scales to skeletal debris during the 20th century are much lower than would be expected if fishing was taking small pelagics out of the system, preventing consumption by their predators (Rose, 2013). Furthermore, if myctophids are the primary contributors to skeletal debris flux and myctophids are not commercially fished, a decrease in skeletal flux would not be expected to be as large as in the sediments from the Humboldt Current Ecosystem (Rose, 2013). The CCE is more diverse than the Humboldt Current Ecosystem in terms of small pelagic forage fish so the removal of forage fish from the CCE had a less dramatic effect on predator consumption because the higher trophic level predators were able to feed on various different prey items (Rose, 2013).

There is considerable variability within the skeletal debris flux record over the last ~250 years, however, there are some key hiatuses that stand out providing further evidence for a decrease in small pelagic forage fish abundances in the SBB due to the 20th century warming event. There was an anomalously low flux of vertebrae occurring in the late 1930s which coincided with the first period of the 20th century warming event and the first decline in scale flux for sardine, anchovy, and hake (Figure 1.5; Rose, 2013). In addition, there was a sharp decline in total skeletal flux that occurred after the 1970s which coincided with the decrease in total scale flux as well as the second major period of the 20th century warming event. This warming event is characterized by a shift towards a more southern/warmer species assemblage (Rose, 2013) providing further evidence that the decline of small pelagic forage fish is largely driven by large scale warming events. Although the evidence by Rose (2013) clearly suggested that the decline in small pelagics is due to the 20th century warming trend, the short, 250-year time scale does

not provide the long-term resolution to determine if the decline in abundance is due to large scale natural variability.

References:

Agostini, V.N., Francis, R.C., Hollowed, A.B., Pierce, S.D., Wilson, C. and Hendrix, A.N., 2006. The relationship between Pacific hake (Merluccius productus) distribution and poleward subsurface flow in the California Current System. Canadian Journal of Fisheries and Aquatic Sciences. 63(12), 2648-2659.

Alverson, D., & Larkins, H. (1969). Status of Knowledge of The Pacific Hake Resource. California Cooperative Oceanic Fisheries Investigations. 13, 24-31.

Atlas, E., and R. M. Pytkowicz. (1977). Solubility behavior of apatites in seawater. Limnology and Oceanography. 22, 290–300.

Bakun, A. (2006). Wasp-waist populations and marine ecosystem dynamics: Navigating the ‘‘predator pit’’ topographies. Progress in Oceanography. 68, 271-288.

Baumgartner, T. R., Soutar, A., & Ferreira-Bartrina, V. (1992). Reconstruction of the history of pacific sardine and northern anchovy populations over the past two millennia from sediments of the Santa Barbara Basin, California. CalCOFl Rep. 33, 24-40.

Berger, A.M., A.M. Edwards, C.J. Grandin, and K.F. Johnson. (2019). Status of the Pacific Hake (whiting) stock in U.S. and Canadian waters in 2019. Prepared by the Joint Technical Committee of the U.S. and Canada Pacific Hake/Whiting Agreement, National Marine Fisheries Service and Fisheries and Oceans Canada. 249.

Bertrand, A., Chaigneau, A., Peraltilla, S., Ledesma, J., Graco, M., Monetti, F., Chavez, F. (2011). Oxygen: A Fundamental Property Regulating Pelagic Ecosystem Structure in the Coastal Southeastern Tropical Pacific. PLoS ONE, 6, e29558.

Biondi, F., Lange, C., Hughes, M., Berger, W. (1997). Interdecadal signals during the last millennium (AD 1117-1992) in the varve record of Santa Barbara Basin, California. Geophysical Research Letters. 24(2), 193-196.

Brodeur, R., Buchanan, J., & Emmett, R. (2014). Pelagic and demersal fish predators on juvenile and adult forage fishes in the northern California current: spatial and temporal variation. California Cooperative Oceanic Fisheries Investigations Report. 55, 96-116.

California Department of Fish and Wildlife. (2014). Review of selected California fisheries for 2013: Coastal pelagic finfish, market squid, groundfish, highly migratory species, dungeness crab, basses, surfperch, abalone, kelp and edible algae, and marine aquaculture. California Cooperative Oceanic Fisheries Investigations Report, 55, 11-50.

Chavez, F. P., Ryan, J., Lluch-Cota, S., & Niquen C., M. (2003). From Anchovies to Sardines and Back: Multidecadal Change in the Pacific Ocean. Science. 299(5604), 217-221.

Checkley, D. M., Dotson, R. C., & Griffith, D. A. (2000). Continuous, underway sampling of eggs of Pacific sardine (Sardinops sagax) and northern anchovy (Engraulis mordax) in spring 1996 and 1997 off southern and central California. Deep Sea Research Part II: Topical Studies in Oceanography, 47(5-6), 1139-1155.

Checkley, D., Ayon, P., Baumgartner, T., Bernal, M., Coetzee, J., Emmett, R., Guevara-Carrasco, R., Hutchings, L., Ibaibarriaga, L., Nakata, H., Oozeki, Y., Planque, B., Schweigert, J., Stratoudakis, Y., van der Lingen, C. (2009). Habitats. In D. Checkley, J. Alheit, Y. Oozeki, C. Roy (Eds.), Climate Change and Small Pelagic Fish (pp. 12-44): Cambridge University Press.

Checkley, D. M., Jr., Asch, R. G., & Rykaczewski, R. R. (2017). Climate, Anchovy, and Sardine. Annual Review of Marine Science. 9, 469-493.

Cury, P., Bakun, A., Crawford, R., Jarrid, A., Quinones, R., Shannon, L., & Verheye, H. (2000). Small pelagics in upwelling systems: patterns of interaction and structural changes in ‘‘wasp-waist’’ ecosystems. ICES Journal of Marine Science, 57, 603-618.

Davison, P., Lara-Lopez, A., & Koslow, J. A. (2015). Mesopelagic fish biomass in the southern California Current Ecosystem. Deep Sea Research Part II: Topical Studies in Oceanography, 112, 129-142.

Demer, D.A., Zwolinski, J.P., Byers, K.A., Cutter, G.R., Renfree, J.S., Sessions, T.S. and Macewicz, B.J. (2012). Prediction and confirmation of seasonal migration of Pacific sardine (Sardinops sagax) in the California Current Ecosystem. Fishery Bulletin. 110(1), 52-70.

DeVries, T.J., Pearcy, W.G. (1982). Fish debris in sediments of the upwelling zone off central Peru: a late Quaternary record. Deep-Sea Research. 28, 87–109.

Dorn, M.W., 1995. The effects of age composition and oceanographic conditions on the annual migration of Pacific whiting, Merluccius productus. California Cooperative Oceanic Fisheries Investigations Report, pp.97-105.

Espinoza, P., Bertrand, A. (2008). Revisiting Peruvian anchovy (Engraulis ringens) trophodynamics provides a new vision of the Humboldt Current system. Progress in Oceanography, 79, 215-227.

Espinoza, P., Bertrand, A., van der Lingen, C.D., Garrido, S., Rojas de Mendiola, B. (2009). Diet of sardine (Sardinops sagax) in the northern Humboldt Current system and comparison with the diets of clupeoids in this and other eastern boundary upwelling systems. Progress in Oceanography, 83, 242-250.

Field, D. B., Baumgartner, T. R., Charles, C. D., Ferreira-Bartrina, V., & Ohman, M. D. (2006). Planktonic Foraminifera of the California Current Reflect 20th Century Warming. Science. 311, 63-66.

Field, D. B., Baumgartner, T. R., Ferreira, V., Gutierrez, D., Lozano-Montes, H., Salvatteci, R., & Soutar, A. (2009). Variability from scales in marine sediments and other historical records. Climate Change and Small Pelagic Fish. 45-63.

Field, D., Barron, J., Bringue, M., Burky, D., De Bernardi, B., Ferriera-Batrina, V., . . . Baumgartner, T. (in progress). A Sliding Ecosystem Baseline in the California Current from Early 20th Century Warming. Unpublished Manuscript.

Gutiérrez, D., Sifeddine, A., Field, D. B., Ortlieb, L., Vargas, G., Chávez, F., . . . Baumgartner, T. (2009). Rapid reorganization in ocean biogeochemistry off Peru towards the end of the Little Ice Age. Biogeosciences. 6, 835-848.

Hamada, M., & Mikuni, A. (1990). X-ray diffraction analysis of sardine scale ash. Nippon Suisan Gakkaishi. 56(6), 947-951.

Hart, J.L. (1973). Pacific fishes of Canada. Bull. Fish. Res. Board Can. 180, 740.

Hill, K., Dorval, E., Lo, N., Macewicz, B., Show, C., Relix-Uraga, R. (2008). Assessment of the Pacific sardine resource in 2008 for USA management in 2009. Pacific Fishery Management Council, November 2008 Agenda Item G.2.b. 236.

Hutchinson, J. J., & Trueman, C. N. (2006). Stable isotope analyses of collagen in fish scales: limitations set by scale architecture. Journal of Fish Biology. 69(6), 1874-1880.

Jones, W. (2016) The Santa Barbara Basin Fish Assemblage in the Last Two Millennia Inferred from Otoliths in Sediment Cores. Ph.D. Thesis. University of California San Diego. 1-125.

Koehn, L., Essington, T., Marshall, K., Kaplan, I., Sydeman, W., Szoboszlai, A., Thayer, J. (2016). Developing a high taxonomic resolution food web model to assess the functional role of forage fish in the California Current ecosystem. Ecological Modelling. 335, 87-100.

Koslow, J., Goericke, R., McClatchie, S., Vetter, R., & Rogers-Bennett, L. (2010). The California Cooperative Oceanic Fisheries Investigations (CalCOFI): The Continuing Evolution and Contributions of a 60-Year Ocean Observation Program. California Cooperative Oceanic Fisheries Investigations Report.

Koslow, J. A., Davison, P., Lara-Lopez, A., & Ohman, M. D. (2014). Epipelagic and mesopelagic fishes in the southern California Current System: Ecological interactions and oceanographic influences on their abundance. Journal of Marine Systems, 138, 20-28.

Koslow, J., Miller, E., & McGowan, J. (2015). Dramatic declines in coastal and oceanic fish communities off California. Marine Ecology Progress Series, 538, 221-227.

Koslow, J. A., & Davison, P. C. (2016). Productivity and biomass of fishes in the California Current Large Marine Ecosystem: Comparison of fishery-dependent and - independent time series. Environmental Development, 17, 23-32.

Kuwae, M., Yamamoto, M., Sagawa, T., Ikehara, K., Irino, T., Takemura, K., . . . Sugimoto, T. (2017). Multidecadal, centennial, and millennial variability in sardine and anchovy abundances in the western North Pacific and climate–fish linkages during the late Holocene. Progress in Oceanography, 159, 86-98.

Lasker, R., and A. MacCall. (1982). New ideas on the fluctuations of clupeoid stocks off California, In Proceedings of the Joint Oceanographic Assembly 1982-general symposia. Canadian National Committee/Scientific Committee on Oceanic Research. 110-120.

Lindegren, M., Checkley, D.M. Jr., Rouyer, T., MacCall, A.D., Stenseth NC. (2013). Climate, fishing, and fluctuations of sardine and anchovy in the California Current. PNAS. 110, 13672–77.

Livingston, P. A., and K. M. Bailey. "Trophic role of the Pacific whiting, Merluccius productus." Mar. Fish. Rev 47, no. 2 (1985): 16-22.

Lluch-Belda, D., Crawford, R. J., Kawasaki, T., Maccall, A. D., Parrish, R. H., Schwartzlose, R. A., & Smith, P. E. (1989). World-wide fluctuations of sardine and anchovy stocks: the regime problem. South African Journal of Marine Science, 8(1), 195-205.

MacCall, A. D. 1979. Population estimates for the waning years of the Pacific sardine fishery. CalCOFI Rep. 20: 72-82.

MacCall, A. (1990). Dynamic geography of marine fish populations: books in recruitment fishery oceanography. University of Washington Press, Washington.

Mantua, N., & Hare, S. (2002). The Pacific Decadal Oscillation. Journal of Oceanography. 58, 35-44.

Mantua, N. J., Hare, S. R., Zhang, Y., Wallace, J. M., & Francis, R. C. (1997). A Pacific Interdecadal Climate Oscillation with Impacts on Salmon Production. Bulletin of the American Meteorological Society. 78(6), 1069-1079.

McClatchie, S., Goericke, R., Auad, G., & Hill, K. (2010) Re-assessment of the stock-recruit and temperature-recruit relationships for Pacific sardine (Sardinops sagax). Canadian Journal of Fisheries and Aquatic Sciences. 76, 1782-1790.

McClatchie, S. (2012). Sardine biomass is poorly correlated with the Pacific Decadal Oscillation off California. Geophysical Research Letters. 39, 1-6.

McClatchie, S., Field, J., Thompson, A. R., Gerrodette, T., Lowry, M., Fiedler, P. C., . . . Vetter, R. D. (2016). Correction to 'Food limitation of sea lion pups and the decline of forage off central and southern California'. Royal Society Open Science. 3(4), 1-9.

McClatchie, S., Hendy, I. L., Thompson, A. R., & Watson, W. (2017). Collapse and recovery of forage fish populations prior to commercial exploitation. Geophysical Research Letters. 44, 1-9.

Nishimoto, M., & Washburn, L. (2002). Patterns of coastal eddy circulation and abundance of pelagic juvenile fish in the Santa Barbara Channel, California, USA. Marine Ecology Progress Series. 241, 183-199.

O'Connell, J., & Tunnicliffe, V. (2001). The use of sedimentary fish remains for interpretation of long-term fish population fluctuations. Marine Geology. 174(1-4), 177-195.

Pierce D. W. (2001). Distinguishing coupled ocean-atmosphere interactions from background noise in the North Pacific. Progress in Oceanography, 49, 331–352.

Pikitch, E., Rountos, K., Essington, T., Santora, C., Pauly, D., Watson, R., . . . Munch, S. (2012). The global contribution of forage fish to marine fisheries and ecosystems. Fish and Fisheries, 1-22.

Phillips, A., Ralston, S., Brodeur, R., Auth, T., Emmett, R., Johnson, C., & Wespestad, V. (2007). Recent pre-recruit Pacific hake (Merluccius productus) occurrences in the northern California Current suggest a northward expansion of their spawning area. California Cooperative Oceanic Fisheries Investigations Report, 48, 215-229.

Posner, A. S., Blumenthal, N. C., & Betts, F. (1984). Chemistry and Structure of Precipitated Hydroxyapatites. Photosphate Minerals. 330-350.

Radovich, J. (1982). The collapse of the California sardine fishery: What have we learned. CalCOFI Reports. 23, 56-78.

Ralston, S., Sakuma, K., & Field, J. (2013). Interannual varaition in pelagic juvenile rockfish (Sebastes spp.) abundance – going with the flow. Fisheries Oceanography, 22(4), 288-308.

Rose, K. (2013). Fish Scales and Skeletal Debris as Indicators of Changes in Small Pelagic Fishes in the Santa Barbara Basin: Fishing or Natural Variability? Masters Thesis. Hawaii Pacific University. 1-181.

Salvatteci, R., Field, D. B., Baumgartner, T., Ferreira, V., & Gutierrez, D. (2012). Evaluating fish scale preservation in sediment records from the oxygen minimum zone off Peru. Paleobiology. 38(1), 52-78.

Salvatteci, R., Field, D., Sifeddine, A., Ortlieb, L., Ferreira, V., Baumgartner, T., Caquineau, S., Velazco, F., Reyss, J.L., Sanchez-Cabeza, J.A., Gutierrez, D. (2014). Cross-stratigraphies from a seismically active mud lens off Peru indicate horizontal extensions of laminae, missing sequences, and a need for multiple cores for high resolution records. Marine Geology, 357, 72-89.

Salvatteci, R., Field, D., Gutiérrez, D., Baumgartner, T., Ferreira, V., Ortlieb, L., . . . Bertrand, A. (2018). Multifarious anchovy and sardine regimes in the Humboldt Current System during the last 150 years. Global Change Biology.

Salvatteci, R., Gutierrez, D., Field, D., Sifeddine, A., Ortlieb, L., Baumgartner, T., Ferreira, V., & Bertrand, A. (2019). Multidecadal to millennial scale variability in fish populations during the last 25 kyr in the Humboldt Current Ecosystem. Biogeociences.

Schroeder, I., Santora, J., Bograd, S., Hazen, E., Sakuma, K., Moore, A., Edwards, C., Wells, B., & Field, J. (2019). Source water variability as a driver of rockfish recruitment in the California Current Ecosystem: implications for climate change and fisheries management. Canadian Journal of Fisheries and Aquatic Sciences.

Smith, A., Brown, C., Bulman, C., Fulton, E., Johnson, P., Kaplan, I., . . . Tam, J. (2011). Impacts of Fishing Low–Trophic Level Species on Marine Ecosystems. Science, 333, 1147-1150.

Soutar, A. (1967). The accumulation of fish debris in certain California coastal sediments. California Cooperative Oceanic Fisheries Investigations. 11, 136-139.

Soutar, A., & Isaacs, J. D. (1969). History of Fish Populations Inferred from Fish Scales in Anaerobic Sediments off California. California Cooperative Oceanic Fisheries Investigations. 13, 63-70.

Soutar, A., & Isaacs, J. (1974). Abundance of pelagic fish during the 19th and 20th centuries as recorded in anaerobic sediment off the Californias. Fishery Bulletin. 72(2), 257-273.

Soutar, A., & Crill, P. (1977). Sedimentation and climatic patterns in the Santa Barbara Basin during the 19th and 20th centuries. GSA Bulletin. 88(8), 1161–1172.

Szoboszlai, A.I., Thayer, J.A., Wood, S.A., Sydeman, W.J. and Koehn, L.E. (2015). Forage species in predator diets: synthesis of data from the California Current. Ecological Informatics, 29, pp.45-56Takasuka, A., Oozeki, Y., Kubota, H., & Lluch-Cota, S. E. (2008). Contrasting spawning temperature optima: Why are anchovy and sardine regime shifts synchronous across the North Pacific? Progress in Oceanography, 77(2-3), 225-232.

Tunnicliffe, V., O'Connell, J., & Mcquoid, M. (2001). A Holocene record of marine fish remains from the Northeastern Pacific. Marine Geology. 174(1-4), 197-2.

CHAPTER 2: Comparison of Sediment Cores and Variations in Small Pelagic Forage Fish Amidst Recent Ocean Warming

Abstract

Evidence from both fossil fish scale records and surveys of fish abundance suggest that small pelagic forage fish abundances in the California Current Ecosystem (CCE) have been declining since the late 20th century, however, the low values in the 1900s have never been put into the context of long-term records. This study compiled scale fluxes from sardine, anchovy, hake, and myctophid as well as a novel record of skeletal debris from three kasten sediment cores as well as numerous box core records from the Santa Barbara Basin (SBB) to develop a Paleo Forage Fish Index. The Paleo Forage Fish Index, which is a normalized compilation of the five time series, revealed periods of extended negative anomalies beginning around the 1930s and from the 1960s to the end of the record following a shift in plankton assemblages toward subtropical taxa, which suggests that the 20th century warming trend influences the abundance, distribution, and/or species assemblage of small pelagic forage fish in the CCE. In addition, this study developed a rigorous outlier detection procedure and determined that up to 30% of the sampling intervals contain identified outliers, although the presence of outliers do not have a major effect on the overall nature of the records. Comparison between cores shows significant differences between kasten cores and between composite core records, which emphasizes the need for a multi-core, composite record to average out decadal to interdecadal scale differences between cores. Furthermore, the skeletal debris record was determined to be a compilation of multiple species with vertebrae primarily coming from fish between two and eight centimeters in length.

2.1 Introduction

In the early 20th century, the peak of the California sardine fishery coincided with the dramatic decline in sardine abundance, which started the debate as to whether the decline was attributed to natural variability or overexploitation from commercial fishing. The California Cooperative Oceanic and Fisheries Investigations program (CalCOFI) was created to determine the cause of the sardine crash and has been monitoring the California Current Ecosystem (CCE) for over 70 years. However, it was Soutar and Isaacs' (1967; 1969) groundbreaking work using fish debris records that found that sardine populations are subject to natural variability throughout the last ~2,000 years. Nonetheless, evidence from both fossil fish scale records and surveys of fish abundance suggest that small pelagic forage fish abundances in the CCE have been declining since the late 20th century (Rose, 2013; Koslow and Davison, 2016; Field et al., in progress), which may point towards a response to climate change and increasing ocean temperatures.

Small pelagic fish are highly variable and play a large ecological role within the coastal food web. A decline in the total biomass of this mid trophic level has the ability to cascade up to higher trophic levels. For example, the unusual increase in California sea lion strandings in Santa Barbara, California was attributed to the reduced availability of prey with high fat and oil content, such as sardine and anchovy, even though market squid and rockfish were relatively abundant at the time (McClatchie et al., 2016). In addition, vertically migrating myctophids are an integral part of the trophic dynamic providing a link between surface production and the deep sea (Davison et al., 2015; Koslow et al., 2010).

A ~250-year fish debris record shows that a decline in forage fish beginning in the mid-1930s may be due to the long-term warming trend (Rose, 2013). Although, this decline has not been put into the context of long-term records that may suggest that the recent decline is affected by natural variability or some anthropogenic cause such as fishing. While there is some evidence that the warming trend has been impacting total fish abundance, it is very clear that the 20th century warming has been modifying species composition of plankton and fish in the CCE (Field et al., 2006; Koslow et al., 2015). For example, some evidence suggests declines or shifts in distributions of many small forage fish populations that have cool-water, more northerly affinities, such as northern anchovy and Pacific hake (Koslow et al., 2015). However, some species with warm water affinities, such as jack smelt, Pacific mackerel, and jack mackerel, actually increased in abundance in the Southern California Bight (SCB) based on time series from the 1950s or more recent (Moser et al., 2001; Koslow and Davison, 2016; Davison et al., 2015). Temperate, cool water fish typically have greater population biomass, associated with higher levels of productivity, than subtropical fish species so a shift in species composition has the potential to alter the relative biomass in the region. The decline in some of the most abundant cool-water forage fish species may be due to the effects of the 20th century warming trend, but natural variability, due to the boom and bust life history of these fish, compounded by anthropogenic influences such as direct fishing and altering of the food web structure, confound our ability to establish causality.

Records of sardine, anchovy, and hake scales show consistent negative anomalies below the pre-20th century historic baseline beginning around 1925 (Field et al., in progress) and further decline after the mid-1970s (Rose, 2013; Field et al., in progress). However, myctophid scale flux

fluctuates throughout the 19th and 20th century without a clear long-term trend, but with consistently low scale flux after the mid-1960s (Rose, 2013). A skeletal debris record, developed from sediment cores, indicates that the lowest fluxes of total skeletal debris in the last ~250 years occur after the 1970s (Rose, 2013), however it is unclear if the skeletal debris record reflects a composite from multiple fish species or is dominated by a single taxon.

Fish debris (i.e. scales v. skeletal debris) arrives to the sediment in different fashions. Scales are shed throughout a fish's lifetime (Field et al., 2009), whereas skeletal debris primarily reaches the seafloor after a predation event. Because bones and vertebrae arrive to the seafloor after a mortality event, much of the skeletal debris likely passes through the guts of a predator, reflecting prey consumption and thus is a function of availability to predators (Rose 2013, Salvatteci et al., 2012). Although, skeletal debris may also be deposited as a chunk of fish sinking to the seafloor as a result of sloppy feeding.

A major issue causing uncertainty in fish debris records is the role of outliers for both scales and skeletal debris. In some cases, a fish may die and its carcass, or a portion of its carcass, may be directly deposited to the seafloor. Additionally, the nature of the bathymetry may affect fish debris settling on the seafloor and could cause debris to collect in micro-accumulation zones creating an anomalous spike in fish debris within a small interval of the sediment core thus generating an outlier. Prior to this study, it was unclear how much these outliers contribute to downcore variability and the total flux throughout multiple cores. Although several studies have identified and removed outliers (O'Connell and Tunnicliffe, 2001; Salvatteci et al. 2012; Rose, 2013), the issues regarding the frequency of outliers from a piece of fish and/or micro-accumulation zones have yet to be carefully addressed or resolved. The nature of the data in the

present study lends itself to the first rigorous outlier analysis because the sediment core is cut into six vertical slabs, allowing outliers to be detected as anomalous fish debris counts among different samples of the same sampling interval.

This study develops a ~2000-year composite time series and a Paleo Forage Fish Index from three kasten cores from the Santa Barbara Basin (SBB). The time series include scales of sardine, anchovy, and hake, which were previously studied from various cores taken within the SBB (Soutar, 1967; Soutar and Isaacs, 1974; Baumgartner et al., 1992; McClatchie et al., 2017), as well as a novel scale record of myctophid and a new skeletal debris index. Together, these are used to address the recent low values of pelagic forage fish scales and skeletal debris over the past ~2000 years, which could ideally be used to inform scientists, managers, policy makers, and the public on the relative roles of the current warming trend, commercial fishing, and natural variability on small pelagic forage fish populations. In addition, the examination of fish debris counts of different slabs within the same core as well as from different cores will allow for identification and quantification of the likelihood of outliers and how outliers affect downcore and between core records.

2.2. Materials and Methodological Approach

2.2.1 Processing and Sampling Sediment Cores

The current study analyzes data from three kasten sediment cores (SBKC 9110-1301, SBKC 9110-1302, and SBKC 9210-1001; SBKC: Santa Barbara Kasten Core) taken by T. Baumgartner, V. Ferreria-Bartrina, W. Riedel, and A. Soutar, with support from California Sea Grant (Baumgartner

et al., 1996). The sediment cores were taken from the SBB from approximately 590 m depth on October 13, 1991 (for cores SBKC 1301 and SBKC 1302) and October 10, 1992 (for SBKC 1001; Figure 2.1; Table 2.1). After a core is taken, it is sectioned into different blocks. Then, each block is left alone for the water to drain, which causes the top of the core to shrink relative to the bottom of the core.

Subsampling of the section was done much later. Due to the shrinkage, a trim slab was removed from each block when it was subsampled. Each sediment sample had approximate dimensions of 305 x 14 x 14.3 cm (Baumgartner et al., 1996), however some sampling intervals include the trim slab which was accounted for in the area calculation. Once the core was drained and sectioned, the sediment core was subsampled into six vertical slabs (Figure A1). Two slabs cut one cm thick were X-radiographed and the varves were used for chronological construction. The other four slabs were cut 2.5 cm thick for subsampling. The core was then photographed and cut into lengthwise sections.

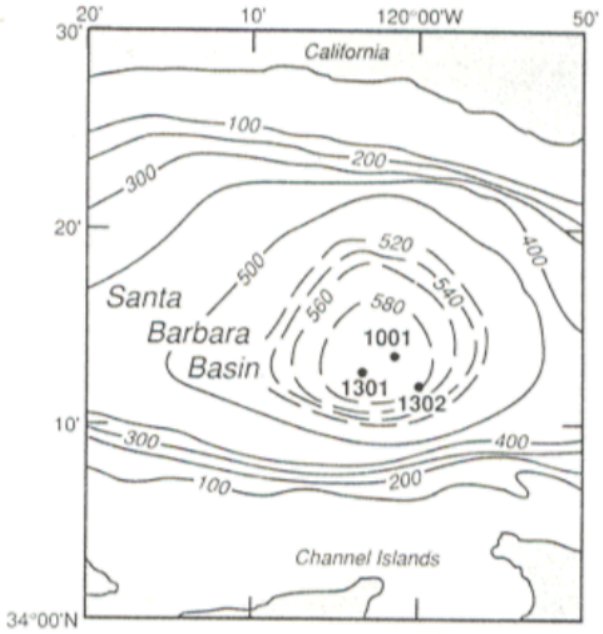

Figure 2.1. Map of the SBB showing bathymetry (m) and location of the three kasten cores used in the current study (Baumgartner et al., 1996).

Table 2.1. Summary of each of the kasten cores used in the current study.

Core	Location	Depth	Number of Sampling Intervals	Total Area for debris extraction	5-year sampling chronology	Varve Count Chronology	Radiocarbon Adjusted Chronology
SBKC 9110-1301	34°12.0'N, 120°0.2'W	588 m	310	43120 cm^2	1924 – 374	1924 – 263	1924 – 25
SBKC 9110-1302	34°12.7'N, 120°3.4'W	588 m	354	51023 cm^2	1924 – 154	1924 – 23 BCE	1924 – 306 BCE
SBKC 9210-1001	34°13.4'N, 120°1.6'W	590 m	330	45640 cm^2	1934 – 284	1934 – 173	1934 – 79 BCE

Subsampling of continuous five-year varve intervals was done with an independent varve count for each different core, but the same varve count for different slabs within a core. These subsamples were then heated in a hydrogen peroxide solution and sieved for fish debris. Core

SBKC 1301 and SBKC 1001 were sieved at 500 um size fractions throughout the entire core whereas SBKC 1302 was sieved at 700 um size fractions from the top of the core to the end of section one and then sieved at 350 um size fractions for the entirety of section one. This change in size fraction is noted in the current study and adjusted accordingly. The fish debris were stored in a 70% ethanol solution until quantification.

The scales extracted from the kasten cores were identified using the aid of a reference collection to a species level where possible and bones were categorized as either vertebrae, otolith, mandible, or other bones. Several people identified and quantified the fish debris (Andy Soutar, John Field, David Field, Hector Lozano, Christina Morales) and each trained the next. Due to the low numbers of otoliths and mandibles in the sediment record, this study focuses analyses on bones and vertebrae, however, otoliths and mandibles were used in the Paleo Forage Fish Index. The fish debris was quantified as either a whole scale/bone/vertebra or a fragment. To be considered a whole scale/bone/vertebra, more than half of the scale/bone/vertebra must be present. This approach prevents overestimation of fish debris, so a piece of debris was not counted twice. After the fish debris was quantified, both scale and vertebrae widths were measured, however, scale widths were not analyzed in the current study.

Additionally, box core data from Rose (2013) and Soutar and Isaacs (1974) were combined to increase the sampling area of the last 200 years. These cores were taken between 1973 and 2008 from the SBB.

2.2.2 Chronological Background

The SBB is characterized by unique conditions, including low oxygen concentration and high sedimentations rates, which allow for the preservation of fish debris and annually layered (varved) sediments (Field et al., 2009). Early chronostratigraphic studies of the SBB, using sediment cores and traps, proposed that each light-dark sediment layer consisted of one annum (Soutar and Isaacs, 1969; Hülsemann and Emery, 1961; Soutar et al., 1977). The light laminae are less dense consisting of more biological material, primarily diatom frustules, resulting from productive spring blooms, whereas, the dark laminae are denser and comprised of terrestrial materials due to winter runoff (Soutar and Isaacs, 1969; Hülsemann and Emery, 1961). Comparisons of Pb^{210} age determinations were consistent with varve-based ages (Soutar and Crill, 1977), which led to the establishment of a chronology based on varve count. However, more recent analyses comparing planktonic foraminiferal carbonate and terrestrial organic C^{14} measurements showed that the varves do not consistently represent annual layers, suggesting that varve count-based chronology records do not reveal a complete sequence of continuous annual varves (Hendy et al., 2013; Schimmelmann et al., 2013; 2016). Possible reasons for not having continuous annual layers may come from erasure or bioturbation of laminae, the occurrence of slumps that consist of varved sequences, or the presence of seasonal laminae that occur within an annual varve sequence (Field et al., 2009).

The scale record by Baumgartner et al. (1992) adjusted the preliminary chronology of approximately 10-year sampling intervals based on the one-centimeter sampling procedure to sampling intervals based on varve counts from x-radiographs. Baumgartner et al. (1992) suspected that varve counts underestimated years due to poorly preserved and non-varved

intervals, due to either an increase in oxygen concentration that allows micro-fauna to mix sediments; lower sedimentation rates, which make varves less identifiable; and/or disappearance of varves as a result of turbidite layers. In order to establish tie points to calendar dates further downcore, Baumgartner et al. (1992) compared varve thickness from a sediment core to *Pinus flexis* tree ring widths since both varve thickness and tree ring width rely on annual rainfall. They anchored the chronology around the dates 770 and 1405 based on the tree rings although the overall uncertainty was estimated to be about 50 years around the year 1000 which is roughly a five percent uncertainty throughout the entire core (Baumgartner et al., 1992).

The recent studies using marine and terrestrial radiocarbon dating agree with Baumgartner's assumption of an underestimation of years but show that the varve counts underestimate time by hundreds of years by about the year 10 and question the original assumption of identifying continuous varves that always represent each and every year (Hendy et al., 2013; Schimmelmann et al., 2013). They further argue that pre-18th century laminations are made up of both annual varves and laminations that represent multiple years (Hendy et al., 2013; Schimmelmann et al., 2013). However, Hendy et al. (2013) could not completely distinguish whether turbidites and erosion of sedimentary layers caused undercounting of the varve age or if the laminations are not consistently annual. Hendy et al. (2013) did note that varves are particularly difficult to see during exceptionally dry periods in time, such as the Medieval Climate Anomaly (MCA). Furthermore, the fact that average varve thickness is much higher in the 20th century reiterates that much of the last 2,000 years experienced lower sedimentation rate (Du et al., 2018; Biondi et al., 1997), which would imply that the varves are

harder to identify in an x-radiograph or a contrasting light dark layer is not present for every year (due to reduced terrestrial input).

There is considerable evidence indicating that annual couplets are not always identifiable. Baumgartner and Soutar re-examined preliminary five-year sampling intervals from the kasten cores used in the current study and found that careful evaluation resulted in each sampling interval consisting of five to nine varves. In an examination of multiple box cores from the SBB, D. Field noted that not all varves were identifiable in all cores and that many thin, light-dark laminations could questionably be identified as one or two years (Field, D.B. personal communication). This observation reiterates that identification of varves based on visual x-radiograph varve counting frequently underestimates years depending on oxygen levels, terrestrial runoff, and marine productivity. Additionally, visual varve counting varies with experience, judgement, and access to multiple x-rays from different cores (as well as different angles of the core). Nonetheless, it is still unclear if large sequences of varves are erased by turbidites.

2.2.3 Outlier Analysis

In order to identify outliers for removal, we developed a rigorous outlier detection procedure hereby referred to as *Outliers from the Median of Standard Deviations (OMSD)*. Since the sediment cores were processed into six vertical slabs, four of which containing fish debris counts, the variance between scale counts in neighboring samples taken from the same time interval of the core were quantified and highly anomalous fish debris counts were identified as outliers.

The fundamental issue with identifying outliers is getting a representative estimate of the central tendency of the variability from the four different samples within the five-year sampling interval. Calculating the standard deviation from four samples of each interval is insufficient to define the variability, as some intervals may be biased high or low due to the number of fish debris and/or presence of an outlier in a given sampling interval. Therefore, an estimate of the central tendency of the standard deviations of all intervals within the core was determined to be the best estimate of variance expected between fish debris counts within a given sampling interval. However, the mean of standard deviations from all sampling intervals was found to bias the estimate of average variation between counts in an interval. In some cases (e.g. bones), many sampling intervals with very large outliers would produce a large mean of the standard deviations causing the anomalous value to not be detected by the 'typical standard deviation outlier analysis' (i.e. when an outlier is greater than two, three, or four standard deviations from the mean). Furthermore, the mean of the standard deviations appeared to be biased by low fish debris counts (e.g. a common occurrence for sardine) that would result in an average of the standard deviation to be low causing non-anomalous values to be detected as outliers using the 'typical standard deviation method'.

Therefore, the Median of Standard Deviations (MSD) for each fish debris type was calculated, which is a measure of the central tendency of the variance in fish debris counts from all the sampling intervals within a core. The MSD is the median of *all* the standard deviations from the different sampling intervals of a core that have a mean fish debris count greater than one (Figure A2). The median minimizes the influence of extremely large outlier values. Additionally, not including standard deviations of sampling intervals with low scale counts (e.g. a

mean of a sampling interval being less than one) reduces the bias by low/zero scale counts that result in low standard deviations within an interval.

For each potential outlier for each fish debris type, the mean fish debris flux for the sampling interval plus two, three, and four MSD were compared to the potential outlier and ranked corresponding to the criteria below (Figure A2). Since potential outliers are compared with the mean of counts from each sampling interval, this method is a conservative estimate for screening outliers since an outlier within a sample size of four would result in an inaccurately high mean.

- Rank 3 "Likely": If the flagged value is greater than *two* MSD from the sampling interval's mean, then that sampling interval is ranked a 3 and is considered *Likely to Contain an Outlier*. In a normally distributed dataset, approximately 95 percent of the data lie within two standard deviations from the mean. For non-parametric data, Chebyshev's inequality rule states that up to nearly 25 percent of non-normal data could lie outside of two standard deviations, though the fish debris counts within an interval are expected to be normally distributed in the absence of outliers.
- Rank 2 "Highly Likely": If the anomalous value is greater than *three* MSD from the mean of the sampling interval, then the sampling interval is ranked a 2 and is *Highly Likely to Contain an Outlier* given that less than one percent of normal data and 11 percent of non-normal data lie outside of three standard deviations according to Chebyshev's inequality rule.
- Rank 1 "Virtually Certain": If the flagged value is greater than *four* MSD from the sampling interval's mean, that sampling interval is ranked a 1 and is *Virtually Certain to Contain an*

Outlier since virtually all normal data and 94% of non-normal data lie within four standard deviations from the mean.

In the case where there are two anomalously high values in one sampling interval (usually consisting of counts from neighboring slabs), the mean of the four samples may be strongly biased by the presence of two outliers. This scenario could occur when a chunk of fish is deposited to the sea floor and settles in a horizontal position and the slabs are cut through the buried piece of fish. The mean of the sampling interval may be larger than the second highest (yet potentially anomalous) fish debris count. In this situation, the larger anomalous value was ranked first (Figure A3). Then, if the value was determined to be an outlier, the mean was recalculated removing the ranked outlier value and the subsequent flagged, potential outlier value(s) were compared to two, three, and four MSD from the newly calculated mean(s).

In some scenarios, there may be additional evidence for the presence of an outlier. A debris outlier may have been deposited to the seafloor as a combination of scales, bones and/or vertebrae from a conglomerated piece of sinking fish. If a sample (i.e. same slab of the same sampling interval) within the same core contains outliers for multiple types of fish debris (i.e. scales and/or bone and/or vertebrae), then this provides additional evidence that the anomalous fish debris counts are more likely to be outliers so the ranks of both types of fish debris increased by one (Figure A4). However, if a scale outlier is associated with both bone and vertebrae, each rank was only increased by one.

Furthermore, a chunk of fish (i.e. an outlier) may span two or more adjacent sampling intervals of the same slab. This would result from a piece of fish arriving to the seafloor and

settling in the sediments in a vertical position occupying multiple five-year varve intervals. If both are determined to be outliers (*rank 1, 2 or 3*), the rank of each of these adjacent samples increased by one from their previously recorded rank (Figure A5). However, ranks did not increase by greater than one for any of the scenarios with additional evidence of an outlier. So, an outlier that was increased in rank by one due to another outlier directly above or below it, would not increase by an additional rank if the outlier were also associated with another form of fish debris.

Once all of the potential outliers were identified and ranked, the outliers ranked *Virtually Certain to Contain an Outlier (1)* and *Highly Likely to Contain an Outlier (2)* were corrected using the mean of the other non-outlier values in the same sampling interval (e.g. the outlier is not included in the estimated flux of skeletal debris). The determination to correct the outliers considered *Virtually Certain* and *Highly Likely to Contain an Outlier* are based on the OMSD results (Figure 2.3) and average correlations between cores (Table 2.3).

In addition to the rigorous outlier procedure used for scales and skeletal debris classified as bones and vertebrae, counts of jawbones and otoliths were also examined for outliers and removed. Jawbones and otoliths were much less abundant throughout the record so the OMSD procedure is not a fair outlier removal method. Instead, samples that contained more than one otolith subtracted one from the total otolith count. Further each slab of each sampling interval that contained more than one identifiable jawbone/mandible was corrected to one. This procedure is very conservative in order to reduce the risk of overinflating the otolith and jawbone time series and contribution to the Paleo Forage Fish Index.

2.2.4 Chronological Development

Two chronologies were developed, one primarily based on visual varve counts and the other correcting for major offsets identified by Hendy et al. (2013) and Schimmelmann et al. (2013).

A varve count chronology was developed based on all three kasten cores by first correlating major sedimentation features and then fine-tuning age assignments based on variations in scale flux of the different species. Unfortunately, the high-resolution x-radiographs taken at the time of subsampling were not available for the current study. So, major tie points came from homogenous intervals that were excluded from the original five-year sampling intervals representing major turbidites and/or flood layers. The well documented Macoma layer and large turbidite were set at 1832 and 1738, respectively, based on the box core chronology developed by D. Field. Since not every turbidite or flood layer is necessarily present in each core, correlating homogenous layers was based on photographs of x-radiographs from Baumgartner et al. (1996). Fine tuning of age assignments consisted of assigning each five-year sampling interval to a period of time greater than five years based on the alignment of peaks and absences in scale flux between cores. Note that this approach consistently adds years to the sum of the varve count record for each core, thus the age of this varve count chronology is much older than the original varve count and closer to the radiocarbon assignments of Hendy et al. (2013) and Schimmelmann et al. (2013; Table 2.1).

Once all three cores were aligned on the same timescale, the radiocarbon chronology was developed from the varve count chronology by adjustment to that of Schimmelmann et al.'s (2013, 2016) radiocarbon dates based on dates of major homogenous layers that were present

and assumed to be contemporaneous in both records (based on the collective evidence of thickness of layer, proximity to other homogenous sections, and evidence of varve structures). A linear regression was run between the years assigned to major homogenous layers identified in Schimmelmann et al. (2013) with the years from the kasten core varve count chronology believed to the same homogenous layers. The years of the major homogenous layers for both records are shown in Table A1. With the slope of the linear regression, a radiocarbon adjusted chronology was created beginning at the end of the box core record (i.e. 1746).

All analyses and references to years in this study refer to the varve count chronology. Additionally, all years refer to the common era (CE) unless otherwise noted as before common era (BCE).

2.2.5 Development of the Paleo Forage Fish Index

A paleo forage fish index was developed to provide an estimate of total forage fish variability from the fish debris collected from the kasten and box core records. The paleo forage fish index is an average of the normalized natural log of the fluxes from the four taxa of scales as well as a weighted sum of skeletal debris. Since other bones are much more common in the record than vertebrae, otoliths and mandibles, the vertebrae record was multiplied by two and a composite record of otoliths and mandibles was multiplied by five and all weighted skeletal debris records were summed together. The skeletal debris index was weighted to the ratio of skeletal debris. Each of the five records (four taxa of scales and skeletal debris) was then normalized to the period of overlap between the kasten core and box core records (i.e. 1746-1934).

2.2.6 SDR – Biomass Calibration

Box core SDR–biomass/recruitment calibrations were done for each of the scale records where data were available. Sardine biomass and recruitment estimates were obtained from Murphy (1966) for 1932-1949, MacCall (1979) for 1945-1966, and Hill et al. (2008) for 1980-2007. The biomass and recruitment estimates from Murphy and MacCall were averaged for the period of overlap between 1945 and 1949. The period between 1966-1980 were assumed to have biomass and recruitment estimates of zero as surveys did not detect a substantial number of eggs. Anchovy biomass estimates were obtained from Thayer et al. (2017a) for the period between 1951-2017 and recruitment estimates from 1963-1994 were obtained from Jacobson et al. (1995). Hake biomass and recruitment estimates were obtained from Berger et al. (2019) for the period between 1966-2019.

The biomass estimates for anchovy and hake were defined in terms of age-2+ fish. Likewise, the sardine stock assessments from Murphy (1966) and MacCall (1979) used age-2+ fish although Hill et al. (2008) defined sardine biomass using age-1+ fish. In order to adjust the sardine biomass estimates to consistently represent age-2+ fish, the Hill et al. (2008) estimates were multiplied by a ratio of the average weights of age-2 to age-1 fish. The average weights were obtained from Hill et al. (2018).

Using the age-2+ biomass estimates for each taxon, linear regressions based on average two-year intervals were run between SDR with biomass and SDR with recruitment (Figure A16, A18, A20). Since the scale record of sardine, anchovy, and hake primarily originate from younger fish, an index of both adult and recruit (A-R) biomass was created to examine the relationship

between total small pelagic biomass with SDR of a species. For this index, recruitment, in terms of millions of fish, was multiplied by the average weight of an age-0 fish in order to get an estimate of recruit biomass. Adult biomass was then added to a weighted recruit biomass estimate to get a total A-R Biomass Index.

2.2.7 Processing Vertebrae

Vertebrae were measured from samples of fish collected from trawl surveys from Dr. John Field from NMFS Southwest Fisheries Science Center. Table 2.2 lists the samples used in the current study. Each fish was sampled into three sections: anterior, mid, and posterior. From each section, approximately three to eight vertebrae were extracted and soaked in 70% hydrogen peroxide to disaggregate the organic matter. The organic matter was then cleaned off the vertebrae with a brush and the vertebrae were stored in DI water. Photos were taken of each vertebra and the height, width, length and waist were measured using ImageJ (Figure A6). The height, width, and waist measurements are not used in the current study. A collection of vertebrae photos is shown in Appendix II.

Table 2.2. Length of fish from the samples collected from trawl surveys in which vertebrae were extracted. The known maximum length and average length are provided when applicable.

Taxa	Standard Length from Sample (mm)	Maximum Size [Total Length] (mm)		Average Size [Total Length] (mm)	
Pacific Sardine	195	395	(Whitehead and Rodriguez-Sánchez, 1995)	200	(Whitehead, 1985)
Northern Anchovy	122, 98	248	(Lamb and Edgell, 1986)	150	(Frimodt, 1995)
Pacific Hake	57, 53	910	(Cohen et al., 1990)	600	(Cohen et al., 1990)

Smooth Tongue	94, 71	150	(Eschmeyer et al., 1983)	N/A	-
Mexican Lampfish	43, 33	70	(Moser and Ahlstrom, 1996)	N/A	-
Nanobracchia sp.	47, 40	142	(Zahuranec, 2000)	N/A	-
Northern Lampfish	68, 43	130	(Eschmeyer et al., 1983)	N/A	-
Blue Lantern Fish	55, 42	127	(Clemens and Wilby, 1961)	N/A	-

2.3. Results

2.3.1 Patterns of the Scale/Skeletal Deposition Rate Time Series Between Cores

Comparison of the scale and skeletal debris deposition rate (both hereby referred to as SDR) time series between cores from any given debris type reveals both reproducibility and some differences between cores. The sardine and hake SDR time series for each core with and without outlier removal are shown in Figure 2.2 and the remaining time series for anchovy and myctophid scales as well as bone and vertebrae can be found in Figure A7 and the summary statistics of each core are reported in Table A2.

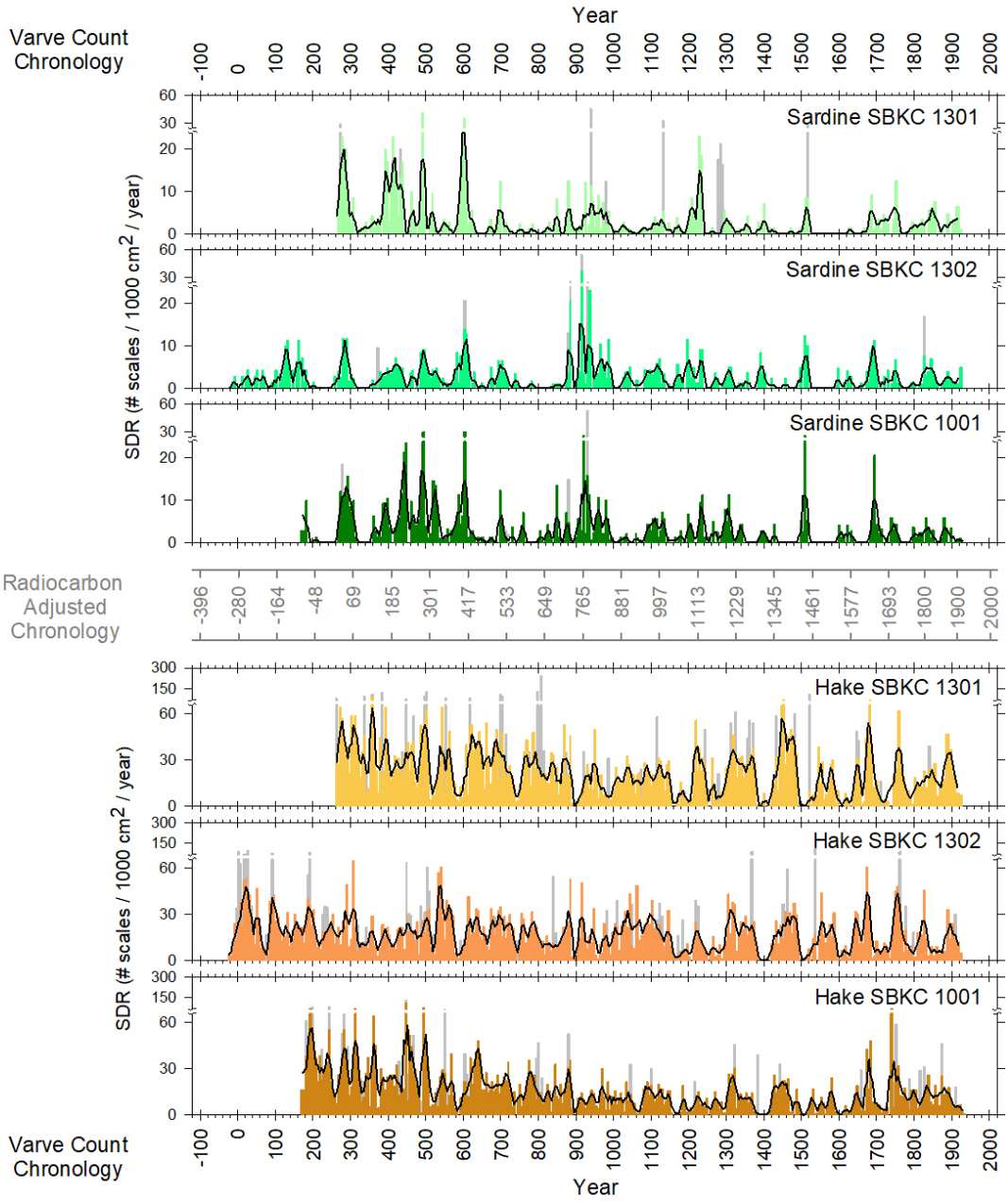

Figure 2.2. Time series of sardine and hake scale fluxes derived from five-year sampling intervals (shaded region) with three-term smoothing (bold black line) after outliers were removed. The grey bars indicate a sampling interval containing an outlier that was removed using the OMSD removal criteria, which corrected the flux to the colored values. The varve count chronology is shown on the top and bottom corresponding to the tick marks and the radiocarbon adjusted chronology is shown between the two debris types. Any years in the text refer to the varve count chronology. Time series for anchovy, myctophid, bones, and vertebrae can be found in the appendix.

Within the sardine record, all three cores show a peak in flux of about ten SDR around 1500 in the middle of an approximately 200-year period of absence (Figure 2.2). Furthermore, there are reproducible characteristics in the sardine record from around 300 to 700. Within this time period, there are shared absences around 320, 430, 560, and 640. Between these shared absences, there are between four and six peaks in scale flux. The exact nature of the peaks varies in both shape and duration. For example, there is a clear peak around 400 in both SBKC 1301 and SBKC 1302 although the magnitude of these peaks varies between the two cores. In SBKC 1001, this same peak is represented as two separate peaks ranging approximately 100 years.

The hake record also has well defined peaks and minimums that can be seen in all three cores. The hake record has pronounced minimums that occur around 590, 1160, 1400, 1500, and 1720 that are seen in each core. However, there are on occasion, minimums in one core that do not correspond to minimums in other cores (e.g. 1850). While a well-defined period of high abundance exists from about 1420 to 1500, the size of the maximum values vary in all three cores by about a factor of two (e.g. SBKC 1301 has a flux of about 50 SDR whereas SBKC 1001 is about 25 SDR; Figure 2.2).

To compare the mean fluxes between cores taken within the SBB, six separate two-way ANOVAs were conducted to test for differences between cores and between sampling intervals for each debris type. For each debris type, the ANOVAs detected significant differences between cores and between sampling intervals (Table A3). However, when 18 one-way ANOVAs were conducted to test for differences between the four slabs of the same core for each debris type, only four records (i.e. one core for one debris type) resulted in significant differences between slabs (Table A4). This indicates that the other 14 records did not have detectable differences

between slabs of the same core. The averages between cores vary for each debris type (Table A2), however, within the time series, different cores may have higher fluxes than others for extended periods of time. For example, in the sardine record, SBKC 1302 has the lowest average debris flux, however the series of peaks between 900 – 1000 are greater than the corresponding peaks in SBKC 1301 (Figure 2.2).

To further quantify shared variability between cores, correlation coefficients are reported in Table 2.3 for each combination of the three cores, as well as the average of the three coefficients, which indicates the average shared downcore variability between the three cores. Although the ANOVAs identified the mean flux to differ from core to core, the correlations (after outlier removal) show that sardine, anchovy, and hake all shared about 40% of their downcore variability between cores based on the three-core average while the myctophid records shared 30% of their downcore variability (Table 2.3). In contrast, bone and vertebrae each shared less than ten percent of the variability between cores.

2.3.2 Identification and Removal of Outliers

Identified Outliers

The Outliers from the Median of Standard Deviations (OMSD) procedure consistently identified outliers from each type of fish debris in all three kasten cores, though the relative number of outliers identified varied by debris type, core, and the relative portions of categories of likelihood of containing an outlier (i.e. *Virtually Certain (1)*, *Highly Likely (2)*, or *Likely(3*)). The percent of sampling intervals containing an identified outlier for each debris type within each core is shown in Figure 2.3, with darker colors indicating higher likelihood of a sampling interval

containing an outlier. Since the core lengths differ, percentage of total sampling intervals is used for comparison between cores.

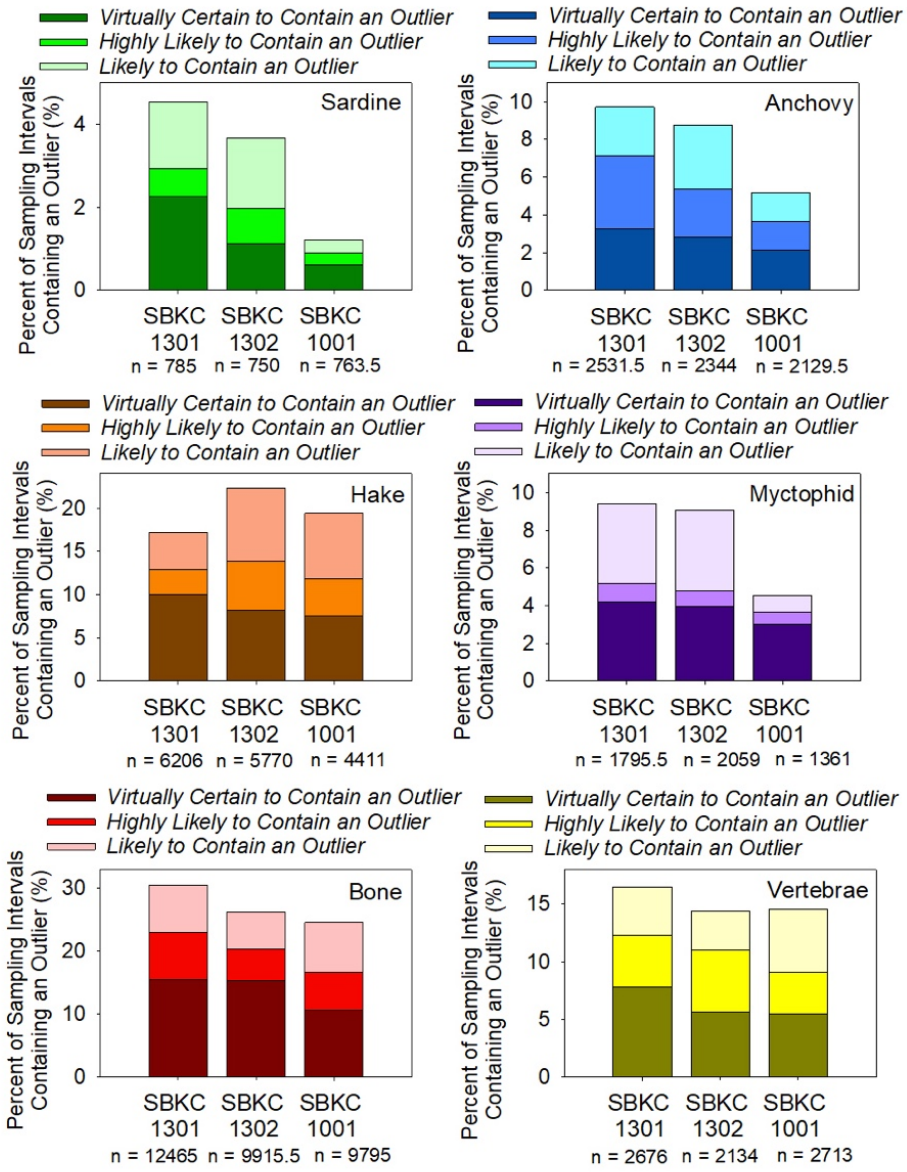

Figure 2.3. The percent of sampling intervals containing outliers identified via the OMSD procedure from three kasten sediment cores (SBKC 1301, SBKC 1302, SBKC 1001). The OMSD procedure ranks the outliers as: Virtually Certain (1) to Contain an Outlier, Highly Likely (2) to Contain and Outlier, and Likely (3) to Contain an Outlier. SBKC 1301 contains 309 sampling intervals, SBKC 1302 contains 354 sampling intervals, and SBKC 1001 contains 330 sampling intervals. n represents the total number of fish debris of a specific type that was extracted from the core.

The average percentage of intervals from all three cores containing outliers ranked *Virtually* Certain *(1), Highly Likely (2), or Likely (3)* for the flux of any debris type were compared with the average flux of that debris type. There is a positive relationship ($R^2 = 0.89$; DF = 6, $p < 0.005$) between the average percent of intervals containing identified outliers with the average amount of fish debris flux to the seafloor across the various debris types (Figure A8). The sardine scale record has the fewest identified outliers and the lowest average flux (Figure 2.3; Table A2). For other species, anchovy and myctophid are similar in both the percent of sampling intervals with identified outliers and average scale flux. Hake has the highest scale flux out of the four species, coinciding with the highest percentage of scale outliers (Figure A9) and nearly double the amount of sampling intervals containing outliers than both anchovy and myctophid scales, independently.

Since skeletal debris arrives to the seafloor in a different fashion than fish scales, skeletal debris may have higher frequencies of outliers than scales. The bone record clearly contains the most outliers throughout the record (Figure 2.3) and bone flux is nearly double the flux of hake scales for all three cores. The OMSD procedure identified less vertebrae outliers than both the bone and the hake records, though the flux of hake was nearly double the flux of vertebrae. The total percent of sampling intervals containing vertebrae outliers is nearly double the sampling intervals containing anchovy outliers even though the total debris fluxes of the two records are similar, which suggests that skeletal debris arrives to the seafloor as outliers more frequently than do scales.

Within a debris type, the percent of sampling intervals ranked *Virtually Certain (1) to Contain an Outlier* is often larger than the percent of intervals ranked *Highly Likely (2)* and *Likely*

(3) to Contain an Outlier and sometimes greater than twice these categories. Within the bone record, the percent of sampling intervals containing a rank *1* outlier is always greater than the other two likelihood categories (Figure 2.3). While the rank *1* and *2* outliers are much less likely to be mis-identified as outliers, the sum of these categories are larger than the rank 3 outliers for all debris types of each core.

Correlation Between Cores Before and After Outlier Removal

The decision to remove rank *1* and *2* outliers was based on the comparison of correlations between cores before and after removal of outliers for different outlier removal scenarios (e.g. removal of rank *1, 2,* and *3*; removal of rank *1* and *2*; and removal of only rank *1* outliers). Correlations between cores and the average correlation between all three cores can be found in Table 2.3. The shared variability between two cores generally increased as outliers were removed, however the shared variance differed between each pair of cores. For all debris types except vertebrae, the average correlation between the three cores is always higher when the outliers considered *Virtually Certain (1) and Highly Likely (2)* were removed (Table 2.3). Removing rank *1*, *2*, and *3* outliers resulted in an increase in shared variability for most debris types compared to the data without outlier removal but did not always result in the greatest shared variance (i.e. sardine, hake, and myctophid; Table 2.3). Therefore, this study removes outliers ranked *1* and *2* since this removal scenario results in the highest shared variability for the greatest number of debris types.

In some cases, the removal of outliers resulted in a large increase in shared variability between cores. For example, the average correlation of myctophid scales between cores

increased five-fold after the outliers ranked *Virtually Certain (1) and Highly Likely (2)* were removed (Table 2.3). In contrast, the bone record shared virtually no significant variability between cores prior to outlier correction. Additionally, the average correlation between cores for the vertebrae record was slightly higher before outlier removal.

Table 2.3. Coefficient of determination (r^2) for correlations between cores and the three-core average for scenarios without outliers removed and with outliers ranked Virtually Certain (1) and Highly Likely (2) to Contain Outliers removed. The coefficient of determination for the three-core average for the removal scenario where all outliers ranked Virtually Certain (1), Highly Likely (2), and Likely (3) were removed are also shown. Underlined values indicate that the correlation between cores that do not have outliers removed is stronger than the correlation between cores with the Rank 1 and 2 outliers removed.

	SBKC 1301 – SBKC 1302		SBKC 1301 – SBKC 1001		SBKC 1302 – SBKC 1001		**3-Core Average**		
	No outliers removed	Rank 1 & 2 removed	No outliers removed	Rank 1 & 2 removed	No outliers removed	Rank 1 & 2 removed	**No outliers removed**	**Rank 1 & 2 removed**	Rank 1, 2, & 3 removed
Sardine	0.28	0.38	0.35	0.42	0.48	0.46	**0.37**	**0.42**	0.40
Anchovy	0.41	0.42	0.50	0.57	0.29	0.26	**0.40**	**0.41**	0.42
Hake	0.20	0.42	0.36	0.50	0.20	0.23	**0.25**	**0.38**	0.37
Myctophid	0.05	0.36	0.11	0.24	0.02	0.28	**0.06**	**0.30**	0.27
Bone	0.01	0.09	0.03	0.16	0.02	0.01	**0.02**	**0.09**	0.10
Vertebrae	0.16	0.04	0.04	0.08	0.10	0.08	**0.10**	**0.07**	0.07

Comparing the corrected fish debris fluxes with the removed outliers shows many sampling intervals where the removal of the rank *1* or *2* outliers increases reproducibility between cores (Figure 2.2). The grey bars in Figure 2.2 indicate outliers ranked *Virtually Certain (1)* and *Highly Likely (2) to Contain an Outlier* that were corrected in the time series. For example, in the sardine flux record, there are outliers in SBKC 1301 around the year 1280 and in SBKC 1302 around 360 that were removed and would otherwise produce a peak in SDR where there is not one in the other two cores. Similarly, in the hake record, there was a sampling interval around 1520 in SBKC 1301 with high scale flux in the middle of an absence of scales.

Furthermore, close examination of outliers in Figure 2.2 also reveals that it is possible that samples can be misidentified and removed as outliers when they were not. For example, an outlier was removed in the SBKC 1301 sardine record around 1507 that corresponds to high scale flux in the other two cores, suggesting that this is a natural peak in sardine scales that occurs throughout the SBB.

Differences in Outliers Between Cores

For each debris type except hake, the percent of sampling intervals containing an outlier considered *Virtually Certain (1) or Highly Likely (2) to Contain an Outlier* is highest in SBKC 1301 and lowest in SBKC 1001 (Figure 2.3). In the hake scale record, SBKC 1302 has the highest percentage of rank *1* and *2* outliers followed by SBKC 1301 and SBKC 1001, respectively. However, none of the chi square results testing for a difference in the percentage of identified outliers between cores were significant (Table A5). The insignificant results for each core indicate that although cores differ in the percentage of outliers identified, this difference could have arisen from chance alone.

Probability of Occurrence of an Outlier Increases with Increasing Debris Flux

Examination of occurrence of outliers in the time series shows that outliers may be more likely to occur in a given interval when debris flux in that interval is high than when flux in an interval is low. Comparison of the frequency of non-outliers and rank *3* outliers with sampling intervals containing rank *1* and *2* outliers, shows that the intervals containing outliers ranked *1* and *2* are generally associated with higher scale fluxes (Figure 2.4). Note that the scale fluxes in

Figure 2.4 are corrected and do not contain identified outliers. A two-sided independent Mann Whitney-U (Wilcoxon) test with continuity correction comparing the median flux of these two categories (i.e. the intervals with non-outliers and rank *3* outliers compared with intervals containing rank *1* and *2* outliers) shows that when detected outliers are present, the distributions of fluxes are significantly higher for all records of fish debris except vertebrae (Table A6). Therefore, when the flux of a sampling interval is higher, indicating there are more fish in the water column, it is more likely to have an outlier from a piece of fish.

In some of the histograms in Figure 2.4, there are sampling intervals considered *Virtually Certain (1) or Highly Likely (2) to Contain an Outlier* where there is very small or zero scale flux in that sampling interval. This is because the data used for these histograms removed the outliers. Therefore, a sampling interval that contains very low fish debris flux other than the anomalous outlier can still contain an identified outlier, even though it is less likely to occur in these intervals than intervals with higher fluxes.

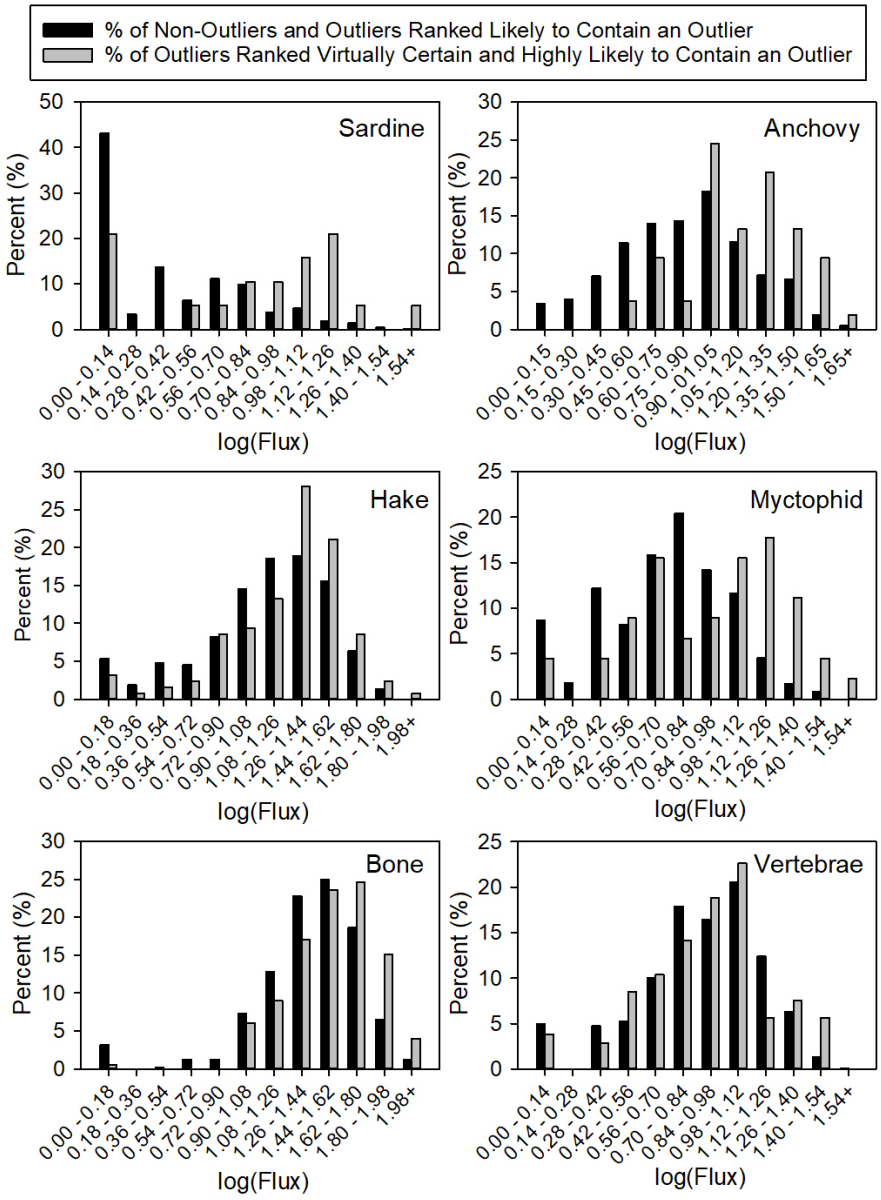

Figure 2.4. Histograms of each debris type showing the distribution of non-outliers and those ranked Likely (3) to Contain an Outlier are shown in black and those ranked Virtually Certain (1) and Highly Likely (2) to Contain an Outlier are shown in grey. Because the flux varies by debris type, the percentages are shown for comparison between debris types.

2.3.3 Composite Time Series

Patterns of Fish Debris Deposition Rate

A composite time series for each debris type was created using the average fluxes from the three kasten sediment cores (Figure 2.5) with outliers ranked *1* and *2* removed. For the bone and vertebrae composite time series, SBKC 1302 was not used due to the change in sieve size during the sampling procedure. As can be seen in Figure 2.5, the SDR magnitude varies by debris type with bone having the greatest mean flux followed by hake, vertebrae, anchovy, myctophid, and sardine, respectively (Table A2).

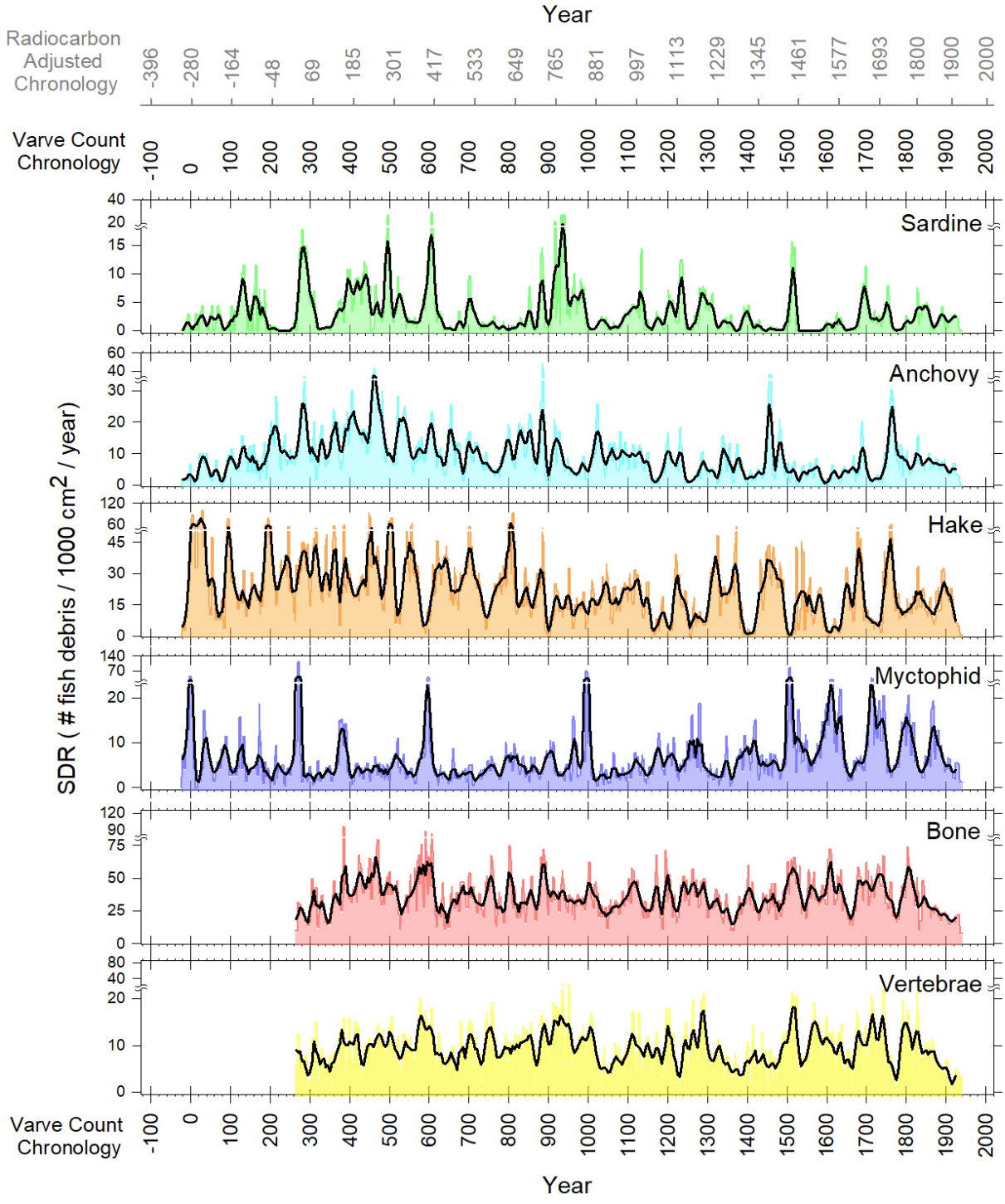

Figure 2.5. Composite kasten core time series of the flux of sardine, anchovy, hake, and myctophid scales as well as bones and vertebrae. The composite scale time series are made up of an average scale flux from all three cores (i.e. SBKC 1301, SBKC 1302, SBKC 1001) whereas the composite bone SDR records are based on the average flux of SBKC 1301 and SBKC 1302.

The colored shaded region is derived from five-year sampling intervals based on data with rank 1 and 2 outliers removed. The bold black lines represent three-term smoothing.

The composite sardine SDR time series consists of many periods of low or zero scale flux lasting roughly 20 to 100 years. Due to the high frequency of low scale flux, the sardine record is highly variable with the greatest coefficient of variation (CV), almost double that of anchovy, hake, and myctophid scales, respectively (Table A2). There are peaks of relatively high scale flux around 15 SDR on centennial time scales prior to 700 with a mean flux of about five SDR during the period between 250 and 700 (Figure 2.5). After 700 the scale flux is lower with a mean flux of 2.5 SDR and there are a few extended periods of low scale flux that last up to 150 years (i.e. ~1530 – 1660).

The anchovy composite record is also highly variable with the second highest CV (Table A2) and short intervals with low flux generally lasting 10 to 40 years. Similar to sardine, the composite anchovy SDR time series has periods of higher flux earlier in the record (e.g. before 700) with a mean flux of around 12 SDR from approximately 700 to the end of the record, whereas the period from 700 to 1934 has a mean flux of 7.4 SDR (Figure 2.5).

The composite hake record consists of the highest mean flux of all scale types although it is less variable with the lowest CV of all scale types (Table A2). Prior to 500, the flux of scales is high with low SDRs of about 20 (Figure 2.5). After 500, the peak in fluxes is still high, reaching approximately 30 SDR, although there are also periods of low scale flux dipping below ten SDR that usually last less than 50 years. After around 1400, the hake record starts to have periods of clear minimums of less than five SDR that last ten to 40 years and coincide with the Little Ice Age (LIA).

There are no periods throughout the entire record where the myctophid composite flux is zero and there is low variability throughout the record with the second lowest CV of all scale types, although a value very similar to hake (Table A2). In contrast to many of the debris types, the myctophid composite record has relatively lower scale flux from the beginning of the record to about 1500 with a mean flux of approximately 5.9 SDR, but no intervals of sustained flux of less than one. After 1500 the average flux is 10.4 SDR and consists of high peaks that last up to 80 years followed by periods of relatively lower scale flux lasting decades, but with values that are still higher than the lows prior to 1500 (Figure 2.5).

The bone and vertebrae composite records are much less variable than the scale records (Table A2) and do not have any zero fluxes throughout the time series. The bone record has the highest mean flux and bone and vertebrae have the lowest CVs of all debris types, respectively. While there are some clear decadal and interdecadal variations in the skeletal debris records, the long-term centennial scale variability is less obvious than can be seen in the scale records (Figure 2.5).

Correlation Between Debris Types

To determine the relationships between species and skeletal debris, correlations were done using the three-term smoothed, composite data and shown in Table 2.4. Within the scale records, the strongest correlation is between anchovy with hake scales ($R^2 = 0.13$), though it is a weak, but a highly significant positive relationship followed closely by sardine with anchovy, which also have a weak, positive relationship ($R^2 = 0.11$). The correlations between myctophid

with anchovy and myctophid with hake are both negative and significant, though weak. There are not significant relationships between sardine with hake or sardine with myctophid.

These relationships can be seen when visually comparing the composite time series (Figure 2.5). Many of the peaks and troughs in anchovy closely align with the peaks and troughs seen in the hake record. For example, there are clear minimums in both records around 760, 900, 1160, 1250, 1400, and 1730. In contrast to these shared flux characteristics, there is clearly a negative relationship that can be seen between hake and myctophid, particularly in the latter part of the record after about 1200. Many of the peaks in myctophid scale flux align with minimums in the hake record and vice versa (e.g. 600, 1280, 1450, 1500, 1600, and 1720).

Comparison of the scale fluxes with the skeletal debris records show that there is a significant relationship between skeletal debris and all scale records, except anchovy (Table 2.4). Bone and vertebrae have the strongest positive relationship, which is expected since both debris types reach the seafloor in a similar fashion. Sardine and myctophid have a relatively higher correlation with both bone and vertebrae suggesting that these species may be major contributors to the skeletal debris record. The hake record, however, has a weak, but significant negative relationship with both bone and vertebrae.

Similar to the correlation between scale types, the relationships between scales and skeletal debris can be seen in the composite time series (Figure 2.5). There is high shared variability ($R^2 = 0.49$) that can be seen between the bone and vertebrae record such as the shared minimums around 520, 660, 1050, 1380, 1670, and 1780. Although the correlations are not quite as strong, the relatively high shared variability can be seen between sardine scales and skeletal debris as well as myctophid flux and skeletal debris. For example, the sardine record shares

downcore variability with both the bone and vertebrae records such as the peaks at 400, 600, 740, and 1510 as well as the minimum around 1780. Likewise, the myctophid SDR record shares much of the downcore variability with the bone and vertebrae flux, specifically towards the end of the record after 1400 (e.g. the minimums around 1400, 1480, 1550, 1650, and 1780).

*Table 2.4. Correlation coefficient (R-value) and coefficient of determination (R^2-value) between composite fish debris types based on a linear regression of the three-term smoothed data. Bold values indicate that the correlation is significant at a 0.05 level and the level of significance is demarcated by: * p≤0.05; ** p≤0.01; ***p≤0.001; ****p≤0.0001.*

	Sardine	Anchovy	Hake	Myctophid	Bone
Sardine	1	-	-	-	-
Anchovy	**0.33 (0.11) ******	1	-	-	-
Hake	0.01 (0.00)	**0.36 (0.13) ******	1	-	-
Myctophid	0.05 (0.00)	**-0.24 (0.06) ******	**-0.29 (0.09) ******	1	-
Bone	**0.28 (0.08) ******	0.09 (0.01)	**-0.11 (0.01) ***	**0.29 (0.09) ******	1
Vertebrae	**0.33 (0.11) ******	-0.03 (0.00)	**-0.22 (0.05) ******	**0.31 (0.10) ******	**0.70 (0.49) ******

To examine if the abundance of a species at one point in time, affects another later in time, autocorrelations and correlations between species were conducted with a lag at five, ten, and fifteen years (Table A7). For most of the correlations between debris types, the relationships are weaker with a lag. However, there are some examples where the correlation coefficient between two species is greater when one species is lagged behind the other. For example, when hake is lagged behind anchovy five years, the correlation coefficient is greater which may suggest that high abundances of anchovy results in higher numbers of hake several years later.

Comparison of the Composite Kasten Core with the Composite Box Core Records

When comparing the composite kasten core records with the box core records, it is clear that the magnitude of the fish debris fluxes differs, however, much of the temporal variation is shared between composite core types (Figure A10, A11). A Mann-Whitney U (Wilcoxon) test between the kasten core with the box core for the period of overlap (i.e. 1746-1934) determined that the composite core types were significantly different for all six of the records (Table A8). Within the sardine, anchovy, and hake records, the relative peaks and troughs in SDR occur around the same time, however, the average flux in the box score is greater than that of the kasten core for each of these three species. In the myctophid scale records, the downcore changes coincide between the two core types, although the flux in the kasten core is frequently greater than in the box core. Nonetheless, the shared variance between core types varies by debris type for the period of overlap. The shared variance (R^2) between the composite kasten with the composite box core records during the period of overlap for sardine, anchovy, hake, myctophid, bone, and vertebrae are 0.30, 0.36, 0.41, 0.23, 0.24, and 0.08, respectively. In some cases such as hake, bone, and vertebrae, the coefficient of determination is greater between composite core types than between individual kasten cores (Table A9).

The composite skeletal debris records from the kasten and box cores do not share the same degree of shared downcore variability as seen in the scale time series. Within the bone record, an approximately 30-year peak in the kasten core around 1800 corresponds to multiple peaks in the box core. After 1800, the box core is more variable with many peaks of higher flux than the kasten core, though this is expected due to the two-year sampling intervals. In the vertebrae record, the SDR in the box core is almost always greater than in the kasten core, and

at times up to nearly three times higher flux. However, there is some shared variability between the two core types such as the minimum around 1775 (Figure A11). Additionally, the vertebrae SDR time series in the box core has a minimum around 1809, whereas the kasten core shows this decline nearly 10 years later.

Paleo Forage Fish Index

The Paleo Forage Fish Index is composed of a compilation of the normalized natural log of fish debris fluxes from both kasten and box cores from the SBB ranging from 260 to 2006 (Figure 2.6). Given that there were differences between the three kasten cores and between the averages of composite kasten and composite box core records, the data were normalized to each composite record based on the, respective, period of overlap between the two cores (1746-1934) in order to compare anomalies to the same time period.

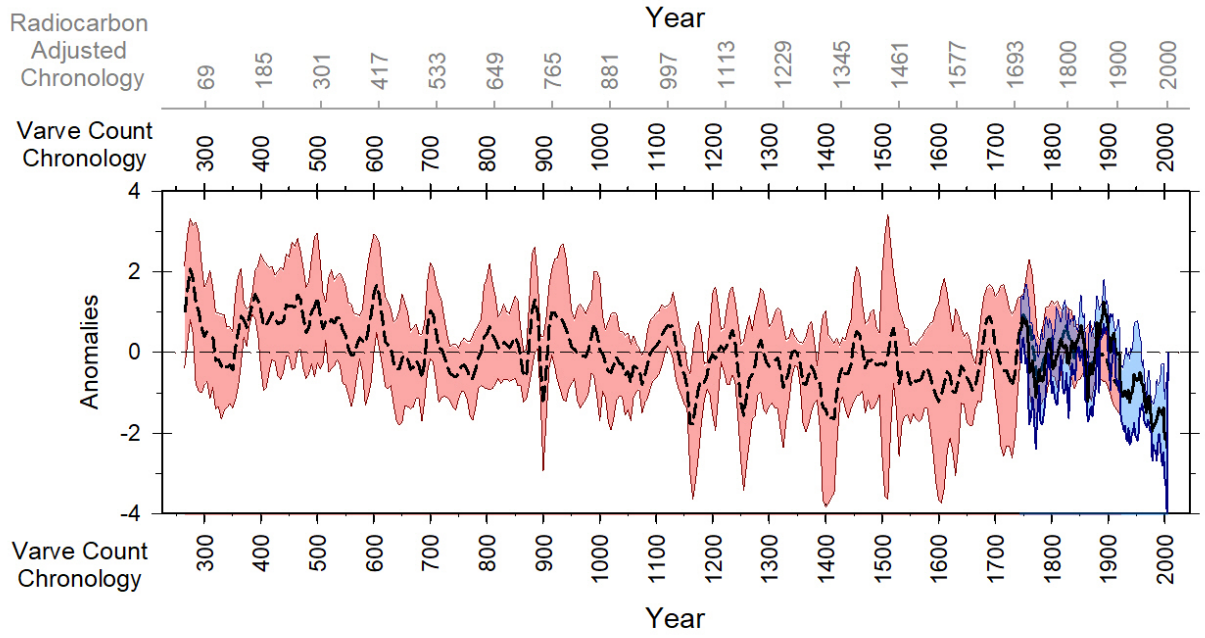

Figure 2.6. Paleo Forage Fish Index derived from the natural log of normalized debris fluxes from 260-2006. The fluxes were normalized to the period of overlap (1746-1934) for each

respective core type. Therefore, the baseline represents the period between 1746-1934. The shading indicates two standard errors and the red represents the kasten core while the blue represents the box core record. Both the varve count and radiocarbon adjusted chronology are shown. A cropped Paleo Forage Fish Index from 1730 to 2004 is shown in Figure A14.

The Paleo Forage Fish Index based on the kasten core ranged from values above and below two from the baseline with the 95% confidence intervals nearing four and negative four. The index was greater than two for one five-year interval in 275. In the early part of the record from around 260 to 1000, the Paleo Forage Fish Index is primarily above the baseline. Within this period of high values, there are six instances where the lower bounds of the 95% confidence interval is above the baseline suggesting that all species are simultaneously abundant.

In contrast, from approximately 1000 to the end of the kasten core record, the index is predominately below the baseline suggesting that at least several taxa occurred in relatively low abundances. The kasten core Paleo Forage Fish Index reached values less than negative one five times throughout the entire record: 900, 1165, 1255, 1405, and 1600. Since 1000, the upper confidence interval was below the baseline six times: 1075, 1155, 1185, 1385, 1660, and in 1915 to the end of the kasten core. The negative confidence limit suggests that many debris types in the Paleo Forage Fish Index are at low abundances during this time.

The box core Paleo Forage Fish Index ranges from 1746 to 2006 and resolves more high frequency changes due to the two-year sampling resolution. The values of the index range from positive one to less than one below the baseline until around 1920 and the 95% confidence interval straddles the baseline as this is the period of overlap to which the values are normalized. From 1746 to 1920, there are five periods where the lower bounds of the confidence interval are above the baseline suggesting an abundance of multiple taxa: 1748, 1844, 1854, 1880, 1886, and

1910. On the other hand, there are three periods when the upper confidence interval is below the baseline in 1776, 1802, and 1862. After 1920, the index remains below the baseline with values approaching less than negative two around 2000 to the end of the record. Within this period, the 95% confidence intervals are below the baseline from 1922 to 1930, 1934, and 1938, and for a prolonged period of time from 1960 to 2006. This is the longest period of time where the confidence limits are consistently below the baseline.

Welch's t-tests were run to determine if the mean of the negative anomalies in the 20th century is different from anomalies in the last two millennia (Table A10). First, a series of Welch's t-tests were run between anomalies from the early 20th century (1922-1942) with negative anomalies from 1155-1180, 1250-1260, 1395-1420, and 1595-1605. The t-tests indicated that the means in the period between 1922 and 1942 are not different from the negative anomalies from 1155-1180, 1250-1260, and 1595-1605. Although, the mean of the negative anomalies from 1395-1420 are significantly less than the anomalies from the 1920s to 1940s. Next, the period from 1964 to 2004 was compared to the same four periods in time. The anomalies from 1155-1180, 1250-1260, and 1395-1420 were not significantly different from the anomalies from 1964 to the end of the record. However, the 1960s anomalies were significantly less than the anomalies in the period from 1595-1605. Finally, the late 20th century (1976-2006) anomalies were compared to the anomalies in the last 2,000 years and the Welch's t-test determined that anomalies from 1976-2006 were significantly less than any of the periods in the last two millennia.

Reconstructing Biomass/Recruitment Estimates from Fish Debris Time Series

In order to determine how well the SDR record resembles the biomass of sardine, anchovy, and hake, linear regressions between the natural log of SDR with biomass, recruitment, and the calculated A-R Biomass index were done. The biomass and recruitment indices were averaged into two-year intervals to compare to the SDR records.

Comparison of the natural log of sardine SDR with age 1-2+ biomass, age-2+ biomass, recruitment, and the A-R Biomass Index from 1930 to 2006 showed shared variability as well as some distinct differences between the records (Figure A15). All five measures of abundance showed high sardine abundances in the early part of the record in the 1930s and then declined to near zero by the 1950s. The natural log of the SDR record has a few years with non-zero scale fluxes, whereas, the biomass and recruitment estimates remain at zero until the 1990s. Nonetheless, fish catch records show occasional landings during this time. Furthermore, all records show an increase in abundance around the 1990s and the 21st century, however, the biomass and recruitment estimates increase to about one quarter that of the 1930s whereas the SDR record increases above the level of the 1930s.

Since the sardine biomass estimates were conducted using a combination of age-1+ and age-2+ individuals, the age-1+ biomass was converted into age-2+ biomass using a ratio of average weights of age-2+ and age-1+ sardine. Linear regressions between the natural log of SDR and both biomass indices produced significant results, however, the regression detected the greatest shared variability with the age-2+ biomass estimates (R^2 = 0.34; Figure A16). The calculated A-R Biomass Index for sardine shared the second most variability with the natural log SDR record (R^2 = 0.33), suggesting that the age-2+ individuals play an important role in the scale

flux records. Finally, the recruitment index shared the least amount of variability with the natural log of SDR ($R^2 = 0.23$) likely due to the high variability of the recruitment record.

The correlations between Northern anchovy natural log of SDR with age-2+ biomass ($R^2 = 0.07$), age-0 recruitment ($R^2 = 0.06$), and the A-R Biomass Index ($R^2 = 0.16$) were insignificant with some major differences between abundance measures (Figure A17, A18). The recruitment estimates, and thus the A-R Biomass Index, were only available from 1964 to 1994. The natural log of SDR and age-2+ biomass estimates showed high anchovy abundance in the 1960s and then again in the 1970s although the timing of the peaks varied. By the 1980s, anchovy SDR declined until the mid-2000s, whereas the age-2+ biomass estimates showed a peak in the 1980s and was low from 1990 to the mid-2000s. The anchovy A-R Biomass Index largely resembles the recruitment timeseries with a large peak in the 1970s and a secondary peak in the 1980s.

The hake natural log SDR timeseries shares many general characteristics with both the age-2+ biomass timeseries ($R^2 = 0.19$) and the A-R Biomass Index ($R^2 = 0.25$), however the timing of the peaks and troughs varies a bit (Figure A19, A20). The natural log of the SDR record shows a small peak in the 1970s whereas both the biomass indices show a slow increasing trend. All three records suggest an increase in hake abundance in the early 1980s, with a major peak in the late 1980s and early 1990s, although the timing of the peaks is off by about four years. The abundance estimates decline after the major peak and then show another moderate peak around 2000. In contrast to the abundance estimates, the natural log of the SDR record is not a good reflection of age-0 recruitment, sharing virtually no variability. The recruitment time series is highly variable showing major peaks in the early 1980s and 2000s.

There is skepticism toward calibrating SDR to biomass since small pelagics distributions are variable and the scale record is predominately made up age-1 fish (Soutar and Isaacs, 1969; Rose 2013), thus primarily representing younger age classes. However, assuming that the scale flux records are representative of abundance and stock structure of the populations, biomass time series for sardine, anchovy, and hake were created based on the A-R Biomass Indices (Figure A21) and a combined biomass time series is shown in Figure 2.7. The sardine reconstructed biomass record exhibited the lowest biomass throughout the record with an average of about 1,900,000 mt per year. Early in the sardine biomass record between 260-650, there are periods reaching nearly 9,000,000 mt per year, although there are many periods with less than 500,000 mt per year. The anchovy biomass record indicated a higher biomass than the sardine record with about 3,700,000 mt per year with no sampling intervals less than 2,000,000 mt per year. The hake biomass timeseries consisted of the highest biomass throughout the record with an average of 5,950,000 mt per year. When examining the combined biomass time series, forage fish biomass from the three major taxa vary on a centennial scale with lower biomass in the late 20th century than the 1800s and early 1900s.

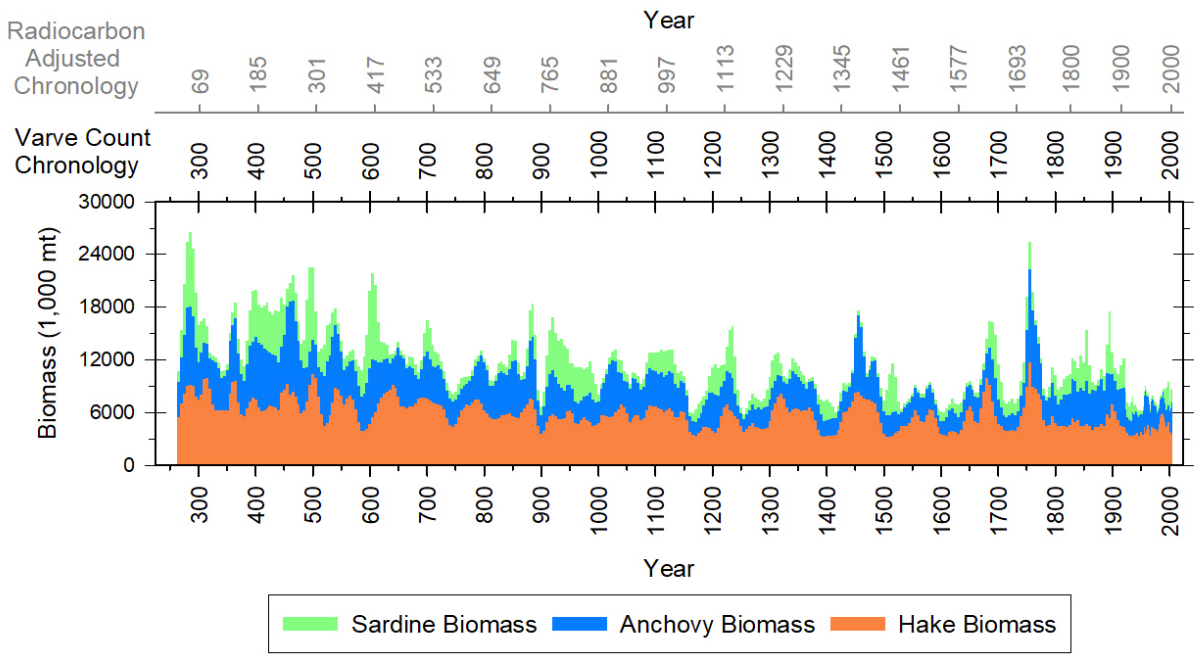

Figure 2.7. Combined biomass time series of three of the major forage fish taxa with biomass and recruitment estimates. SDR was calibrated with biomass using a liner regression with the A-R Biomass Index. Individual biomass time series are shown in Figure A21.

Variability in Vertebrae

Vertebrae lengths were measured from SBKC 1301 and a histogram of the lengths are shown in Figure 2.8. Additionally, vertebrae lengths were measured from samples collected via trawls survey (Figure A22), which can be used to help infer fish lengths from the vertebrae lengths measured from SBKC 1301.

Most of the vertebrae from SBKC 1301 were between 0.4 and 1.4 mm in length, with a maximum vertebrae length of 3.8 mm. A Hartigan Dip Test was conducted to test for unimodality using the maximum difference between the observed distribution and a unimodal distribution aimed to minimize the maximum difference. The dip test results indicated that the vertebrae

length distribution was multimodal (D = 0.0677, p-value < 2.2e-16), which shows that multiple size classes compose the vertebrae record.

A linear regression was run between the fish lengths and vertebrae lengths from the trawl survey samples in order to determine a relationship between vertebrae length and the size of fish. Using the regression equation, inferred fish length was calculated. Most of the fish that contributed to the vertebrae record range between 20-80 mm in length, which would correspond to age-0 juveniles for anchovy, sardine and hake, but would be consistent with both juvenile and adult life history stages for most myctophids.

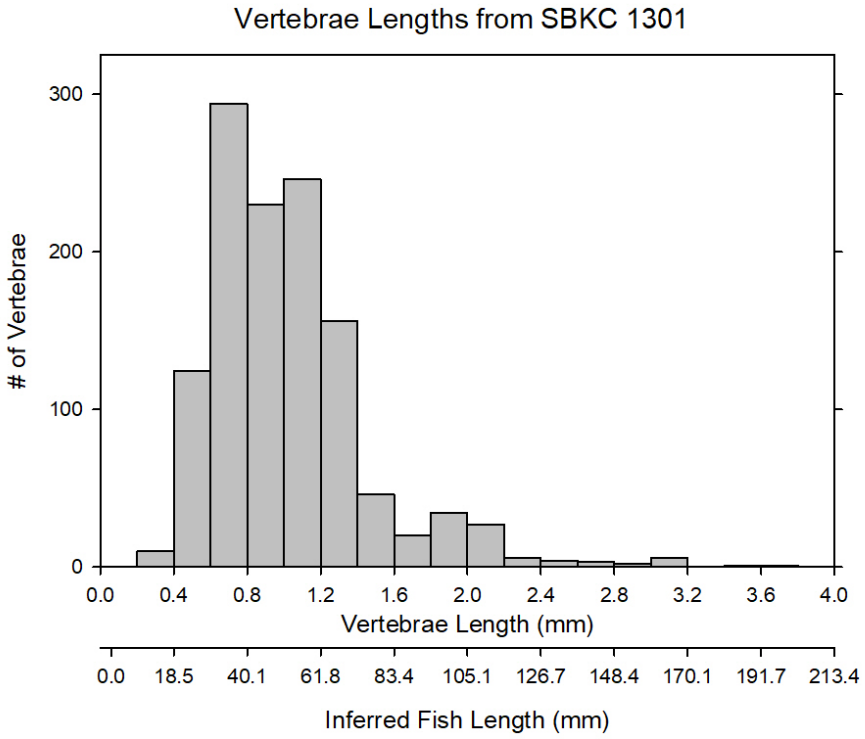

Figure 2.8. Histogram of vertebrae lengths measured from SBKC 1301 as well as inferred fish length based on comparison with vertebrae measurements collected from trawl samples.

2.4. Discussion

The SBB offers a detailed record of fish remains which provide evidence of long-term variability in small pelagic forage fish populations (Soutar and Isaacs, 1969; 1974; Baumgartner et al., 1992; Field et al., 2009; Salvatteci et al., 2019; O'Connell and Tunnicliffe, 2001). This study uses the largest volume of sediment ever compiled and examined to provide a nearly 2,000-year composite kasten core record to reconstruct population variability of sardine, anchovy, and hake scales, as well as a novel record of myctophid scales and a skeletal debris index composed of a compilation of many species. Multiple replicate counts from multiple cores provide the best outlier detection method of any paleo fish debris study to date which is discussed first. Then, comparisons between kasten cores and between composite core records are reviewed followed by the calibrations between SDR and biomass and potential causes for deviations between these two records. Finally, the Paleo Forage Fish Index is examined to compare the major forage fish contributors in the CCE and why the 20th century consists of the lowest values on record.

2.4.1 Nature of Outliers

The rigorous *Outliers from the Median of Standard Deviations (OMSD)* approach conducted in the present study is the first to develop a rigorous procedure to identify outliers and quantify the frequency of anomalous values when using fish debris within the sediment record to reconstruct long-term population variability. The outlier detection design is possible due to multiple replicate slabs per core in order to identify outliers and multiple cores to compare the frequency of outliers between cores. In many published studies, large peaks in SDR could be attributed to rapid increases in fish populations although some of these random pulses of flux

can cause false peaks in the SDR record. Some studies, such as O'Connell and Tunnicliffe (2001) and Rose (2013) identified outliers in their records by comparing the anomalous value to a threshold of two standard deviations away from the mean. This two standard deviation method may be fairly conservative, however, this approach takes the standard deviation and mean based on the entire core which may be biased by period of naturally occurring high scale fluxes. Additionally, this method does not identify many of the highly anomalous outliers since the outlier values are included in the mean and standard deviation calculation biasing the outlier threshold high. In contrast to the high proportion of sampling intervals containing outliers in the current study, O'Connell and Tunnicliffe (2001) identified less than one percent of samples as outliers and Rose (2013) corrected only one outlier from the scale record.

One of the major challenges in detecting outliers in the current study is determining a representative central tendency of the variability within a sampling interval. The median of all the standard deviations (MSD) from sampling intervals with means greater than one was used to reduce bias from sampling intervals with anomalously high debris counts from outliers (e.g. bone). Additionally, eliminating sampling intervals with a mean less than one reduces potential bias from sampling intervals with a high frequency of low debris counts (e.g. sardine), which would otherwise result in a low MSD. The MSD values are similar for each debris type between cores indicating that the MSD provides consistent outlier thresholds between cores. Additionally, debris types with similar average fluxes have similar MSD values.

Outliers could arise in several different ways. Since many small pelagics naturally lose their scales throughout their lifetime, scale outliers likely come from conglomerated pieces of fish due to sloppy feeding, though compact fecal matter and perhaps micro-accumulation zones

in the sediment could also produce concentrated pulses of fish remains. Scale outliers may range from a small piece of skin to a large chunk of fish that was not consumed as it sank to the seafloor. In some cases, outliers were determined to span multiple slabs or sampling intervals suggestive of a large piece of fish. For example, a sampling interval in the hake record consisted of four, two, 23, and 51 scales in each of the four slabs used for fish debris extraction. Since there is a thin chronological development slab in between the two anomalously high scale counts, the chunk of fish debris may be larger than the one-centimeter thick chronology slab. Additionally, another sampling interval in the hake record was made up of six, 34, 134, and two scales in each of the four samples. Since the number of scales along the lateral line of a hake range from 125 to 144 (Cohen et al., 1990), a single deposit of approximately 160 scales within two samples suggests that a large piece of fish was instantaneously deposited to the seafloor.

Skeletal debris, on the other hand, is more likely to arrive to the seafloor after a mortality event, such that the bone and vertebrae record is naturally made up of either chunks of fish (outliers) or fecal debris, which could be concentrated or spread out over the seafloor. Thus, the OMSD procedure only detects the most anomalous skeletal debris counts, likely coming from large pieces of fish. Within the bone record of all three cores, there are multiple examples of three or more sampling intervals from the same slab containing highly anomalous outliers suggesting that a piece of fish spanned multiple sampling intervals. Further, there is a sampling interval in the vertebrae record containing 33, 16, 34, and three vertebrae in each of the samples which did not correspond to anomalously high scale flux in the other cores. Additionally, there was a single sample containing 134 vertebrae surrounded by samples consisting of zero or one vertebrae per sample. Since many small pelagics have approximately 45-90 vertebrae (Hubbs,

1925; Clarke, 1936; Hart, 1973), it is likely that this sample contains multiple pieces of fish or a packed fecal excretion.

Fish debris sometimes pass through the guts of predators and are deposited to the seafloor via concentrated fecal excretions (Robinson and Bailey, 1981; Starensinic et al., 1983). Due to a high surface area to volume ratio, most scales are either digested or poorly preserved within fecal waste (O'Connell and Tunnicliffe, 2001). Unlike scales, skeletal debris is more likely to be passed through the guts of a predator intact, although the degree of degradation may vary. For example, bones and vertebrae were found to pass through the guts of some predators (e.g. black rockfish, hake, and most pinnipeds) but not others (e.g. lingcod; DeVries and Percy, 1982; Pierce et al., 1991; O'Connell and Tunnicliffe, 2001).

The finding of a greater proportion of outliers when the flux of that debris type is higher may be due an increase in regional abundance of forage fish and/or their predators. The positive relationship between the percentage of outliers identified with the average flux to the seafloor for each different debris type may indicate higher fluxes associated with higher biomass. When a species is more abundant, it is more available to predators and thus more likely to be eaten and deposited as outliers to the seafloor. However, the type of predator, rates of scale loss, and predator abundance could also affect the frequency of outliers.

2.4.2 Effects of Removing Outliers

Since the decision to remove outliers identified by the OMSD was based on the strongest correlations between cores before and after outlier removal (Table 2.3), it was determined that removal of outliers ranked Virtually Certain and Highly Likely for all debris types markedly

improved the relationships between cores. The average three-core correlation coefficients for sardine and anchovy in the current study (R = 0.65 and R = 0.64, respectively) are slightly greater than the correlation coefficients reported in Baumgartner et al. (1992; R = 0.53 and R = 0.54, respectively). The increase in shared variability may be attributed to the removal of outliers. Nonetheless, it could also be due to the use of smoothed composite data, which are known to increase correlations, however, autocorrelation from smoothed data has less of an effect with larger datasets/longer time series. Granted the cores in the present study share more variability than in past studies, the increase in shared variability is less than five percent despite roughly six times more sediment surface area from the kasten cores than in Baumgartner et al.'s (1992) piston cores. The two piston cores used in Baumgartner et al. (1992) have a surface area of nearly 100 cm^2 whereas the three kasten cores have approximately 600 cm^2 of sediment. The marginal increase in shared downcore variance suggests that the large increase in sampling area and removal of outliers in the present study does not necessarily result in a huge increase in shared downcore variance between cores.

Nonetheless, some of the records showed that a pulse of high flux in one core, identified as an outlier, was associated with low fluxes in other cores indicating that many true outliers were identified and removed (Figure 2.2). In contrast, there are cases when an identified outlier in one core is associated with high flux in the other cores suggesting that the high flux should not be identified as an outlier leading to an increase in Type 1 errors. The OMSD procedure may not detect all outliers stemming from chunks of fish, although these minor outliers do not have large effects on the SDR records.

Although up to 30 percent of sampling intervals were identified as containing outliers (Figure 2.3), as in the case of bones, the outliers do not have drastic effects on the overall timeseries. Since the outliers are more likely to occur when debris flux is higher, the majority of the outliers mostly just increase the magnitude of the flux during times when flux is already high. Thus, the removal of outliers typically does not change the overall shape and variability of the timeseries as seen in the comparison of three-core average correlation coefficients before and after outlier removal (Table 2.3). The three-core average coefficient of determination increased by an average of about 0.03 after outlier removal for sardine, anchovy, and hake suggesting that the presence of outliers did not highly affect the shared variance between cores. However, the myctophid coefficient of determination increased by 0.24 after outlier removal, probably because the average flux of myctophid is around five scales per year while there are some sampling intervals containing outliers with fluxes approaching 400 SDR, which would dramatically increase shared variability between cores. On the one hand, myctophid predators may be sloppy feeders depositing many chunks to the seafloor or the predators may not degrade scales during digestion which could lead to fecal excretions that are fully packed with myctophid scales. Although, on the other hand, myctophid species may be more deciduous than other small pelagic taxa. For example, myctophids from midwater trawl surveys commonly lose all or at least most of their scales, whereas sardine and anchovy often lose many but not all of their scales (Field, J.C., personal communication).

2.4.3 Differentiations in the Chronologies

There may be uncertainty in each of the two chronologies developed, whereby the varve count chronology is younger and the radiocarbon adjusted chronology is older and perhaps more accurate (Table 2.1). While varve count chronologies have been shown to miss some years due to erasure of laminations, the varve count chronology developed in the current study has fewer missed/undercounted varves because some five-year intervals are extended to longer intervals between homogenous sections to increase the shared variability. This approach added about 50 years to the original varve counts compared to Schimmelmann et al.'s (2016) 400-year correction to Baumgartner et al.'s (1992) composite time series.

Since the radiocarbon adjusted chronology modified the varve count chronology based on the line of best fit from the linear regression, the radiocarbon chronology provides better absolute dates. The adjusted radiocarbon chronology is not a perfect match with that of Hendy et al. (2013), although it provides the ability to compare the composite time series and Paleo Forage Fish Index to other long-term records.

One of the issues with adjusting the varve count chronology to the radiocarbon chronology is that many of the homogenous layers with radiocarbon dates provided by Hendy et al. (2013) could not be associated to homogenous layers in the kasten cores. In addition, many of the homogenous layers that were identified in one of the kasten cores were not present in the other cores in the current study. It is unclear if the homogenous layers result in deletions of material from bioturbations, which could explain why the varve count chronology is so much younger than Hendy et al.'s radiocarbon chronology.

In addition, another issue that may affect the chronological adjustments is that Hendy et al. (2013) made many corrections for changes in reservoir age, which, if applied to our chronology, at times would result in many five-year sampling intervals to become less than five years. These fine tuning of adjustments were not done in the current study in order to maintain the integrity of the five-year sampling intervals.

The chronology of the box core record, on the other hand, is similar to Hendy et al.'s (2013) chronology. While both chronologies are based on varve counts, more box cores in the current study revealed more varves down to the Macoma layer, which is set at 1832 in the current study and 1841 by Hendy et al. (2013). The chronologies are more closely aligned at the large olivine homogenous layer at the bottom of the box core record dated here with varve counts at 1746 and 1738 by Hendy et al. (2013).

2.4.4 Differences and Similarities Between Cores

Emphasis on using a compilation of many cores for reconstruction of paleo fish abundances has been emphasized in many studies (Baumgartner et al., 1992; Field et al., 2009; O'Connell and Tunnicliffe, 2001; Salvatteci et al., 2018) and this study uses a three-core composite kasten record along with different slabs (of varying surface area) from more than 20 box cores (Rose, 2013; Soutar and Isaacs, 1974) to increase sampling area within the last 200 years. Based on the cores used in the current study, there are differences in average scale flux between cores (Table A2) and composites of cores further reiterating the importance of a multi-core record to average out the differences in average scale flux.

While the shared variance between cores in the present study is similar with that of Baumgartner et al. (1992), there are greater between-core differences found here (i.e. F-ratio is larger), which may be due to the chronostratigraphic match (or mismatch) between cores. Chronological uncertainties may stem from misidentifying/miscounting varves, interruption of homogenous layers across different sampling intervals in different cores, or in the case of the current study, lack of available x-radiographs of varves for all core sections. The current study developed the varve count chronology using photos of the cores prior to sampling to match varves and homogenous layers in addition to the comparison of peaks and absences in the SDR time series between cores. There was often a lack of clear varve sequences in the x-radiographs throughout the cores to tie the chronologies of each core together. Additionally, comparison of peaks in SDR using the smoothed data may result in differences in chronology between cores, which also would have increased the noise.

Another factor that could have played a role in the differences in average flux between the three kasten cores is the change in sieve size in SBKC 1302. SBKC 1302 did not have the lowest mean scale flux for the anchovy, hake, or myctophid records suggesting that the change in sieve size did not affect the retention of scales. SBKC 1302 contained the lowest average flux in the sardine record, however, sardine have the largest scales of the four major taxa further suggesting that the low scale flux was not a function of sieve size in SBKC 1302. The skeletal debris records, however, recorded much lower mean skeletal debris flux in SBKC 1302 than in the other two cores. It is likely that small, thin bones, such as spines, and fragmented bones passed through the larger sieve size and these bones are not reflected in the timeseries. The composite kasten core for the bone and skeletal debris records do not include SBKC 1302 for this reason.

While the relative peaks and troughs in debris flux align between the composite kasten and box core records, the significant differences in average flux between these composite core records revealed by the Mann Whitney-U tests shows that even multi-core averages result in some differences (Table A8). In some cases, such as in sardine, anchovy, and hake, the average flux in the box core record is greater than the average flux in the composite kasten cores for the period of overlap. However, the average myctophid SDR is greater in the box core suggesting that this is not a systematic difference and is a function of debris type. Furthermore, there are periods in time where the flux of the kasten core is greater than the flux of the box core in the sardine, anchovy, and hake records and vice versa for myctophid. It is possible that there may be bias in the sampling procedure as there could be differences in the frequency of scales identified versus scales categorized as unidentifiable between core types, but this seems unlikely to explain many of the observed differences.

Although the correlation coefficients between the individual kasten cores are similar to the correlations between composite core records, there may be several reasons why the correlation is stronger between the kasten cores for some debris types and between the composite records for others (Table A9). On the one hand, the correlation between the three kasten cores are from less sediment areas and are not composites from multiple cores, which could suggest weaker correlations as seen in the hake, bone, and vertebrae records. On the other hand, the kasten cores are about four times longer than the box cores with periods of higher flux and extended periods of low flux which may increase shared variability between the kasten cores such as in sardine, anchovy, and myctophid scales. Chronological uncertainties could affect both the correlations between kasten cores as well as between composite core types, however the

chronostratigraphic match between core tops may have less uncertainty than further downcore. The examination of the reproducibility between kasten cores and between composite core types further emphasizes the need for a multicore record.

2.4.5 The Effect of Fishing on SDR Variability

Based on the scale record, the development of commercial fisheries did not appear to have a large impact on the variability of SDR. Salvatteci et al. (2012) determined that the ratio of scales to skeletal debris increased during the development of the Peruvian anchoveta fishery, possibly suggesting that scale loss would be higher during fishery operations due to increased trauma to the fish or an increase in scale loss due to predator avoidance mechanisms. Alternatively, the high ratio of scales to skeletal debris could be due to the skeletal debris being removed from the system and used for fish meal. Using the idea that commercial fishing increased the flux of scales to the seafloor, the SDR of sardine and anchovy scales did not increase during the development of the fisheries suggesting that fishing did not greatly impact the variability of SDR. At the beginning of the sardine fishery, there was an increase in SDR in the 1910-1920s, however, since fish catch was low at this time, a large increase in scales would not be expected to be due to the fishery. Furthermore, there was a decline in sardine SDR in the 1930s during the heyday of the fishery. Similarly, anchovy scale flux remains fairly constant from the development of the fishery around 1965 to the peak of the fishery in the 1980s.

The hake scale flux record, however, showed evidence of a decline in scales around 1965 during the development of the foreign fleet hake fishery off the west coast of the United States. There was an additional decline in the late 1980s, which coincides with the development of the

US hake fishery and increased landings off California. However, hake scales collected from the SBB primarily originate from juveniles (Soutar and Isaacs, 1974; Rose, 2013), whereas the hake caught in the fishery are predominantly adults. The correlations in the current study between hake SDR with the A-R Biomass Index was greater than with the age-2+ biomass estimates further suggesting that recruits and juvenile hake play a major role in the hake SDR records. This may suggest that the decline in hake SDR was attributed to a decline in abundance or shift in distribution of juvenile hake and would not represent a large effect from the fishery.

2.4.6 Species Specific Relationships between SDR with Abundance, Migration, and SST

There are many factors that may affect the variability of scale flux as it is deposited to the seafloor. The most obvious explanation for variations in SDR is changes in species abundance. However, migration and changes in distribution may also play major roles in the variability of the SDR records. One way to consider consequences of potential changes in distribution on SDR is to examine deviations in the ratio of scale flux to biomass and compare them to other sources of information such as SST records, fish catch, or the distribution of eggs and larvae. Since the biomass estimates in the current study are calibrated from SDR with the A-R (Adult and Recruit) Biomass Index, total biomass is always larger than the age-2+ biomass estimates (since recruit biomass is included).

Scale widths examined from other studies indicate that most of the sardine and anchovy scales found within the sediment record originate from one-year old fish or recent recruits (Soutar and Isaacs, 1969; Rose, 2013). There is a presence of scales that originate from age-2+ fish, although these are more common in the anchovy record (Rose, 2013). While there is no

clearly documented relationship between hake scale width and age, a comparison between the average scale width from the sediment with scales collected from samples of hake between 13-15 cm suggests that the scales collected from the sediments primarily correspond to age-1 fish (Rose, 2013). However, it is likely that additional age classes contribute to the hake scale record as well.

Sardine

Although major changes in the sardine SDR record follow periods of high and low biomass throughout most of the 20th century, the ratio of SDR to biomass is anomalously higher in the 1990s than in the 1930s (Figure A15), which could be explained by numerous factors. One explanation for the deviation between the ratio of scale flux to biomass in the 1930s and 1990s is that there could be inaccuracies in the biomass estimates in more recent decades due to the lack of high-volume fishery-dependent data that was available in the 1930s.

In contrast, if the biomass estimates are assumed to be fairly representative of changes in population abundance since the 1930s, then the differences in the ratio of SDR to biomass could be due to changes in sardine distribution, perhaps following MacCall's Basin Model Hypothesis (MacCall, 1990). This hypothesis suggests that when fish abundance is high, as in the 1930s and 1940s, the distribution of the population expands; however, when population abundance is low (i.e. 1990s), the distribution of fish contracts within their central range. Since biomass estimates and fish catch are greater during warmer periods, population numbers and subsequent range expansion may be more favorable in anomalously high SSTs and the positive phase of the Pacific Decadal Oscillation (PDO) beginning around 1925. However, periods of high

sardine abundance associated with low SSTs may indicate that there are also other factors that influence sardine population variability.

Although egg and larval information are not available for periods before the development of CalCOFI in 1949, the Canadian sardine fishery developed in 1916 suggesting that sardine were already present in the far northern region of their distribution with larger individuals migrating further north (Field et al., 2009). The increased abundance and wide distribution of the sardine population at the time, which could be due to higher SSTs, may help explain the low scale to biomass ratio seen in the 1930s. Landings of Pacific sardine are well known to have collapsed sequentially from north to south during the 1940s and 1950s (Radovich 1982). It is known that in the mid-1940s, there was a shift from positive to negative PDO associated with low SSTs, which may be an underlying cause of the population collapse and movement of sardine south.

When abundance was low from 1950-1984, a period coinciding with predominately low SSTs, sardine egg and larvae distribution maps suggest that sardine were primarily distributed in the southern region of the Southern California Bight (SCB) and near Punta Eugenia, Mexico (Moser, 2001), which would result in few scales being lost in or around the SBB. Yet, there are still the occasional presence of scales and fish catch (Rose, 2013) during this time. Additionally, there is a presence of scales around the 1958/59 El Niño along with a small increase in sardine landings despite the biomass estimates showing no change, which may suggest that the increase in SST due to the El Niño caused distributional shift towards the northern region of the SCB. Since maps of sardine egg and larvae distribution show an increase in abundance in the northern part of the SCB during periods of high SST and a more southerly distribution during years with low

SST, it seems probable that an increase in SST could result in high levels of SDR in the basin due to a northward shift in population distribution.

In the 1990s, the ratio of sardine scales to biomass is anomalously high, which may suggest that a greater proportion of the population is distributed around the SBB. The distribution of sardine eggs collected by CUFES (Continuous Underway Fish Egg Sampler) since 1996 (Checkley et al., 2000; Weber, 2019) suggests that sardine are primarily distributed offshore, both north and south of Point Conception, which may suggest increased flux to the basin. During years with high SST, sardine are typically distributed closer to shore, such as in 1996-1998, whereas sardine are typically found further from shore in cooler years (i.e. 1999-2001; Weber 2019). The coastal distribution during periods with warmer SST may imply that more scales are deposited to the SBB. However, regardless of the distribution, recruits are often more coastal than adults and schools are constantly shifting adding potential variability to the flux of sardine scales.

An interesting observation in recent layers of the sediment records, along with some historical observations, is the high sardine scale flux during periods of anomalously low SST which is not consistent with the notion of higher sardine recruitment in warmer years (Zwokinski and Demer, 2012). The peaks in scale flux during the anomalously cool periods from 1890 to 1900 and 1910 to 1925 are about two and three times greater than the SDR during the heyday of the sardine fishery, respectively. Evidence for low SSTs comes from ICOADS SST time series, with additional evidence from shifting plankton assemblages with primarily subtropical species dominating during warmer years and subpolar and temperate species more prevalent during cool SSTs (Field et al., 2006).

Since the late 1800s and early 20th century are predominately cool in the CCE, it is possible that the high SDR is due to a concentration of sardine in and around the basin; however, observations from naturalists show that the presence of sardine was recorded in the northern region of the CCE, around British Columbia (Field et al., 2009), supporting the notion that the population was large enough to expand north at this time. Interestingly, the low sardine flux from 1900-1910 corresponds to a period of relatively warm waters (based on the presence of subtropical plankton and low numbers of subpolar and temperate taxa) amidst an extended period of low SSTs (Field et al., 2006). The low sardine SDR could be due to lower recruitment during the time, being distributed away from the SBB, or some other factor. The sardine scale flux in the late 19th and 20th centuries may suggest that sardine are not strictly associated with warm water and many other factors may play a role in their abundance and distribution. Alternatively, SST could be a proxy for some other process, and the relationship between SST and the other process varies through time.

Anchovy

The lack of a significant relationship between SDR and the A-R Biomass Index could be due to multiple factors. A potential source of variation between SDR and biomass may stem from inaccurate biomass estimates. Thayer et al. (2017a), which were used for the adult biomass estimates in the A-R Biomass Index, corrected for hyperstability when the population contracts whereas the recruitment estimates from Jacobson et al. (1995) did not account for the nearshore concentration of fish. However, the correlations between SDR and biomass estimates from Thayer et al. (2017a) as well as between SDR with recruitment estimates from Jacobson et al.

(1995) were also insignificant suggesting that there may be other factors impacting the relationship between SDR and estimates of abundance. Additionally, the short time series of both biomass and recruitment estimates may influence the deviations of scale flux to biomass. The correlation between SDR and the A-R Biomass Index may be better if updated recruitment estimates were available. For example, both biomass (from Thayer et al., 2017a) and SDR begin to increase in the beginning of the 21st century until the end of the record in 2006.

On the one hand, the insignificant relationship between SDR with biomass may be due to changes in SST. Anchovy are known to be associated with coastal upwelling and the gradient between low and high SSTs, typically between 13-15ºC (Weber, 2019), which may affect population abundance and distribution. During years when upwelling weakens and/or SST increases, such as El Niño years, the anchovy population may be more likely to decline and contract into coastal waters of the northern SCB (Hewitt, 1980; Weber, 2019) resulting in a higher ratio of scales to biomass. For example, anchovy were distributed further north around the SBB during the warmer years such as the 1958/59 El Niño (Kramer, 1970), supporting this notion. Furthermore, in the 1990s, during the positive phase of the PDO and anomalously high SSTs, the ratio of SDR to biomass was high (Figure A17), which could reflect a small anchovy population closer to the SBB.

In contrast, when abundance is high, the population may expand its distribution offshore as well as north and south of their central distribution. The early 1970s was a period of lower SST coinciding with relatively high biomass and high SDR suggesting that the population may be abundant and distributed north and south of the SBB, but still centered around the basin. In anomalously cool years, such as in the 1950s, anchovy eggs are often distributed from the

southern part of the SCB to Punta Eugena off Baja California (Hewitt, 1980; Weber 2019), which may result in low SDR in the SBB. These relationships between abundance and the ratio of scales to biomass may suggest that when biomass is low, SDR may be a reflection of anchovy abundance, whereas when biomass is high, SDR could be more affected by distribution.

On the other hand, the early 20th century is an anomalously cold period with relatively high anchovy scale flux suggesting that factors other than SST affect the relationship between SDR and biomass. In contrast, there is a low ratio of SDR to biomass during the mid 1980s, coinciding with high SST, implying that high SDR may not always be due to a northerly, coastal contraction of the population associated with warm water. The anomalously high SST in the late 20th and early 21st centuries might suggest that the anchovy population was concentrated near the SBB, however, the low SDR values at the end of the record indicate that something else may be influencing anchovy SDR variability.

Hake

The calibration between hake scale flux and the A-R Biomass Index was better than other abundance estimates indicating that hake SDR is a combination of recruits and adults, which is consistent with the inferred ages based on scale widths from Rose (2013). SDR often increases after large recruitment pulses, such as in 1986 (Figure A19), further suggesting that the hake SDR record is largely driven by juveniles and recruits.

One factor that may impact the relationship between SDR and biomass is changes in distribution as a result of deviations in SST. During warm years, hake are typically distributed north and usually offshore around Point Conception and the SBB (Hollowed, 1992). In addition,

the ratio of hake scales to biomass is generally higher during periods of high SST, such as from 1983 to 1998. The distribution of hake north of Point Conception may lead to an increase in scale flux in the SBB cores since the California Current can transport scales south and into the basin. In contrast, hake larvae are typically found south of the Channel Islands during cold years (Hollowed, 1992), which may explain why there is low flux to the SBB during cooler years (e.g. 1970s). The distribution of fish offshore and south of the Channel Islands may cause scales that are lost to be transported south by the California Current since the northward flowing Southern California Counter Current is typically considered closer to shore.

Despite higher hake SDR coinciding with higher SSTs in the modern record, there is evidence that high (low) hake SDR can occur during periods of anomalously low (high) SSTs suggesting that SST is not the sole driver of hake SDR variability. For example, there is high scale flux from around 1880 to 1920, which is associated with the coolest waters in the last 150 years (based on IOCADS SST time series). Further, the hake SDR values in the 21st century are the lowest on record corresponding with periods of anomalously high SST. Therefore, the variability in hake SDR is likely to be influenced by many different factors.

Myctophid

Currently, there are no accurate myctophid biomass estimates to be used for SDR calibrations; although, visual comparison of SDR with mesopelagic biomass estimates based on larval abundance and acoustic/trawl surveys (e.g. Koslow and Davison, 2016) suggests that there is unlikely to be a strong relationship between myctophid SDR and biomass. The decline in myctophid biomass at the end of the 20th century does not match the timing of the decline in

SDR suggesting that there are other factors that may play a role in the variability of myctophid scale flux. Myctophid SDR is not expected to be heavily affected by migration and changes in distribution since most myctophids do not participate in coastal, horizontal migrations. Some species participate in diel vertical migration, however, their spatial distribution does not vary as widely as epipelagics thus myctophid scale loss may not be a function of horizontal changes in distribution.

Since myctophids primarily inhabit the mesopelagic, variations in myctophid SDR are less likely to be due to changes in SST. However, some myctophid species are associated with warm water whereas others prefer cooler water so changes in ocean temperature may affect species assemblages (Koslow et al., 2014). As SST continues to increase in the 20th century, myctophid biomass in the CCE may become dominated by warm affinity species, which may affect rates of scale loss since these species may have differential scale shedding rates.

The 1950s was a period with low SST coinciding with high SDR and moderate biomass estimates (Koslow and Davison, 2016) suggesting that the mesopelagic could have been dominated by taxa with cool water affinities with high rates of scale loss. The 1990s, however, was warmer with high biomass (Koslow and Davison, 2016) and relatively low scale flux implying that deviations in the ratio of SDR to biomass might be affected by changes in species assemblage with warmer affinity myctophids losing less scales than cool-water taxa. The 21st century coincides with relatively low SDR and biomass estimates (Koslow and Davison, 2016), which may suggest that myctophid abundance is low despite the notion that myctophid species with warm water affinities lose less scales than taxa with cool water affinities.

Another factor that may affect myctophid SDR is changes in midwater oxygen concentration. From 2000 to 2008, mean oxygen concentration at 300 m declined by about 20% within and outside the SBB and the oxygen minimum zone shoaled by about 40 m coinciding with a decline in myctophid biomass (Bograd et al., 2008; McClatchie et al., 2010) and a period of low scale flux.

2.4.7 Meaning of the Skeletal Debris Record

While both the fluxes of scales and skeletal debris are a function of fish abundance, the differential mechanisms of loss (and perhaps sinking) means these two records could be considered semi-independent. Fish scales from the four major species in the current study are continuously lost throughout the fish's lifetime, though rates of loss could vary with age, and may be higher during predator avoidance (Field et al., 2009). In contrast, skeletal debris are only deposited to the seafloor after a mortality event, primarily via fecal plumes or as conglomerated chunks of fish due to sloppy feeding, which makes skeletal debris a better representation of regional prey availability and consumption compared to scale deposition.

Since the size and shape of a scale differs from that of skeletal debris (or a chunk of fish containing skeletal debris), the sinking rate of each debris type may be subject to differential horizontal transport via currents. Scales are often longer, wider, and thinner than skeletal debris with a higher ratio of surface area to volume, which may cause the scales to sink slower through the water column. As a result, scales may be more likely to be affected by currents and arrive to the SBB from a broader geographic range. In the spring and summer, the California Current may transport fish debris that was lost north of the SCB south into the SBB as the current wraps

around San Miguel Island. In the fall and winter, however, scales and skeletal debris may be more likely to be transported to the SBB from the southern region of the SCB from the Southern California Counter Current. Thus, scales may be transported into the SBB from fish located further north or south and represent a wider distribution of fish causing overall differences in flux between scales and skeletal debris.

One of the biggest issues with the skeletal debris record is ascertaining the relative contributors to the bone and vertebrae SDR timeseries and determining if the skeletal debris records should be incorporated in the Paleo Forage Fish Index, since skeletal debris may be primarily composed of one or two taxa. A study identifying otoliths using shape and elemental composition from SBB box cores determined that nearly 85% of the otoliths originated from meso- or bathypelagic species and less than half of one percent came from sardine (Jones, 2016). However, positive correlations in the current study between skeletal debris with both sardine and myctophid scales suggests that the skeletal debris record is made up of multiple species, including at least sardine and myctophid. When visually comparing the composite time series, it is clear that the bone and vertebrae records take features of multiple SDR records such as the high skeletal debris SDR around 600 coinciding with high flux of both sardine and myctophid scales during the same period (Figure A2).

It is also likely that species that do not make up a major proportion of the scale record contribute to the skeletal debris time series. There are periods in time where skeletal debris SDR is high coinciding with low fluxes of sardine and myctophid scales suggesting that skeletal debris may arrive to the seafloor from different taxa. Additionally, Jones (2016) found that hake, rockfish, and anchovy made up seven, five, and four percent of the otolith record, respectively.

These species may have lower scale shedding rates, such as rockfish (Patterson et al., 2002), or may only be abundant in the SBB during some periods in time. For example, Pacific saury larvae were found in coastal waters from 1951-1976 during the period of cooler SST and then shifted their distribution more offshore after the 1976 regime shift associated with warmer SST (Moser et al., 2001).

After converting vertebrae length measurements from SBKC 1301 to estimated fish length, most fish that contribute to the vertebrae record are between two and eight centimeters in length (Figure 2.8). While it is clear that vertebrae length increases as fish length increases, this size range coincides with the four species of myctophids in which samples were obtained for the current study as well as juvenile Pacific hake and small northern anchovy. Additionally, the multimodal distribution in vertebrae length indicates that there are multiple size classes, and therefore, species, contributing to the record. The examination of vertebrae further suggests that the skeletal debris record is made up of many different taxa, and thus it is justified to incorporate skeletal debris in the Paleo Forage Fish Index.

2.4.8 Historical Changes in Small Pelagic Fish Abundance

The largest centennial scale change in the Paleo Forage Fish Index occurs around the year 1000, whereas there is less of a detectable change in forage fish abundance during the shift from the Medieval Climate Anomaly (MCA) to the Little Ice Age (LIA; Figure 2.6), which could suggest that there was a large-scale shift in climatic, circulation, and/or productivity in the CCE around the year 1000. The Paleo Forage Fish Index and the relative abundance of *Gephyrocapsa oceanica*, which has been used as a proxy for SST (Beufort and Grelaud, 2017), follow the same

general trend over the last two millennia. Both records are primarily above the baseline/abundant during the early part of the record until about 1000 (~900 radiocarbon adjusted chronology) followed by a period of predominately negative anomalies/less abundant from around 1000 to 1700 (~900-1700 radiocarbon adjusted years).

G. oceanica is abundant from before 300 to around 1000, indicative of a much warmer California Current (Beufort and Grelaud, 2017) and coincides with high fish debris flux which has been shown to increase during periods of high SST. Further, both the flux of fish debris and the relative abundance of *G. oceanica* show evidence of a decline around 1000 until at least the 1600s, largely following the low SSTs associated with the MCA. The relationship between *G. oceanica* with the Paleo Forage Fish Index might suggest that fish debris flux in the SBB is biased high during periods of anomalously high SSTs, which may be a result of a greater density of small pelagics in the northern SCB around the SBB. However, a time series of at least 24 diatoms and 10 silicoflagellates did not detect a noticeable shift towards taxa with warm-water affinities around 1000 (Barron et al., 2008), suggesting that the relative abundance of a single species (i.e. *G. oceanica*) may not be an accurate proxy for SST.

Nevertheless, an additional piece of evidence that may suggest that *G. oceanica* follows long-term SST patterns is the increase in the relative abundance during the 20th century (Beufort and Grelaud, 2017), which coincides with some of the highest SST anomalies in the last two millennia. Despite the notion that scale flux increases with high SST, the Paleo Forage Fish Index shows the lowest values on record in the 20th century, possibly suggesting the presence of a large-scale climate shift which may be attributed to anthropogenic influences such as increased

emissions of greenhouse gasses due to industrialization in the early 20th century or even effects from changes in land use much earlier in time (Ruddiman, 2003).

Similar to the Paleo Forage Fish Index, Finney et al. (2010) detected a large shift in fish productivity around 1000. Finney et al. (2010) showed a negative relationship between sockeye salmon abundances in Alaska with sardine and anchovy from the SBB from around 300 to 1900, which he speculated may be attributed to shifts in primary production due to large-scale changes in SST that could be associated with variations in the Aleutian Low-Pressure System. For example, the northeastern Pacific was likely cooler during the LIA, with conditions similar to the positive PDO, and associated with higher levels of productivity and increased Alaskan salmon abundances. However, the CCE was relatively warmer which may have coincided with lower primary production resulting in low Paleo Forage Fish Index values from around 1400 to 1700. Nonetheless, sardine and anchovy positively covary with Alaskan salmon during most of the 20th century, which further suggests that large-scale climatic forcing influenced fish abundances prior to the 19th century. Beginning around the 1800s, a climate reorganization throughout the northeastern (or greater) Pacific may have been affecting the composition, distribution, and abundance of small pelagic fishes in a way that is different than the past millennia.

In contrast to the dramatic shift from positive to negative anomalies seen around the year 1000, the Paleo Forage Fish Index does not show a clear change in forage fish abundance from the MCA to the LIA, which has been noted in the literature in terms of changes in SST, precipitation, and plankton assemblages (Graham et al., 2007; Barron et al., 2008). The MCA is described as having cool SST (Graham et al., 2007) in the CCE between ~800 and 1350 and coincides with periods of negative forage fish abundance anomalies following the notion that low

SDR is attributed to low SST. The LIA, however, is typically characterized as warmer SST in the CCE between ~1400 and 1800 (Graham et al., 2007), which might suggest higher fish abundances based on the relationship with SST in the past two millennia. However, the average value of the Paleo Forage Fish Index during the LIA is negative and less than the average Paleo Forage Fish Index value during the MCA. This relationship may suggest that small pelagic abundances were not largely impacted by the climate shift from the MCA to the LIA and other large-scale factors particularly on multi-decadal to centennial timescales may have played a role in the historical abundance and distribution of forage fish.

2.4.9 Major Forage Fish in the 20th Century

Throughout periods of the 1930s and from the 1960s to the end of the record, the Paleo Forage Fish Index, along with the 95% confidence limits (Figure A14), have been below the baseline, which may suggest that forage fish abundances have been declining due to increases in SST associated with the 20th century warming trend, however, many other factors could also play a role in the reduction of fish. The Paleo Forage Fish Index and composite SDR records suggested that high fish debris flux was generally associated with higher SSTs, however, the 20th century is unlike the last two millennia and the high SSTs correspond to anomalously low forage fish abundances. This unexpected relationship could be evidence of a climate reorganization following the LIA that could be due to anthropogenic induced warming as a result of changes in land use and increased emissions.

Since the Paleo Forage Fish Index is based on the composite box core record in the 20th century, which is composed of various slabs of multiple different cores, comparisons of box core

flux in the 1970s to the end of the record determined that the box cores were not biased towards lower flux in this period. However, the lowest values on record from 2000 to 2006 are derived from a single box core and caution must be taken when interpreting these values.

Extended periods of anomalously low values in the Paleo Forage Fish Index persisted in the 1930s and 1960s, which may be impacted by a number of different factors. On the one hand, the negative abundance anomalies in the early 20th century could be attributed to natural variations in population abundance since the 1930s and 1960s are not significantly different than other periods of low abundance in the last two millennia. Small pelagic forage fish are known to vary with factors such as SST which may cause natural fluctuations in abundance associated with large-scale forcings such as PDO. On the other hand, these periods of extended low values could be the first evidence of impacts on forage fish abundance from the 20th century warming trend. The warming trend was first detected from a shift towards primarily subtropical plankton in 1925 with further evidence of warming in the 1970s (Field et al., 2006). The shift in plankton assemblages may parallel the low abundances of forage fish, which may both be subject to changes in temperature.

The anomalously low values in the Paleo Forage Fish Index after the 1970s are likely due to increases in SST, although many factors can impact forage fish abundances and distribution. In 1976/77 there was a regime shift associated with a deepening of the Aleutian Low-pressure System (i.e. positive phase of the PDO) and an increase in SST in the eastern Pacific (i.e. CCE: McGowan et al., 2003), which coincided with the beginning of the longest period of negative anomalies in the Paleo Forage Fish Index (Table A10). Following the negative trend of the Paleo Forage Fish Index, the southern California power plant intake time series revealed that nearshore

fish abundances declined dramatically from 1970 to the 2000s, predominately in fishes with cool water affinities (Koslow et al., 2015). This decline of cool water, coastal taxa further could suggest that the increase in SST following the 1976/77 regime shift lead to a shift in abundance, distribution, and species assemblage of small pelagics.

The development of commercial fishing is unlikely to be the primary cause of the declination of forage fish abundance since the 1930s reduction of forage fish occurred prior to the development of the anchovy and hake fisheries. Soutar and Isaacs (1974) were the first to suggest that the 1940s reduction of California sardine may be attributed to natural variability rather than overfishing. Rose (2013) compared mean scale flux before and after the fishery for sardine, anchovy, and hake was considered fully developed (i.e. 1934, 1967, and 1984, respectively) and determined that despite a significant difference in mean flux before and after the fisheries, the timing of the declines better corresponded to the warming events. Additionally, the upper bound of the 95% confidence interval of the Paleo Forage Fish Index (Figure A14) is below the baseline for parts of the 1930s and 1960s suggesting that all species and skeletal debris is low during this period and the low values are not attributed to a low abundance of a single species being fished. Miller and McGowan (2013) analyzed the power plant cooling water intake time series and found a declination of fish abundances in the SCB that included both exploited and unexploited taxa. Since evidence of unexploited species, such as myctophids, declined in the late 20th century, the reduction of biomass is not likely to be greatly impacted by commercial fishing, but rather driven by the increase in SST.

In the 21st century, paleo sediment records and biomass estimates indicate that small pelagic forage fish abundance remains low, commonly at or below abundance levels of the 1970s

(Hill et al., 2016; Thayer et al., 2017a; Berger et al., 2019). Pacific sardine are an actively managed coastal pelagic species, however the fishery has been closed since 2015 and the stock is currently declared overfished. While the term 'overfished' may not be the best language, sardine biomass estimates are below a fishable threshold, which is likely in part due to a low abundance, perhaps associated with the increase in SST. Northern anchovy are considered a monitored taxon although formal assessments are less frequent. However, recent catch rates are an order of magnitude less than historical catch rates (NMFS, 2009), which may suggest that abundances are low and the low catch is not due to low effort.

The continued decline of small pelagics has been and will further impact the CCE. Small pelagics are important forage for many large predators in the CCE including piscivorous fish, marine mammals, seabirds, and elasmobranchs (Koehn et al., 2016). Forage fish, such as sardine and anchovy, are more nutritious than other prey items due to their high fat and oil content (Koehn et al., 2016). In the early 20th century, there were fewer large predators, specifically marine mammals, than in the late 20th and 21st century and these populations have been recovering since the 1960s. As forage for these predators continues to decline, the large predators will have to prey switch and find areas of high food. In the last few decades, the largest removal of forage fish in the CCE came from demersal fish, marine mammals, and seabirds, respectively (Thayer et al., 2017b). In 2016, there was an increase in juvenile sea lion strandings associated with starving pups in southern California that was speculated to be due to the lack of nutritious available prey (McClatchie et al., 2016). As SST continues to increase throughout the 21st century, the future of small pelagics and those that rely on forage fish is questionable.

2.5. Conclusion

The OMSD procedure developed here found that the debris records may range between slightly over one percent (e.g. sardine SBKC 1001) and up to 30% (e.g. bone SBKC 1301) of sampling intervals that contain outliers, although outliers predominantly occur during periods of high fish debris flux and had a minor effect on the overall nature of the downcore records.

Examination of the three cores in the current study demonstrated the importance of using a multi-core composite record to reconstruct population variability since there are some differences in average flux and downcore patterns between cores. Comparisons between the three individual kasten cores as well as between composite kasten and composite box core records revealed significant differences in average flux. Although, in some cases a core with higher average flux could have a period of time with lower flux than the other cores. The observation that fluxes of some debris types are greater in the box cores while others are greater in the kasten cores suggests that this difference in average flux is a function of debris type. In addition to differences in average fluxes, many of the differences in shared downcore variability between the three kasten cores are likely caused by small differences in chronology along with differences in core specific debris flux.

The novel, skeletal debris record is largely composed of sampling intervals containing identified outliers, which may partially explain why there is less shared variability between cores. Since all skeletal debris are deposited to the seafloor after mortality events and a portion is likely deposited as conglomerated chunks of fish from sloppy feeding, the skeletal debris record reflects prey availability and total consumption. The multimodal distribution of vertebrae measurements from SBKC 1301 suggest that the vertebrae come from fish of different size

classes, most often between two and eight centimeters in length. Likewise, the weak positive correlations between skeletal debris with sardine and myctophid scales suggest that at least these two species contribute to the variability in skeletal debris. Nonetheless, it is likely that other taxa that are highly abundant at any given time also contribute to the skeletal debris record, particularly since there are periods of high skeletal debris flux when both sardine and myctophid SDR are low. The determination that the skeletal debris record is a compilation of at least multiple species, thus reflecting prey availability, and are deposited to the seafloor in a different fashion than scales justifies the inclusion of skeletal debris record into the Paleo Forage Fish Index.

Comparisons of the composite records and Paleo Forage Fish Index, representing a compilation of the five time series, suggests that SDR may be biased high during periods of anomalously high SST, which may be attributed to changes in abundance or shifts in species distribution toward the SBB. However, the SDR during the 20th century does not follow this trend with anomalously high SSTs coinciding with the lowest Paleo Forage Fish Index values on record. The Paleo Forage Fish Index indicates that the period of prolonged negative anomalies is first detected in the 1930s, before commercial fishing of most species, with further decline seen after the 1960s and 1970s, which suggests that the 20th century warming trend may play a major role in the low SDRs. Since the end of the record, biomass estimates of all four major forage fish taxa remain low amidst rising temperatures.

References:

Barron, J., Bukry, D., Field, D. (2008). Santa Barbara Basin diatom and silicoflagellate response to global climate anomalies during the past 2200 years. Quaternary International. 1-11.

Baumgartner, T. R., Soutar, A., & Ferreira-Bartrina, V. (1992). Reconstruction of the history of pacific sardine and northern anchovy populations over the past two millennia from sediments of the Santa Barbara Basin, California. CalCOFl Rep. 33, 24-40.

Baumgartner, T.R., Soutar, A., Riedel, W. (1996). Natural time scales of variability in coastal pelagic fish populations of the California Current over the past 1500 years: Response to global climate change and biological interaction. California Sea Grant Report, R-040, 31-37.

Beamish, R., Benson, A., Sweeting, R., Neville, C. (2004). Regimes and the history of the major fisheries off Canada's west coast. Progress in Oceanography, 60, 355-385.

Beaufort, L., Grelaud, M. (2017). A 2700-year record of ENSO and PDO variability from the Californian margin based on coccolithophore assemblages and calcification. Progress in Earth and Planetary Science, 4:5.

Berger, A.M., A.M. Edwards, C.J. Grandin, and K.F. Johnson. (2019). Status of the Pacific Hake (whiting) stock in U.S. and Canadian waters in 2019. Prepared by the Joint Technical Committee of the U.S. and Canada Pacific Hake/Whiting Agreement, National Marine Fisheries Service and Fisheries and Oceans Canada. 249.

Bograd, S. J., C. G. Castro, E. Di Lorenzo, D. M. Palacios, H. Bailey, W. Gilly, and F. P. Chavez (2008), Oxygen declines and the shoaling of the hypoxic boundary in the California Current, Geophys. Res. Lett., 35.

Checkley, D. M., Dotson, R. C., & Griffith, D. A. (2000). Continuous, underway sampling of eggs of Pacific sardine (Sardinops sagax) and northern anchovy (Engraulis mordax) in spring 1996 and 1997 off southern and central California. Deep Sea Research Part II: Topical Studies in Oceanography, 47(5-6), 1139-1155.

Clark, F. (1936). Variations in the number of vertebrae of the Sardine, Sardinops caerulea (Girard). Copia. 3, 147-150.

Clemens, W.A. and Wilby, G.V. (1961). Fishes of the Pacific coast of Canada. 2nd ed. Fish. Res. Bd. Canada Bull. (68):443.

Cohen, D.M., T. Inada, T. Iwamoto and N. Scialabba. (1990). FAO species catalogue. Gadiform fishes of the world (Order Gadiformes). An annotated and illustrated catalogue of cods, hakes, grenadiers and other gadiform fishes known to date. FAO Fish. Synop. 125(10).

Davison, P., Lara-Lopez, A., & Koslow, J. A. (2015). Mesopelagic fish biomass in the southern California current ecosystem. Deep Sea Research Part II: Topical Studies in Oceanography, 112, 129-142.

DeVries, T.J., Pearcy, W.G. (1982). Fish debris in sediments of the upwelling zone off central Peru: a late Quaternary record. Deep-Sea Research. 28, 87–109.

Du, X, Hendy, IL., Schimmelmann, A., 2018, 'A 9000-year flood history for Southern California: A revised stratigraphy of varved sediments in Santa Barbara Basin' Marine Geology. Vol. 397, 129-42.

Eschmeyer, W.N., E.S. Herald and H. Hammann. (1983). A field guide to Pacific coast fishes of North America. Boston (MA, USA): Houghton Mifflin Company.

Field, D., Barron, J., Bringue, M., Burky, D., De Bernardi, B., Ferriera-Batrina, V., . . . Baumgartner, T. (in progress). A Sliding Ecosystem Baseline in the California Current from Early 20th Century Warming. Unpublished Manuscript.

Field, D. B., Baumgartner, T. R., Charles, C. D., Ferreira-Bartrina, V., & Ohman, M. D. (2006). Planktonic Foraminifera of the California Current Reflect 20th Century Warming. Science. 311, 63-66.

Field, D. B., Baumgartner, T. R., Ferreira, V., Gutierrez, D., Lozano-Montes, H., Salvatteci, R., & Soutar, A. (2009). Variability from scales in marine sediments and other historical records. Climate Change and Small Pelagic Fish. 45-63.

Finney B.P., Alheit J., Emeis K-C., Field D.B., Gutierrez D., & Struck U. (2010). Paleoecological studies on variability in marine fish populations: a long-term perspective on the impacts of climatic change on marine ecosystems. J. Mar. Syst. 79, 316–326.

Frimodt, C. (1995). Multilingual illustrated guide to the world's commercial coldwater fish. Fishing News Books, Osney Mead, Oxford, England. 215.

Graham, R., Hughes, M., Ammann, C., Cobb, K., Hoering, M., Kennett, D., Kennett, J., Rein, B., Stott, L., Wigland, P, Xu, T. (2007), Tropical Pacific – mid-latitude teleconnections in medieval times. Climate Change. 83, 241-285.

Hendy, I., Dunn, L., Schimmelmann, A., Pak, D. (2013). Resolving varve and radiocarbon chronology differences during the last 2000 years in the Santa Barbara Basin sedimentary record, California. Quaternary International. 310, 155-168.

Hewitt, R. (1980) Distributional atlas of fish larvae in the California Current region: northern anchovy, *Engraulis mordax* (Girad), 1966-1979.

Hill, K., Dorval, E., Lo, N., Macewicz, B., Show, C., Relix-Uraga, R. (2008). Assessment of the Pacific sardine resource in 2008 for USA management in 2009. Pacific Fishery Management Council, November 2008 Agenda Item G.2.b. 236.

Hill, K., Crone, P., Dorval, E., Macewicz, B. (2016). Assessment of the Pacific sardine resource in 2016 for USA management in 2016-17. NOAA Technical Memorandum NMFS.

Hill, K.T., P.R. Crone and J.P. Zwolinski. (2018). Assessment of the Pacific Sardine Resource in 2018 for U.S. Management in 2018-19. US Department of Commerce. NOAA Technical Memorandum NMFS-SWFSC-600.

Hollowed, A. (1992). Spatial and temporal distributions of Pacific hake, *Merluccius productus,* larvae and estimates of survival during early life stages. CalCOFI Rep. 33, 100-123.

Hubbs, C. (1925) Racial and seasonal variation in the Pacific herring, California sardine and California anchovy. Fish Bulletin No. 8.

Hülsemann, J., and Emery, K. O. (1961). Stratification in recent sediments of the Santa Barbara Basin as controlled by organisms and water characteristics. Jour. Geology, 69, 279-290.

Jacobson, L., Lo, N., Herrick, S., Bishop, T. (1995). Spawning biomass of the northern anchovy in 1995 and status of the coastal pelagic fishery during 1994. NOAA Technical Memorandum NMFS.

Jones, W. (2016). The Santa Barbara Basin Fish Assemblage in the Last Two Millennia Inferred from Otoliths in Sediment Cores. Ph.D. Thesis. University of California San Diego. 1-125.

Koehn, L., Essington, T., Marshall, K., Kaplan, I., Sydeman, W., Szoboszlai, A., Thayer, J. (2016). Developing a high taxonomic resolution food web model to assess the functional role of forage fish in the California Current ecosystem. Ecological Modelling. 335, 87-100.

Koslow, J., Goericke, R., McClatchie, S., Vetter, R., & Rogers-Bennett, L. (2010). The California Cooperative Oceanic Fisheries Investigations (CalCOFI): The Continuing Evolution and Contributions of a 60-Year Ocean Observation Program. California Cooperative Oceanic Fisheries Investigations Report.

Koslow, J., Davison, P., Lara-Lopez, A., Ohman, M. (2014). Epipelagic and mesopelagic fishes in the southern California Current System: Ecological interactions and oceanographic influences on their abundance. Journal of Marine Systems, 138, 20-28.

Koslow, J., Miller, E., & McGowan, J. (2015). Dramatic declines in coastal and oceanic fish communities off California. Marine Ecology Progress Series, 538, 221-227.

Koslow, J. A., & Davison, P. C. (2016). Productivity and biomass of fishes in the California Current Large Marine Ecosystem: Comparison of fishery-dependent and -independent time series. Environmental Development, 17, 23-32.

Kramer, D. (1970). Distributional atlas of eggs and larvae in the California Current region: Pacific sardine, *Sardinops caerulea* (Girard), 1951-1966.

Lamb, A. and P. Edgell. (1986). Coastal fishes of the Pacific northwest. Madeira Park, (BC, Canada): Harbour Publishing Co. Ltd., 224.

MacCall, A. D. 1979. Population estimates for the waning years of the Pacific sardine fishery. CalCOFI Rep. 20: 72-82.

MacCall, A.D. 1990. Dynamic geography of marine fish populations. Seattle, WA: Washington Sea Grant Program.

McClatchie, S., Goericke, R., Cosgrove, R., Auad, G., and Vetter, R. (2010). Oxygen in the Southern California Bight: Multidecadal trends and implications for demersal fisheries. Geophysical Research Letters. 37, 1-5.

McClatchie, S., Field, J., Thompson, A. R., Gerrodette, T., Lowry, M., Fiedler, P. C., . . . Vetter, R. D. (2016). Correction to 'Food limitation of sea lion pups and the decline of forage off central and southern California'. Royal Society Open Science. 3(4), 1-9.

McClatchie, S., Hendy, I. L., Thompson, A. R., & Watson, W. (2017). Collapse and recovery of forage fish populations prior to commercial exploitation. Geophysical Research Letters. 44, 1-9.

McGowan, J. A., Bograd, S. J., Lynn, R. J., & Miller, A. J. (2003). The biological response to the 1977 regime shift in the California Current. Deep Sea Research Part II: Topical Studies in Oceanography, 50(14-16), 2567-2582.

Miller, A., McGowan, J. (2013). Faunal shift in southern California's coastal fishes: A new assemblage and trophic structure takes hold. Estuarine, Coastal and Shelf Science. 29-36.

Moser, H.G. and Ahlstrom, E.H. (1996). Myctophidae: lanternfishes. In H.G. Moser (ed.) The early stages of fishes in the California Current Region. California Cooperative Oceanic Fisheries Investigations (CalCOFI) Atlas No. 33.

Moser, H., Charter, R., Smith, P., Ambrose, D., Watson, W., Charter, S., Sandknop, E.M. (2001). Distributional Atlas of fish larvae and eggs in the Southern California Bight region: 1951–1998. CalCOFI Atlas 34, 1–166.

Murphy, G. I. 1966. Population biology of the Pacific sardine (Sardinops caerulea). Proc. Calif. Acad. Sci. Vol. 34 (1): 1-84.

NMFS (2009). Our living oceans. Report on the status of U.S. living marine resources, 6th edition, Technical Memo NOAA-TM-NMFS-F/SPO-80, U.S. Department of Commerce, National Oceanic and Atmospheric Administration.

O'Connell, J., & Tunnicliffe, V. (2001). The use of sedimentary fish remains for interpretation of long-term fish population fluctuations. Marine Geology. 174(1-4), 177-195.

Patterson, R. T., Prokoph, A., Wright, C., Chang, A., Taylor, L., Lyons, P., Dallimore, A., Kumar, A. (2002). Atlas of common Squamatological (fish scale) material in coastal British Columbia and an assessment of the utility of various scale types in paleofisheries reconstruction. Palaeontologia Electronica. 4(1):88.

Pierce, G. J., Boyle, P. R., & Diack, J. S. (1991). Identification of fish otoliths and bones in faeces and digestive tracts of seals. Journal of Zoology. 224(2), 320-328.

Robinson, B., Bailey, T. (1981). Sinking rates and dissolution of midwater fish fecal matter. Mar. Biol. 65, 135-142.

Rose, K. (2013). Fish Scales and Skeletal Debris as Indicators of Changes in Small Pelagic Fishes in the Santa Barbara Basin: Fishing or Natural Variability? Master's Thesis. Hawaii Pacific University. 1-181.

Ruddiman, W. (2003). The anthropogenic greenhouse era began thousands of years ago. Climate Change. 61, 261-293.

Salvatteci, R., Field, D. B., Baumgartner, T., Ferreira, V., & Gutiérrez, D. (2012). Evaluating fish scale preservation in sediment records from the oxygen minimum zone off Peru. Paleobiology. 38(01), 52-78.

Salvatteci, R., Field, D., Gutiérrez, D., Baumgartner, T., Ferreira, V., Ortlieb, L., . . . Bertrand, A. (2018). Multifarious anchovy and sardine regimes in the Humboldt Current System during the last 150 years. Global Change Biology.

Schimmelmann, A., Hendy, I., Dunn, L., Pak, D., & Lange, C. (2013). Revised ~2000-year chronostratigraphy of partially varved marine sediment in Santa Barbara Basin, California. GFF, 135:3-4, 258-264.

Schimmelmann, A., Lange, C., Schieber, J., Francus, P., Ojala, A., Zolitschka, B. (2016). Varves in marine sediments: A review. Earth-Science Reviews. 159, 215-246).

Soutar, A. (1967). The accumulation of fish debris in certain California coastal sediments. California Cooperative Oceanic Fisheries Investigations. 11, 136-139.

Soutar, A., & Isaacs, J. D. (1969). History of Fish Populations Inferred From Fish Scales In Anaerobic Sediments Off California. California Cooperative Oceanic Fisheries Investigations. 13, 63-70.

Soutar, A., & Isaacs, J. (1974). Abundance of pelagic fish during the 19th and 20th centuries as recorded in anaerobic sediment off the Californias. Fishery Bulletin. 72(2), 257-273.

Soutar, A., & Crill, P. (1977). Sedimentation and climatic patterns in the Santa Barbara Basin during the 19th and 20th centuries. GSA Bulletin. 88(8), 1161-1172.

Soutar, A., Kling, A., Crill, P., Duffrin, E., & Bruland, K. (1977). Monitoring the marine environment through sedimentation. Nature. 266, 136-139.

Starensinic, N., Farrington, J., Gagosain, R., Clifford, C., Hulburt, E. (1983). Downward transport of particulate matter in the Peru coastal upwelling: role of the anchoveta, Engraulis ringens. n: Suess, E. & Theide, J. (Eds.) Coastal Upwelling: Its Sediment Record. Part A.

Responses of the Sedimentary Regime to Present Coastal Upwelling. Plenum, New York, pp. 225–240.

Thayer, J., MacCall, A., Sydeman, W., Davison, P. (2017a). California anchovy population remains low, 2012–16. California Cooperative Oceanic Fisheries Investigations. 58, 1-8.

Thayer, J., Szoboszlai, A. & Sydeman, W. (2017b). Predator forage needs: Comparison and model synthesis. In International Symposium: drivers of dynamics of small pelagic fish resources Mar 6-11, 2017, Victoria, BC, Canada.

Weber, E. (2019). Egg distribution maps for sardine, anchovy, and jack mackerel. NOAA Southwest Fisheries Science Center.

Whitehead, P.J.P. (1985). Clupeoid fishes of the world (suborder Clupeoidei). FAO Species Catalogue. An annotated and illustrated catalogue of the herrings, sardines, pilchards, sprats, shads, anchovies and wolf-herrings. FAO Fish. Synop. 125(7-1), 1- 303.

Whitehead, P.J.P. and Y.R. Rodriguez-Sánchez. (1995). Clupeidae. Sardinas, sardinetas, machuelos, sábalos, piquitingas. In W. Fischer, F. Krupp, W. Schneider, C. Sommer, K.E. Carpenter and V. Niem (eds.) Guia FAO para Identification de Especies para lo Fines de la Pesca. Pacifico Centro-Oriental. 3, 1015-1025.

Zahuranec, B.J. (2000). Zoogeography and systematics of the lanternfishes of the genus Nannobrachium (Myctophidae: Lampanictini). Smithson. Contrib. Zool. 607:1-69.

Zwolinski, J., Demer, D., Byers, K., Cutter, G., Renfree, J., Sessions, T., & Macewicz, B. (2012). Distributions and abundances of Pacific sardine (Sardinops sagax) and other pelagic fishes in the California Current Ecosystem during spring 2006, 2008, and 2010, estimated from acoustic – trawl surveys. Fishery Bulletin. 110(1), 110-122.

APPENDIX I: Supplementary Material

Table of Figures:

Table of Tables:

2. Materials and Methodological Approach

2.1 Processing and Sampling Sediment Cores

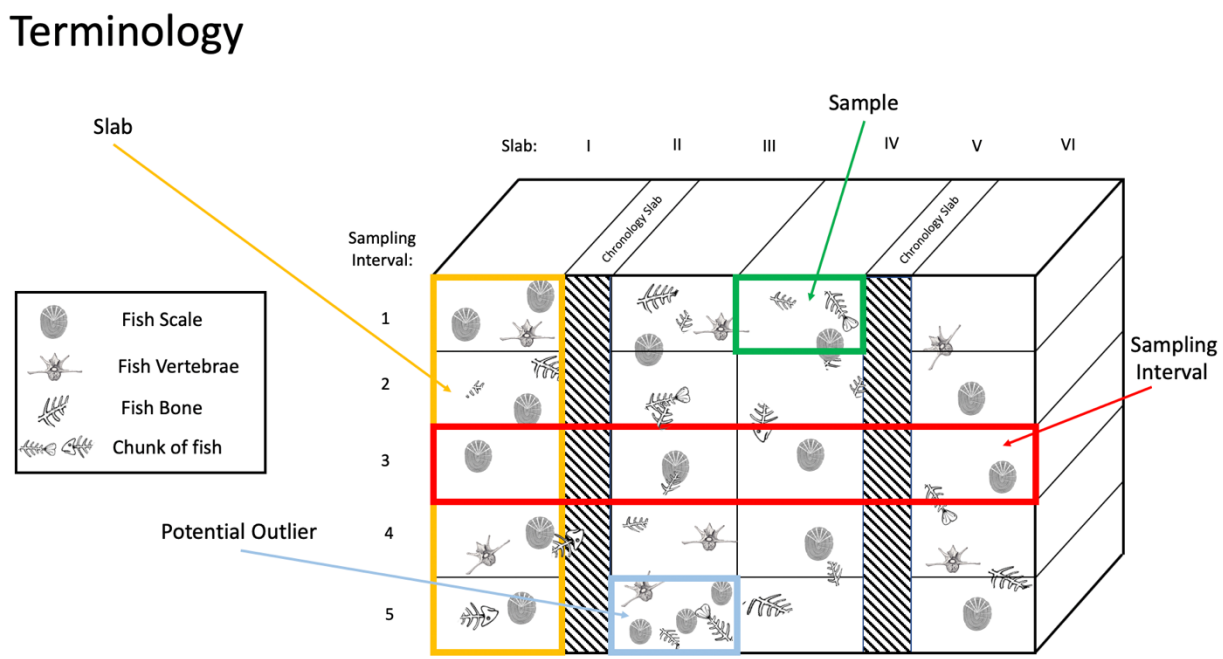

Figure A1. Simple schematic of sampling procedure and terminology.

2.2 Outlier Analysis

Typical Outlier Scenario:

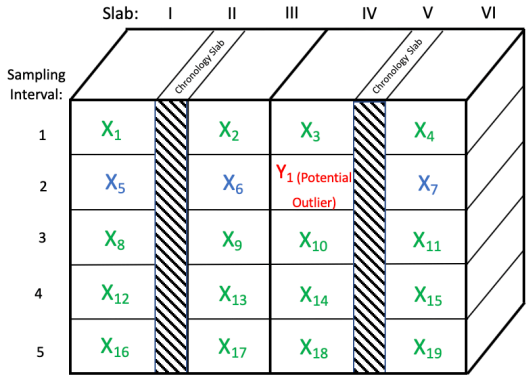

Mean
$\overline{x_1}=\frac{x_1+x_2+x_3+x_4}{4}$
$\overline{x_2}=\frac{x_5+x_6+y_1+x_7}{4}$
$\overline{x_3}=\frac{x_8+x_9+x_{10}+x_{11}}{4}$
$\overline{x_4}=\frac{x_{12}+x_{13}+x_{14}+x_{15}}{4}$
$\overline{x_5}=\frac{x_{16}+x_{17}+x_{18}+x_{19}}{4}$

SD
$\sigma_1 = stdev(x_1 + x_2 + x_3 + x_4)$
$\sigma_2 = stdev(x_5 + x_6 + y_1 + x_7)$
$\sigma_3 = stdev(x_8 + x_9 + x_{10} + x_{11})$
$\sigma_4 = stdev(x_{12} + x_{13} + x_{14} + x_{15})$
$\sigma_5 = stdev(x_{16} + x_{17} + x_{18} + x_{19})$

$MSD = median(\sigma_1, \sigma_2, \sigma_3, \sigma_4, \sigma_5, \ldots, \sigma_n)$
(for intervals with mean ≥ 1)

1. Calculate the mean and standard deviation of each sampling interval (4 samples)
2. Take the median (MSD) of all the standard deviations within the core with a mean greater than 1
3. Compare the anomalous value (potential outlier) with the mean of the sampling intervals +2, +3, +4 MSD
4. Rank outlier accordingly (ranks on following slide)

Figure A2. Conceptual diagram of the OMSD procedure for a typical outlier scenario.

Two or more potential outliers in the same sampling interval:

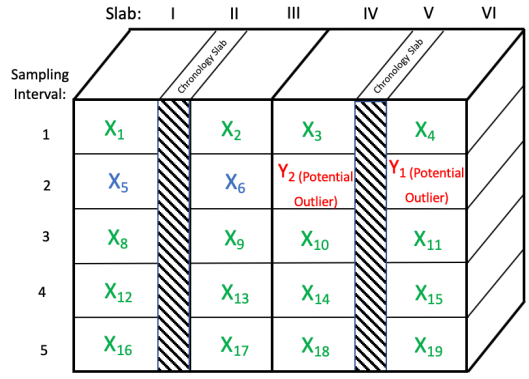

Mean	Second Outlier Mean
$\overline{x_1}=\frac{x_1+x_2+x_3+x_4}{4}$	
$\overline{x_2}=\frac{x_5+x_6+y_2+y_1}{4}$	$\overline{x_2}=\frac{x_5+x_6+y_2}{4}$
$\overline{x_3}=\frac{x_8+x_9+x_{10}+x_{11}}{4}$	
$\overline{x_4}=\frac{x_{12}+x_{13}+x_{14}+x_{15}}{4}$	
$\overline{x_5}=\frac{x_{16}+x_{17}+x_{18}+x_{19}}{4}$	

SD
$\sigma_1 = stdev(x_1 + x_2 + x_3 + x_4)$
$\sigma_2 = stdev(x_5 + x_6 + y_2 + 1)$
$\sigma_3 = stdev(x_8 + x_9 + x_{10} + x_{11})$
$\sigma_4 = stdev(x_{12} + x_{13} + x_{14} + x_{15})$
$\sigma_5 = stdev(x_{16} + x_{17} + x_{18} + x_{19})$

$MSD = median(\sigma_1, \sigma_2, \sigma_3, \sigma_4, \sigma_5, \ldots, \sigma_n)$
(for intervals with mean ≥ 1)

Once the most anomalous value (Y_1) has been identified as an outlier, recalculate the mean without that outlier value.
Then compare the second most anomalous value (Y_2) to the mean of the sampling interval +2, +3, +4 MSD and rank the second outlier accordingly.

Figure A3. Conceptual diagram of the OMSD procedure when there are two or more potential outliers in the same sampling interval.

Additional Evidence From Another Type of Fish Debris:

If a sample contains outliers for multiple types of fish debris (i.e. scales and/or bone and/or vertebrae), then this provides additional evidence that the anomalous fish debris counts are more likely to be outliers.

If a potential outlier in scales is associated with an outlier in bones and/or vertebrae or a potential bone outlier is associated with an outlier of vertebrae within the same sample (i.e. same slab of the same sampling interval), then the ranks of both types of fish debris increase by one

Note: Outlier ranks increase by a maximum of 1 rank.

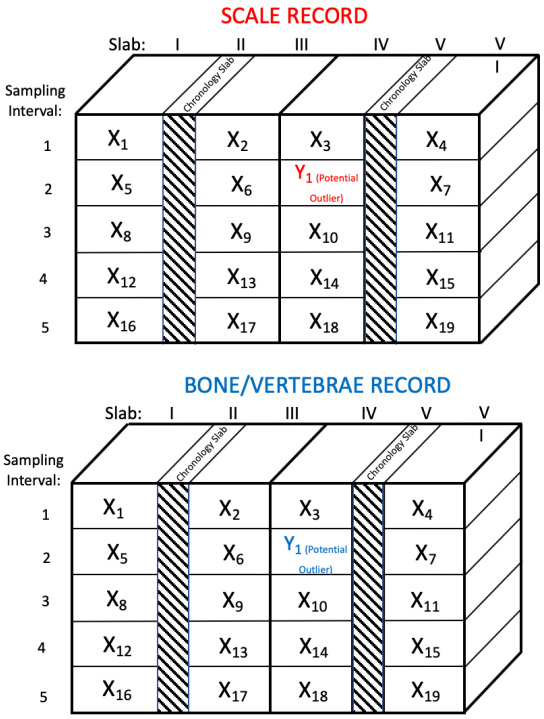

Figure A4. Conceptual diagram of the OMSD procedure when there is additional evidence from another type of fish debris.

Two or more outliers in the same slab in neighboring intervals:

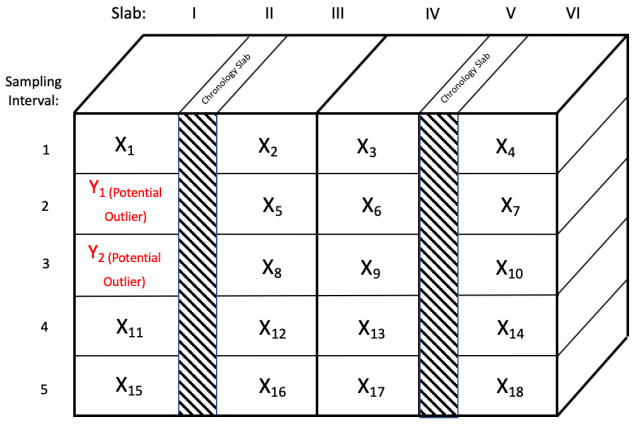

Once the ranks have been obtained, each rank will increase by one due to the additional evidence of an outlier spanning multiple sampling intervals.

Note: Outlier ranks increase by a maximum of 1 rank.

Figure A5. Conceptual diagram of the OMSD procedure when there are two or more potential outliers in the same slab of neighboring intervals.

2.4 Chronological Development

Table A1. Years of major homogenous layers identified in the kasten core associated with those identified by Schimmelmann et al. (2013).

Homogenous Layer Identification	Year based on Schimmelmann et al. (2013)	Year based on kasten core
Large Turbidite	1738	1746
Grey Layer	1380	1537
Thick Grey Layer	53	352
Olivine Layer	33	303

2.6 Processing Vertebrae

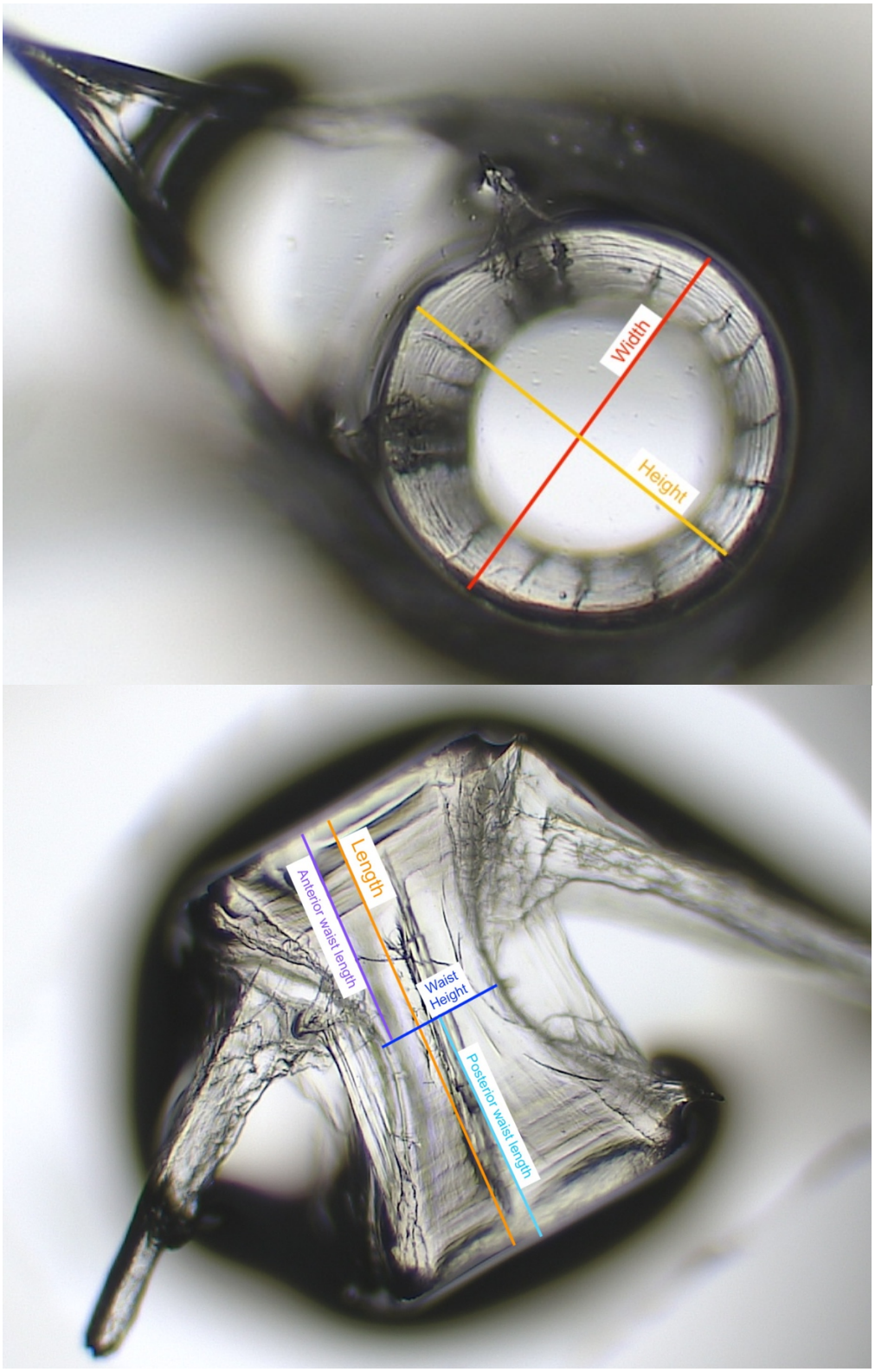

Figure A6. A guide for height, width, length, and waist measurements used in the current study. Only the length measurement is used in the current study.

3. Results

3.1 Patterns of the Scale/Skeletal Deposition Rate Time Series

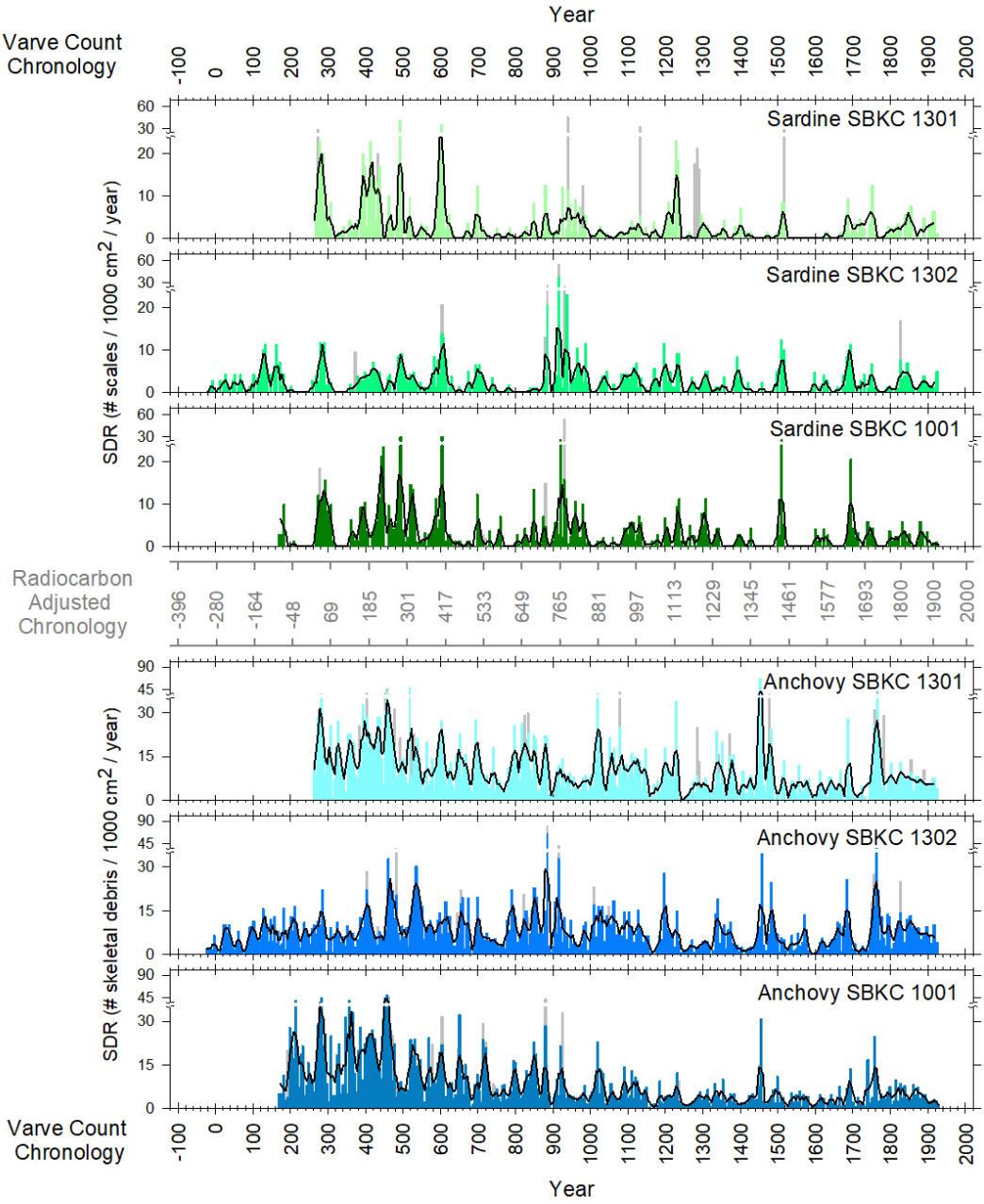

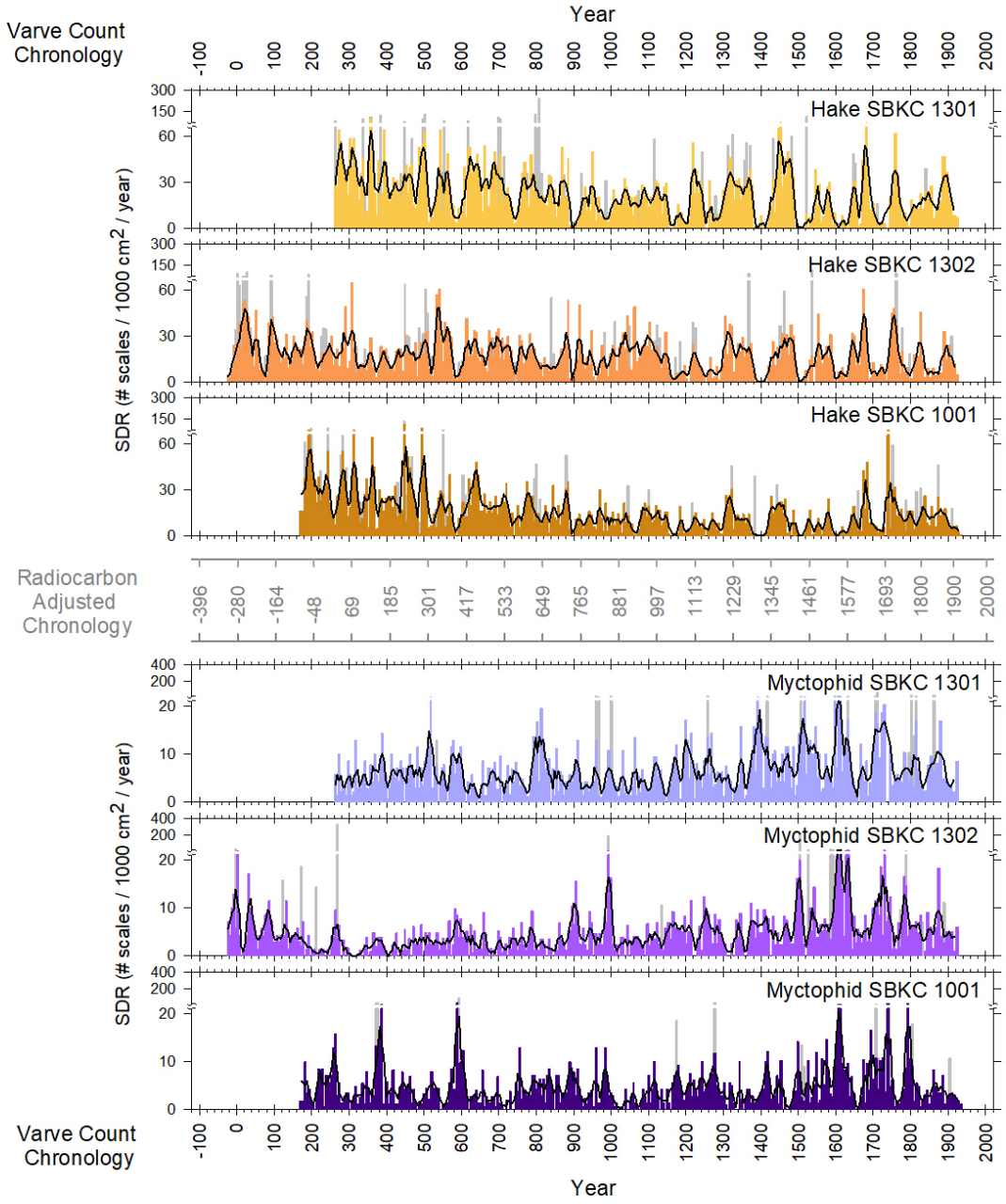
Varve Count Chronology
Year
Hake SBKC 1301
Hake SBKC 1302
Hake SBKC 1001
SDR (# scales / 1000 cm2 / year)
Radiocarbon Adjusted Chronology
Myctophid SBKC 1301
Myctophid SBKC 1302
Myctophid SBKC 1001
Varve Count Chronology
Year

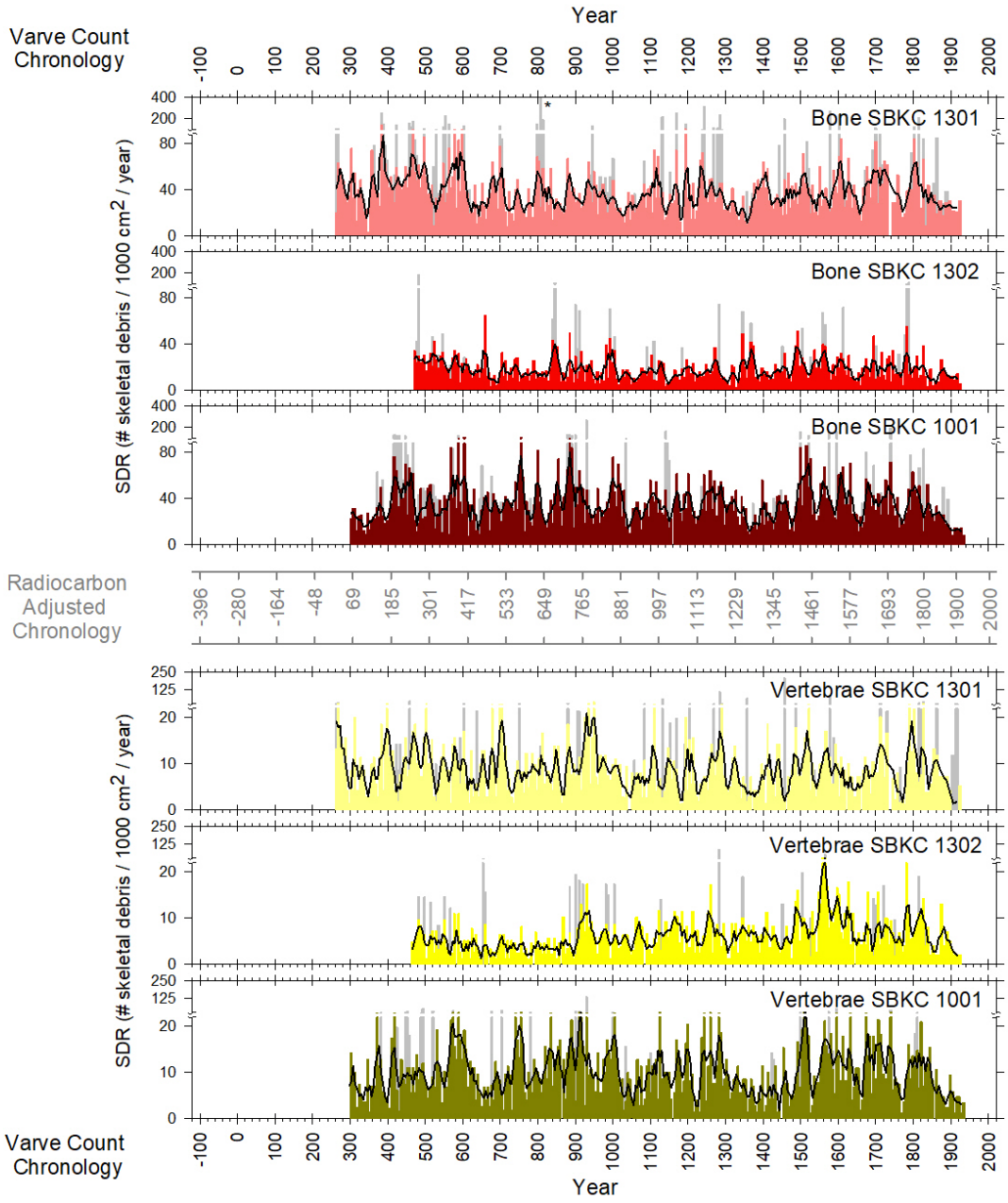

Figure A7. Time series of fish debris fluxes derived from five-year sampling intervals (shaded region) with three-term smoothing (bold black line) after outliers were removed. The grey bars indicate a sampling interval containing an outlier that was removed using the OMSD removal criteria, which corrected the flux to the colored values. The varve count chronology is shown on the top and bottom corresponding to the tick marks and the radiocarbon adjusted chronology is shown between the two debris types.

Table A2. Summary statistics of each core as well as the composite record for each debris type with outliers removed using the three-term (15-year) smoothed data. The units of flux and standard deviation is number of fish debris per 1000 cm^2 per year. The CV is unitless. Note the composite skeletal debris record is only composed of SBKC 1301 and SBKC 1001.

Debris Type	Core	Mean Flux	Median Flux	Standard Deviation	CV (SD/mean)
Sardine	1301	2.86	1.48	4.01	1.40
	1302	2.51	1.78	2.61	1.04
	1001	3.05	1.77	3.62	1.19
	Composite	**2.81**	**1.74**	**2.99**	**1.07**
Anchovy	1301	10.27	8.74	6.84	0.67
	1302	8.16	7.62	5.12	0.63
	1001	8.01	5.29	7.09	0.88
	Composite	**8.81**	**7.67**	**5.56**	**0.63**
Hake	1301	21.74	21.15	13.20	0.61
	1302	16.37	16.58	9.06	0.55
	1001	14.86	12.48	10.37	0.70
	Composite	**17.65**	**17.81**	**9.45**	**0.53**
Myctophid	1301	6.74	5.88	3.69	0.55
	1302	4.90	3.91	3.82	0.78
	1001	4.80	3.96	3.44	0.72
	Composite	**5.48**	**4.67**	**3.05**	**0.55**
Bone	1301	37.65	35.46	12.20	0.34
	1302	20.30	18.10	9.72	0.48
	1001	35.10	33.56	12.33	0.35
	Composite	**36.37**	**35.49**	**10.45**	**0.29**
Vertebrae	1301	8.71	8.35	3.76	0.43
	1302	5.92	5.22	3.06	0.52
	1001	10.05	9.40	4.19	0.42
	Composite	**9.38**	**9.36**	**3.19**	**0.34**

Table A3. Summary of two-way ANOVA without replication to compare the differences between cores. The ANOVA for skeletal debris does not include SBKC 1302.

Debris Type	Source of Variation	F	P-value	df
Sardine	Between-core	5.41	0.0047	2
	Downcore	5.90	<0.0001	331
Anchovy	Between-core	34.86	<0.0001	2
	Downcore	6.10	<0.0001	331
Hake	Between-core	90.07	<0.0001	2
	Downcore	5.56	<0.0001	331
Myctophid	Between-core	65.74	<0.0001	2
	Downcore	4.62	<0.0001	331
Bone	Between-core	11.11	<0.0001	1
	Downcore	2.30	<0.0001	322
Vertebrae	Between-core	25.65	<0.0001	1
	Downcore	1.81	<0.0001	322

Table A4. Summary of two-way ANOVA without replication to compare slabs within a core. Sampling intervals containing samples without flux data were removed. Bold values indicate significance.

Debris Type	Core	F	P-value	df
Sardine	1301	0.514	0.673	3
	1302	2.371	0.069	3
	1001	0.872	0.455	3
Anchovy	**1301**	**11.89**	**<0.001**	**3**
	1302	**4.051**	**0.007**	**3**
	1001	1.009	0.388	3
Hake	1301	2.578	0.053	3
	1302	1.656	0.175	3
	1001	1.317	0.268	3
Myctophid	1301	0.835	0.475	3
	1302	2.019	0.110	3
	1001	2.481	0.060	3
Bone	1301	0.951	0.415	3
	1302	**2.643**	**0.048**	**3**
	1001	1.432	0.232	3
Vertebrae	**1301**	**4.99**	**0.002**	**3**
	1302	2.364	0.069	3
	1001	1.734	0.159	3

3.2 Identification and Correction of Outliers

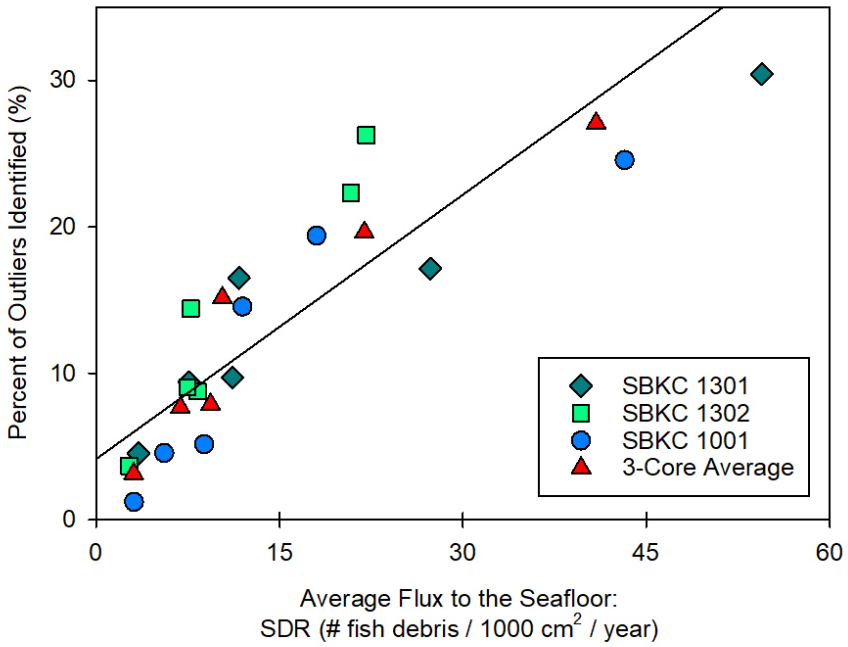

Figure A8. Linear regression of the average percent of outliers identified with the average flux of fish debris to the sea floor by debris type.

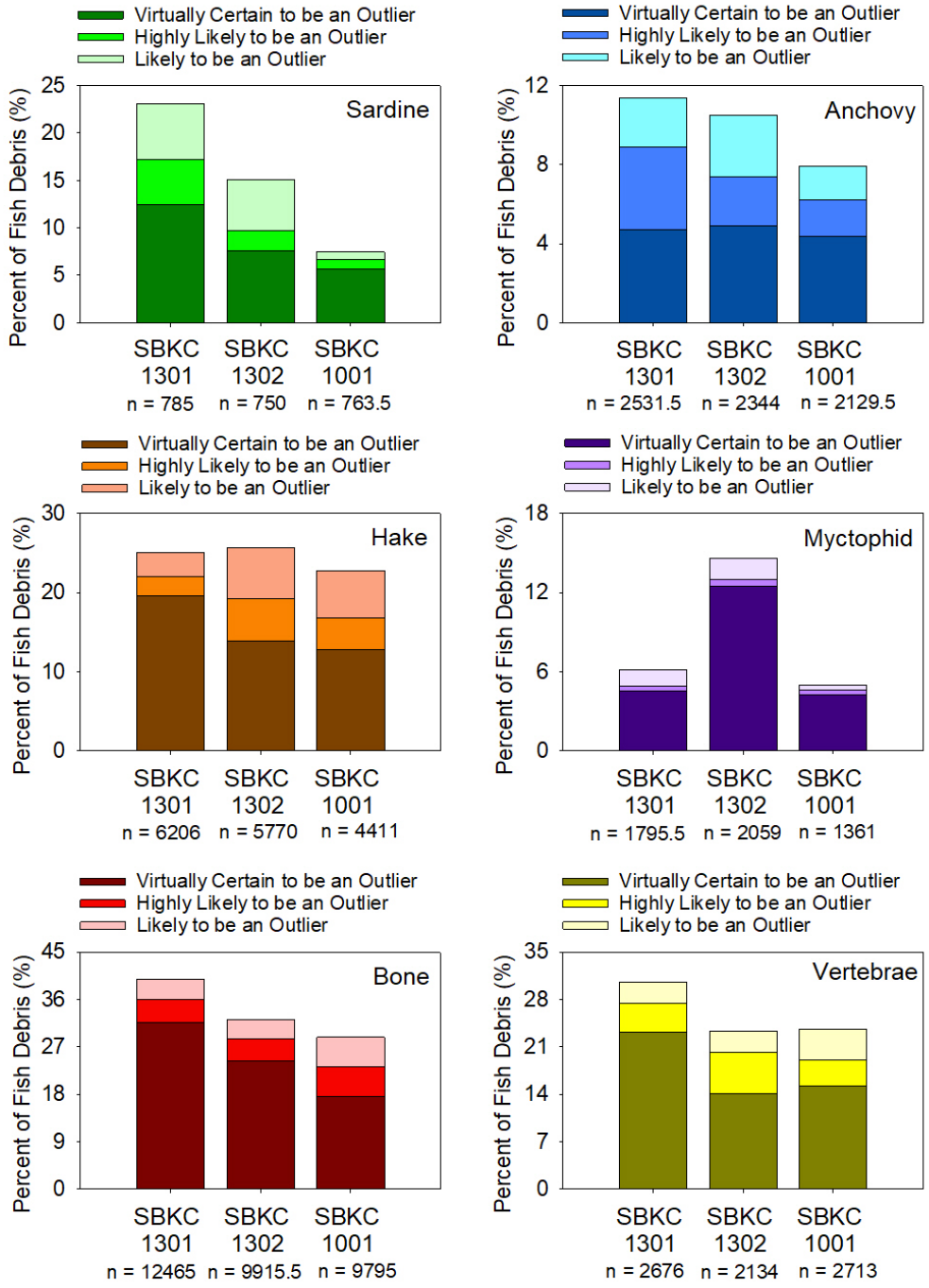

Figure A9. The percent of fish debris identified as outliers via the OMSD procedure from three kasten sediment cores (SBKC 1301, SBKC 1302, SBKC 1001). The OMSD procedure ranks the outliers as: Virtually Certain (1) to be an Outlier, Highly Likely (2) to be an Outlier, and Likely (3) to be an Outlier. n represents the total number of fish debris of a specific type that was extracted from the core.

Table A5. Results of the Chi Square test between cores to determine if there is a difference in the frequency of outliers by core for each debris type.

Debris Type	Chi^2	p-value	DF
Sardine	3.43	0.1804	2
Anchovy	3.83	0.1471	2
Hake	0.62	0.7320	2
Myctophid	0.97	0.6158	2
Bone	4.04	0.1329	2
Vertebrae	1.74	0.4189	2

Table A6. Results from the independent two-sided Mann Whitney-U (Wilcoxon) test with continuity correction applied for the difference between the flux at which non outliers and Rank 3 outliers occur and the flux at which Rank 1 and 2 outliers occur.

Debris Type	Distributions Different?	p-value	Lower 95% CI	Upper 95% CI	Wilcoxon Test Statistic
Sardine	Yes	5.151e-05	-0.754	-0.264	4445
Anchovy	Yes	1.761e-08	-0.382	-0.194	13480
Hake	Yes	0.0005783	-0.186	-0.050	44990
Myctophid	Yes	3.469e-05	-0.348	-0.123	13566
Bone	Yes	5.377e-08	-0.169	-0.079	59406
Vertebrae	No	0.5182	-0.081	0.042	45259

3.3 Composite Time Series

Table A7. Correlation coefficients (R-value) between each debris type SDR with one another lagged at 0-3 sampling intervals (0-15 years). Values in bold indicate that the correlation coefficient is greater with a lag than would be without a lag.

Taxa	Lag Interval	Time Lag (Years)		Sardine	Anchovy	Hake	Myctophid	Bone	Vertebrae
Sardine	0	0		1.00	0.33	0.01	0.05	0.28	0.33
	1	5		0.89	0.27	0.06	-0.03	0.22	0.29
	2	10		0.65	0.18	**0.08**	-0.08	0.12	0.21
	3	15		0.43	0.11	0.06	-0.10	0.03	0.12
Anchovy	0	0		0.33	1.00	0.36	-0.24	0.09	-0.03
	1	5		0.32	0.90	0.29	**-0.27**	0.08	-0.04
	2	10		0.27	0.68	0.22	-0.26	0.04	**-0.07**
	3	15		0.21	0.49	0.17	-0.23	0.02	-0.07
Hake	0	0		0.01	0.36	1.00	-0.29	-0.11	-0.22
	1	5		-0.05	**0.40**	0.88	**-0.33**	**-0.14**	-0.25
	2	10		-0.09	0.40	0.65	-0.32	-0.14	**-0.26**
	3	15		-0.10	0.36	0.40	-0.25	-0.11	-0.21
Myctophid	0	0		0.05	-0.24	-0.29	1.00	0.29	0.31
	1	5		0.16	-0.17	-0.21	0.81	**0.31**	0.31
	2	10		**0.22**	-0.10	-0.12	0.48	0.25	0.26
	3	15		0.20	-0.05	-0.04	0.18	0.14	0.16
Bone	0	0		0.28	0.09	-0.11	0.29	1.00	0.70
	1	5		0.28	0.07	-0.11	0.27	0.85	0.63
	2	10		0.25	0.05	**-0.12**	0.23	0.60	0.50
	3	15		0.24	0.06	-0.12	0.19	0.36	0.37
Vertebrae	0	0		0.33	-0.03	-0.22	0.31	0.70	1.00
	1	5		0.31	**-0.05**	-0.20	0.29	0.62	0.86
	2	10		0.30	-0.06	-0.19	0.26	0.47	0.61
	3	15		0.32	-0.03	-0.15	0.23	0.30	0.38

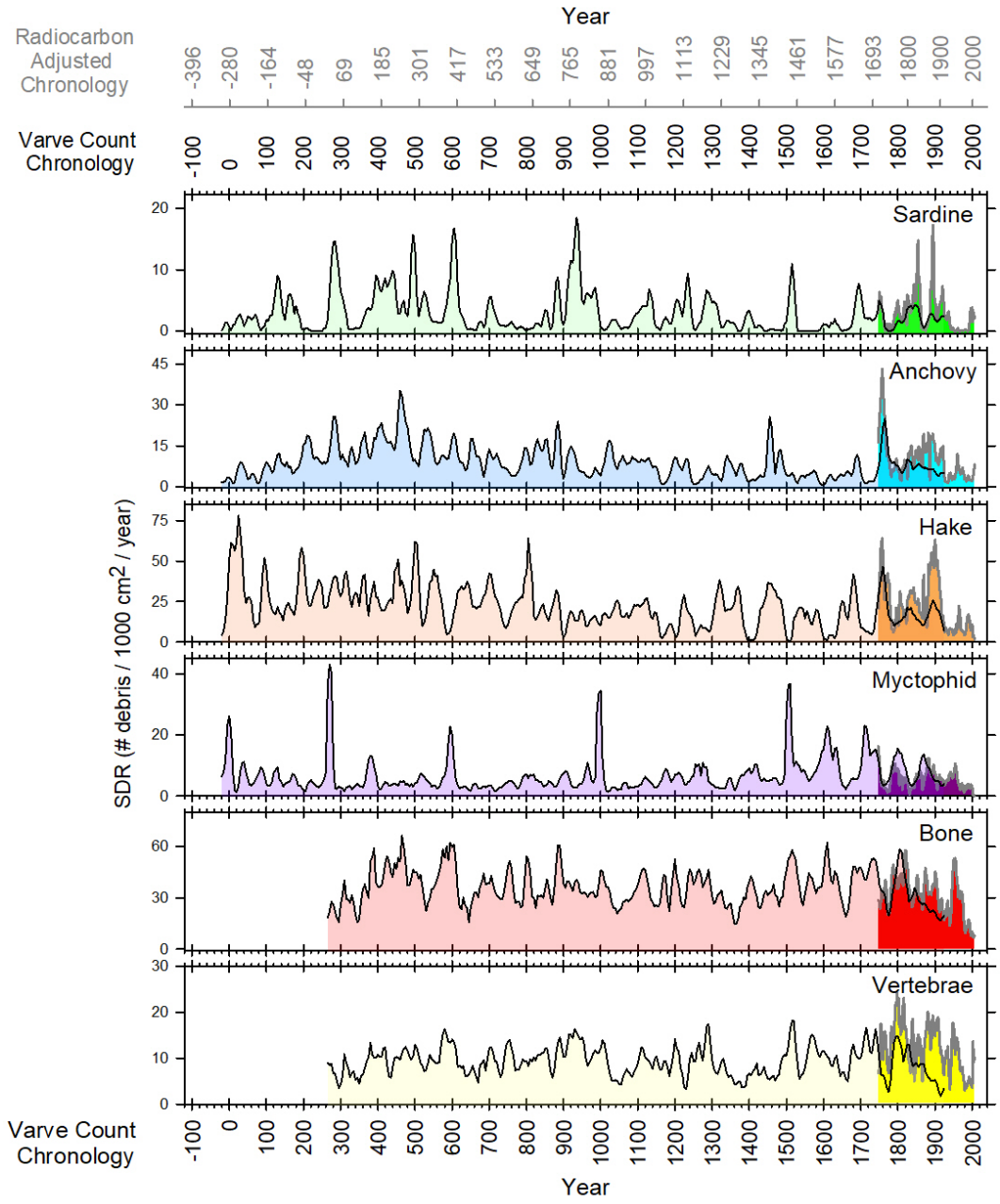

Figure A10. Comparison of the composite kasten core record with the composite box core record from 20 BCE to 2006.

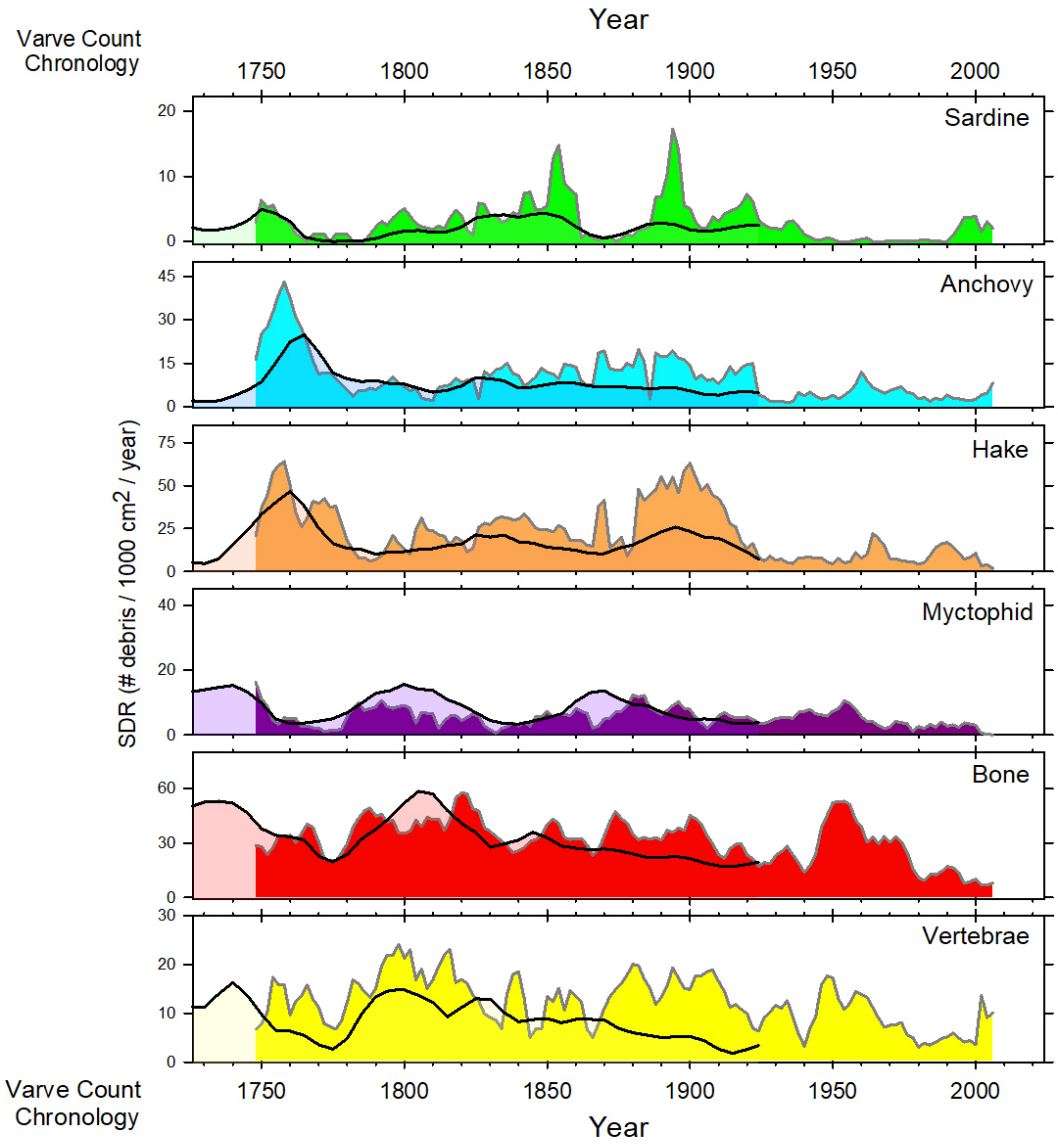

Figure A11. Comparison of the composite kasten core record with the composite box core record from 1746 to 2006. The black line and light shading represents the kasten core and the grey line and dark shading represents the box core record.

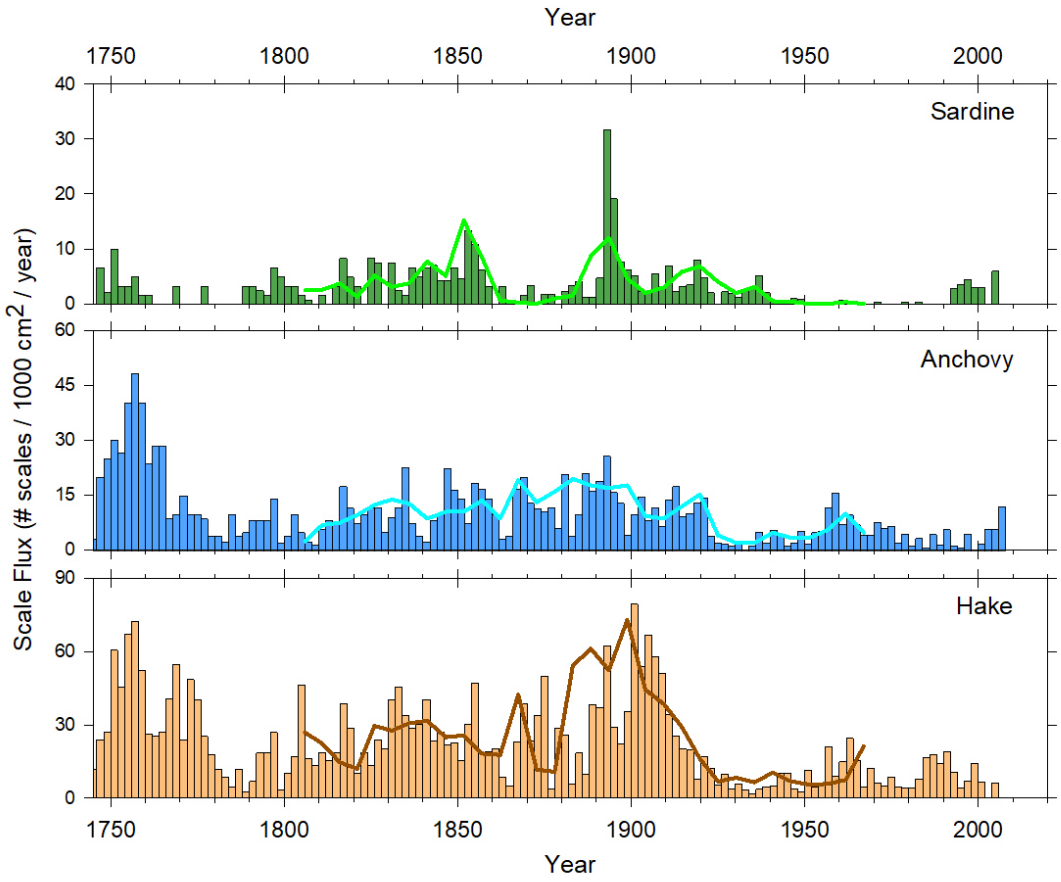

Figure A12. Comparison of the Composite Rose (2013) Box Core with the Composite Soutar and Isaacs (1974) Box Core Record for sardine, anchovy, and hake. The bars represent the Rose (2013) record and the line represents the Soutar and Isaacs (1974) record.

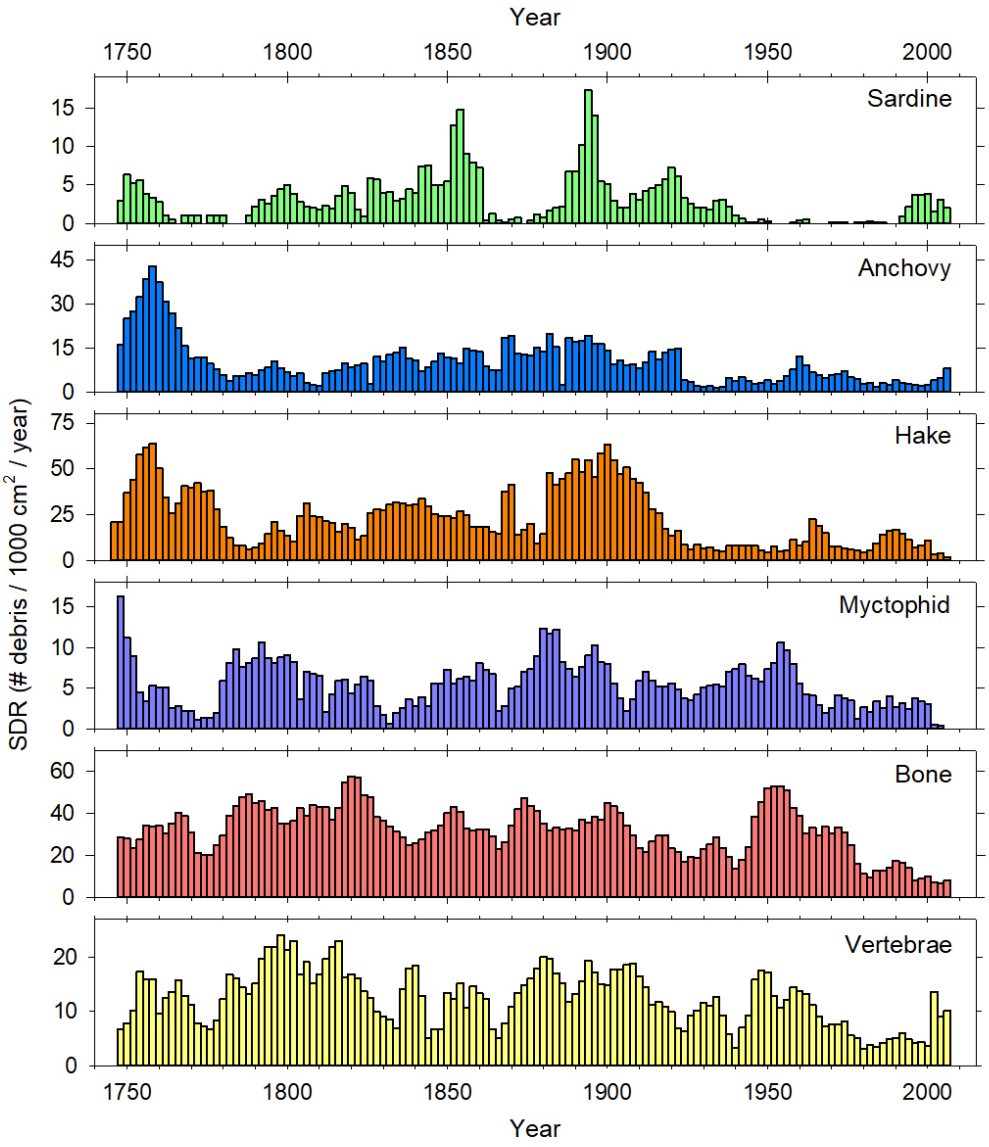

Figure A13. Composite time series of flux of sardine, anchovy, hake, and myctophid scales and well as bone and vertebrae derived from box cores from Rose (2013) and Soutar and Isaacs (1974). Each sampling interval corresponds to 2-year intervals.

Table A8. Results from the independent two-sided Mann Whitney-U (Wilcoxon) test with continuity correction for the difference between the flux of the composite kasten core with the composite box core for the period of overlap from 1746 – 1934.

Debris Type	Distributions Different?	p-value	Lower 95% CI	Upper 95% CI	Wilcoxon Test Statistic
Sardine	Yes	0.016	0.185	0.189	2187
Anchovy	Yes	0.001	1.363	4.97	2379
Hake	Yes	<0.001	-10.067	-5.216	851
Myctophid	Yes	0.025	-3.114	-0.248	1285
Bone	Yes	0.022	0.740	8.381	2164
Vertebrae	Yes	<0.001	4.131	7.673	2865

Table A9. Correlation coefficient and coefficient of determination for correlations between the composite kasten core with the composite box core for the period of overlap (i.e. 1746-1934) as well as the between kasten core correlations.

	Correlation between Composite Kasten with Composite Box Core for the period of overlap (1746-1934)		Correlation Between Kasten Three-Core Average	
	R	R^2	R	R^2
Sardine	0.55	0.30	0.65	0.42
Anchovy	0.60	0.36	0.64	0.41
Hake	0.65	0.41	0.62	0.38
Myctophid	0.48	0.23	0.55	0.30
Bone	0.49	0.24	0.30	0.09
Vertebrae	0.29	0.08	0.26	0.07

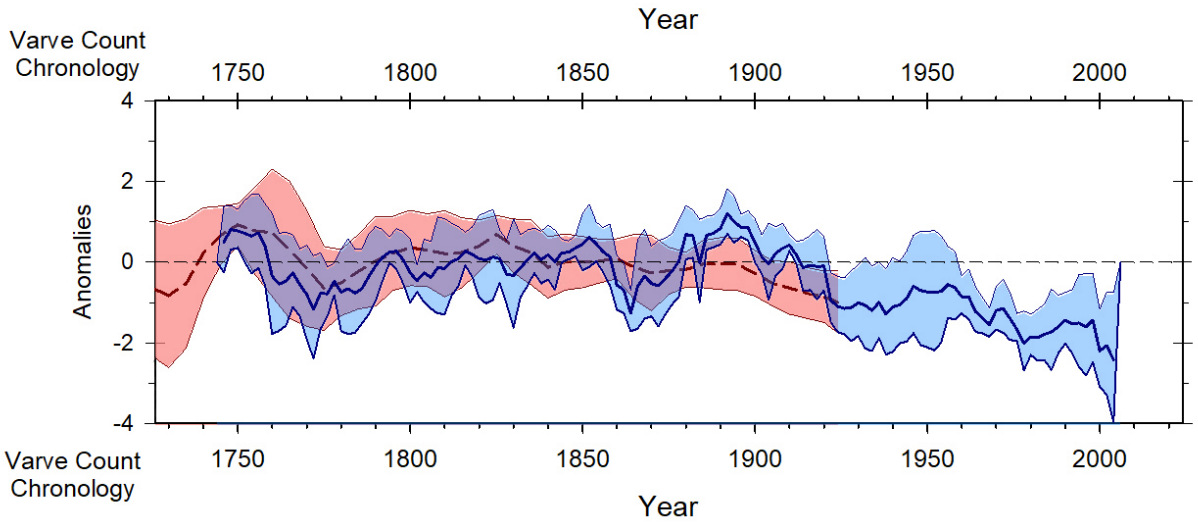

Figure A14. Cropped Paleo Forage Fish Index showing period of overlap between composite kasten and box core records. Red indicates the composite kasten core and the blue represents the composite box core record. The shaded region represents two standard errors.

Table A10. Results from the Welch's t-test comparing negative anomalies from the 20th century with negative anomalies from the last two millennia. Bold values indicate significance.

			Composite Kasten Core			
			1155 – 1180	1250 – 1260	1395 – 1420	1595 – 1605
Composite Box Core	1922 – 1942	T Stat	-0.86	-1.84	**-3.66**	-1.21
		p-value	0.21	0.10	**0.01**	0.16
		DF	5	2	**6**	3
	1964 – 2004	T Stat	1.82	1.79	1.13	**5.22**
		p-value	0.06	0.09	0.14	**0.00**
		DF	6	3	10	**11**
	1976 – 2004	T Stat	**2.44**	**2.60**	**2.13**	**6.53**
		p-value	**0.03**	**0.04**	**0.03**	**0.00**
		DF	**6**	**3**	**10**	**11**

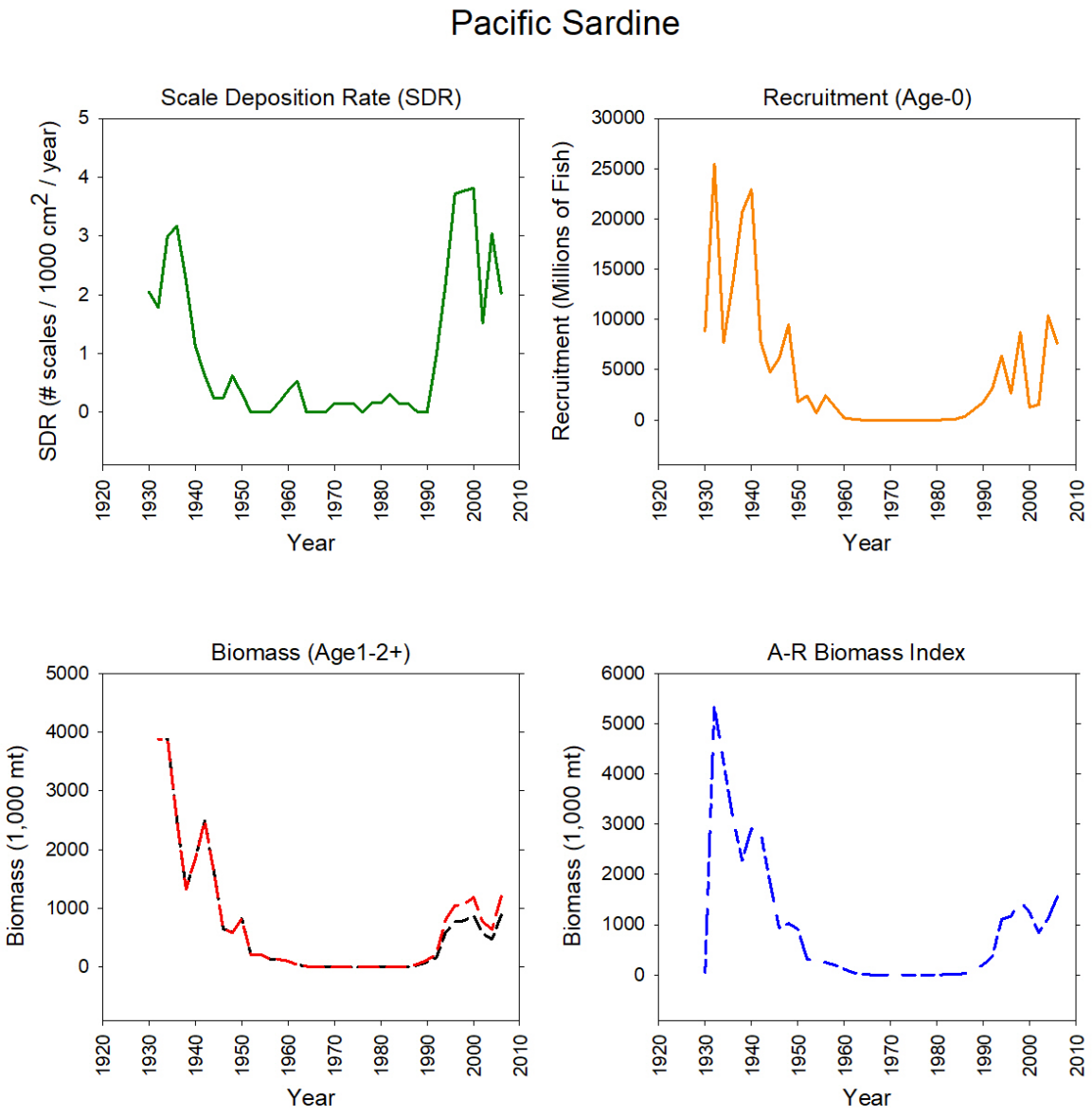

Figure A15. Time series of sardine SDR, recruitment (Murphy, 1966; MacCall, 1979; Hill et al., 2008), biomass (Murphy, 1966; MacCall, 1979; Hill et al., 2008), and the A-R Biomass Index. The Biomass (Age1-2+) time series shows both the biomass estimates from age-1 and age-2 individuals (black dashed line) as well as the converted age-2+ biomass estimates (red dashed line).

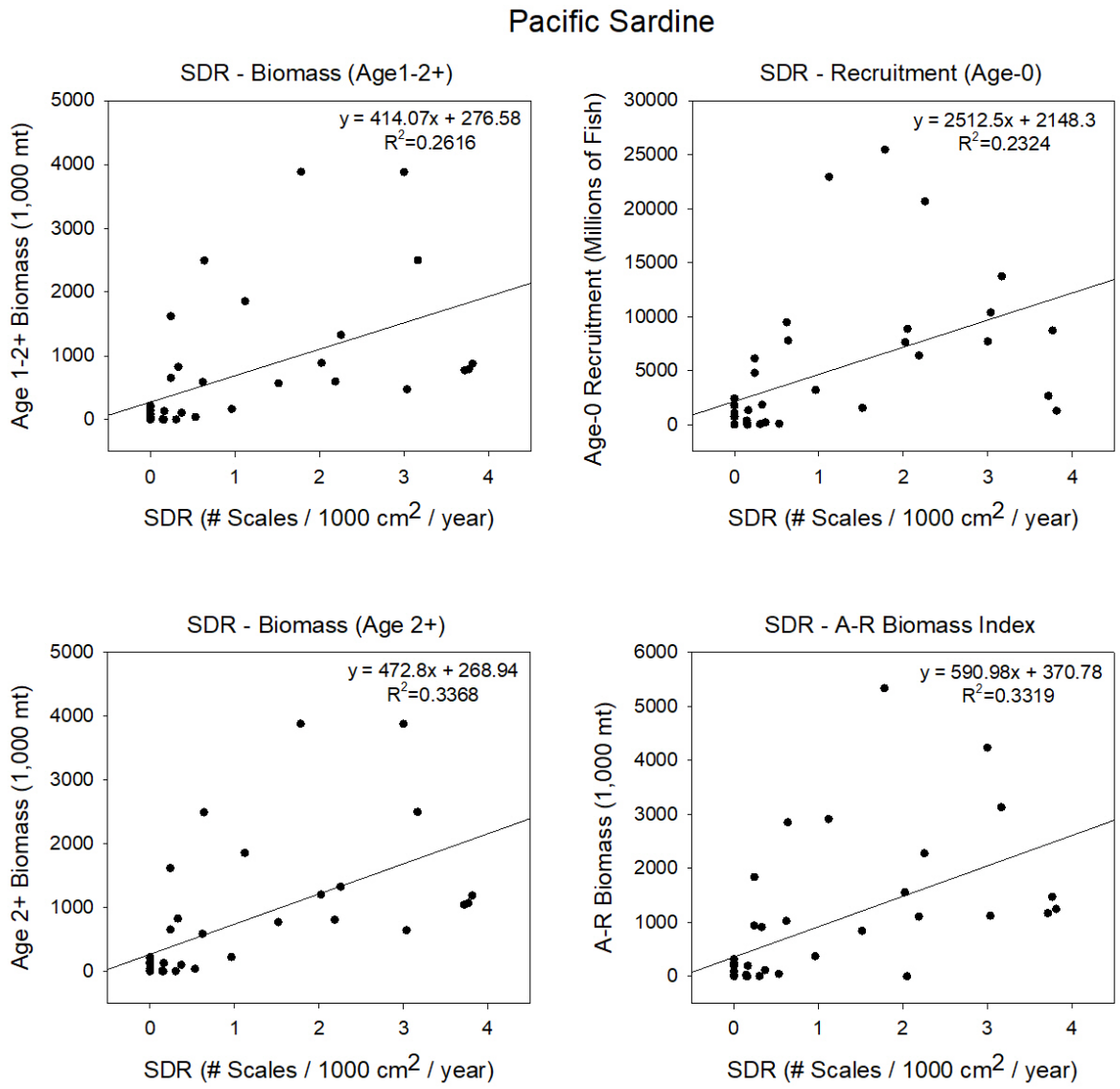

Figure A16. Linear regressions between the natural log of sardine SDR with biomass, recruitment, and the A-R Biomass Index.

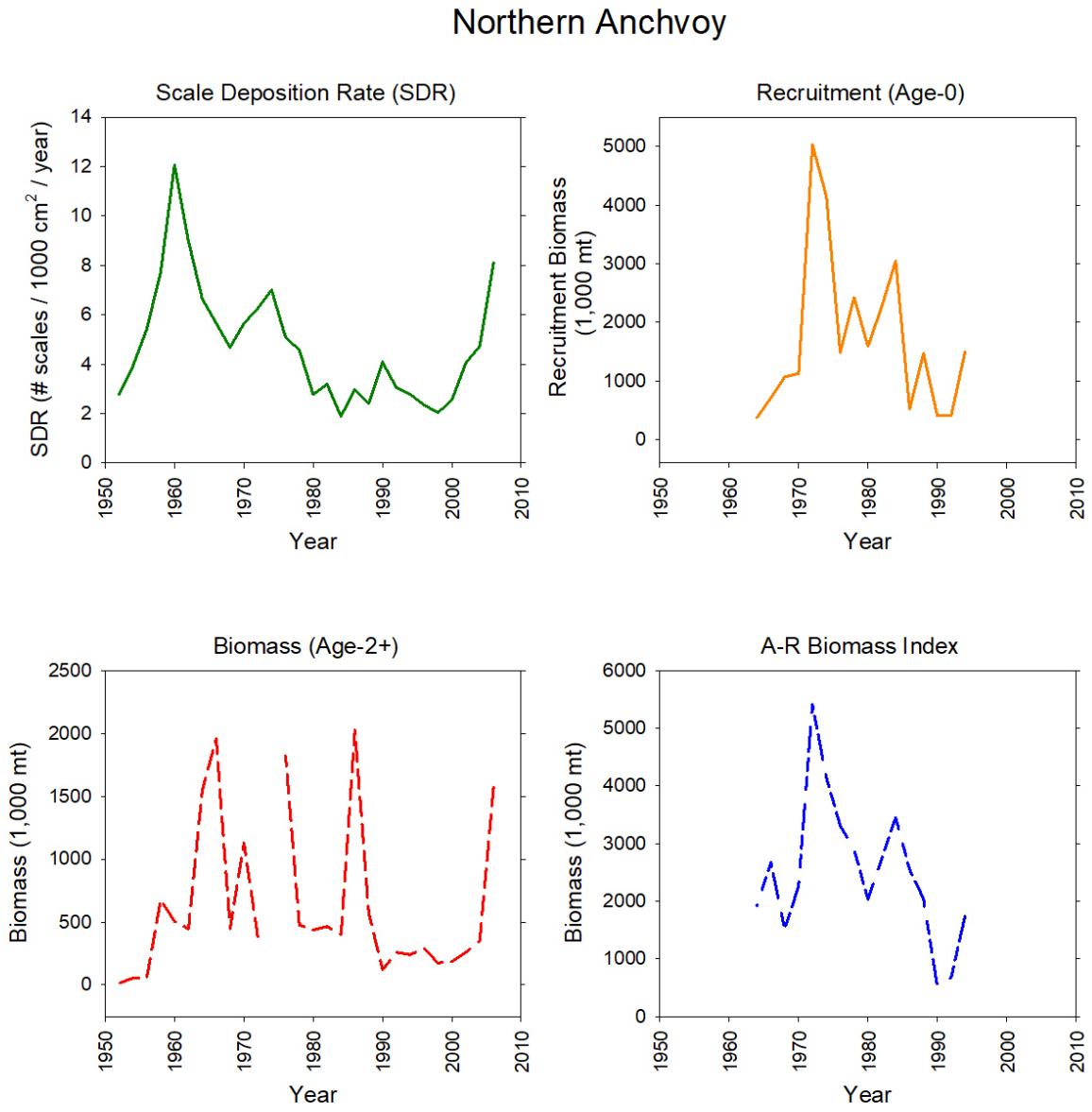

Figure A17. Time series of anchovy SDR, recruitment (Jacobson et al., 1995), biomass (Thayer et al., 2017), and the A-R Biomass Index.

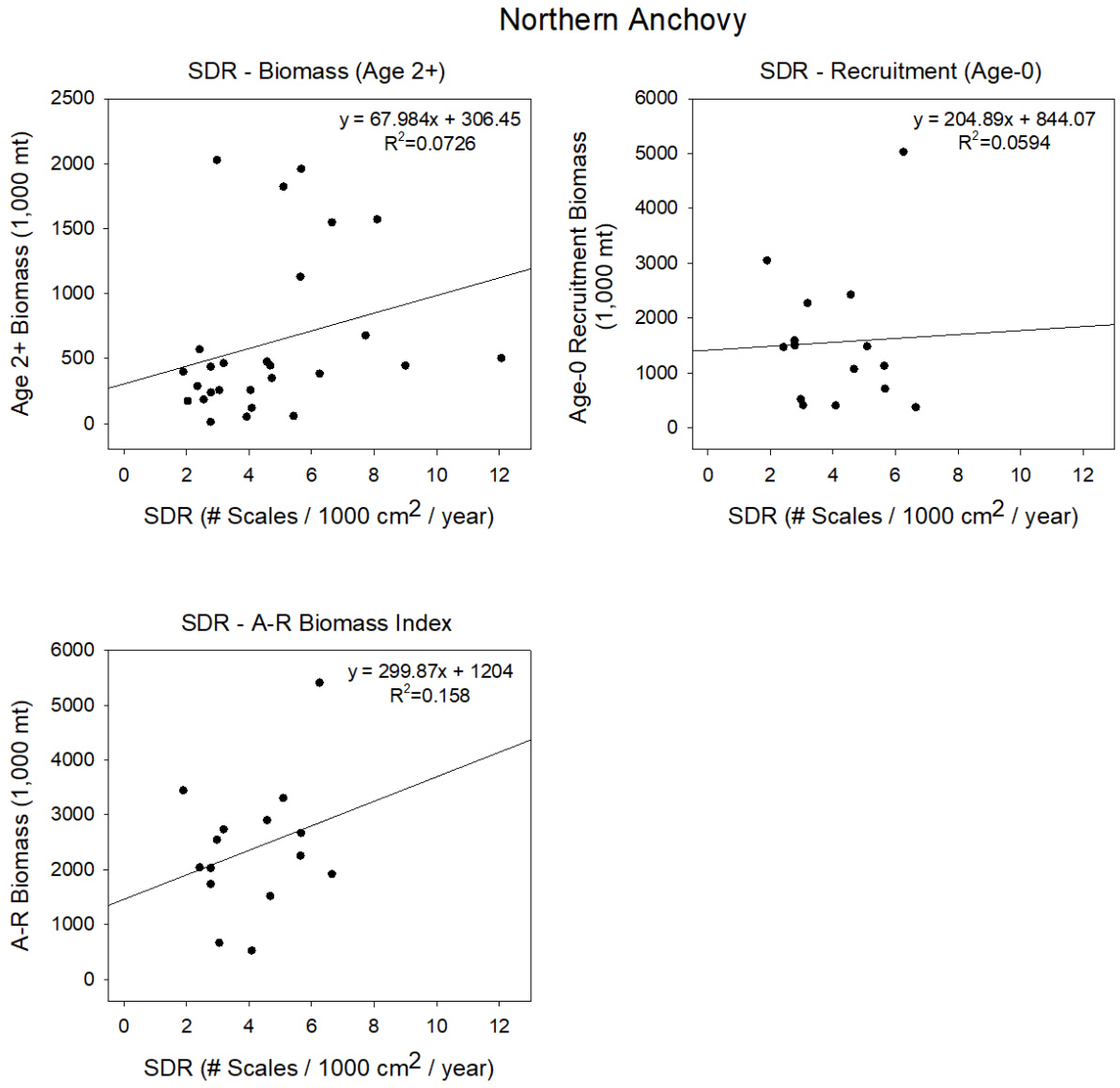

Figure A18. Linear regression between anchovy SDR with biomass, recruitment, and A-R Biomass Index.

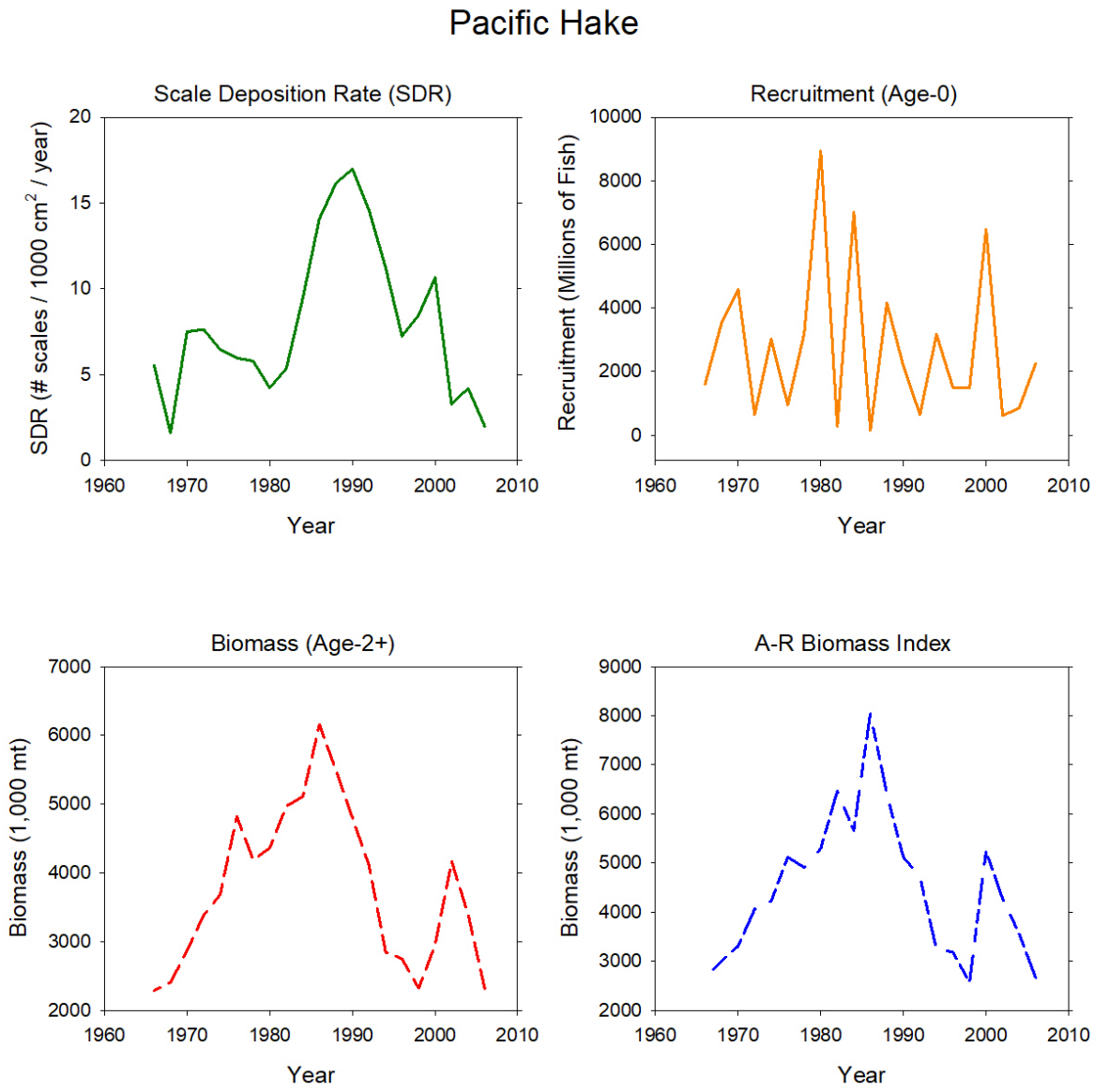

Figure A19. Time series of anchovy SDR, recruitment (Berger et al., 2019), biomass (Berger et al., 2019), and the A-R Biomass Index.

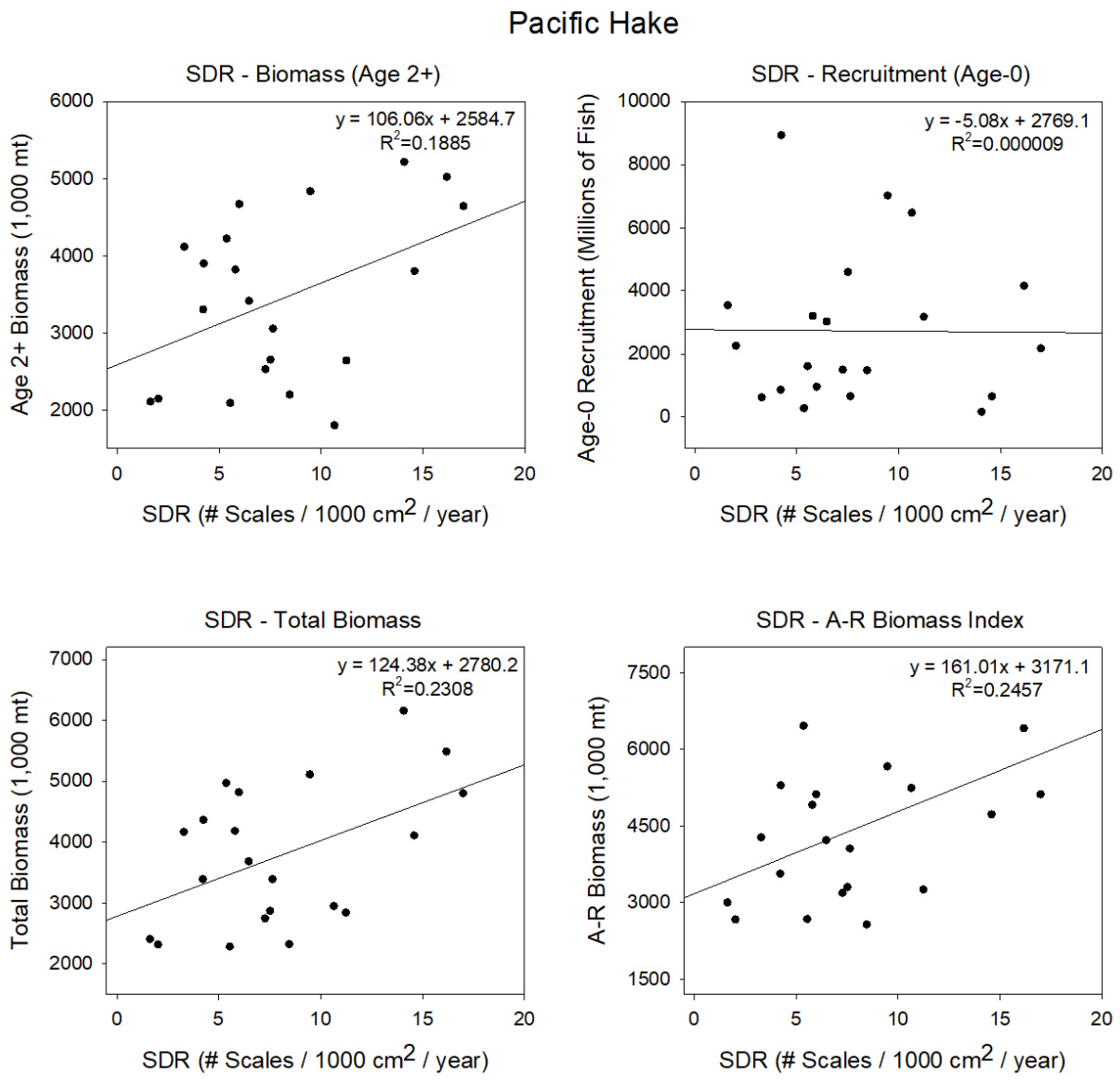

Figure A20. Linear regression between hake SDR with biomass, recruitment, and A-R Biomass Index.

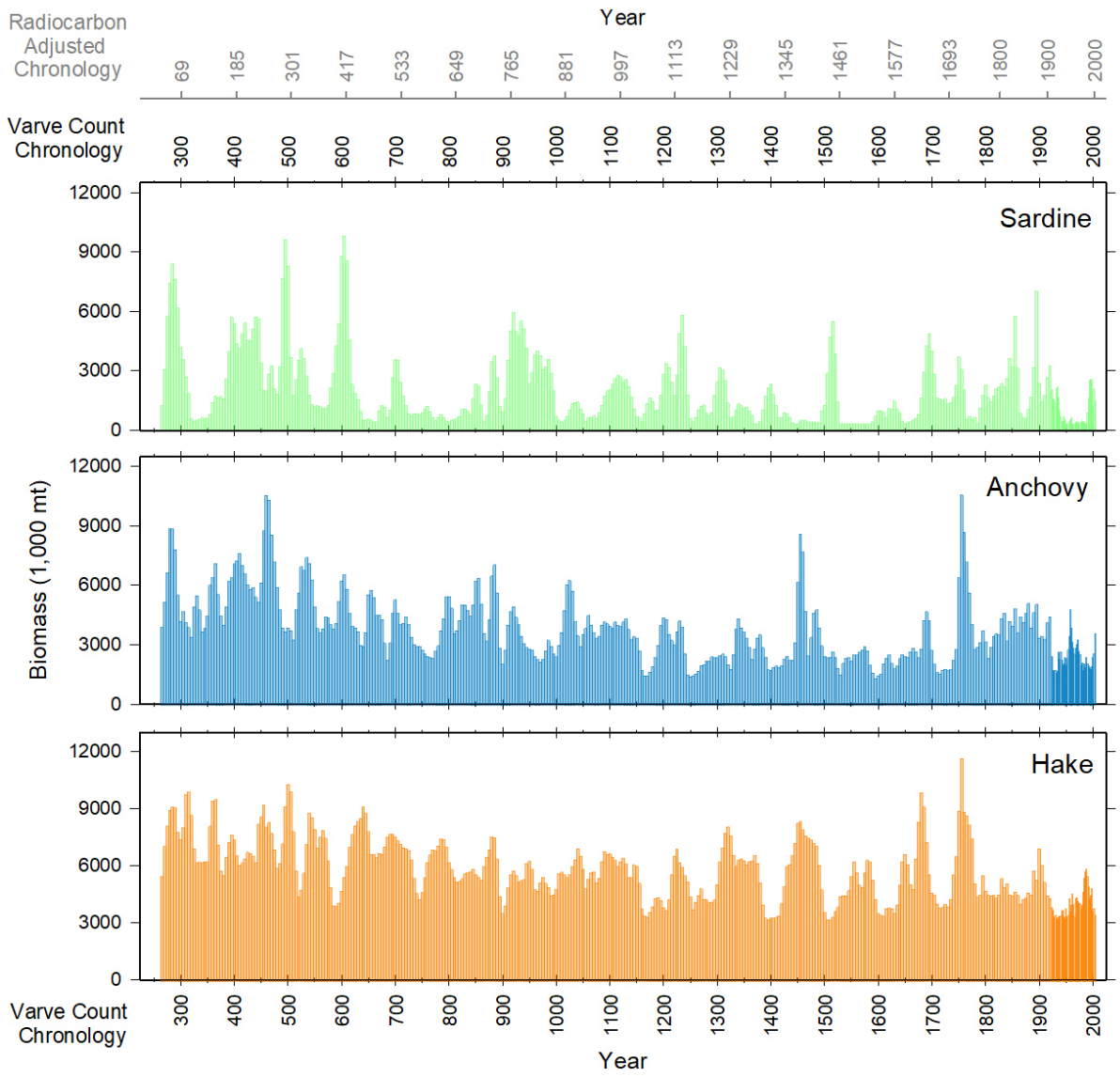

Figure A21. Biomass time series of sardine, anchovy, and hake from 260 to 2006AD. SDR was calibrated with biomass using a linear regression with the A-R Biomass Index. Note that the sampling intervals from 260 – 1746 are in five-year intervals whereas from 1746-2006 there is a two year sampling resolution.

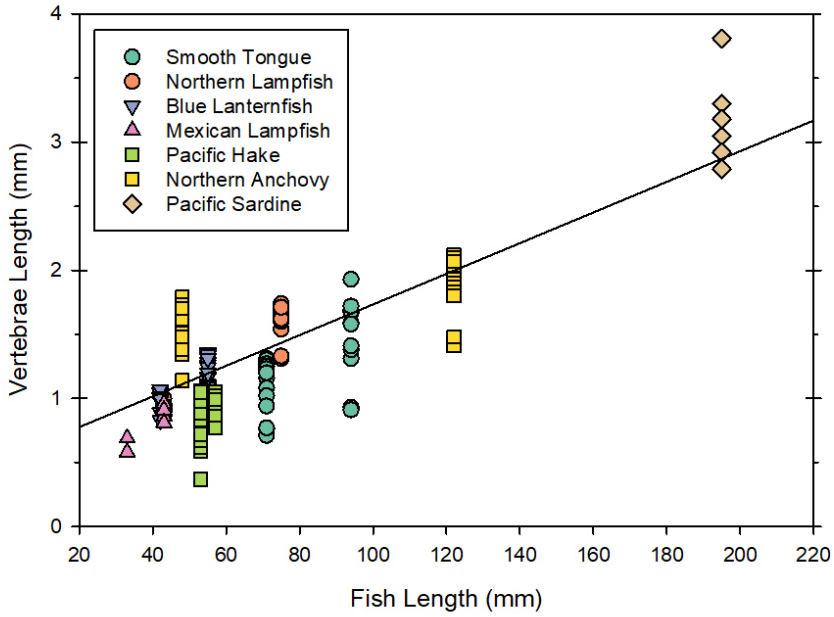

Figure A22. A scatterplot of vertebrae lengths versus the fish lengths the vertebrae were extracted from along with a linear regression to obtain a formula to estimate fish length based on vertebrae length.

APPENDIX II: Vertebrae Image Catalog

Table of Figures:

Blue Lantern Fish

(Blue lanternfish (42 mm) anterior images unavailable)

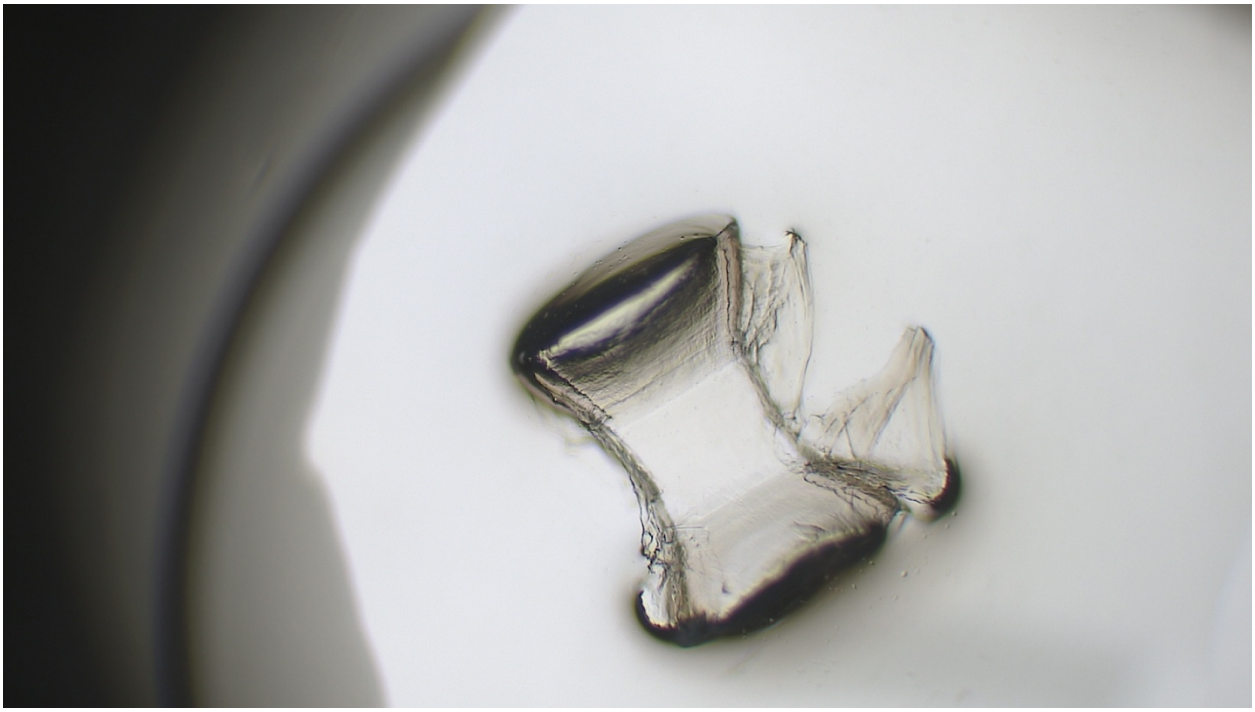

Figure AA1. Blue Lanternfish, 42 mm standard length, Mid, Side View (Mid Centrum View Unavailable)

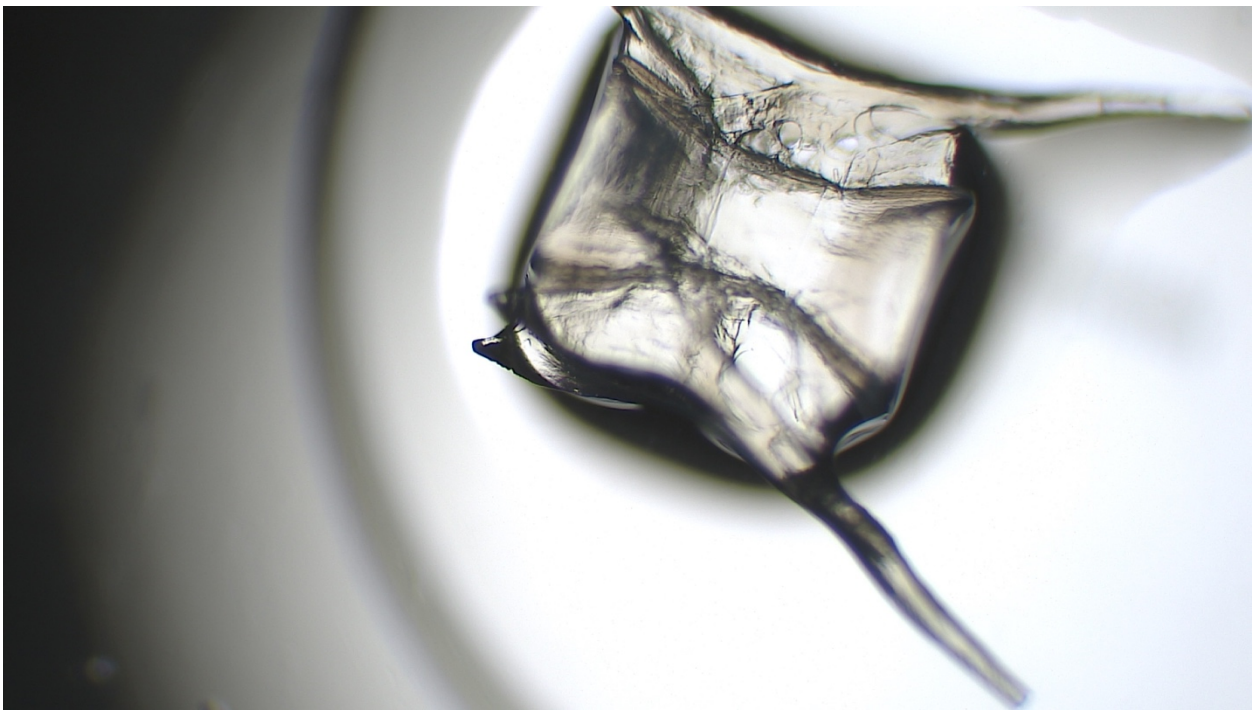

Figure AA2. Blue Lanternfish, 42 mm standard length, Posterior, Side View

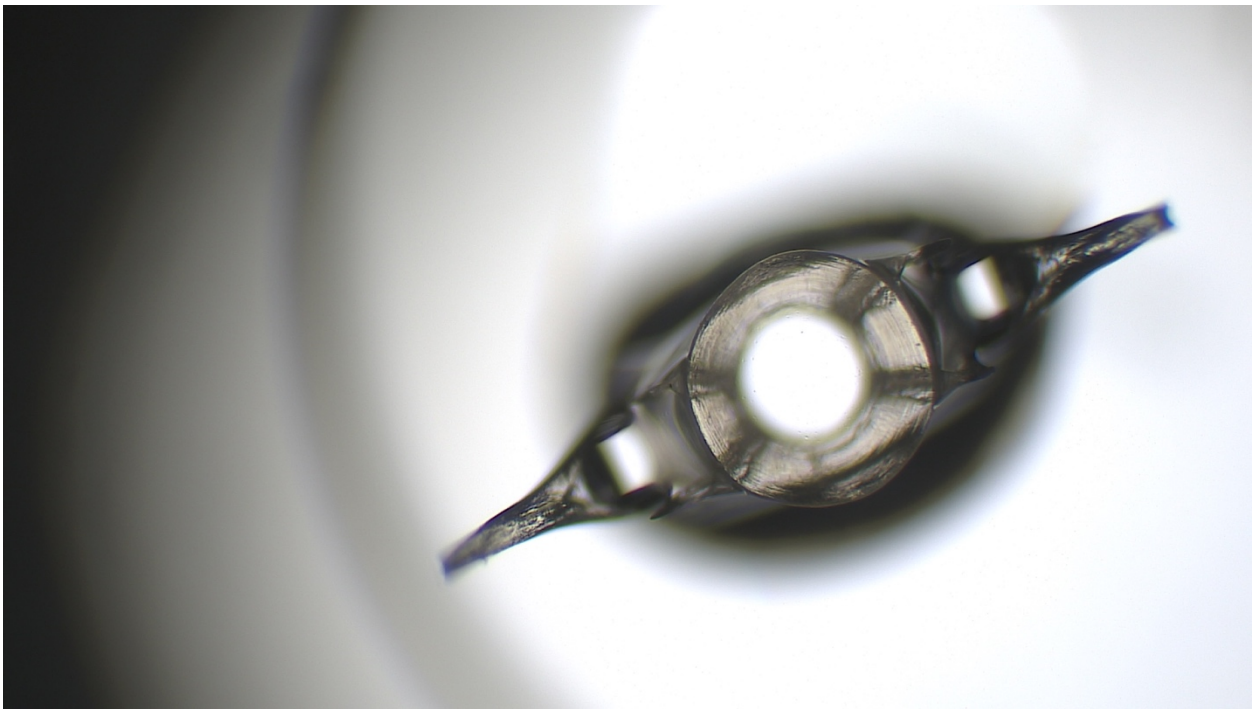

Figure AA3. Blue Lanternfish, 42 mm standard length, Posterior, Centrum View

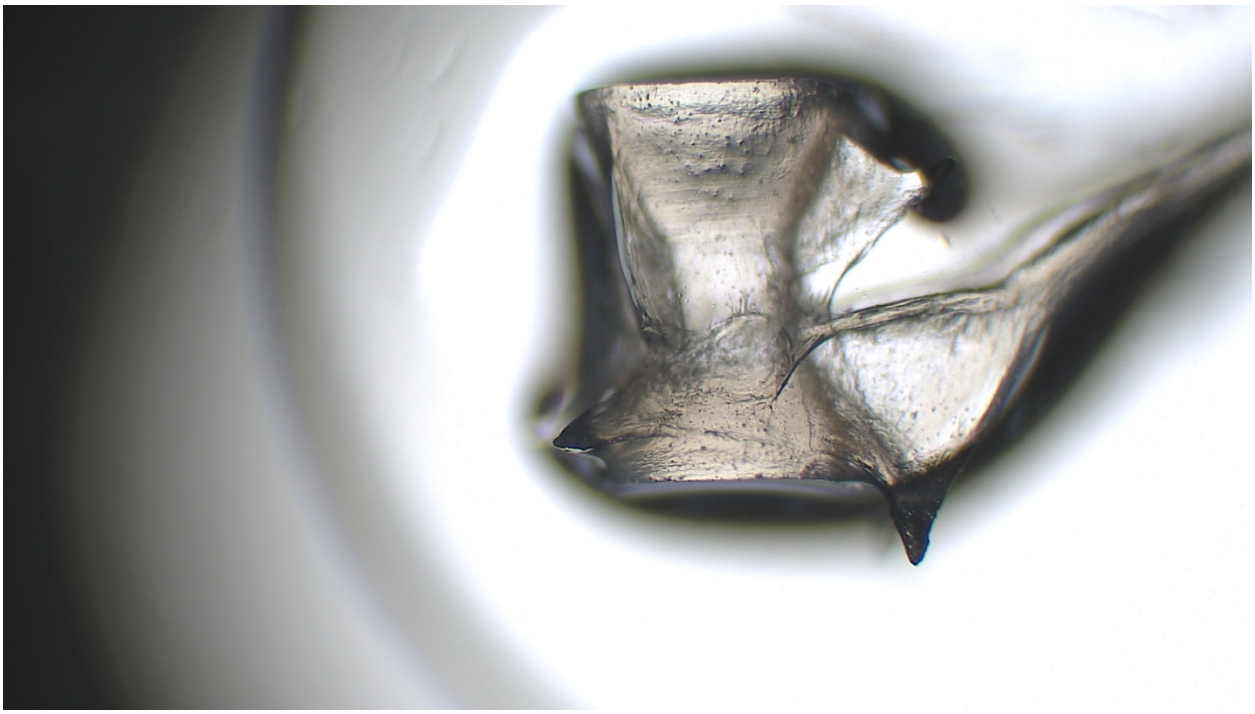

Figure AA4. Blue Lanternfish, 55 mm standard length, Anterior, Side View

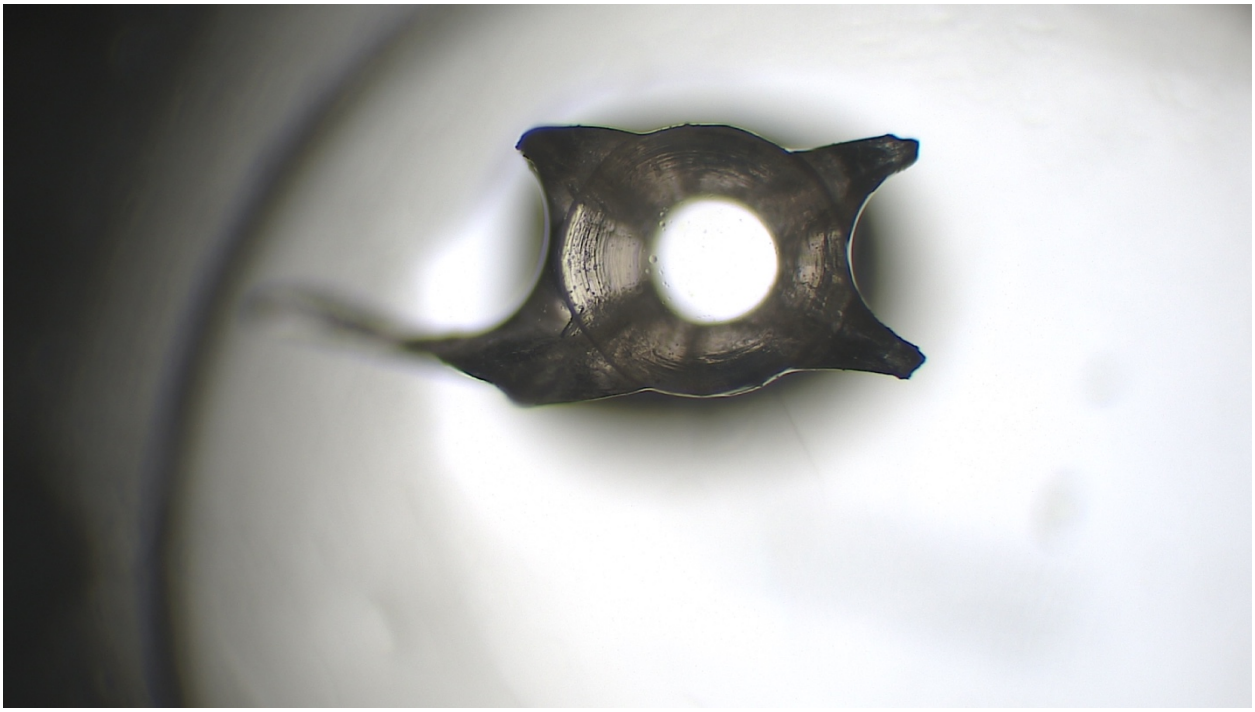

Figure AA5. Blue Lanternfish, 55 mm standard length, Anterior, Centrum View

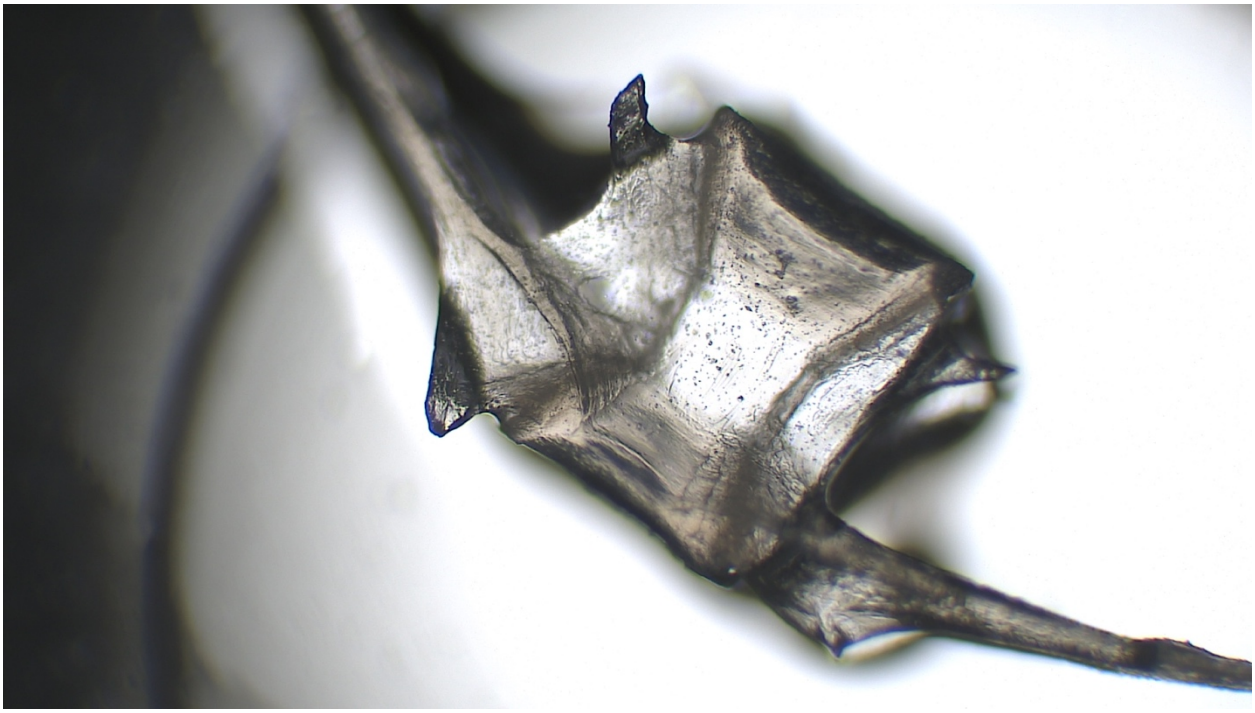

Figure AA6. Blue Lanternfish, 55 mm standard length, Mid, Side View

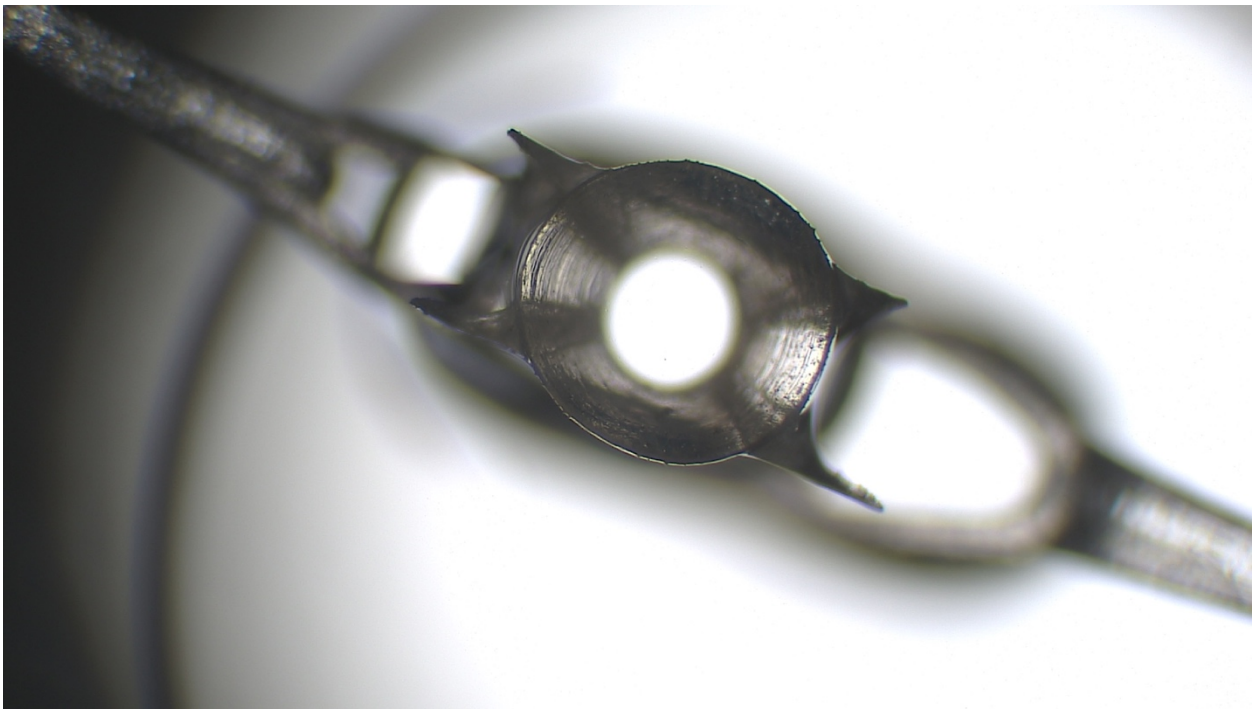

Figure AA7. Blue Lanternfish, 55 mm standard length, Mid, Centrum View

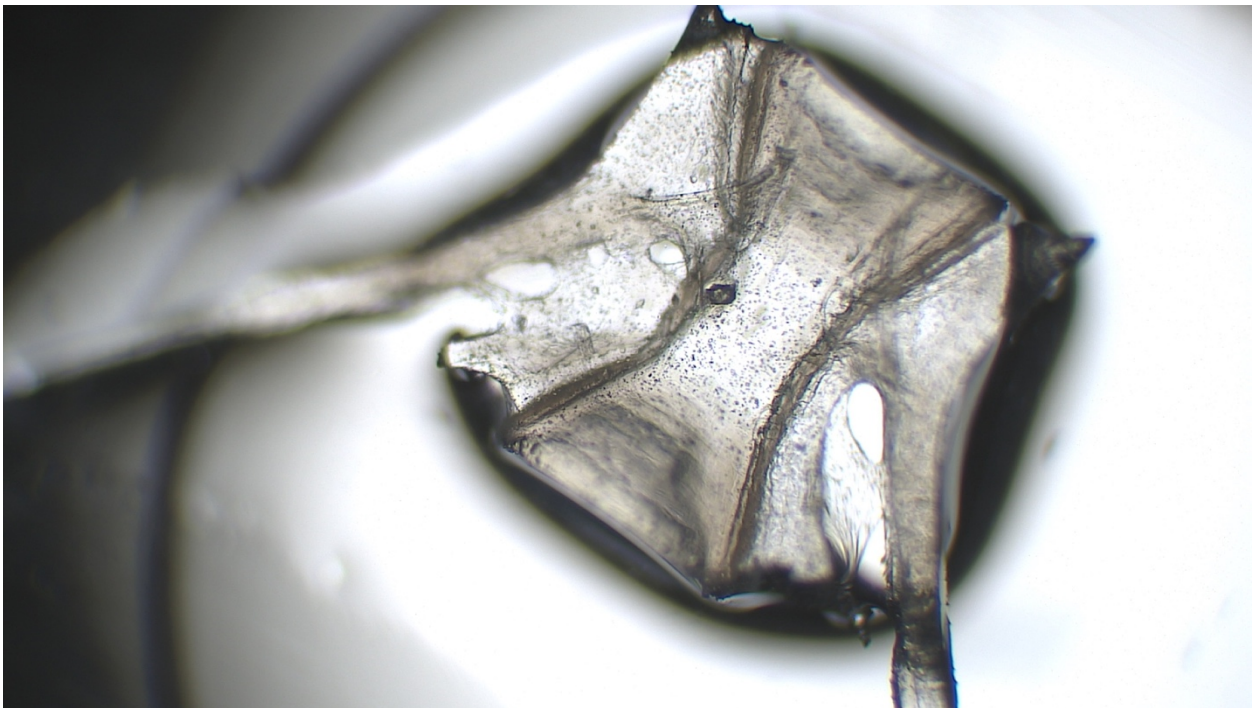

Figure AA8. Blue Lanternfish, 55 mm standard length, Posterior, Side View

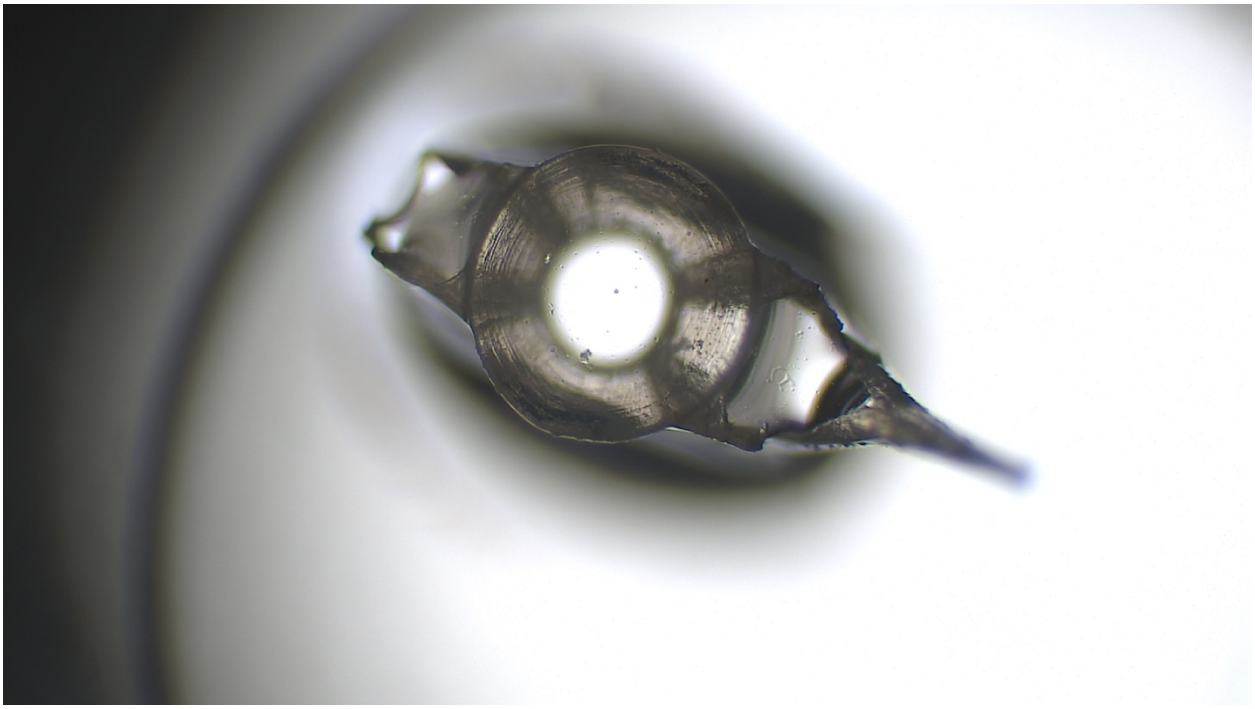

Figure AA9. Blue Lanternfish, 55 mm standard length, Posterior, Centrum View

Mexican Lampfish

(Mexican lampfish (33 mm) anterior and mid images unavailable)

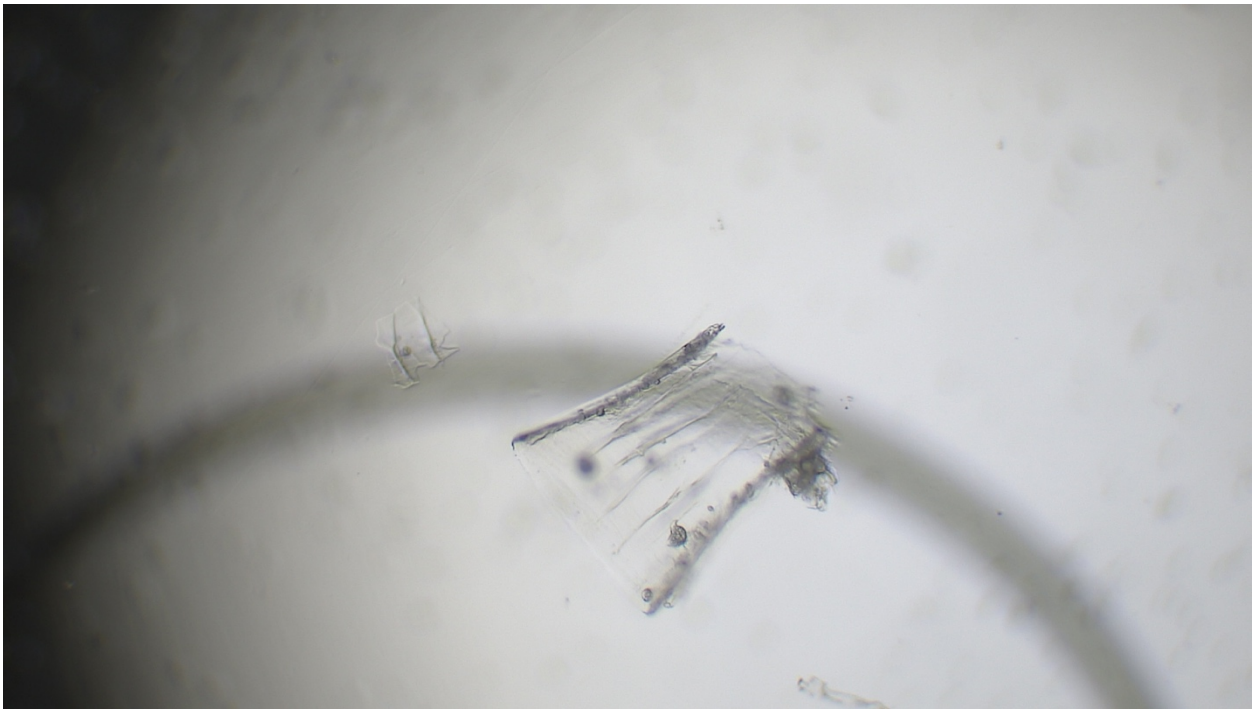

Figure AA10. Mexican Lampfish, 33 mm standard length, Posterior, Side View (Posterior Centrum View Unavailable)

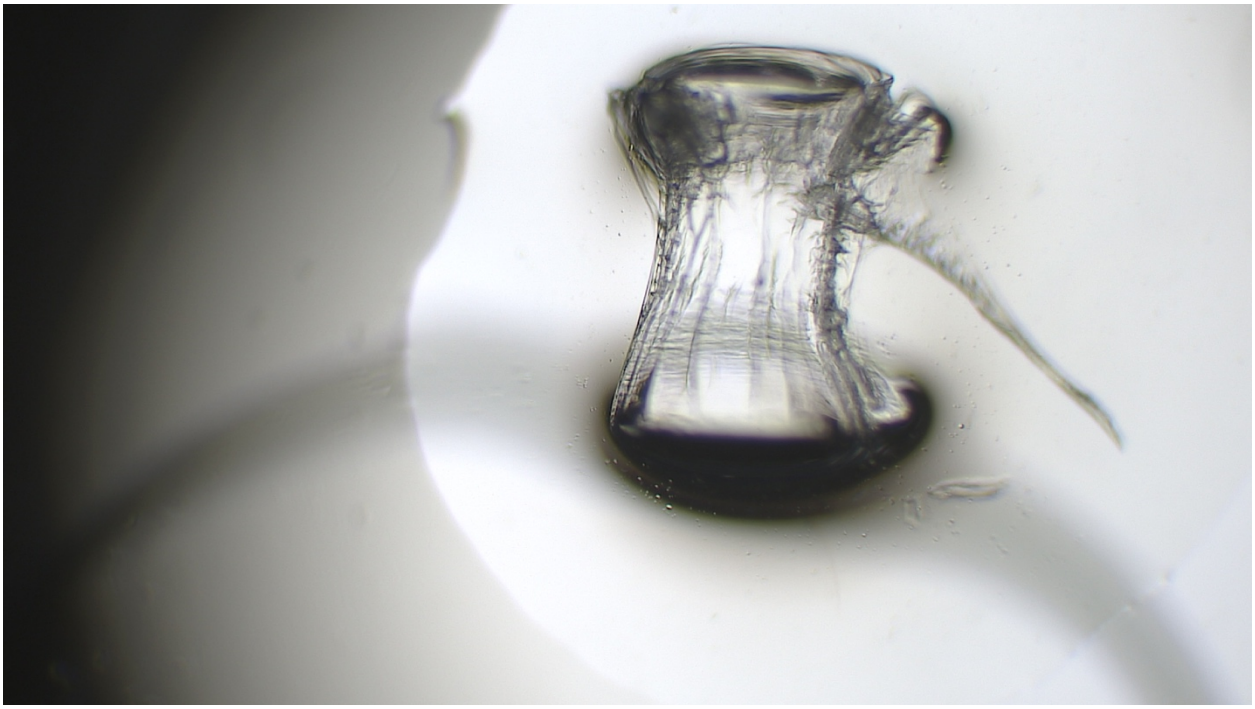

Figure AA11. Mexican Lampfish, 43 mm standard length, Anterior, Side View

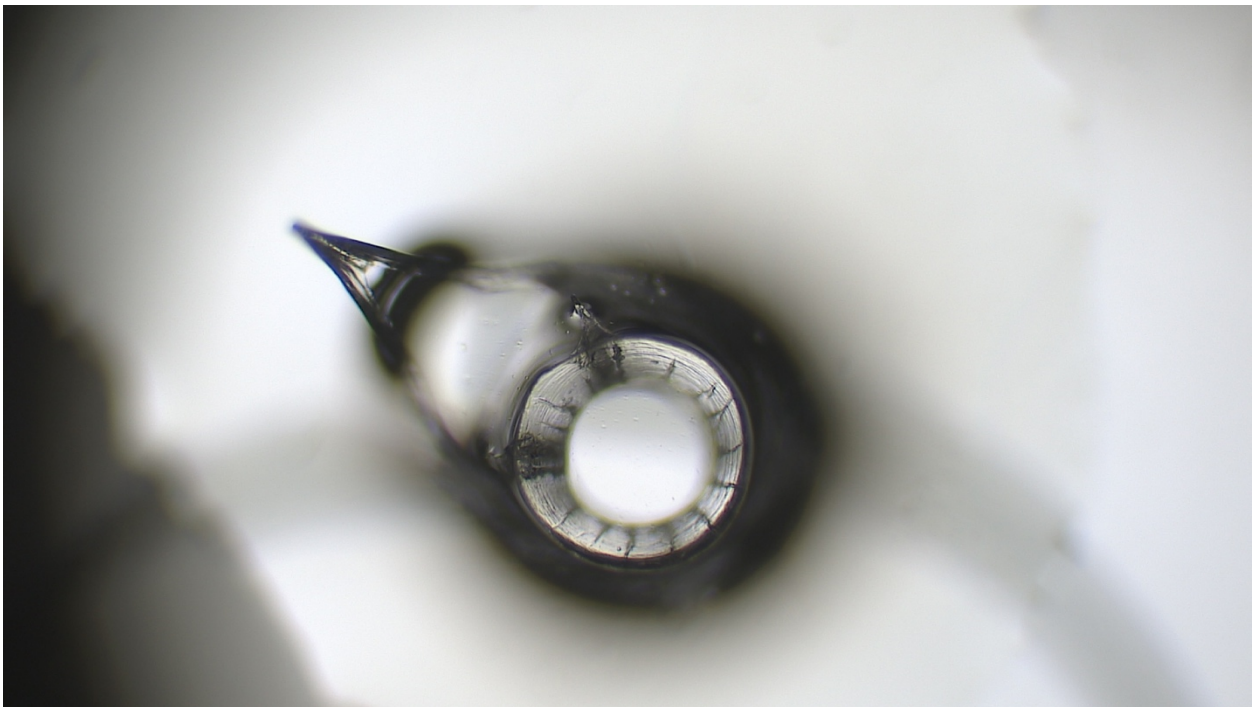

Figure AA12. Mexican Lampfish, 43 mm standard length, Anterior, Centrum View

(Mexican Lampfish (43 mm), mid and posterior images unavailable)

Nanobracchia sp.

Nanobracchia (40 mm) anterior and posterior images unavailable)

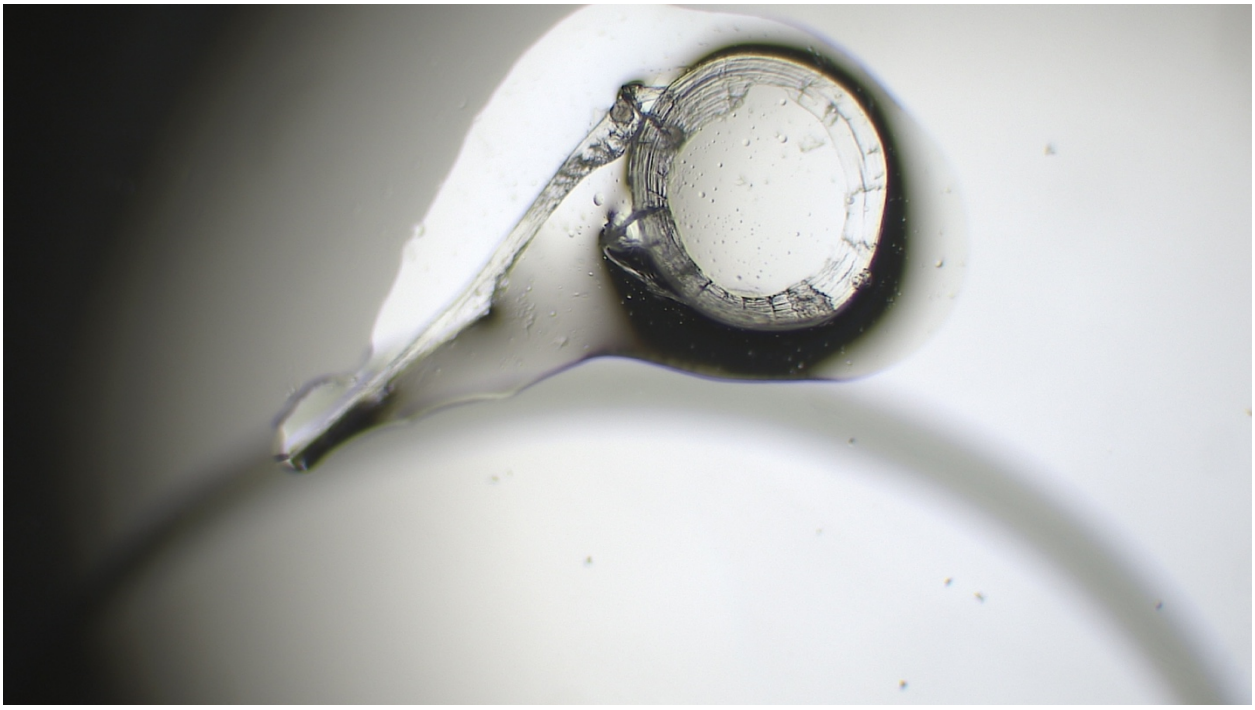

Figure AA13. Nanobracchia sp., 40 mm standard length, Mid, Centrum View)

Northern Anchovy

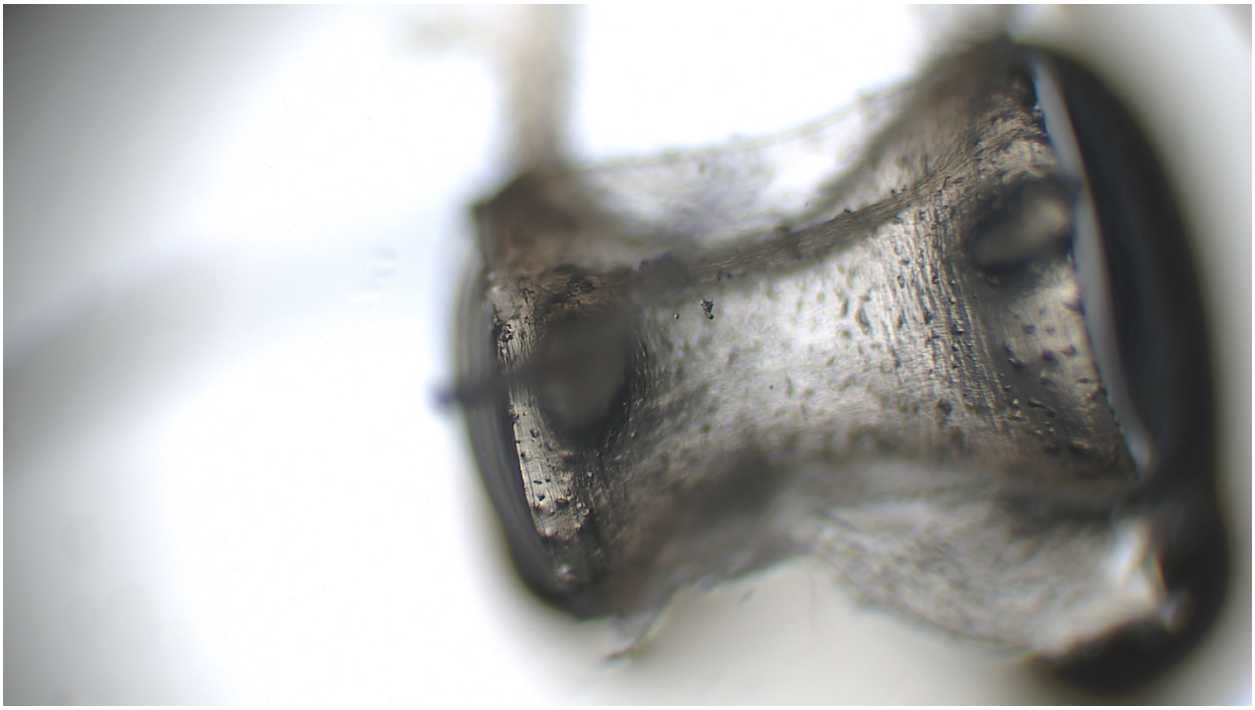

Figure AA14. Northern Anchovy, 48 mm standard length, Anterior, Side View

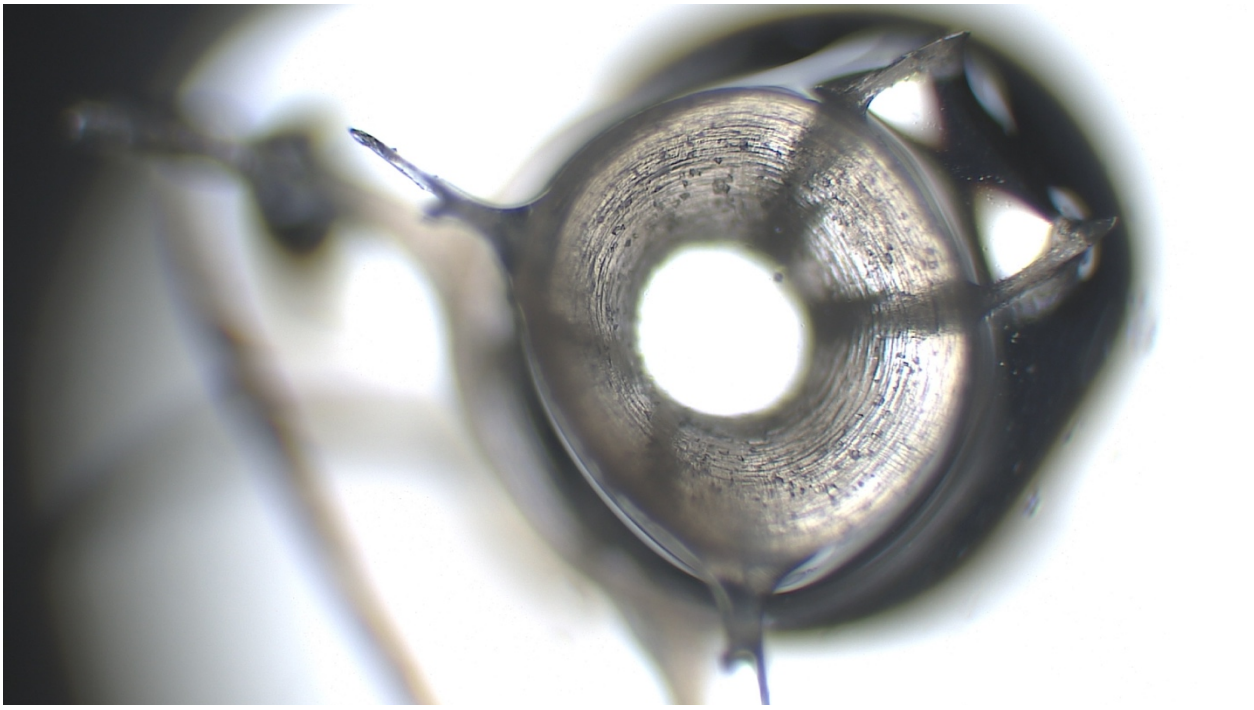

Figure AA15. Northern Anchovy, 48 mm standard length, Anterior, Centrum View

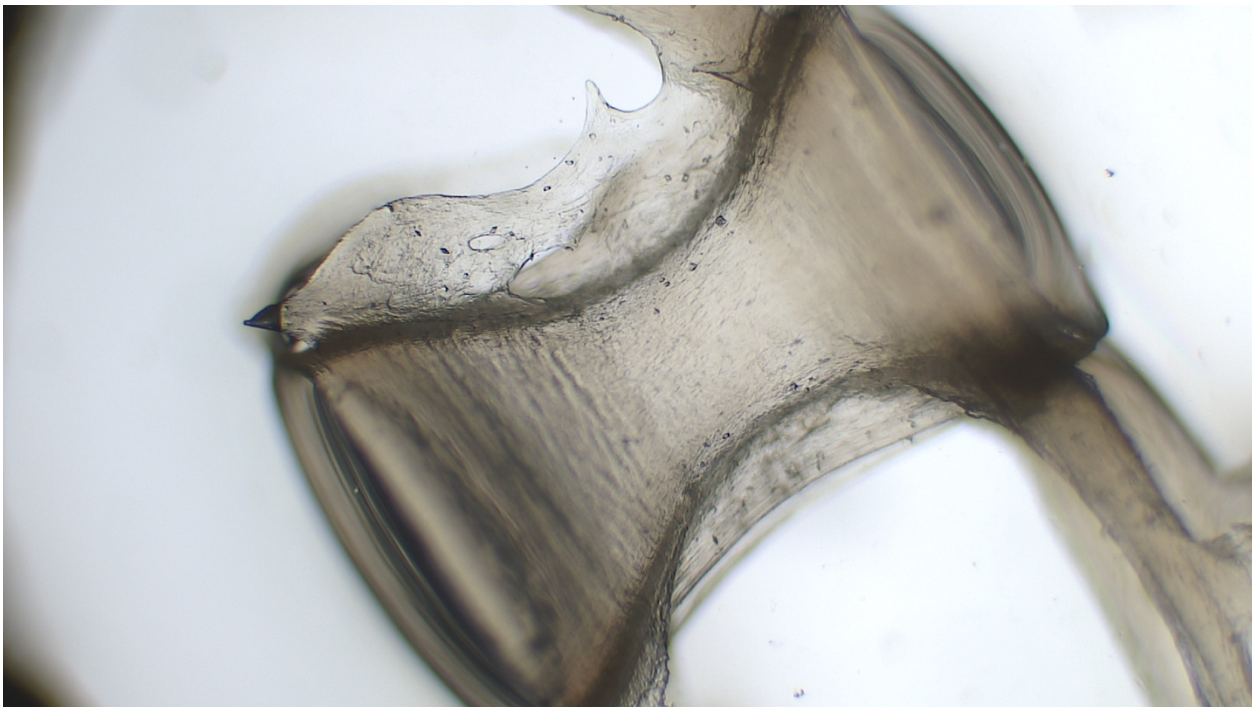

Figure AA16. Northern Anchovy, 48 mm standard length, Mid, Side View

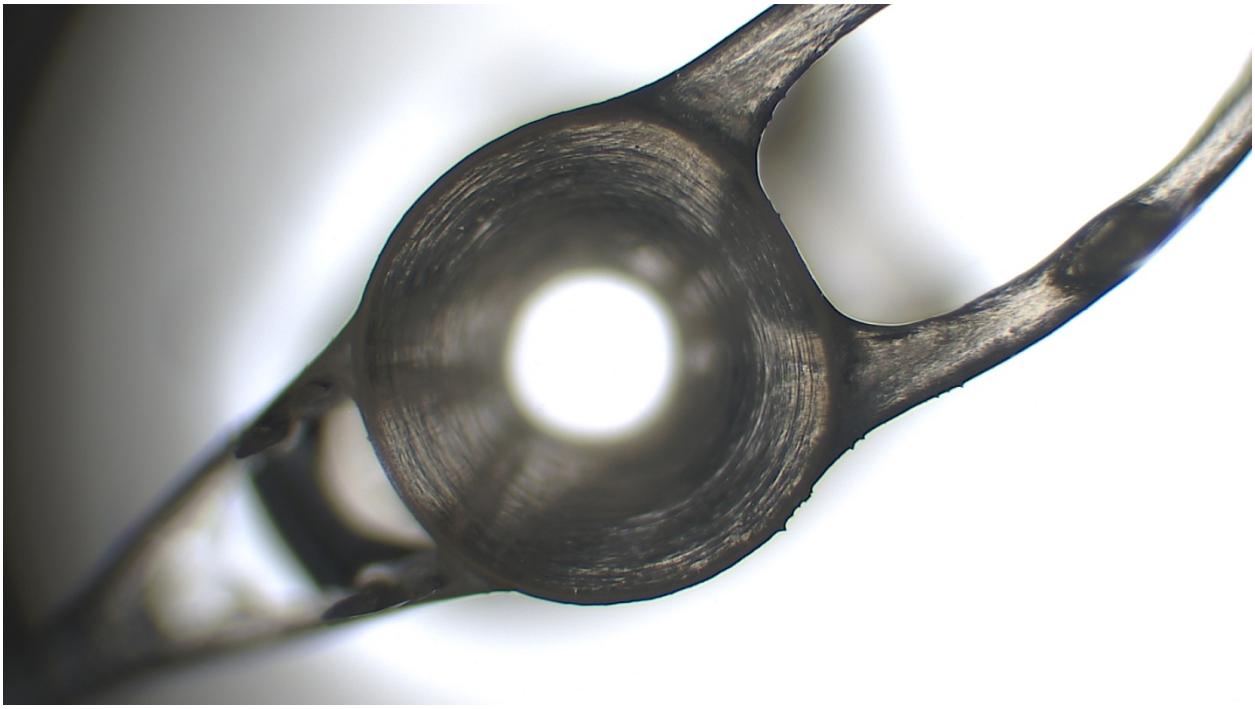

Figure AA17. Northern Anchovy, 48 mm standard length, Mid, Centrum View

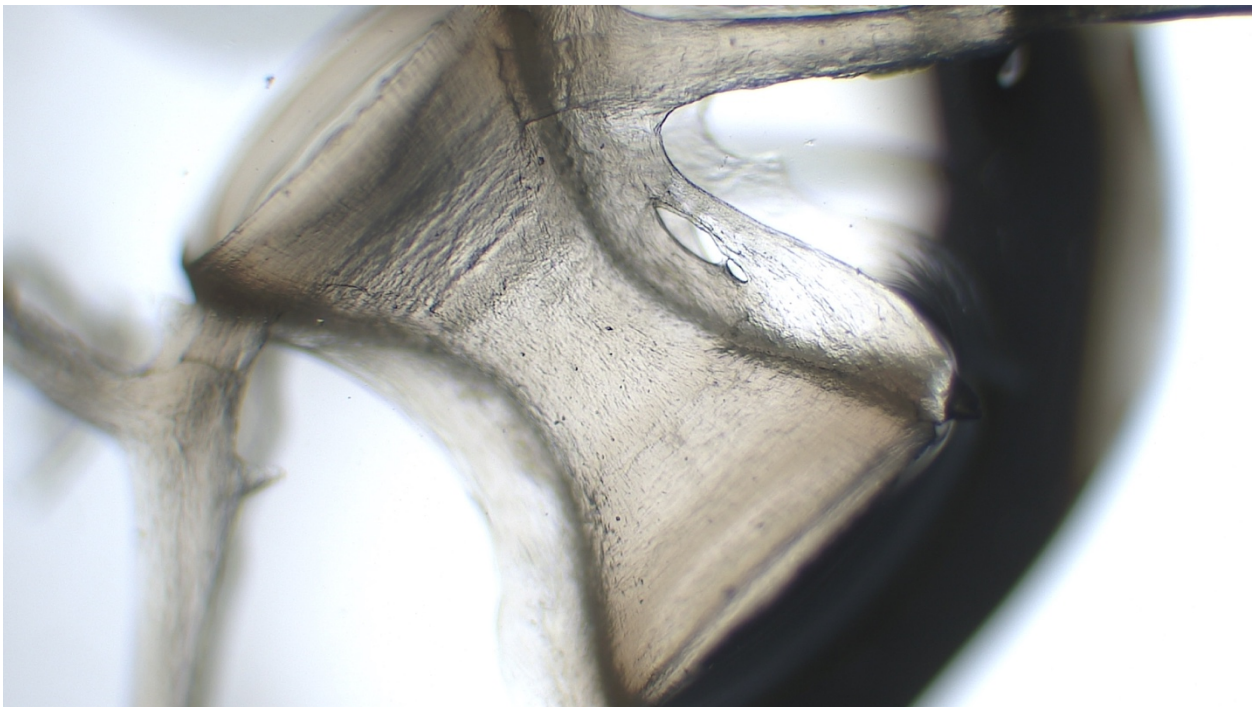

Figure AA18. Northern Anchovy, 48 mm standard length, Posterior, Side View

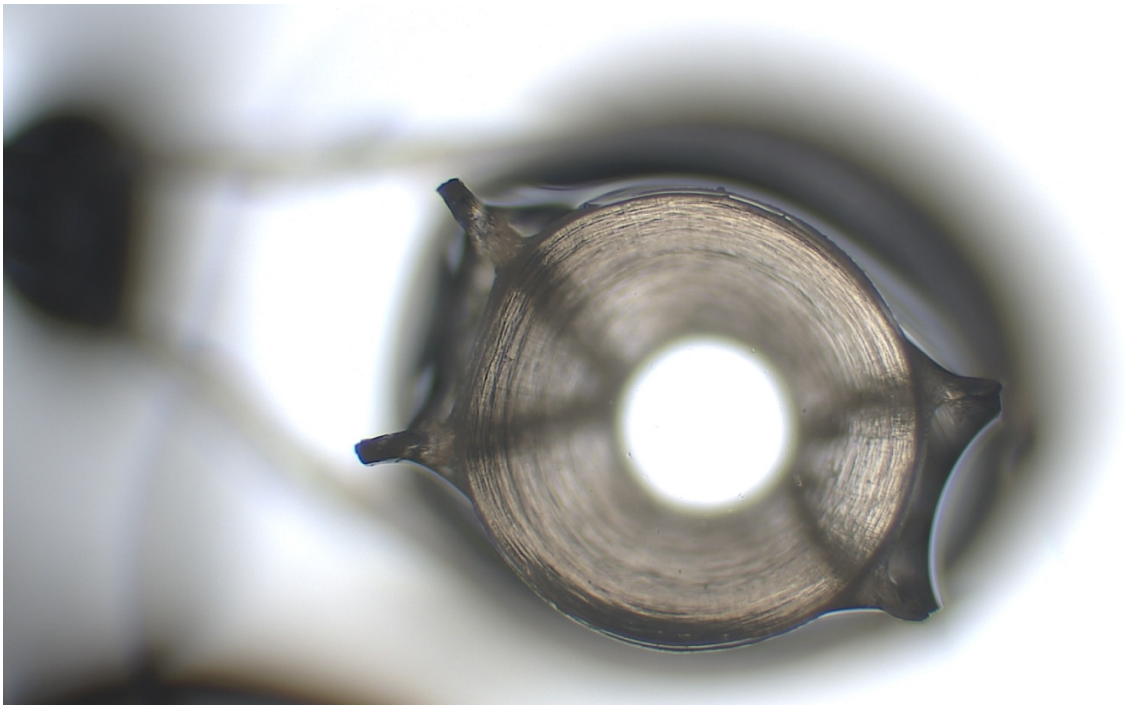

Figure AA19. Northern Anchovy, 48 mm standard length, Posterior, Centrum View

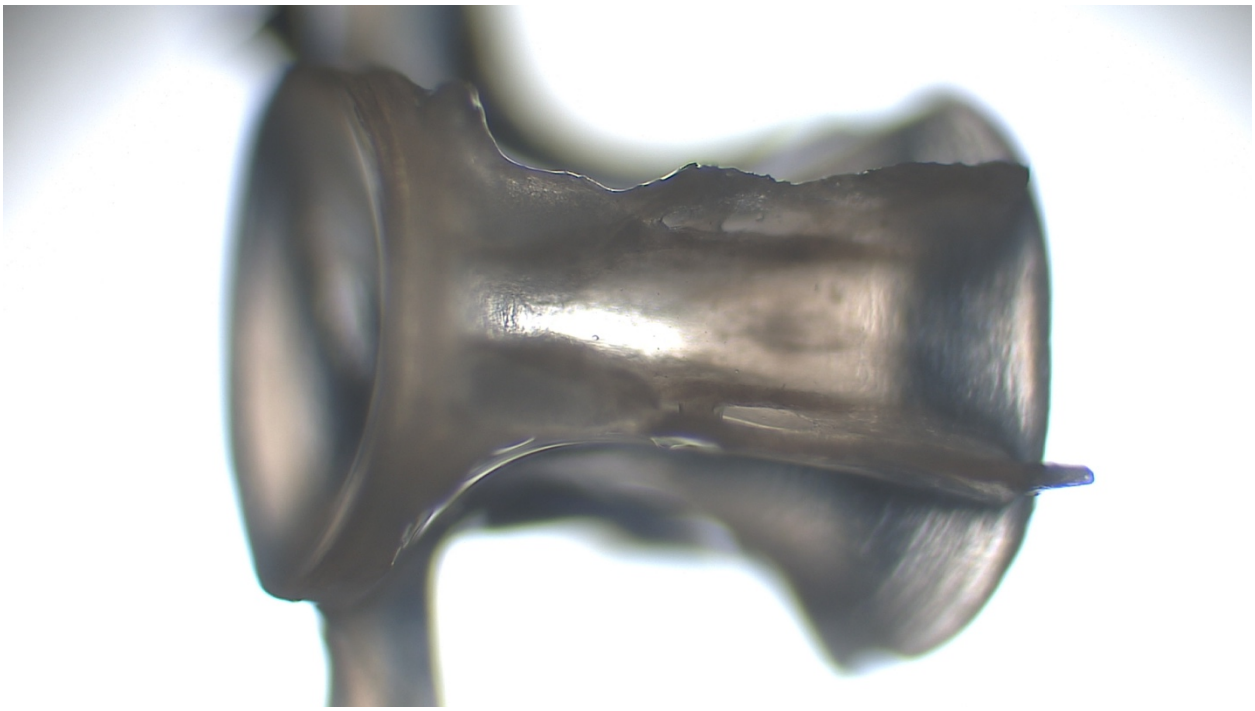

Figure AA20. Northern Anchovy, 122 mm standard length, Anterior, Side View

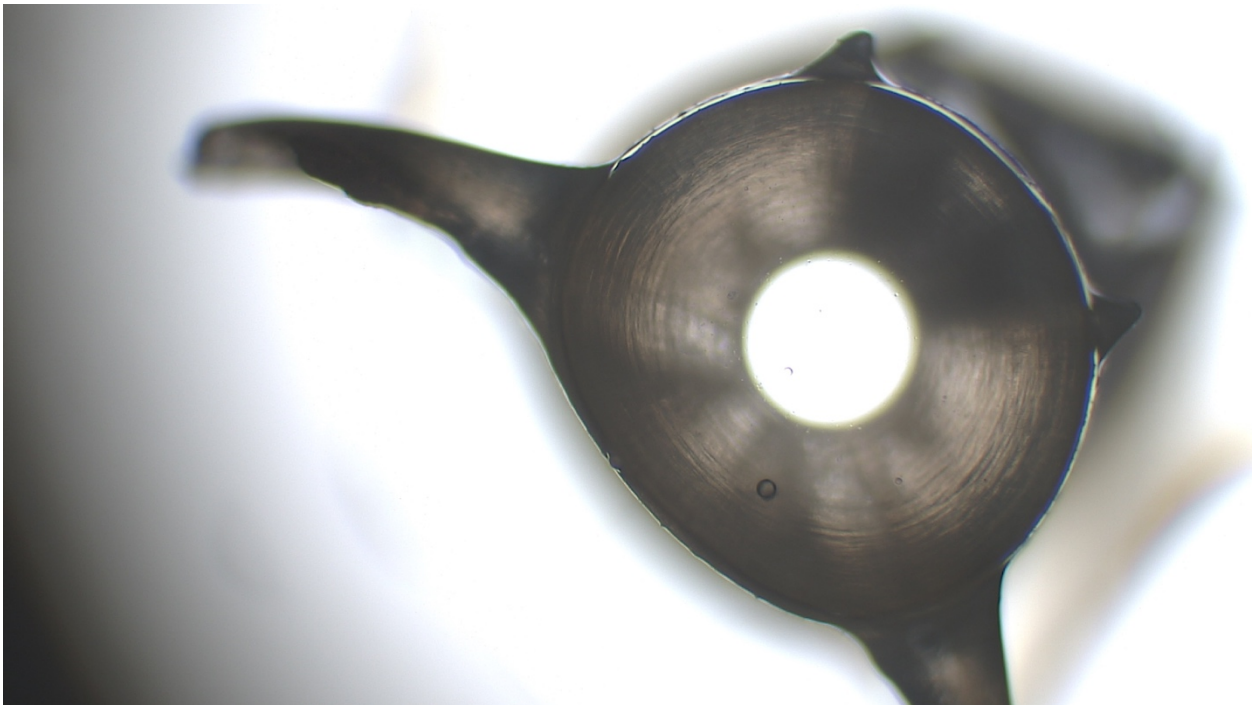

Figure AA21. Northern Anchovy, 122 mm standard length, Anterior, Centrum View

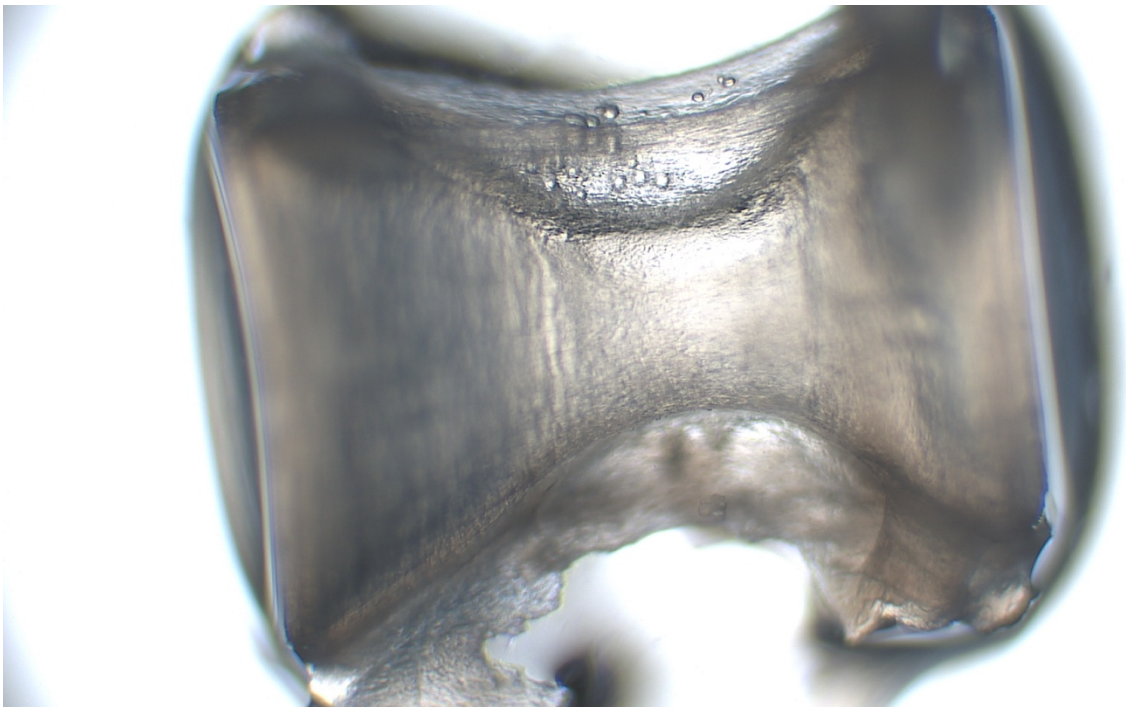

Figure AA22. Northern Anchovy, 122 mm standard length, Mid, Side View

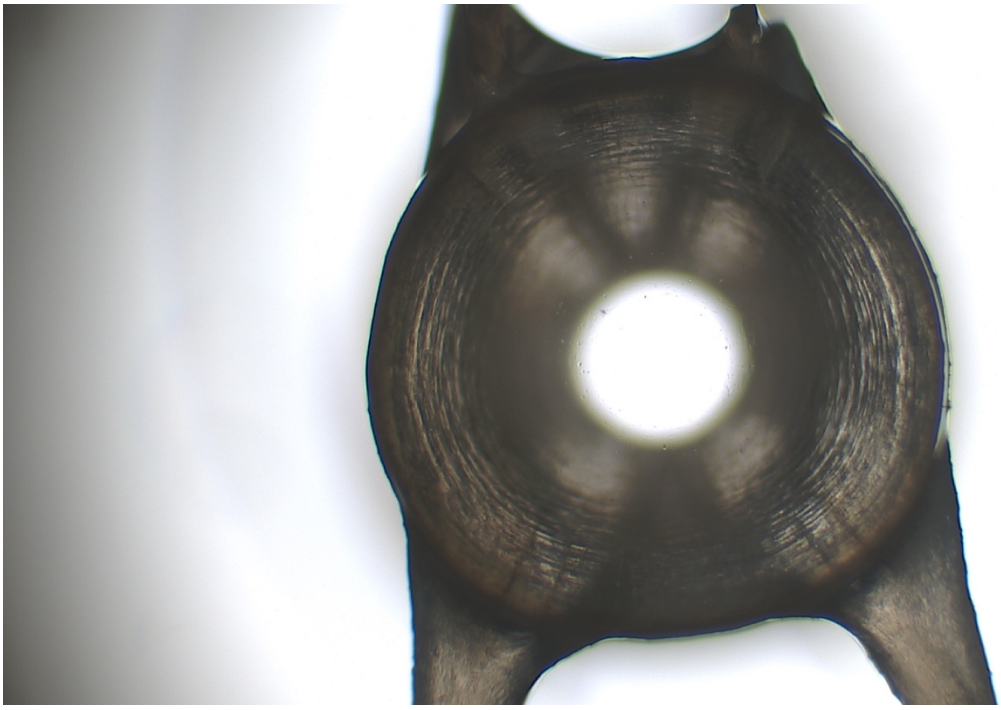

Figure AA23. Northern Anchovy, 122 mm standard length, Mid, Centrum View

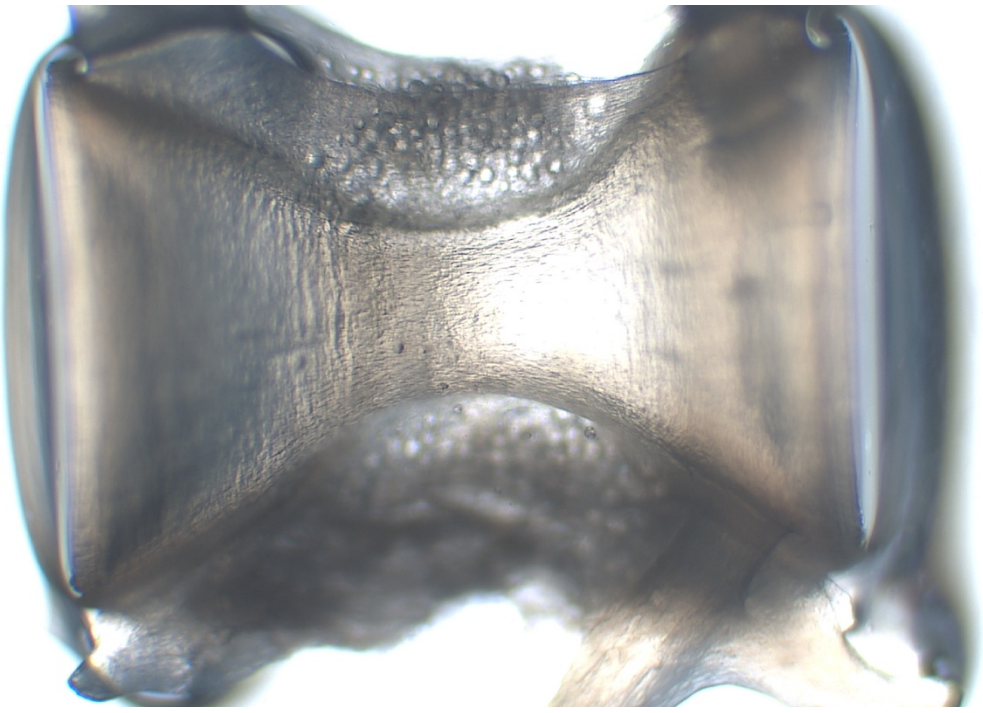

Figure AA24. Northern Anchovy, 122 mm standard length, Posterior, Side View

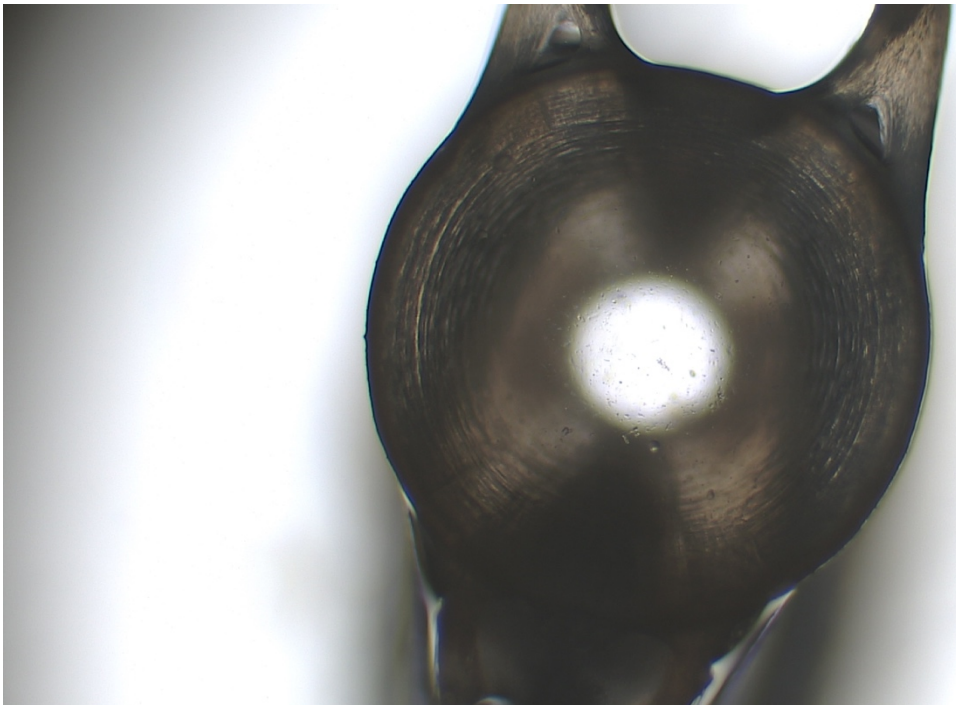

Figure AA25. Northern Anchovy, 122 mm standard length, Posterior, Centrum View

Northern Lampfish

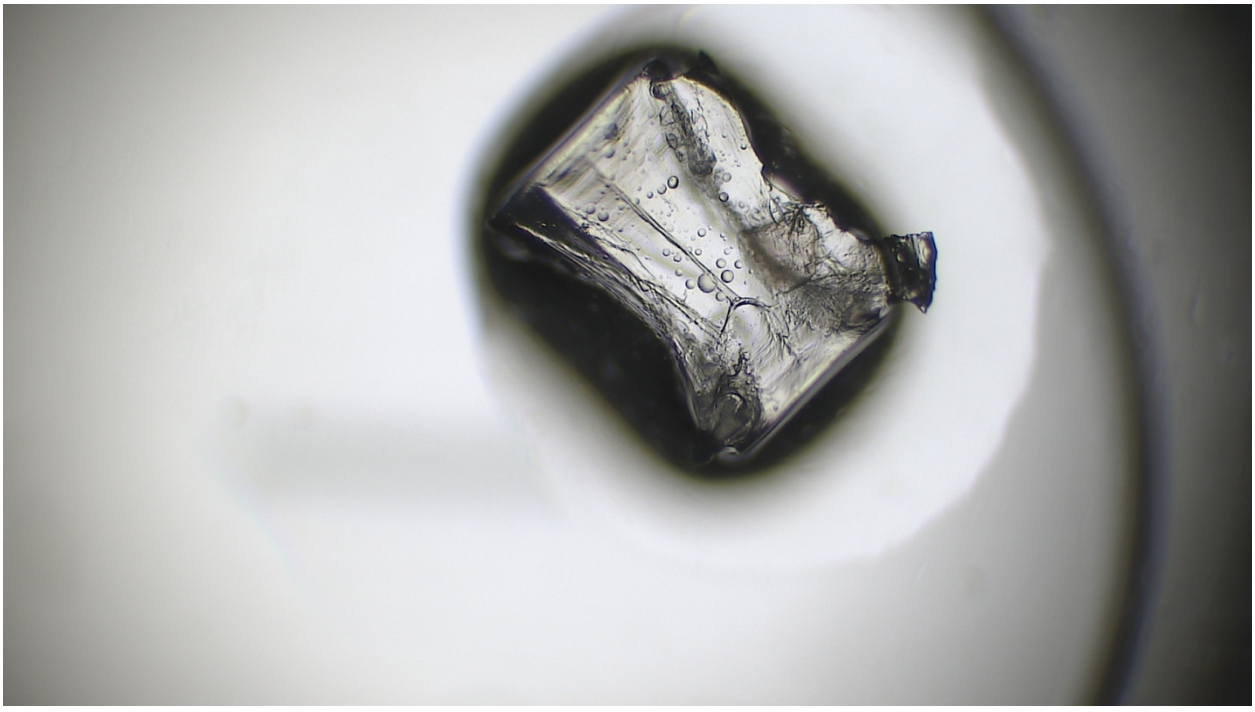

Figure AA26. Northern Lampfish, 43 mm standard length, Anterior, Side View

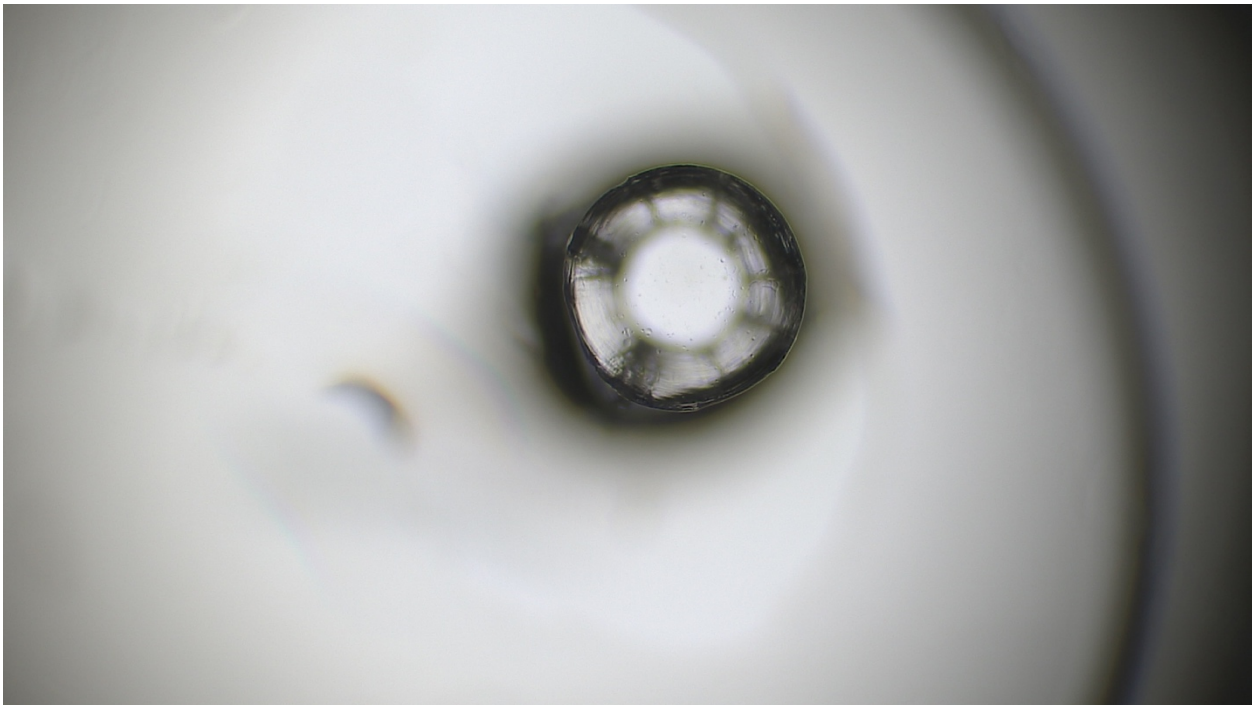

Figure AA27. Northern Lampfish, 43 mm standard length, Anterior, Centrum View

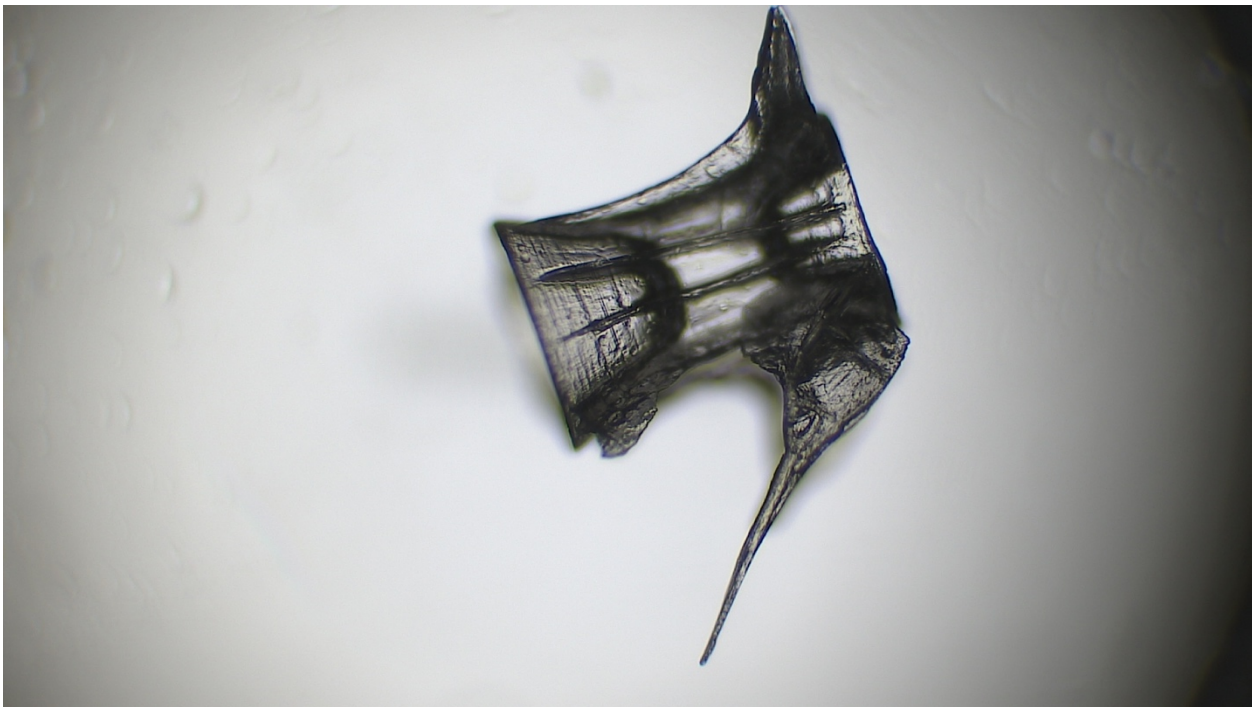

Figure AA28. Northern Lampfish, 43 mm standard length, Mid, Side View

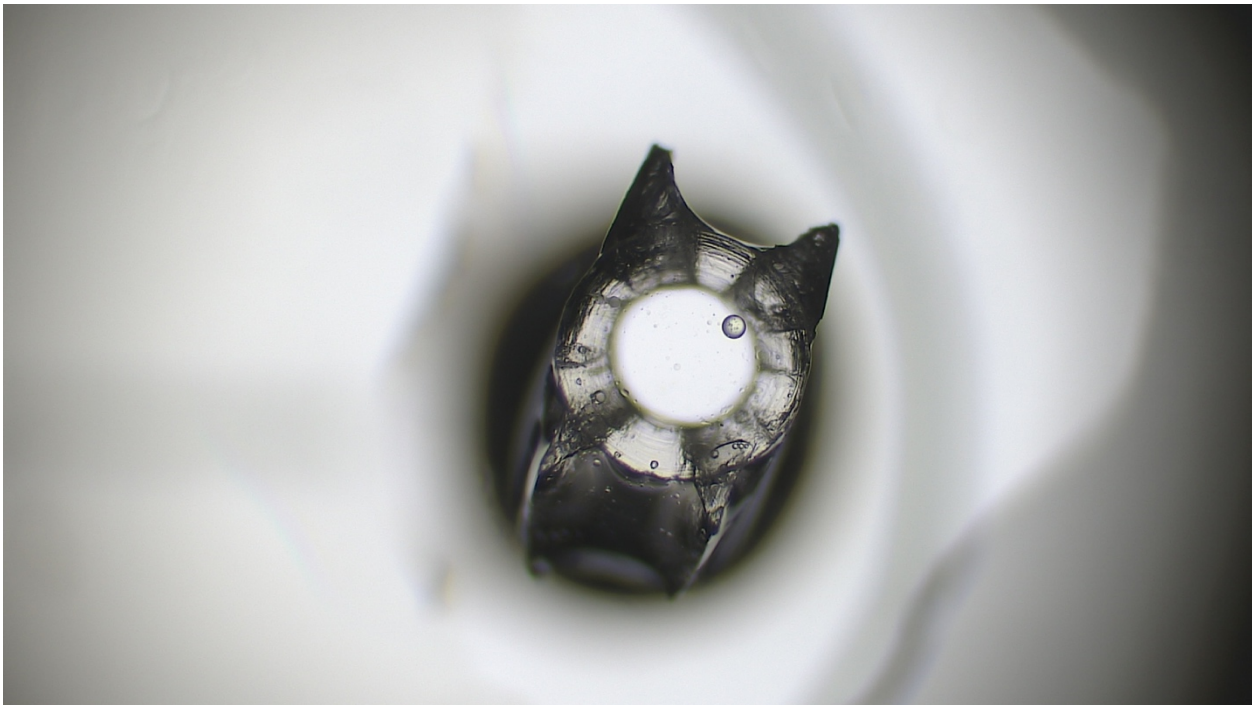

Figure AA29. Northern Lampfish, 43 mm standard length, Mid, Centrum View

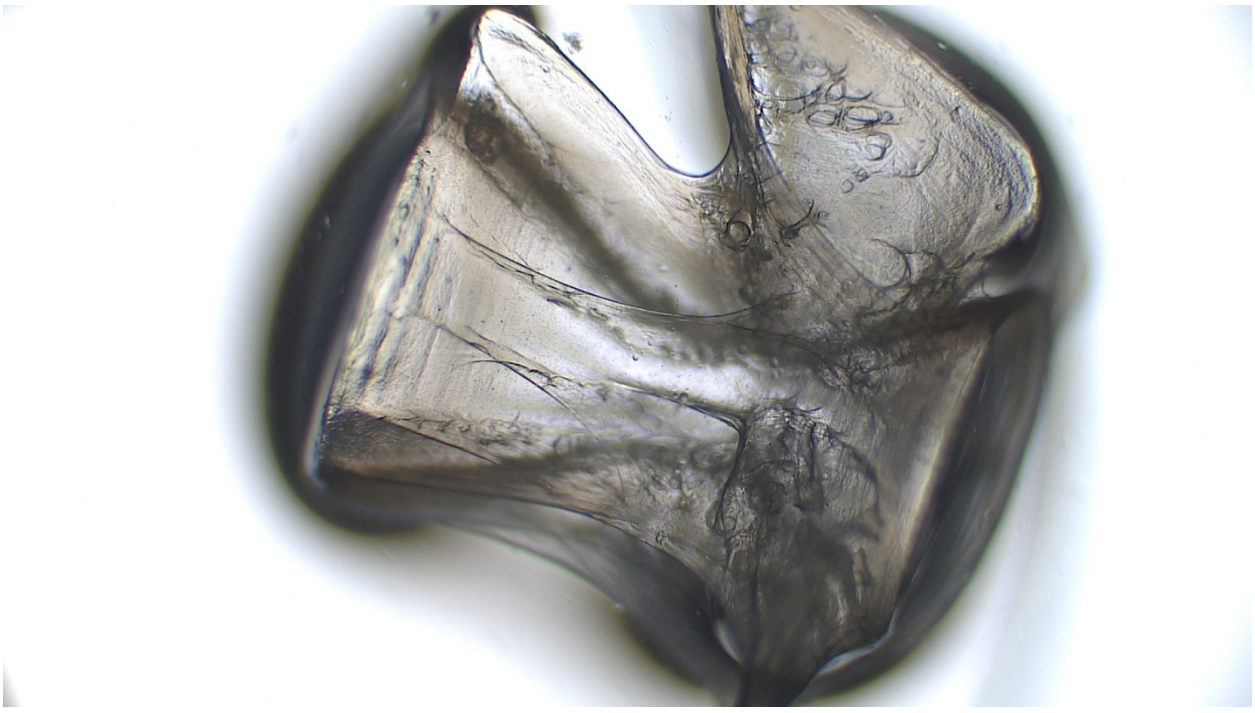

Figure AA30. Northern Lampfish, 75 mm standard length, Anterior, Side View

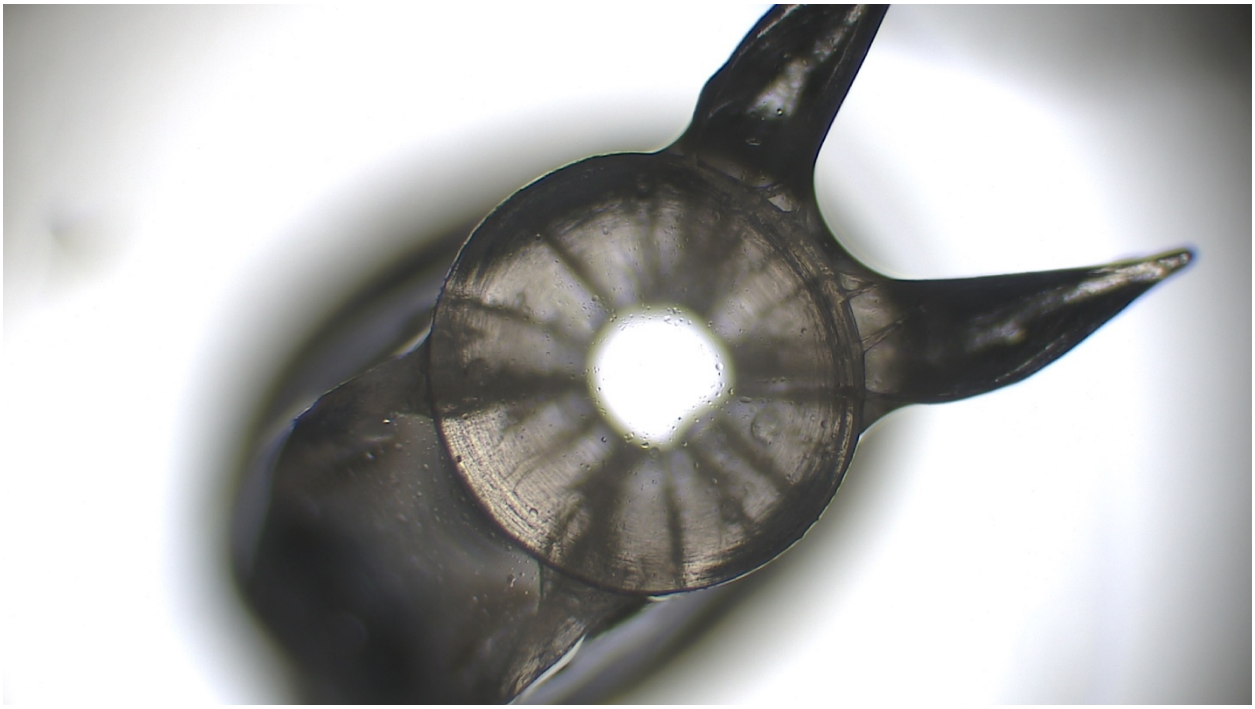

Figure AA31. Northern Lampfish, 75 mm standard length, Anterior, Centrum View

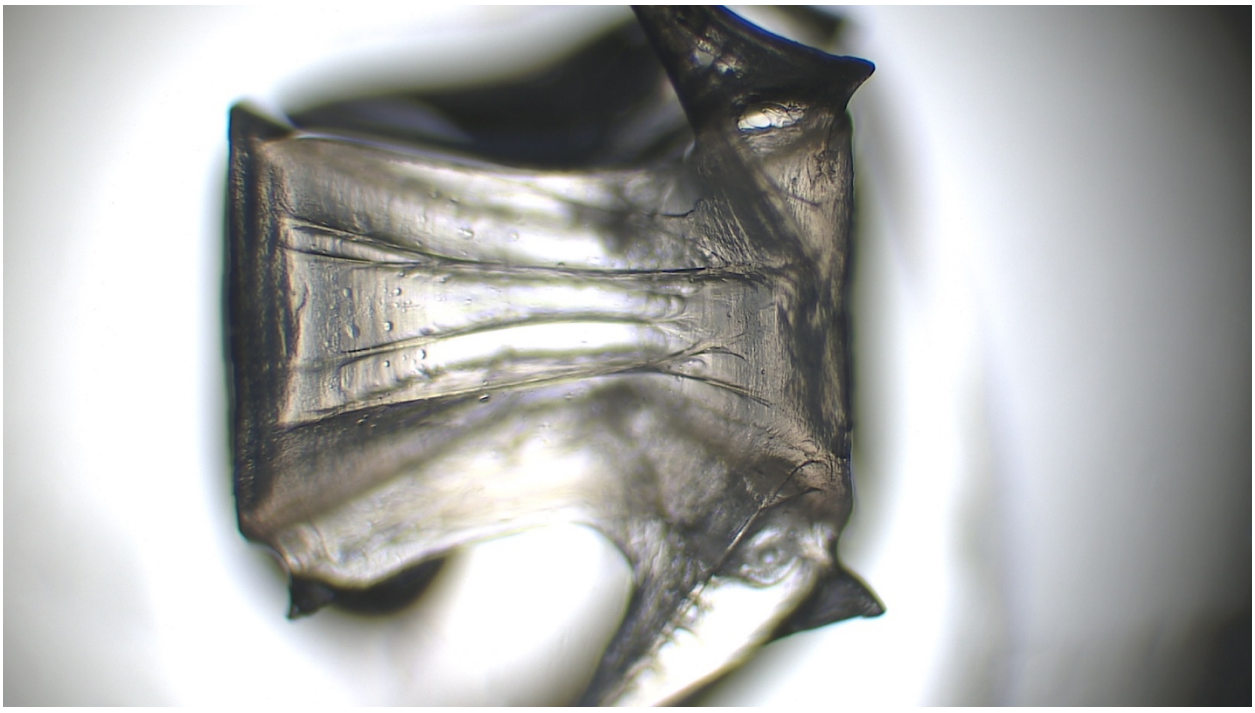

Figure AA32. Northern Lampfish, 75 mm standard length, Mid, Side View

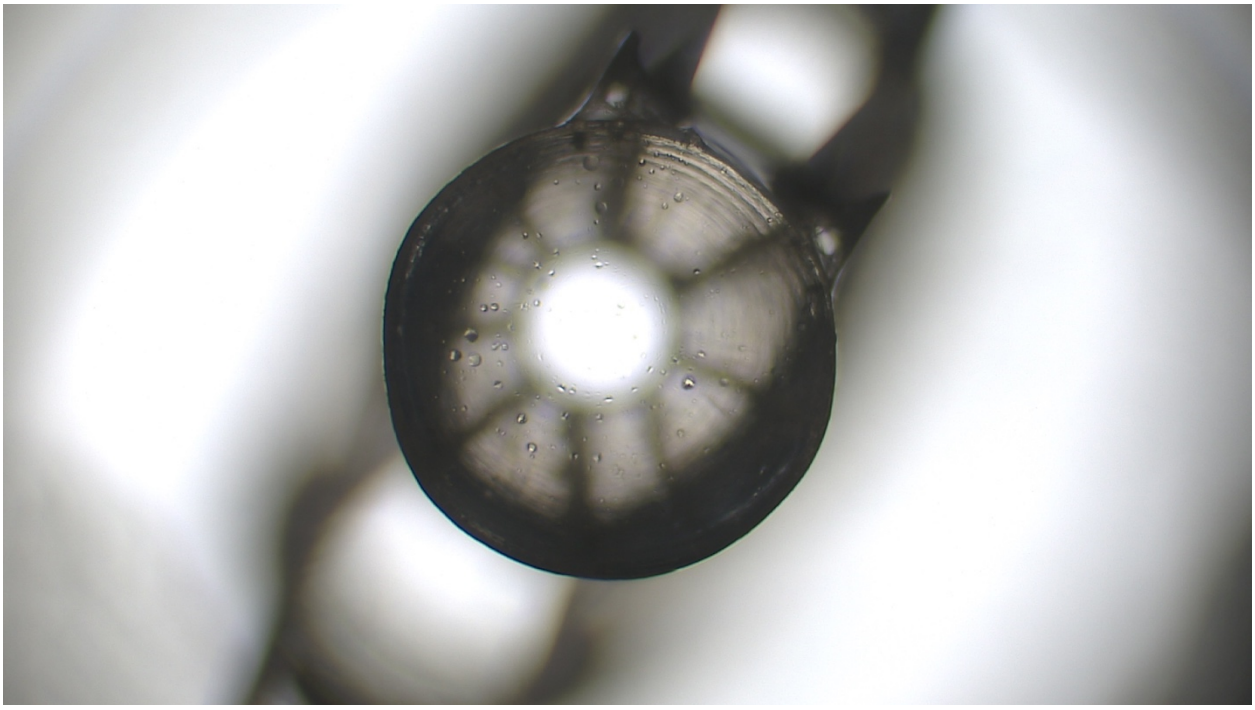

Figure AA33. Northern Lampfish, 75 mm standard length, Mid, Centrum View

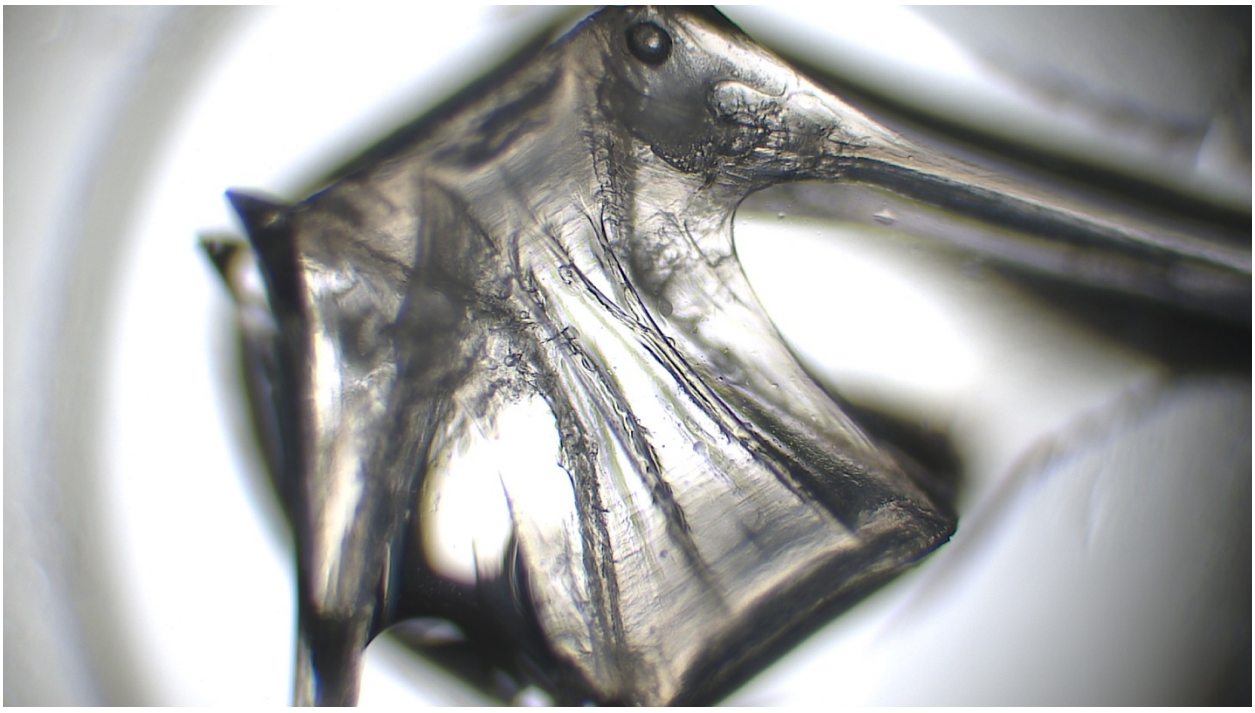

Figure AA34. Northern Lampfish, 75 mm standard length, Posterior, Side View

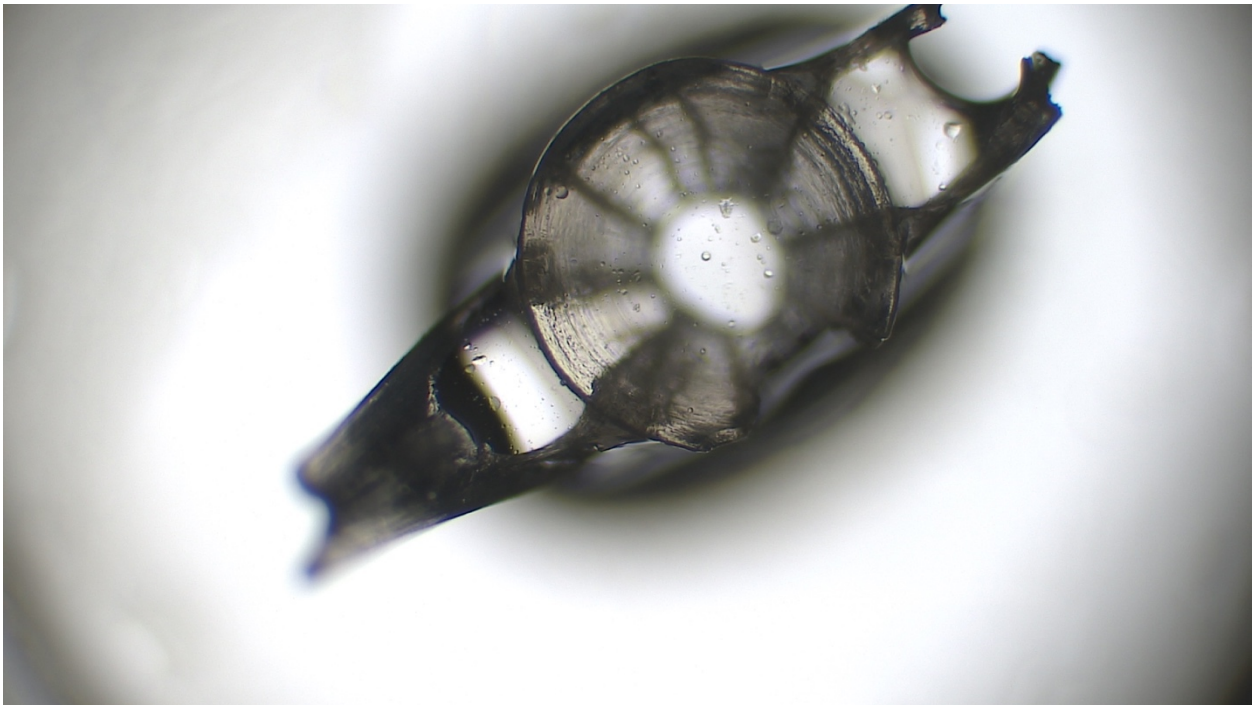

Figure AA35. Northern Lampfish, 75 mm standard length, Posterior, Centrum View

Pacific Hake

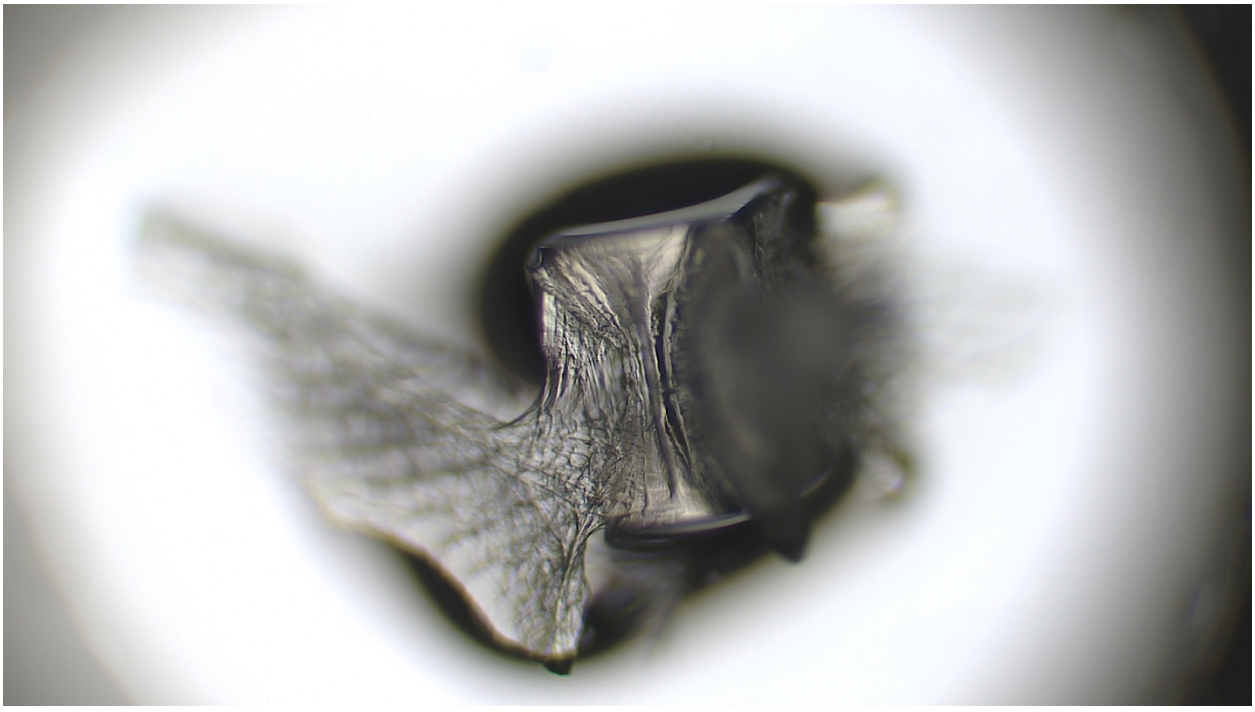

Figure AA36. Pacific Hake, 53 mm standard length, Anterior, Side View

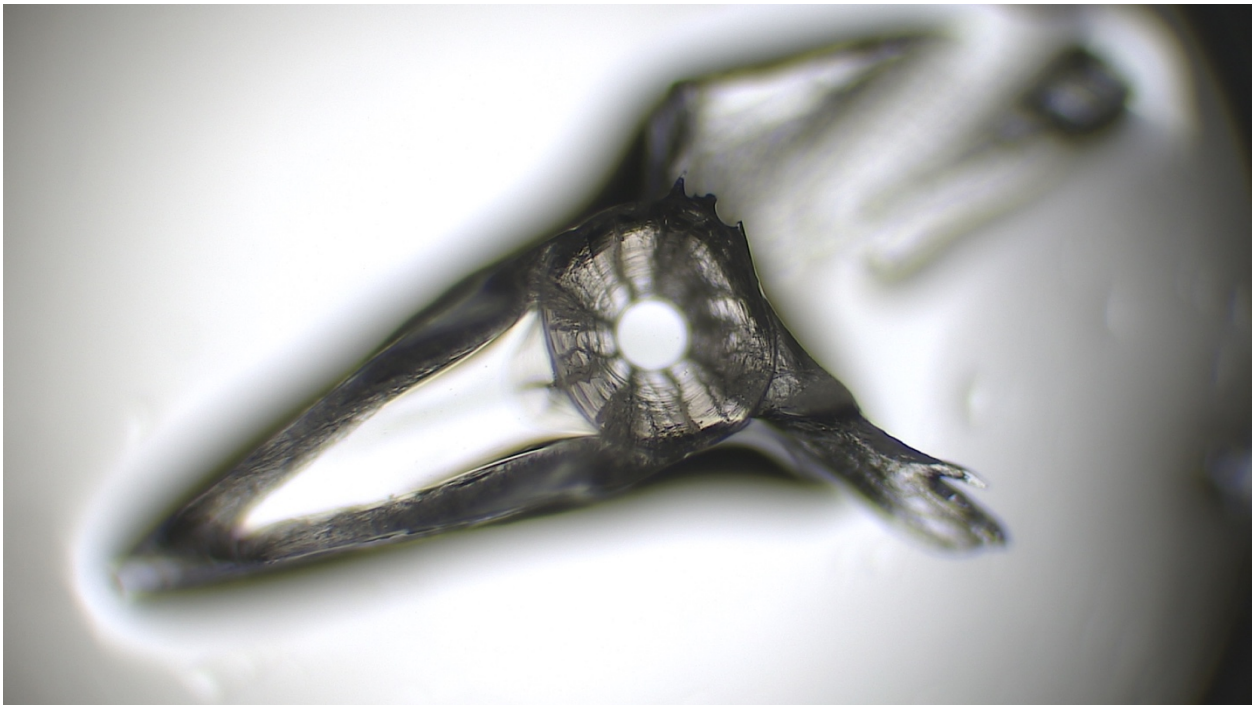

Figure AA37. Pacific Hake, 53 mm standard length, Anterior, Centrum View

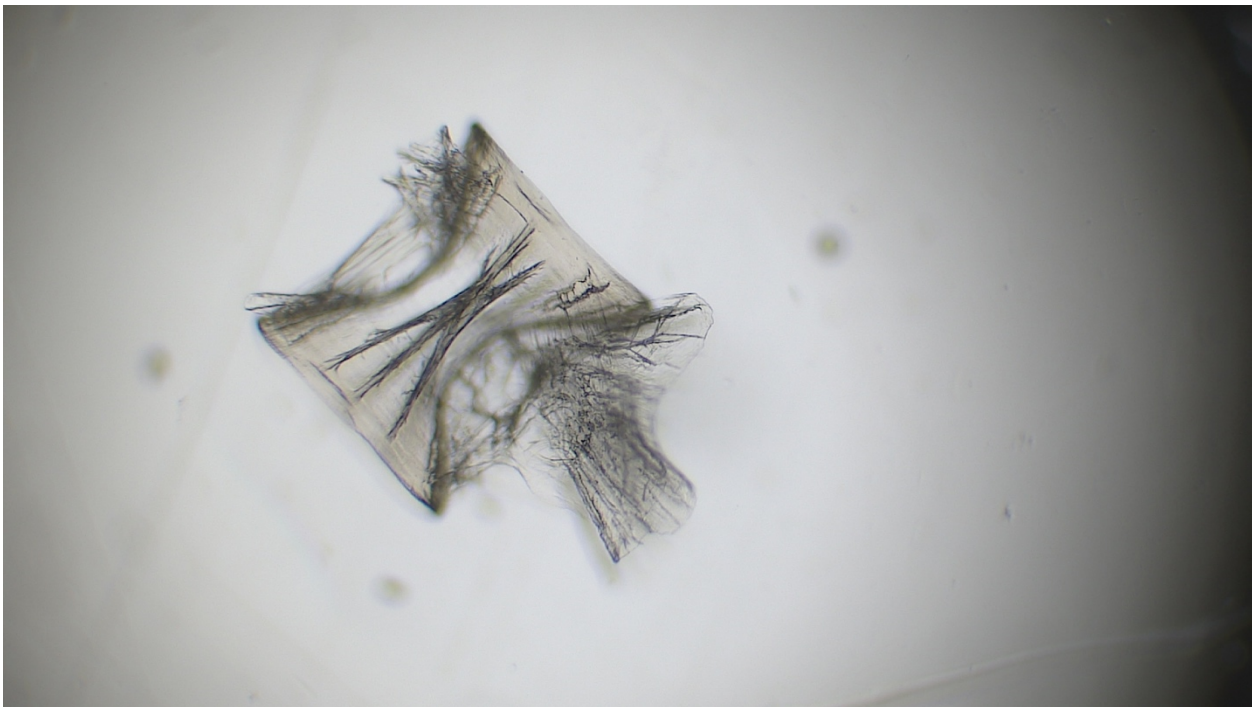

Figure AA38. Pacific Hake, 53 mm standard length, Mid, Side View

Figure AA39. Pacific Hake, 53 mm standard length, Mid, Centrum View

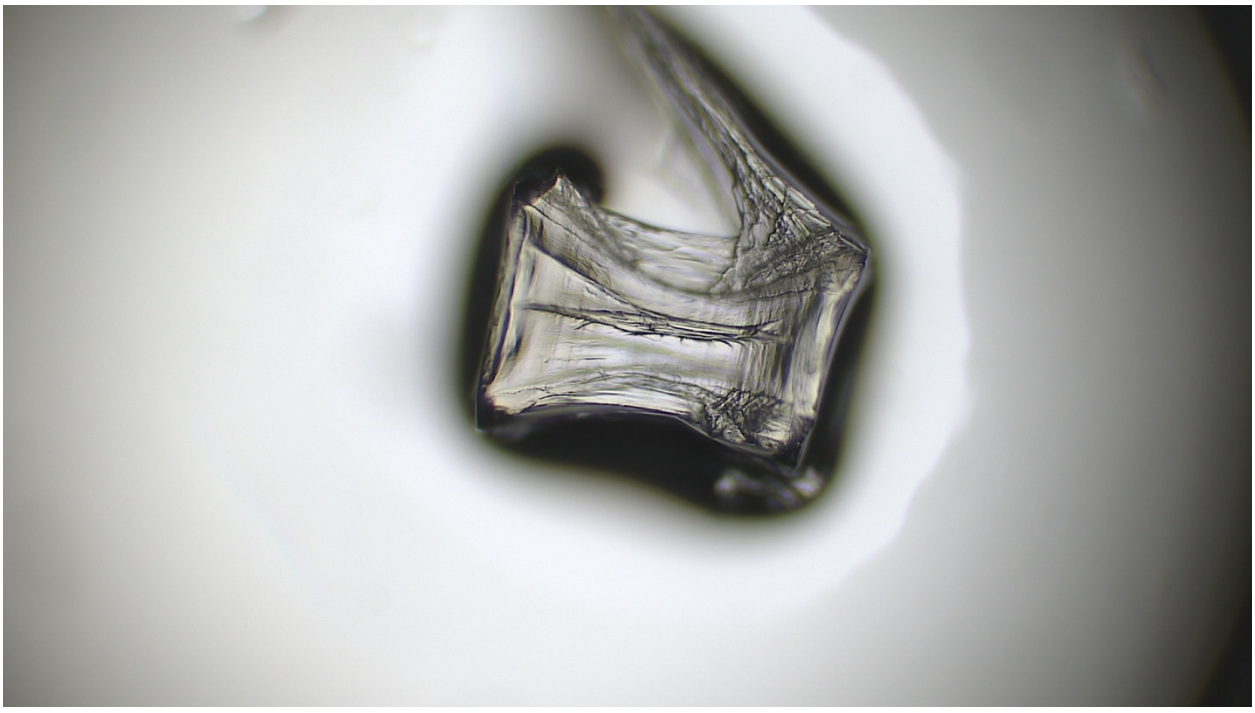

Figure AA40. Pacific Hake, 53 mm standard length, Posterior, Side View

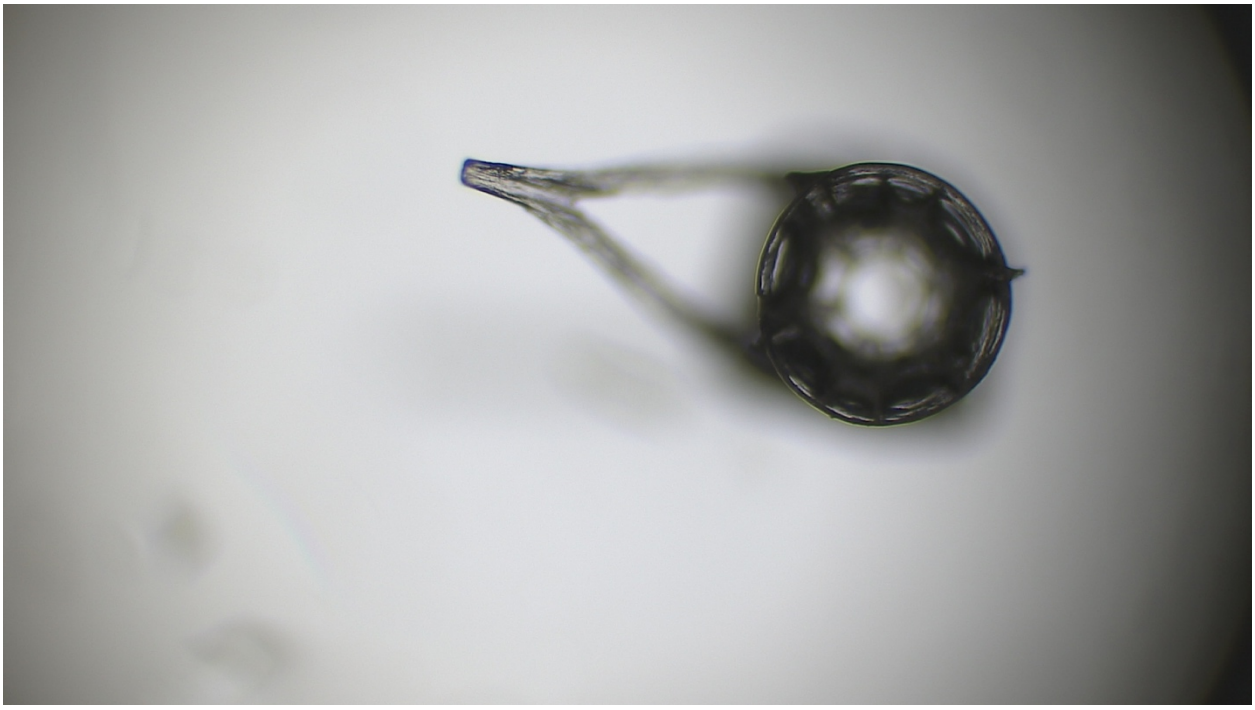

Figure AA41. Pacific Hake, 53 mm standard length, Posterior, Centrum View

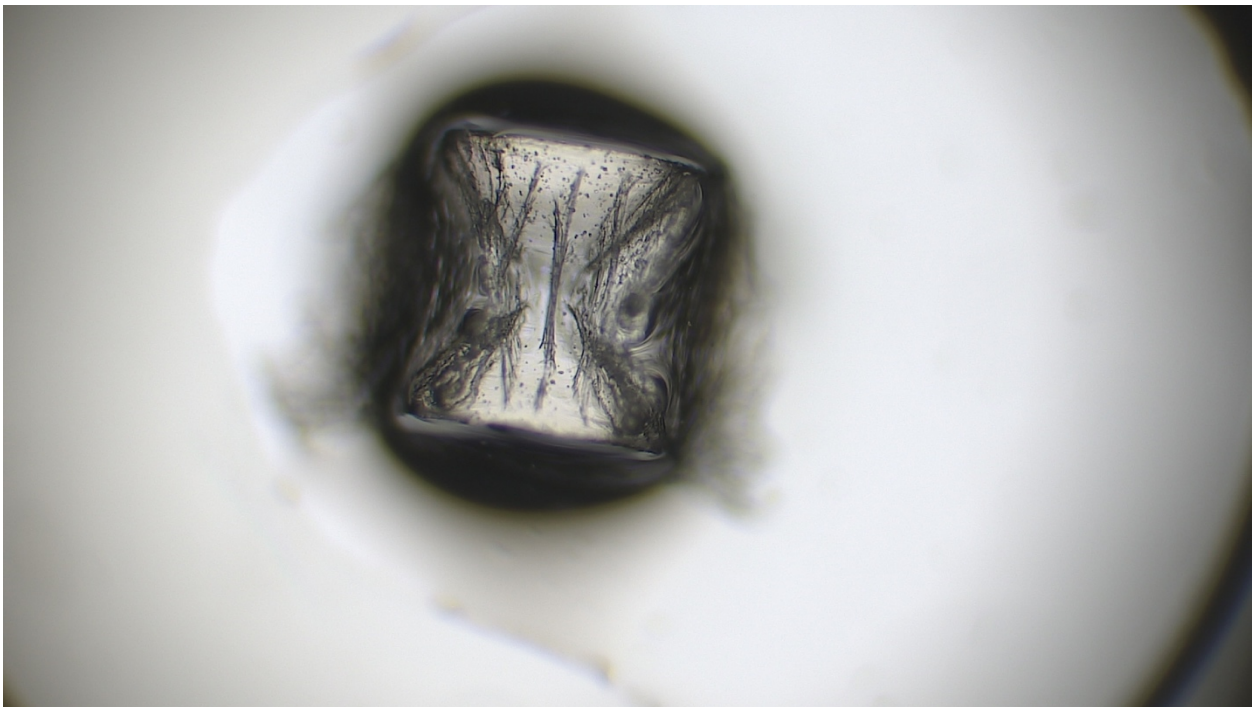

Figure AA42. Pacific Hake, 57 mm standard length, Anterior, Side View

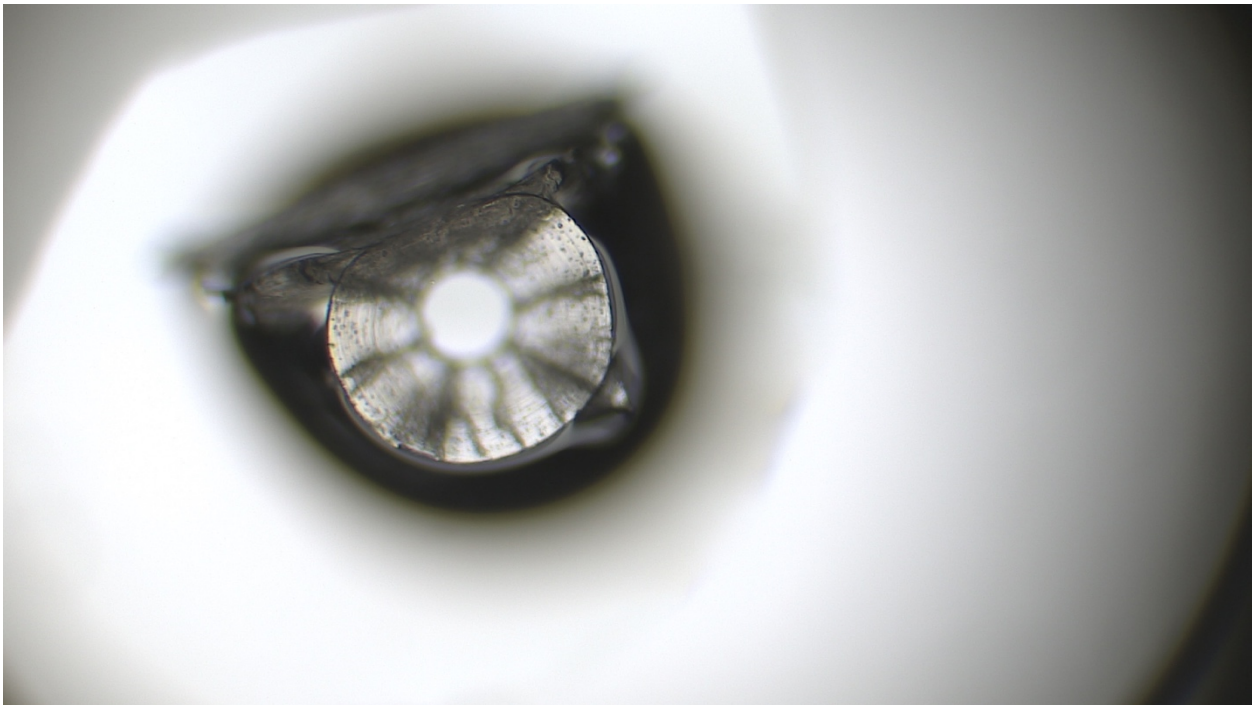

Figure AA43. Pacific Hake, 57 mm standard length, Anterior, Centrum View

(Pacific Hake (57 mm) mid images unavailable)

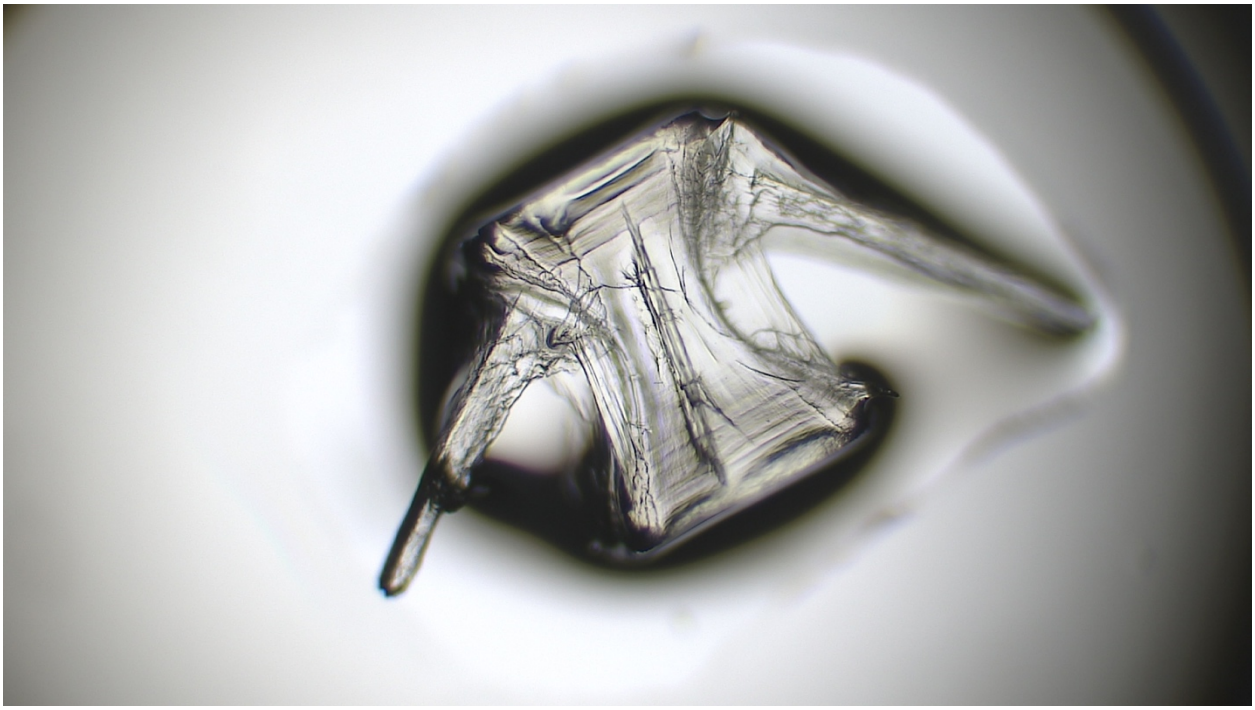

Figure AA44. Pacific Hake, 57 mm standard length, Posterior, Side View

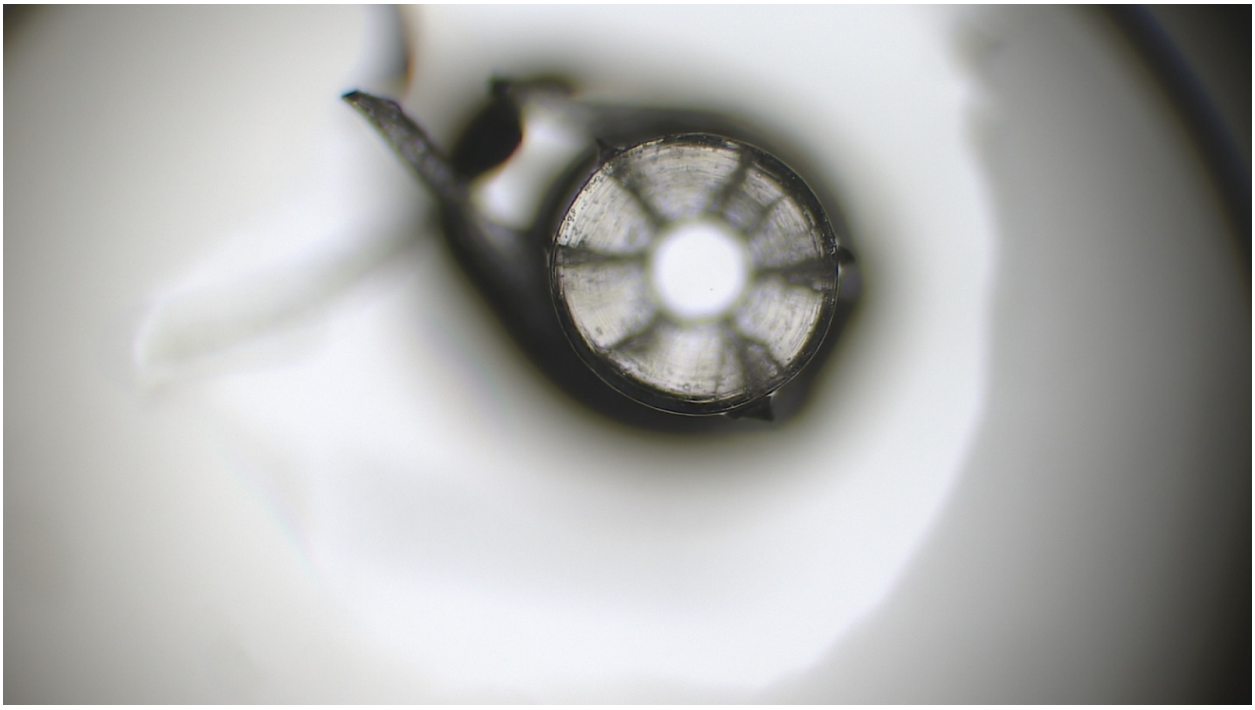

Figure AA45. Pacific Hake, 57 mm standard length, Posterior, Centrum View

Smooth Tongue

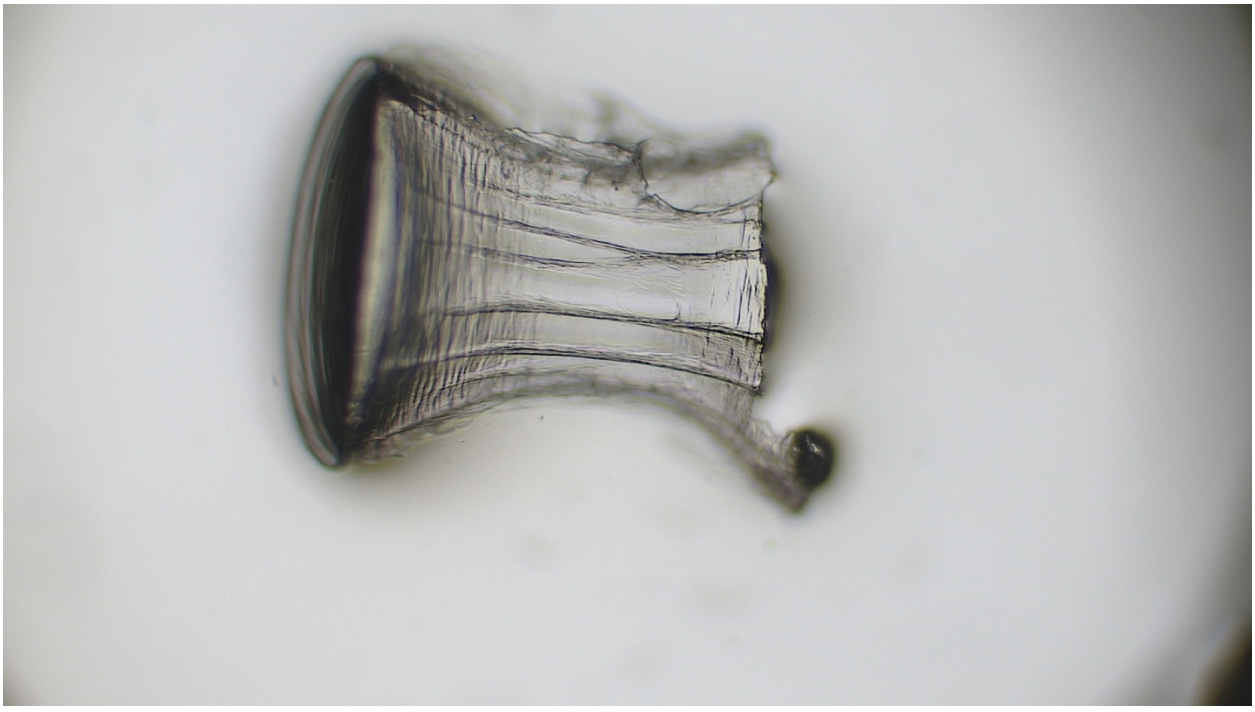

Figure AA46. Smooth Tongue, 71 mm standard length, Anterior, Side View

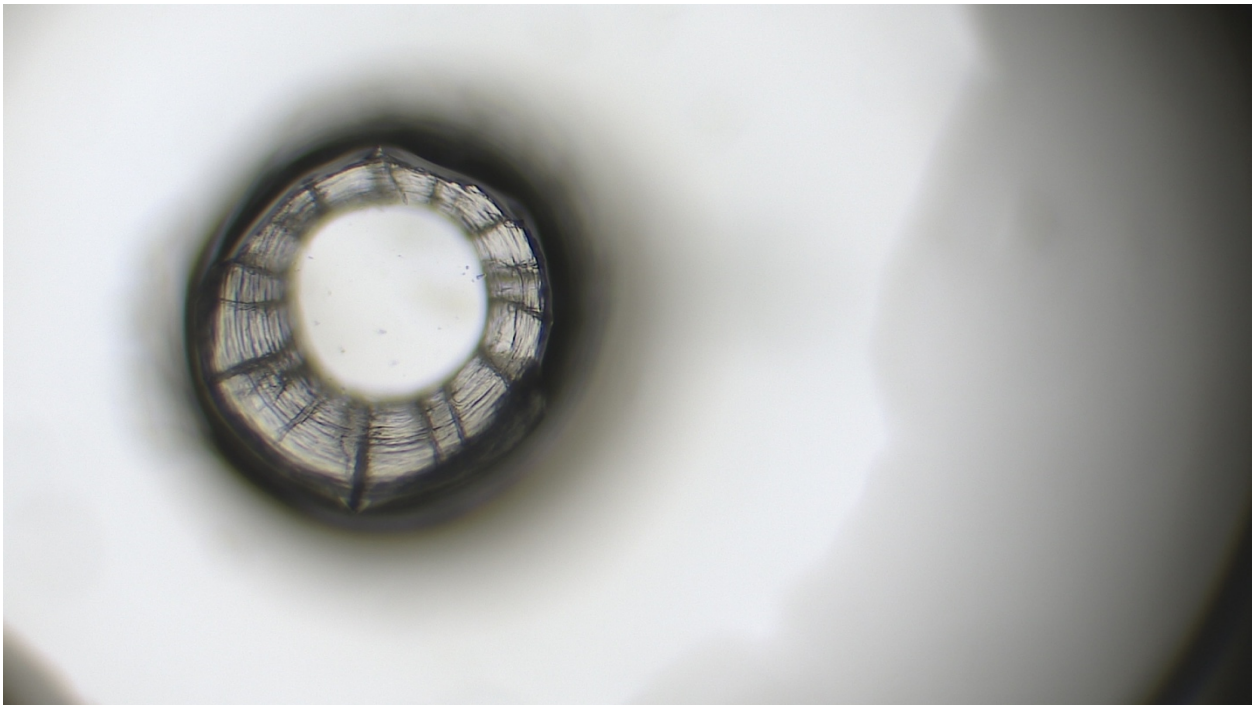

Figure AA47. Smooth Tongue, 71 mm standard length, Anterior, Centrum View

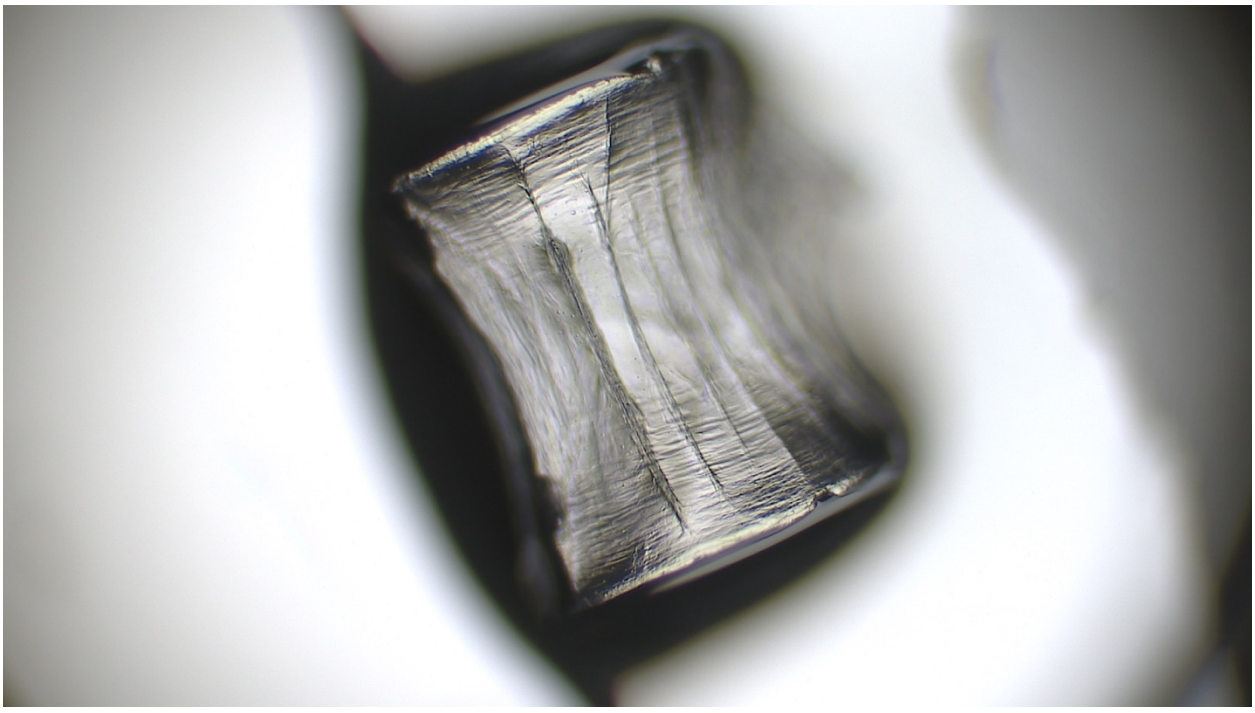

Figure AA48. Smooth Tongue, 71 mm standard length, Mid, Side View

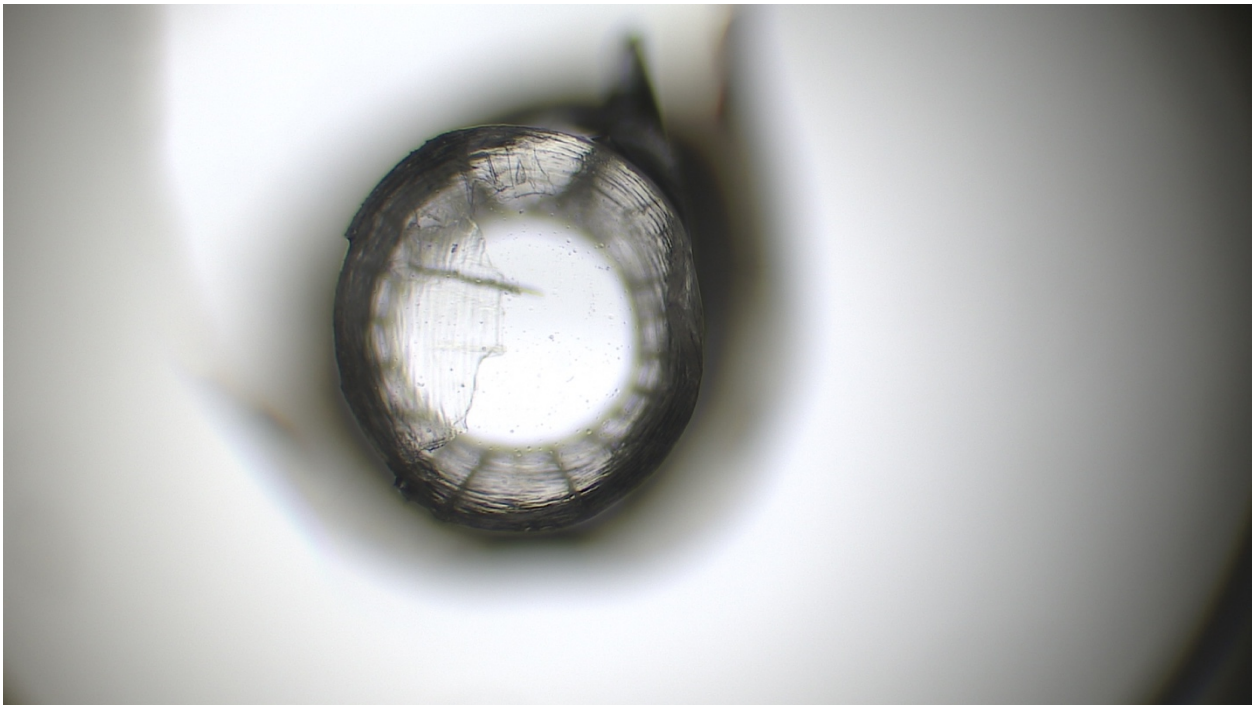

Figure AA49. Smooth Tongue, 71 mm standard length, Mid, Centrum View

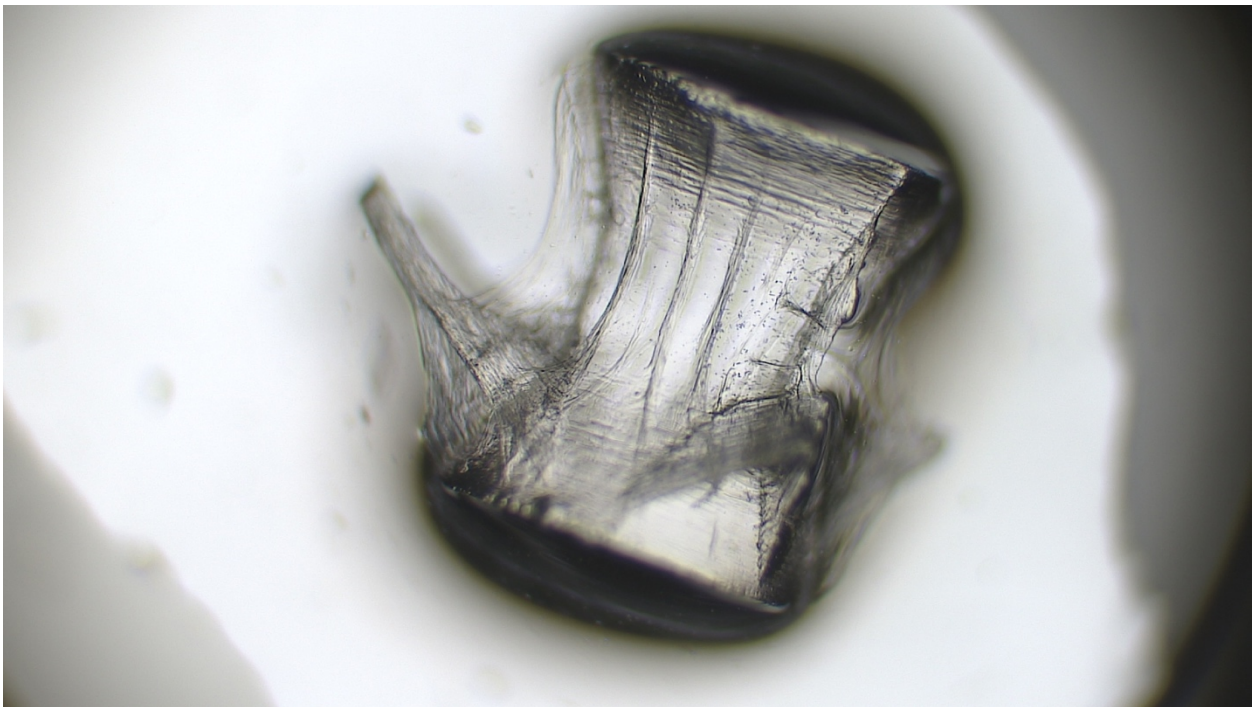

Figure AA50. Smooth Tongue, 71 mm standard length, Posterior, Side View

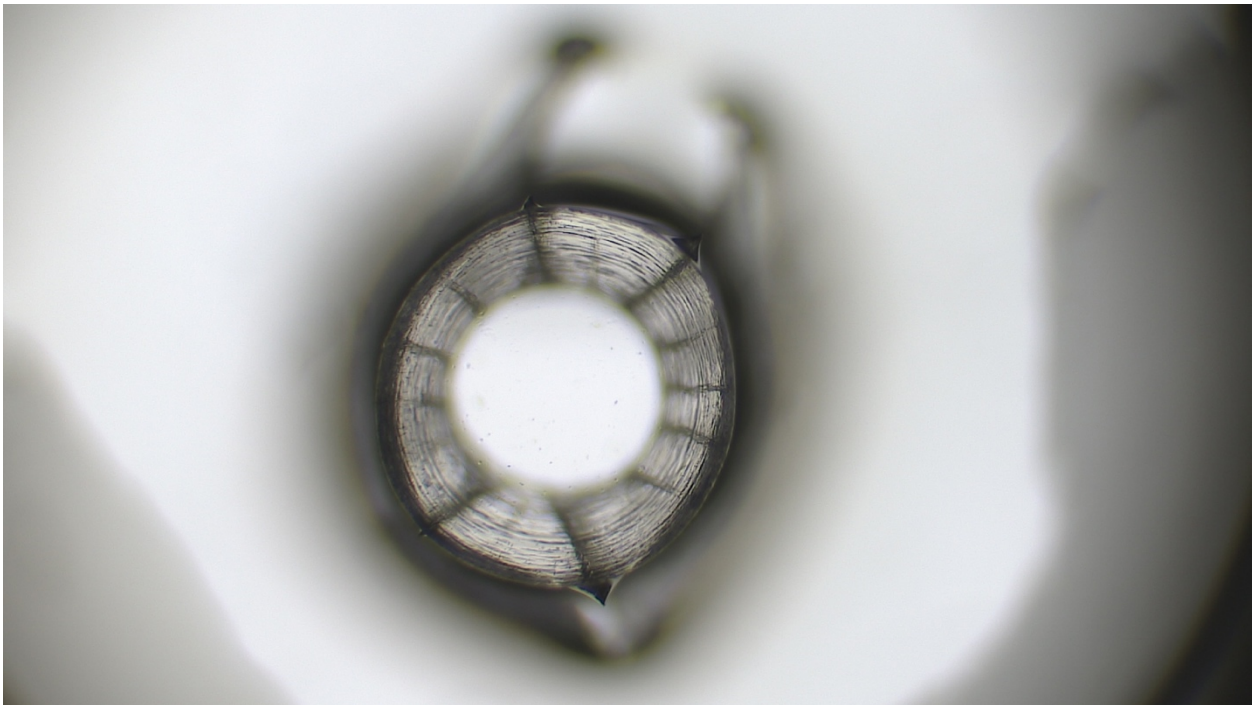

Figure AA51. Smooth Tongue, 71 mm standard length, Posterior, Centrum View

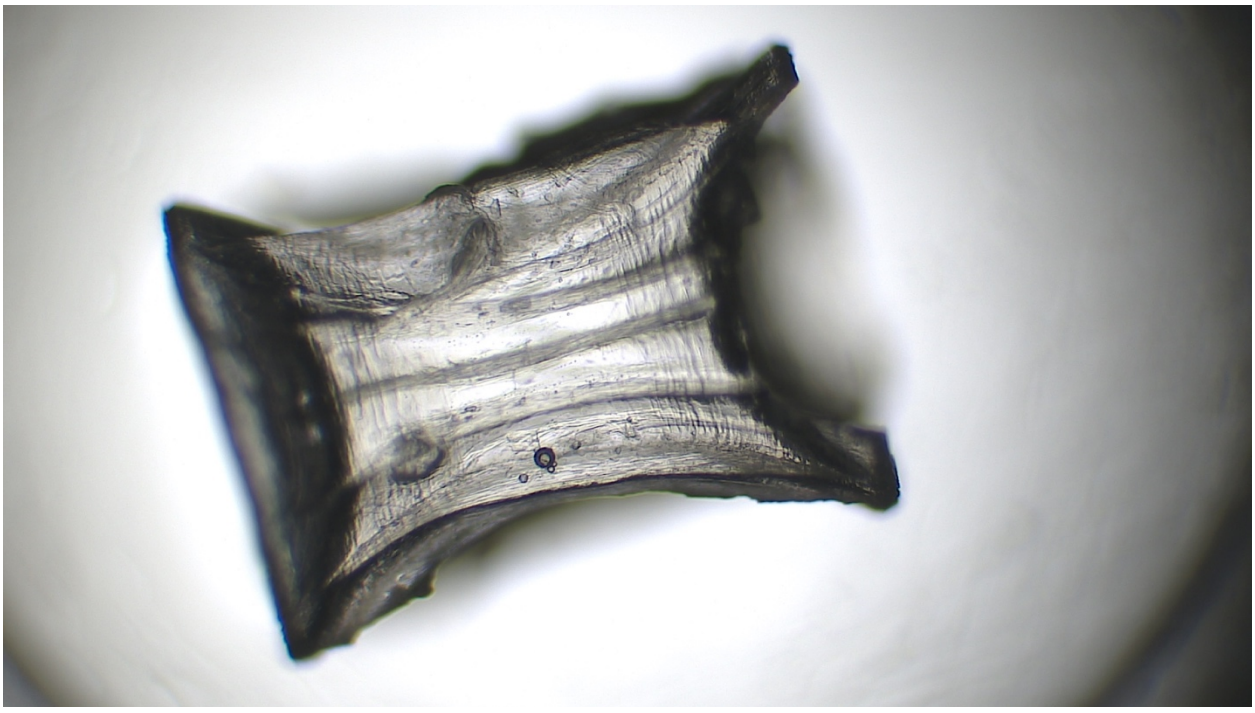

Figure AA52. Smooth Tongue, 94 mm standard length, Anterior, Side View

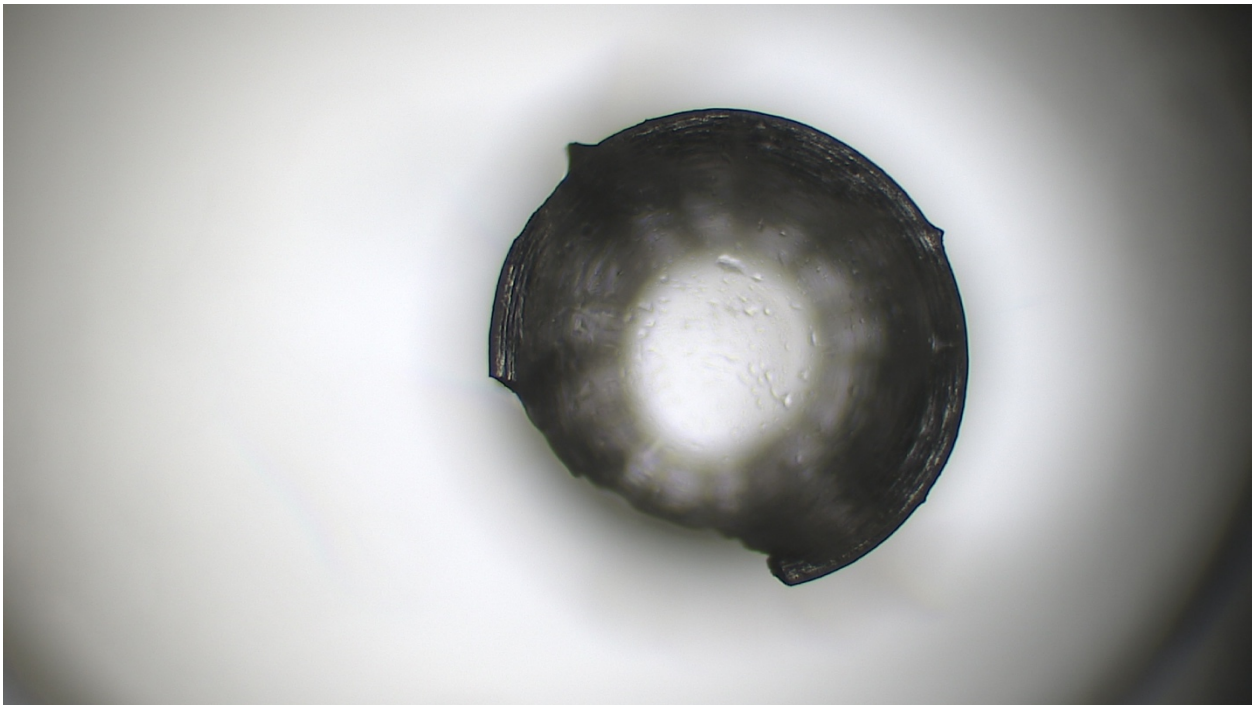

Figure AA53. Smooth Tongue, 94 mm standard length, Anterior, Centrum View

(Smooth Tongue (94 mm) mid images unavailable)

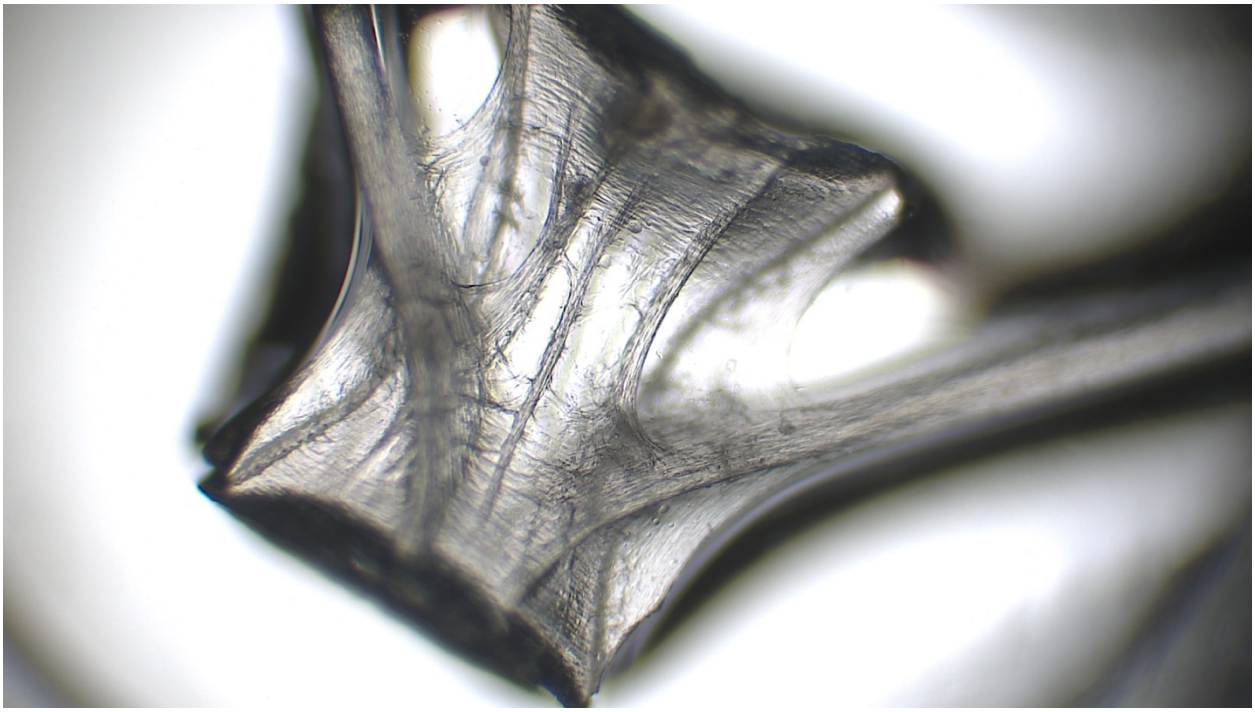

Figure AA54. Smooth Tongue, 94 mm standard length, Posterior, Side View

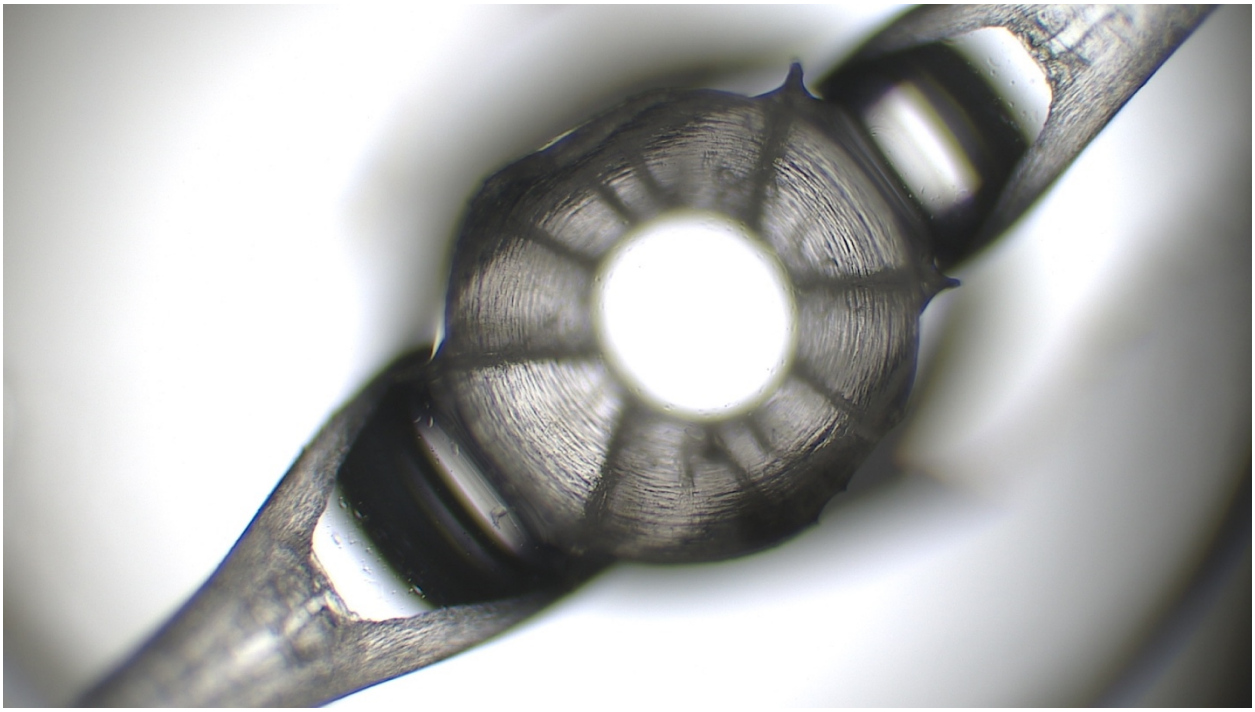

Figure AA55. Smooth Tongue, 94 mm standard length, Posterior, Centrum View